An Investigation into the Influence of Bridging Diamine Linkers on the Substitution Reactions of Dinuclear Platinum^{II} Complexes.

By

Venashree M. Munisamy B.Sc. (Hons), Natal

Submitted in partial fulfilment of the academic requirements for the degree of

Master of Science

in the Faculty of Science & Agriculture

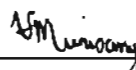School of Chemistry

University of KwaZulu-Natal

Pietermaritzburg

July 2005

Declaration

The work described in this thesis was carried out in the School of Chemistry, University of KwaZulu-Natal, Pietermaritzburg, under the supervision of Professor Deogratius Jaganyi.

These studies represent original work by the author and have not otherwise been submitted in any form for any degree or diploma to any University. Where use has been made of work of others, it is duly accredited in the text.

_____

V. M. Munisamy

I hereby certify that this statement is correct.

_____

Professor D. Jaganyi

Supervisor

Pietermaritzburg

July 2005

This work is dedicated to two very special people:

To my late mother

The one person that has stuck by me
Through the worst times in my life
The person that has lifted me when I had fallen
And comforted me when I was sad
The one person that I know will always be there
And I just wanted to say
Thanks.

To Desigan

Thank you for believing in me when
I found it difficult to believe in myself
For saying what I have needed to hear sometimes,
instead of what I wanted to hear
For siding with me
and for giving me another side to consider.
Thank you for opening yourself up to me...
For trusting me with your thoughts
and disappointments and dreams...
For knowing you can depend on me and
for asking my help when you've needed it.
Thank you for always being honest with me,
being kind to me...being there for me.
Thank You for being a friend to me
in so many ways

Table of Contents

Chapter 3: Kinetic Theory & Techniques

Acknowledgements

Firstly, I would like to thank God, for granting me the strength to see this to completion.

I wish to extend my sincerest gratitude to the following people for their assistance in making the undertaking of this project a success:

- My supervisor, Professor Jaganyi, for always being at hand to offer assistance, ideas and words of encouragement.

- My dad for instilling in me faith, courage and above all his much-appreciated love.

- Drs. Andreas Hofmann and Basam Alzoubi at the Institute for Inorganic Chemistry, University of Erlangen-Nürnberg, Germany for their assistance in elemental analysis.

- The National Research Foundation for their financial support provided for the duration of this project.

- Craig Grimmer, for his timeous running of all NMR samples.

- The academic and technical staff at the School of Chemistry for offering invaluable advice and assistance.

- To my 'support group'; Janine Naidoo and Lynette Mariah, for all their encouragement and laughter during trying times – a heartfelt Thank You!

- My family and friends for all their support and encouragement.

Abstract

Four dinuclear platinum^{II} complexes viz. [{trans-PtCl(NH$_3$)$_2$}$_2$-NH$_2$(CH$_2$)$_n$H$_2$N]Cl$_2$ (where n = 2, 3, 4 and 6) herein referred to as **DiPtEn-Chloro, DiPtProp-Chloro, DiPtBut-Chloro** and **DiPtHex-Chloro** were successfully synthesized and fully characterized with the aid of ^{1}H-NMR, ^{195}Pt-NMR, IR spectroscopy and elemental analysis. The conversion of the chloride moiety to the corresponding aqua moiety, viz. **DiPtEn-Aqua, DiPtProp-Aqua, DiPtBut-Aqua** and **DiPtHex-Aqua**, was successfully achieved via a methathesis reaction using established literature procedures.

pK_a studies were conducted on three of the complexes viz. **DiPtEn-Aqua, DiPtProp-Aqua** and **DiPtBut-Aqua** using UV/Visible spectrophotometry. A single pK_a value was obtained for all complexes. The pK_a value is seen to increase from 4.98 (**DiPtEn-Aqua**) to 5.62 (**DiPtHex-Aqua**), with a corresponding increase in diamine chain length. This phenomenon can be attributed to an increase in electron density around the platinum centre via the inductive effect.

The rate of substitution of the aqua moieties from each of these four complexes by a series of neutral nucleophiles, viz. thiourea (TU), 1,3-dimethyl-2-thiourea (DMTU) and 1,1,3,3-tetramethyl-2-thiourea (TMTU) in aqueous solution was determined under pseudo first-order conditions as a function of concentration and temperature. All reactions studied gave excellent fits to a single exponential and obeyed the simple rate law, $k_{obs} = k_2$[Nu], with the exception of the reaction involving **DiPtEn-Aqua** and **TU**, which was found to exhibit second-order kinetics with the observed rate constants, $k_{obs(1,2)}$ being expressed by the equation, $k_{obs(1,2)} = k_{(1,2)}$[Nu]. The first rate constant k_1 ((5029.24 ± 0.01) x 10^{-3} M^{-1} s^{-1}) was found to be approximately 15 times greater than that for the second rate constant k_2 ((326.6 ± 7.5) x 10^{-3} M^{-1} s^{-1}).

A comparison of the second-order rate constants at 298 K shows that the reactivity of these complexes is dependent on the length of the diamine linker. As the CH$_2$ group is increased the rate of substitution decreases. This has been accounted for in terms of increased electron density around the metal centres through an inductive process. Lengthening of the backbone also increases the flexibility of these complexes resulting in increased steric

hindrance. Although the computational calculation using the B3LYP density functional method with LACVP** pseudopotential basis set indicate that the *trans* effect is increased by addition of the CH_2 group, through the shortening of the Pt-N bond and lengthening of the $Pt-OH_2$ bond, this effect is small. Computational factors have also shown that the frontier molecular orbital energies increase with an increasing number of CH_2 groups. The energy gap, $E_{HOMO} - E_{LUMO}$ was found to increase from **DiPtEn-Aqua** to **DiPtProp-Aqua** indicating a decrease in interaction between the orbitals. The results of the temperature dependence studies indicate that the reactivity is controlled by activation entropy. The substitution mechanism remains associative in nature.

The reaction involving **DiPtEn-Aqua** and **TU** was found to be 10^2 times faster than the other complexes, and it was possible to measure the rate of substitution at each metal centre. This shows that the interaction between the two Pt^{II} centres is dependent on the distance between them. The unusual reactivity of **DiPtEn-Aqua** is thought to be mainly caused by less steric hindrance that the molecule experiences due to lack of flexibility. In addition to this is the proximity of the two Pt^{II} centres, which in this case interact with each other.

List of Abbreviations

AgCl	-	silver chloride
AgClO$_4$	-	silver perchlorate
AgNO$_3$	-	silver nitrate
ApG	-	platinum bound to the N7 atoms of adjacent adenine-guanine sites
BBR3005	-	[{$trans$-PtCl(NH$_3$)$_2$}$_2$-H$_2$N(CH$_2$)$_6$NH$_2$]$^{2+}$
BBR3464	-	[($trans$-PtCl(NH$_3$)$_2$)$_2${μ-$trans$-Pt(NH$_3$)$_2$(H$_2$N(CH$_2$)$_6$NH$_2$)$_2$}]$^{4+}$
DMF	-	dimethylformamide
DMTU	-	1,3-dimethyl-2- thiourea
DNA	-	deoxyribonucleic acid
DNA-PK	-	DNA-dependent protein kinase
EtOH	-	ethanol
GpG	-	platinum bound to two adjacent N7 guanine sites
GSH	-	gluthathione
HClO$_4$	-	perchloric acid
HMG	-	high mobility group
HOMO	-	highest occupied molecular orbital
IR	-	infrared
k_2	-	second-order rate constant (unless otherwise stated)
k_{obs}	-	observed pseudo first-order constant
KCl	-	potassium chloride
LFER	-	linear free energy relationship
LUMO	-	lowest unoccupied molecular orbital
Mesna	-	2-mercaptoethanesulfonate
MMR	-	mismatch repair
NaClO$_4$	-	sodium perchlorate
Naddtc	-	sodium diethyldithiocarbamate
NaOH	-	sodium hydroxide
NER	-	nucleotide excision repair
NMR	-	nuclear magnetic resonance
py	-	pyridine
TMTU	-	1,1,3,3-tetramethyl-2-thiourea

TU	-	thiourea
UV/Vis	-	ultraviolet/visible
X	-	leaving group (unless otherwise stated)
Y	-	entering group (unless otherwise stated)

List of Figures

List of Schemes

List of Tables

Publications and Conference Contributions

Publications:

1. D. Jaganyi, **V. M. Munisamy** & D. Reddy, "Role of Bridging Diamine Linker on the Rate of Ligand Substitution in a Series of Dinuclear Pt^{II} Complexes.": In preparation for submission to *J. Chem. Soc. Dalton Trans.*

Conference Contributions

Part of the work presented in this dissertation has been presented in the form of poster presentations.

Poster Presentations

1. Inorganic Reaction Mechanisms Discussion Group, 5th-7th January 2005, University of Liverpool, **The Role of Bridging Diamine Chain Length in Determining the Rates of Substitution of H$_2$O from a Series of Dinuclear Platinum^{II} Complexes."**

2. 37th Convention of South African Chemical Institute (SACI), Pretoria, South Africa, July 2004, Entitled: **"An Investigation into the Influence of Bridging Diamine Linkers on the Substitution Reactions of Dinuclear Platinum^{II} Complexes."**

Chapter 1

An Introduction into Platinum Chemistry

Chapter 1

An Introduction into Platinum Chemistry

_1.1_ _Background_

Platinum occupies a position of paramount importance in transition metal-complex chemistry. Organometallic and coordination chemistry of platinum is unusual on two accounts:[1]

- due to the variety of compounds this metal forms and,

- owing to the wide variety of reactions that these participate in.

The versatility of platinum chemistry may be accounted for by the fact that coordination compounds of platinum are known in many oxidation states _viz._ 0, +1, +2, +3 and +4. Higher oxidation states are also known but these are rare. The most common of these oxidation states are 0, +2 and +4, with derivatives of Pt^0, Pt^{II} and Pt^{IV} by far the most stable and studies ones.[1]

Pt^{II} coordination complexes were early and important examples of transition metal complexes. Their square planar geometry was first determined in the classic isomer-counting experiments of Werner. Pt^{II} complexes were subsequently used extensively in studies determining the mechanisms of square-planar substitution reactions, since they react at rates that are convenient for such studies in aqueous solutions. Platinum binding to nucleic acids was first investigated in part with the aim of developing heavy metal stains for electron microscope (EM) studies of DNA. The high electron density of platinum complexes has also lead to their use as isomorphous replacement agents for solving macromolecular crystal structures.

Medicinal applications of metals can be traced back almost 5000 years ago. The development of modern medicinal inorganic chemistry was stimulated by the serendipitous discovery of cisplatin, and has been facilitated by the inorganic chemists extensive knowledge of the coordination and redox properties of metal ions. Metal centres, being

positively charged are favoured to bind to negatively charged biomolecules (the constituents of proteins and nucleic acids), offer excellent ligands for binding to metal ions.[2] The potential use of metal complexes in pharmaceuticals is vast and remains to be exploited.

1.2 The Biological Importance of Platinum^{II}-Amine Complexes

Broad interest in the pharmacological properties of metal compounds first arose with the pioneering work of Barnett Rosenburg[3,4], who in the late 1960's fortuitously discovered the electrostatic effects of *cis*-diamminedichloroplatinum^{II} (cisplatin) (*Figure 1.1*) and related complexes. Cisplatin has been a highly successful platinum-based antitumour agent and has been used clinically over the last thirty years and continues to play a central role in cancer chemotherapy. This is due to cisplatin on one hand being able to cure testicular germ-cell cancer in about 90% of its cases, and on the other hand for its notable therapeutic efficacy in a broad range of other solid tumours. Driven by the impressive impact of cisplatin on cancer chemotherapy, great efforts have been made to derive new derivatives with pharmacological properties, hence cisplatin has become the prototype of a unique class of antineoplastic agents now comprising innumerable derivatives, many of which have been abandoned in preclinical or early clinical stages of their development, whilst a few have succeeded in becoming established in routine clinical practice. Among the 33 platinum agents (*Table 1.1*) which have entered clinical trials after the onset of clinical studies with cisplatin in the early 1970's, only carboplatin has received worldwide approval, whilst four others *viz.* oxaliplatin, nedaplatin, lobaplatin and SK12053R have gained regionally limited approval and eight others continue to be evaluated in clinical studies.[3-6]

$$H_3N \overset{\textstyle NH_3}{\underset{\textstyle Cl}{\overset{|}{\underset{|}{-\!\!Pt\!\!-}}}} Cl$$
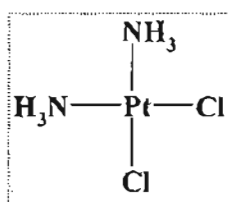
Figure 1.1:   *cis-diamminedichloroplatinum^{II} or cisplatin as it is commonly referred to is a proven and effective chemotherapeutic agent.*

The vast majority of these compounds and all of the clinically established platinum drugs essentially belong to the classic type of uncharged *cis*-configured square-planar Pt^{II} complexes described by the general formula *cis*-$[PtA_2X_2]$, whereby A_2 can be either two monodentate or one bidentate stable amine ligand(s) and X_2 being either two monodentate or one bidentate anionic leaving ligand(s). These types of complexes have been favoured since the early landmark studies conducted by Cleare and Hoeschele[7,8] on structure activity relationships within Pt^{II} compounds, performed soon after the antineoplastic properties of cisplatin was established.[9,10]

Table 1.1:   *Platinum compounds in clinical studies since 1971 in roughly chronological*

order.[11]

Compound	Current Status
1970's	
Cisplatin (CDDP)	Approval Worldwide for a broad range of solid neoplasms
PAD	Abandoned during phase I (insufficient solubility)
Platinum Uracil Blue (PUB)	Abandoned during phase I (cardiac toxicity)
MBA	Abandoned during phase I (one case of severe hypersensitivity)
JM-20 (SHP)	Abandoned during phase I (severe allergic reactions)
JM-74 (PHM)	Abandoned during phase II (nephrotoxicity, inferior activity)
Neo-SHP	Abandoned during phase II (nephrotoxicity, inferior activity)
Neo-PHM	Abandoned during phase I (insufficient solubility)
1980's	
Carboplatin (CBCDA; JM-8)	Approval Worldwide for a broad range of solid neoplasms
Iproplatin (CHIP; JM-9)	Abandoned during Phase III (lower activity than carboplatin)
JM-82 (DACCP)	Abandoned during Phase II (chemical instability, low activity)
JM-11	Abandoned after pharmocokinetic study
Spiroplatin (TNO-6)	Abandoned during Phase II (nephrotoxicity)
Oxaliplatin (l-OHP)	Approved in over 60 countries for metastatic colorectal cancer
Nedaplatin (254-S)	Approved in Japan for several solid neoplasms
CI-973 (NK-121)	Abandoned during Phase II (lack of activity)
DWA2114R (miboplatin)	Abandoned during Phase III (no advantage over cisplatin)
Enloplatin	Abandoned during Phase II (nephrotoxicity)
Zeniplatin	Abandoned during Phase II (nephrotoxicity)
1990's	
Lobaplatin (D-19466)	Approved in China
Ormaplatin (tetraplatin)	Abandoned during Phase I (neurotoxicity)
Cycloplatam	. Phase II
JM-216 (satraplatin)	Phase III
SKI 2053R	Approved in South Korea for advanced gastric cancer
ZD0473 (AMD473)	Phase III
SPI-77 (liposomal CDDP)	Phase II
BBR3464	Phase II
2000's	
AP5280	Phase I

1.3   The First Generation: Cisplatin

Cis-diamminedichloroplatinum[II] (cisplatin) has been known as Peyrone's salt since the mid nineteenth century. Interest in its potential pharmacological properties arose only in the late 1960's, when cisplatin and its Pt[IV] analogue (*cis*-diamminetetrachloroplatinum[IV]) was identified by Barnett Rosenburg as strong inhibitors of bacterial proliferation in a set of experiments, that were performed in order to investigate the effects of electric fields on cell division. Subsequently, their cytostatic activity was examined in tumour-bearing animals, with the encouraging result of complete inhibition of murine solid sarcoma-180[2] by cisplatin.

Clinical trials of cisplatin were thereafter initiated in 1971, but anticancer activity was associated with severe renal toxicity. This could be circumvented by pre-hydration, followed by slow infusion, and by the end of the 1970's cisplatin became the mainstay in combination chemotherapy of advanced and metastatic testicular germ-cell cancer, which has since become a highly curable disease. Currently, cisplatin is one of the most commonly used compounds for the treatment of a wide spectrum of human malignancies. As a single agent, or in combination, cisplatin is now the mainstay of treatment for testicular, ovarian, bladder, cervical, head and neck, as well as small-cell or non-small-cell lung cancers.[5,12,13]

Cisplatin is usually administered in chloride-containing solution as short intravenous infusion following either a single-dose or a split-dose schedule. In aqueous solutions, the chloride ligands are easily replaced by aqua ligands, leading to a much more reactive species. Part of these aqua ligands may be deprotonated to hydroxo ligands consequently resulting in a lowering of the reactivity of the complex. These hydrolysis reactions result in a mixture comprising mainly of mixed chloro/aqua and chloro/hydroxo, and in much smaller portions aqua/hydroxo, diaqua/dihydroxo species (*Figure 1.2*). Hydrolytic activation of cisplatin is to some extent suppressed by high chloride ion concentrations in extracellular fluids, but is assumed to be promoted by the low chloride ion concentration present within the cell. However, one should bear in mind that the assumptions made are based on chemical equilibria and this is not attained within biological systems.
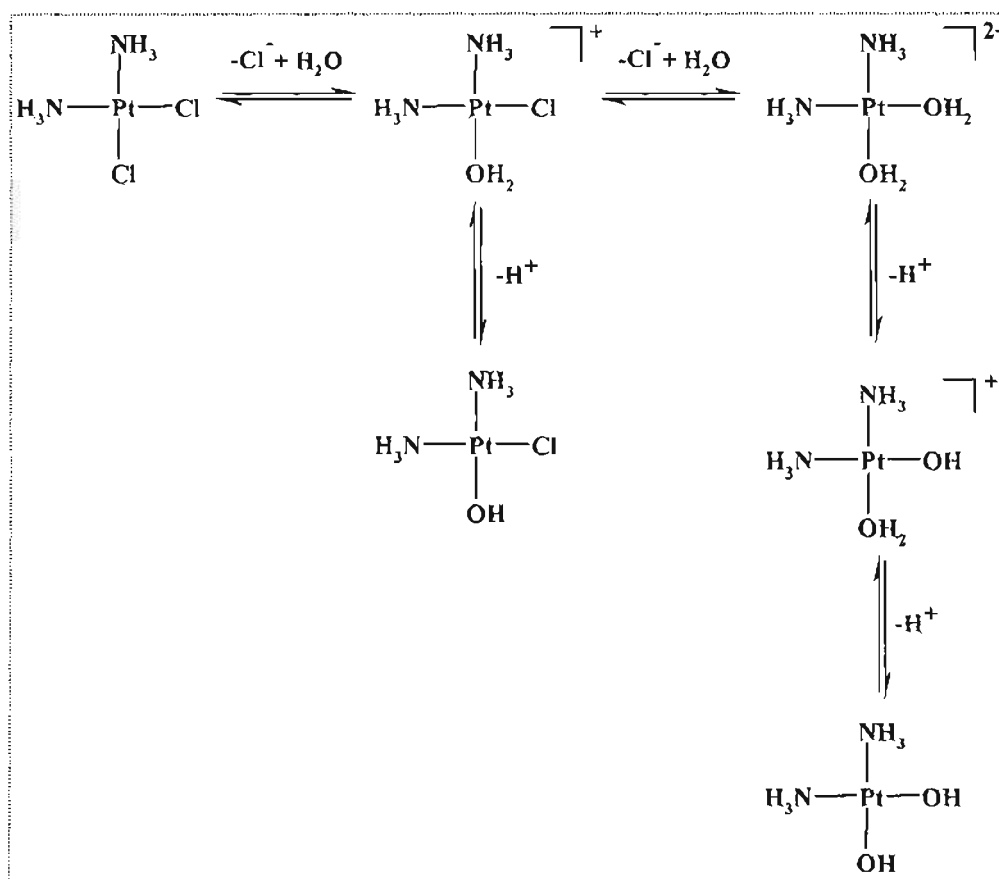
Figure 1.2: **Structures of cisplatin and its hydrolysis products**

The nephrotoxicity of cisplatin severely hampered its early clinical development, until pre-hydration and forced diuresis[14-16] were successfully introduced to prevent renal failure. Further frequent adverse effects include cumulative peripheral sensory neuropathy, nausea, vomiting and myellosupression.[17-19] Hence, the administration of cisplatin is normally accompanied by chemoprotective agents, which help alleviate side effects on normal tissues without compromising antitumour efficacy. These include many sulfur-containing agents such as glutathione, sodium thiosulphate, sodium diethyldithiocarbamate (Naddtc), 2-mercaptoethanesulfonate (mesna) and amifostine.[20]

These disadvantages have provided the impetus for the development of new and improved platinum antitumour drugs and these have mainly focused on the development of new derivatives that display altered pharmacokinetic and pharmocodynamic properties. The methods used in synthesizing new platinum drugs that display antitumuor activity have

adhered to a set of structure activity relationships that were developed by Cleare and Hoeschele.[9,11] These can be summarized as follows:

1. The first structure-activity relationship revealed that the *cis* isomers of both $Pt(NH_3)_2Cl_2$ and $Pt(NH_3)_2Cl_4$ uniquely interfered with the cell division in *E. coli*, but the equivalent *trans*-isomers (*Figure 1.3*) were ineffective.

cis-[Pt(NH₃)₂Cl₂]

cis-[Pt(NH₃)₂Cl₄]

trans-[Pt(NH₃)₂Cl₂]

trans-[Pt(NH₃)₂Cl₄]
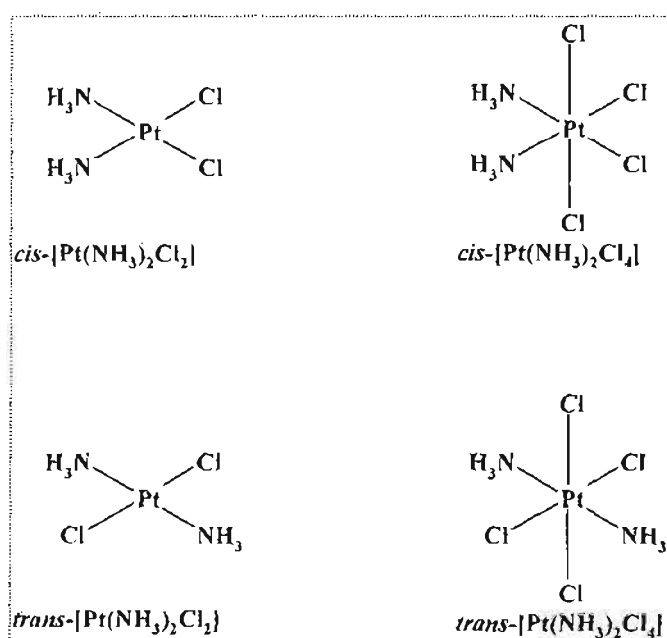
Figure 1.3:   *Structures of the original platinum complexes studied for antibacterial and antitumour activity.*

2. The leaving group, *X*, should be anionic with intermediate binding strength to platinum and must exhibit a weak *trans*-effect to avoid labilization of the amine moiety, *e.g.* Cl^- or SO_4^{2-}. Complexes with other leaving groups such as NO_3^-, have been found to be highly toxic, whilst those with inert leaving groups have been shown to be inactive.

3. The amine group in the form of a monodentate or bidentate ligand, should possess at least one N-H moiety, which whilst still not fully understood, is thought to play a role in hydrogen bonding interactions with the DNA fragment.

Altering the structure of the leaving group of cisplatin to less labile leaving groups appears to influence tissue and intracellular distribution of the platinum complexes and improve the drugs toxicity profile, whilst the more stable (carrier) amine group usually determines the structure of the adduct formed upon interaction with DNA, believed to be the ultimate target for antitumour activity.

Therefore, adducts produced by cisplatin and most of the classical platinum analogues are identical, and this explains their very similar patterns of tumour sensitivity and susceptibility to resistance. An important question in platinum-based anticancer chemotherapy and biology is whether the original structure-activity relationships adequately describe the range of complexes with useful antitumour activity. Complexes that are structurally unique to cisplatin may be processed in a different manner by the cells.

1.3.1 Mechanism of action of cisplatin

Cisplatin reacts with many cellular components that have nucleophilic sites such as deoxyribo nucleic acid (DNA), ribo nucleic acid (RNA), proteins, membrane phospholipids, cytoskeletal microfilaments and thiol containing molecules.[21] Currently, the cellular target for platinum complexes is generally accepted to be DNA. Approximately 1% of the total cellular platinum binds to DNA, inducing various types of inter- and intra-strand cross-links (*Figure 1.4*).[22]

Cisplatin reacts preferentially with DNA (*Figure 1.5*) by coordination to the N7 atoms of purine nucleobases, which are exposed in the major groove of the double helix and are not involved in base-pair hydrogen bonding. The resulting adducts may be grouped into one of six categories *viz.*[23-25]

-    1,2-intrastrand d(GpG)[†] adducts between an adjacent guanines;
-    1,2-intrastrand d(ApG)[‡] adducts between an adjacent guanine and adenine;
-    intrastrand adducts between purines separated by one or more intervening bases;
-    interstrand adducts linking the two strands of the DNA double helix;
-    monofunctional adducts coordinated to a single purine and

---

[†]   *Platinum bound to two adjacent N7-guanine sites.*
[‡]   *Platinum bound to the N7 atoms of adjacent adenine-guanine sites.*

- protein-DNA cross links where cisplatin coordinates a protein molecule and a nucleobase.

Up to 90% of total platinum-DNA adducts comprise of 1,2-intrastrand cross-links involving adjacent bases, with the most frequent adduct being the 1,2-intrastrand cross-link involving two adjacent guanines. This adduct is *ca.* 2-3 times more frequent than 1,2-intrastrand d(ApG) adducts between an adjacent guanine and adenine. All types of DNA cross-links exert distorting effects on DNA, which have been extensively studied in double-stranded oligonucleotides.[8]

MONOFUNCTIONAL   **INTRASTRAND**

INTERSTRAND   **INTERMOLECULAR**
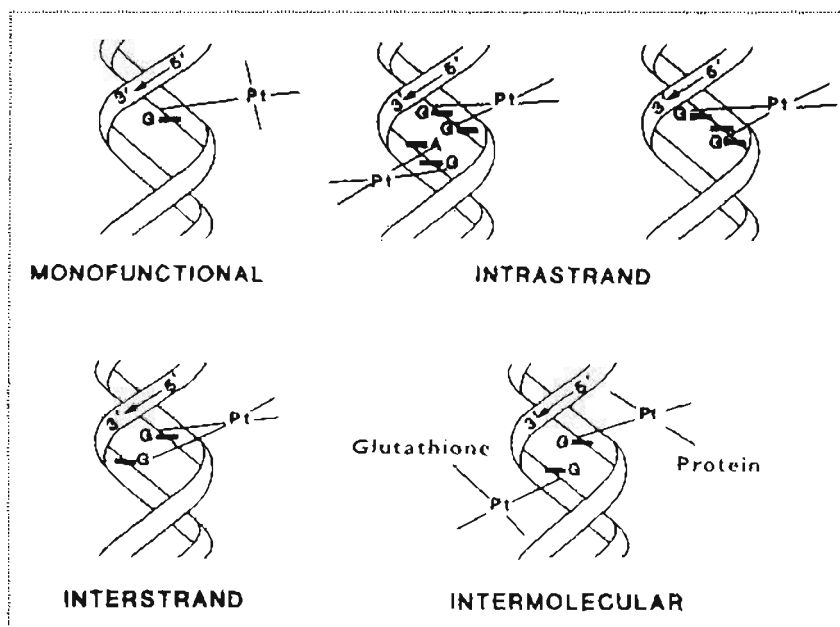
Figure 1.4: <u>Diagram illustrating the main adducts formed during the interaction of cisplatin with DNA.</u>[26]
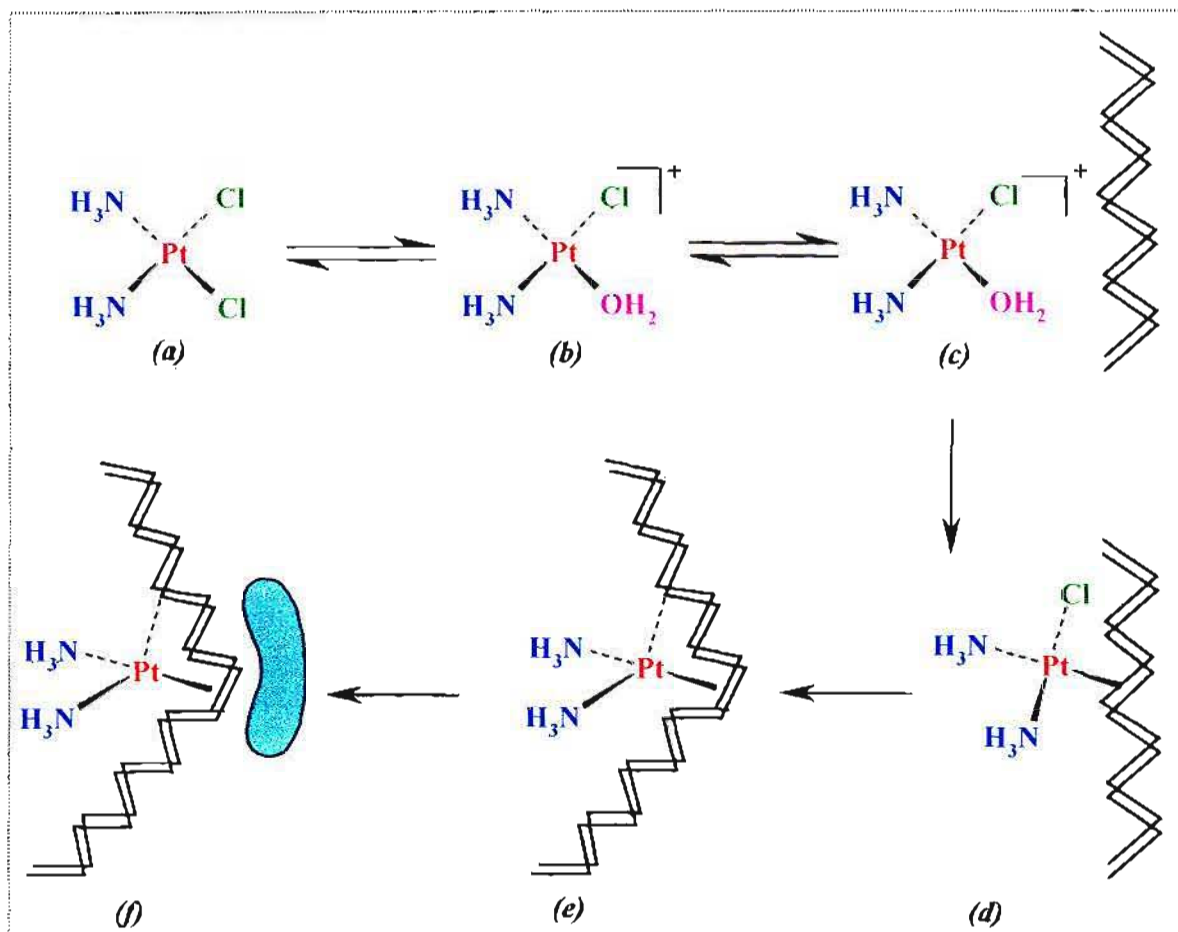
Figure 1.5: *The sequence of events in cisplatin binding to DNA.*[25]

The consequences of these cross-links to the cell and how they bring about cell death remain unknown. However, results to date in numerous cell lines suggest that cisplatin-damaged DNA causes cell-cycle perturbation, an arrest in the G2-phase (a second gap or growth phase which is the period between the completion of DNA synthesis and mitosis) to repair damage, and in the absence of adequate repair, the cells eventually undergo an abortive attempt at mitosis that results in cell death via an apoptotic mechanism (*Figure 1.6*).[26-29] It has been suggested that the G2 arrest is due to inhibition of transcription of genes essential for passage mitosis. High concentrations of cisplatin may also induce an S phase (synthesis phase where DNA synthesis occurs) arrest followed by apoptosis instead of just slowing progression to the G2 phase. However, it still remains unknown as to which of these above mentioned cellular effects trigger the apoptotic pathway and knowledge of the signal transduction pathways involved in cisplatin-induced apoptosis is far from complete.

Cisplatin

Cell Survival

DNA damage

$p53^+$ or $p53^-$

$p53^+$

recovery

G1 phase   S phase   G2 phase

lethal mitosis

Cell cycle arrest and repair

APOPTOSIS
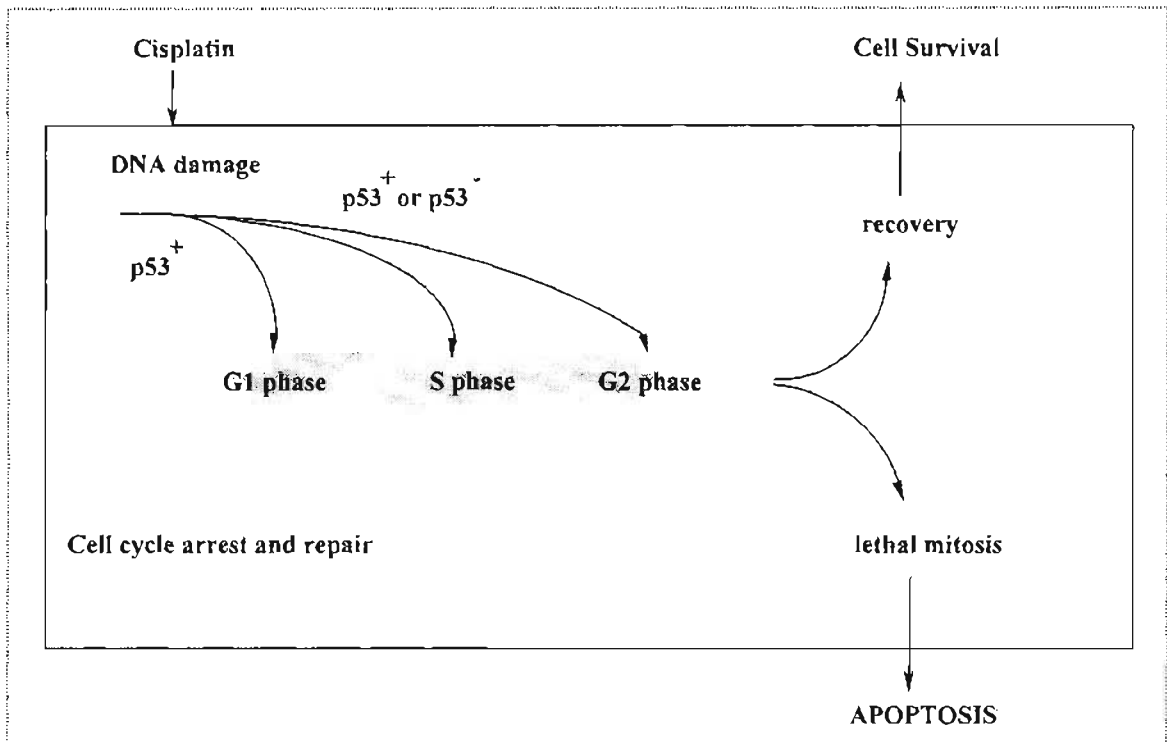
Figure 1.6: *The cell-cycle perturbations that occur as a consequence of DNA damage induced by cisplatin. The gray box represents the period during which cells arrest at various phases of the cell cycle with the intent to repair the damage. [p53 is a protein that mediates cell cycle arrest and may also protect cells from apoptosis. G1 represents a gap or growth phase, which is the period between mitosis and the start of DNA synthesis]*

1.3.2 Mechanism of Cisplatin Resistance

The occurrence of resistance is a common drawback of cancer chemotherapy, and cisplatin is no exception. Moreover, the patterns of resistance vary considerably between tumour types. The degree of resistance responsible for these relapses is usually of the order of 2-4 fold, which may not appear to be very high. But for cisplatin, which is routinely used in dosages at the limit of its systemic cytotoxicity, these levels of resistance can completely eliminate clinical effectiveness. In addition to the development of acquired resistance, some tumours such as colorectal cancer and nonsmall lung cell cancer (NSCLC) are predominantly sensitive to cisplatin treatment.

With a better understanding of how cisplatin exerts its antitumour effects, much insight into mechanisms of resistance to cisplatin has been gained from preclinical laboratory-based investigations using different cancer cell lines. Cellular resistance to cisplatin is multifactorial and has been reviewed in detail.[30-32] Two broad causes of resistance has been observed:-

- prevention of adequate amounts of the drug from reaching and binding to its cellular target, DNA;[33,34]
- a failure of cell death occurring after binding of platinum to DNA.[35]

More specifically, these mechanisms of resistance are believed to include one of the following and can be represented schematically by *Figure 1.7*:[30,31]

- reduced platinum accumulation;
- increased cytoplasmic detoxification by glutathione and/or metallothioneins;
- increased DNA repair (mainly through NER machinery) and/or tolerance of platinum-DNA adducts and;
- overexpression and mutation of other genes.

Reduced Pt accumulation and increased cytoplasmic detoxification by glutathione and metallothioneins represent the major causes of inadequate drug concentrations reaching DNA. Once DNA binding has occurred, resistance mechanisms include increased DNA

repair of adducts, and an ability to tolerate greater levels of DNA damage with concomitant failure to engage programmed cell death pathways. The elucidation of these major biochemical mechanisms of resistance has been critical in providing a basis for the development of platinum-based compounds capable of circumventing cisplatin resistance.
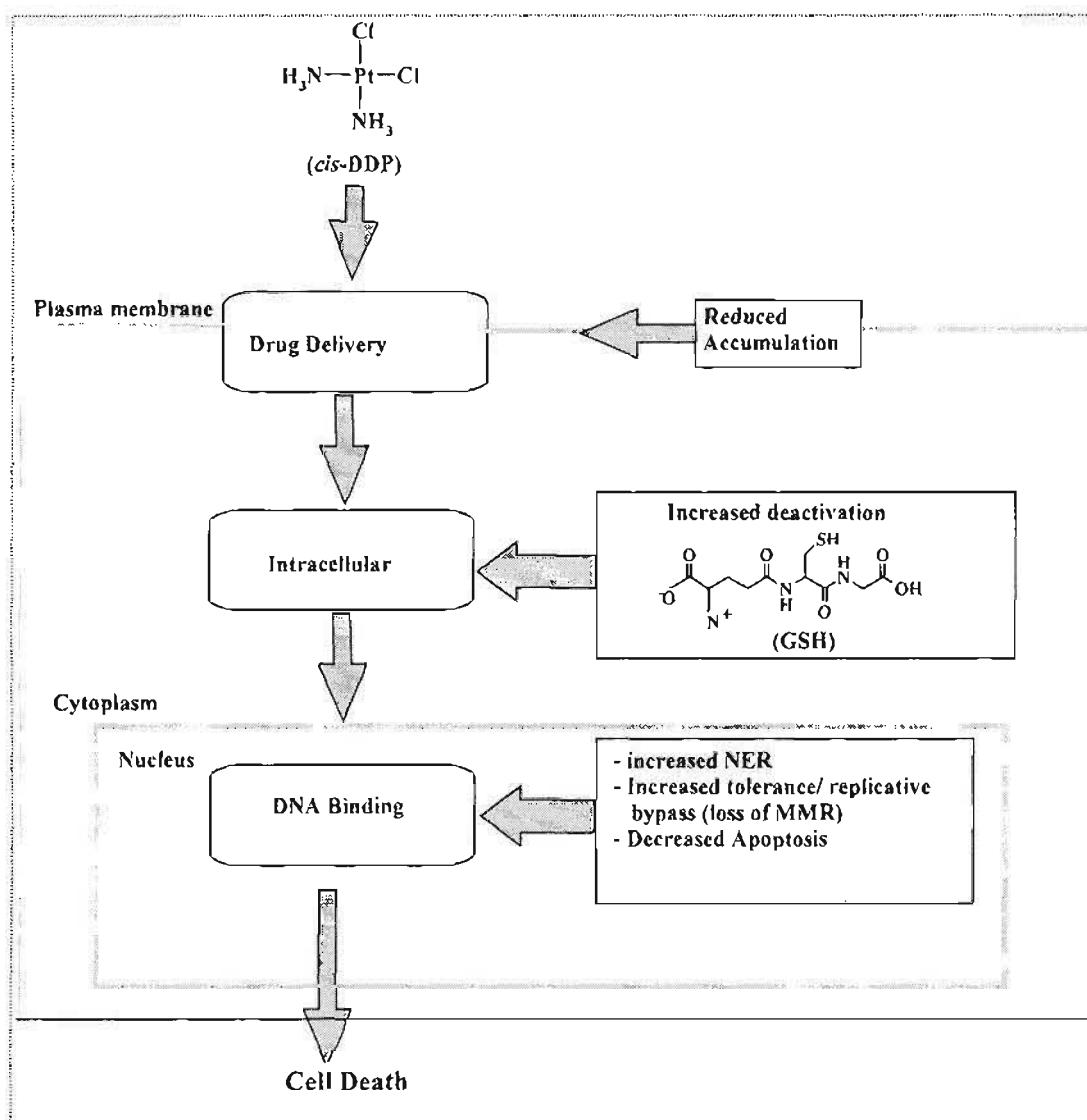
Figure 1.7:   *Schematic drawing of the major biochemical mechanism of resistance to cisplatin. Resistance mechanisms may operate prior to or after binding of cis-DDP to DNA. MMR = mismatch repair; NER = nucleotide excision repair; GSH = glutathione.*[12]

1.3.3 DNA-Repair Mechanism

The mechanism of cisplatin-induced DNA damage towards cell killing is beginning to be disentangled. Previously, cisplatin cytotoxicity was thought to be the result of cisplatin inhibition of DNA synthesis. However, DNA-repair deficient cells die at concentrations of cisplatin that do not inhibit DNA synthesis. Moreover, DNA repair-proficient cells survive at concentrations of cisplatin high enough to inhibit DNA synthesis and arrest the cell in the S phase.[27] Therefore, cisplatin-induced cell death does not always correlate with inhibition of DNA synthesis. Evidence gathered recently, has indicated that the mechanism whereby cisplatin can kill cells is via apoptosis.[28,29] Apoptosis is an ubiquitous, genetically regulated cell mechanism of active cell death that is conserved in multicellular organisms.[36-38] It has unique morphological and biochemical features that include cell shrinkage, blebbing[†] of the cell surface, loss of cell-cell contact, chromatin condensation and fragmentation.

The specific mechanism that triggers apoptosis in response to cisplatin still remains undefined. Logically, such mechanisms must include ways to detect damage as well as to determine whether or not the damage is severe enough to be lethal. Much attention has therefore been focused on identification and characterization of proteins that recognize cisplatin-induced DNA damage.[39] Currently, several families of protein are implicated as being important. These include:

- Nucleotide excision repair (NER) proteins;
- Mismatch repair (MMR) proteins;
- DNA-dependent protein kinase (DNA-PK) and
- High-mobility group (HMG) proteins.

[†]   *An elevation in the skin filled with a serous fluid.*

1.4 The Second Generation: Carboplatin and its Analogues

To date, only one of the second generation platinum compounds (*Figure 1.8*), *cis*-diammine-1,1'-cyclobutanedicarboxylatoplatinum[II] (*carboplatin*) has received worldwide clinical acceptance. Carboplatin exhibits reduced side effects, with myelosuppression being dose limiting.[40,41] Whilst the lower toxicity of carboplatin has facilitated its worldwide approval and use, it is however, only active against the same tumour lines as cisplatin.[42] Therefore, it may be deduced that the discovery of carboplatin has somewhat made platinum based chemotherapy safer, but its spectrum of activity remains very similar to that of cisplatin. More importantly, the problems of intrinsic and acquired cisplatin resistance persist.[43,44]

In recent years, two other second-generation drugs have been developed and approved for several indications in certain countries. These include, *cis*-diammineglycolatoplatinum[II] (*nedaplatin*), which has received approval in Japan and *trans*-L-Diaminocyclohexane)oxalatoplatinum[II] (*oxaliplatin*) has received approval for clinical use in Europe, China and the United States, both of which have been shown to exhibit improved toxicological properties compared to that of cisplatin.

(1)

diamine-[1,1-cyclobutanedicarboxylato(2-)]-*O,O'*-platinum[II]

carboplatin

(2)

(*trans*-L-diaminocyclohexane)oxalatoplatinum[II]

oxaliplatin

(3)

cis-diamine-glycoloato-*O,O'*-platinum[II]

nedaplatin
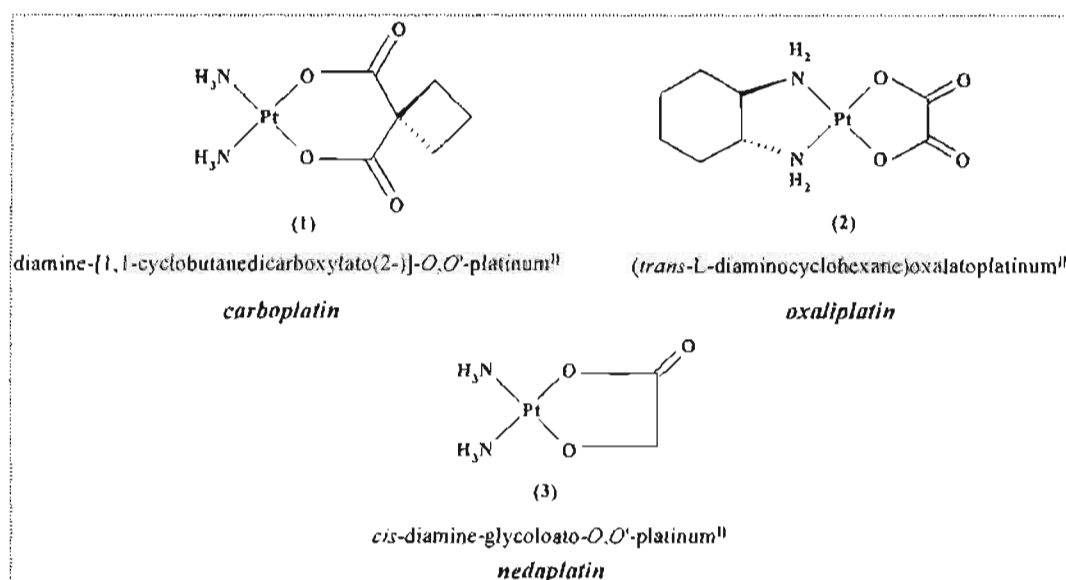
Figure 1.8:   *Second generation platinum-based antitumour drugs currently being used in the treatment of cancer.*

1.5 *Nonclassical Platinum Antitumour Agents: Perspectives for Design and Development of New Drugs Complementary to Cisplatin.*

An important question in platinum antitumour chemistry is whether the original structure-activity relationships adequately describe the range of complexes with useful antitumour activity. Cells may process complexes that are structurally different from cisplatin in an entirely different manner. The determining factors of cytotoxicity may therefore not follow the same patterns as found by cisplatin and its analogues. Besides affecting cellular uptake and interaction with biomolecules such as glutathione, the lesions induced in DNA will be different from those of cisplatin. Altered DNA binding and conformational changes may affect inhibition of DNA synthesis and / or differential repair of the drug-DNA lesion. The binding of GSH or other thiols to platinum may also be modulated by steric effects. This warranted a new approach to the design of Pt drugs that can circumvent cisplatin resistance by developing compounds that are capable of forming radically different Pt-DNA adducts to current platinum drugs.

In recent years the antitumour activity of a number of well-defined platinum complexes differing in structure from the parent cisplatin have been reported.[43] The fact that these complexes have shown antitumour activity serves as an indication that cisplatin-like lesions are *not* unique arbiters of cytotoxicity and antitumour activity. What is important however, is to examine how radically different are the mechanisms of action of these compounds as compared to that of the parent drug. The biological consequences of these new mechanisms in terms of spectrum of antitumour activity, especially activity in cisplatin resistant lines is also important.

At least four series have been recognized that violate the empirical structure-activity relationships for platinum antitumour drugs *viz*:[45]

- Dinuclear bis(platinum) Complexes: To this endeavour Farrell[46] and co-workers have successfully synthesized multinuclear complexes with bridging ligands, particularly dinuclear platinum complexes with the general formula

[{PtCl$_2$(NH$_3$)$_2$}μ-H$_2$N-R-NH$_2$]Cl$_2$ (where R is a linear or substituted aliphatic linker), that has exhibited activity against both cisplatin-sensitive and cisplatin resistant cells. These complexes are one of the very first class of antitumour agents based on the dinuclear family.

- Complexes of formula trans-[PtCl$_2$(py)$_2$] (where py = pyridine) are more cytotoxic than their cis counterparts, and, in fact, demonstrate equivalent activity to cisplatin in tissue culture.[47] The presence of the planar ligand dramatically enhances the cytotoxicity of the trans complexes.

- Cationic Complexes: Two series of cationic complexes have been reported with antitumour activity. The general structures are [PtCl(R'R"SO)(diam)]NO$_3$][48] and cis-[PtCl(NH$_3$)$_2$amine]$^+$ (amine = pyridine or pyramidine).[49] In the case of asymmetrical sulfoxides, such as methyl-p-(tolyl)sulfoxide)MeTolSO), preparation of the optically pure forms demonstrated a distinct effect of chirality of the sulfoxide ligand on the biological activity.

- the ability to alter the type of antitumour activity is demonstrated by complexes containing redox active ligands such as nitroimidazoles in cis and trans-[PtCl$_2$(NH$_3$)(NO$_2$Im)], which, in contrast to cisplatin, are more cytotoxic in hypoxic cells than in air.[50]

1.5.1 Activation of the trans Geometry in Platinum Complexes

The paradigm of structure-activity relationships of platinum antitumour complexes is that the trans geometry is therapeutically inactive. An important point to remember is that trans-DDP is cytotoxic, albeit much reduced in comparison to the cis isomer. Possible explanations for the differences observed in cytotoxicity can be accounted for by the fact that cis compounds form platinum-DNA adducts that inhibit DNA replication to a greater extent than those formed from trans-DDP[51,52], or alternatively, that DNA adducts formed by the trans compounds may be repaired more rapidly.[53] Sequencing studies and adduct analysis[54] of DNA modified by trans-DDP show a preference for GC (guanine-cytosine) crosslinking in comparison to cis-DDP. The trans isomer also produces bidentate adducts

on DNA, such as a 1,3-intrastrand crosslink, which are assumed to account for its cytotoxicity. The structures of the d(GpTpG)[55] and d(GpCpG)[56] adducts have been characterized by nuclear magnetic resonance studies. The intervening base (C or T in the above studies) is destacked and "bulged out", this feature may contribute significantly to disruption of the DNA helix. The monofunctional *trans*-DDP-DNA intermediate is longer lived than its *cis*-DDP analogue and may react readily with glutathione, preventing closure to the bidentate lesion.[57,58]

It has been reported that the presence of a planar ligand such as pyridine greatly enhances the cytotoxicity of the *trans*-structure, such that its cytotoxicity is equivalent to its *cis* isomer and indeed cisplatin itself. This feature has been shown to be the general property of complexes with planar ligands, as exemplified by the structural classes shown in *Figure 1. 9*.

The cytotoxicity of *trans* complexes containing planar ligands is highlighted by a remarkably low resistance factor in both murine and human tumour cisplatin-resistance cell lines (*Table 1.2*). These trends are further confirmed by results from the ovarian carcinoma panel of Harrap[43], where the pattern of activity and indeed range of cytotoxicity are remarkably different from those of the clinically used agents.[59]

trans-[PtCl₂(py)₂]   trans-[PtCl₂(NH₃)(quin)]   trans-[PtCl₂(R'R"SO)(quin)]

R' = Me, R" = Me, Ph, Bz
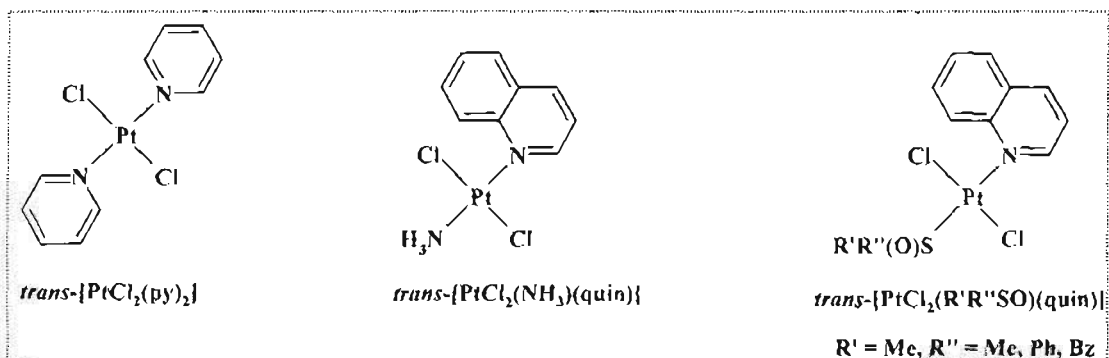
Figure 1.9:   *Structures of trans-platinum complexes with cytotoxicity equivalent to that of cis-DDP.*

Table 1.2: *Cytotoxicity of Selected trans-Platinum[11] Complexes in L1210 Leukemia Cells.[45]*

	ID_{50} (μM)		
Complex	*L1210/0[†]*	*L1210/DDP[‡]*	*L1210/dach[ſ]*
trans-[PtCl₂(py)₂]	1.20	1.1 (0.92)	2.26 (1.88)
trans-[PtCl₂(Tz)₂]	1.60	7.4 (4.63)	5.96 (3.73)
trans-[PtCl₂(Me₂SO)quin]	0.36	0.38 (1.06)	0.39 (1.08)
trans-[PtCl₂(NH₃)quin]	0.51	1.35 (2.65)	0.96 (1.88)
Cisplatin	0.33	9.22 (28)	1.81 (5.48)
trans-[PtCl₂(NH₃)₂]	15.7	22.0 (1.40)	1.6 (1.25)
[Pt(R,R-dach)SO₄]	0.23	0.75 (3.26)	5.65 (25)

The following features may be extracted from these data:[45]

- in tissue culture *trans*-platinum complexes with planar ligands may be equally cytotoxic as cisplatin and dramatically more so than *trans*-[PtCl₂(NH₃)₂];

- *trans*-platinum complexes give a different pattern of cytotoxicity in comparison to cisplatin;

- replacement of NH₃ by pyridine even in *cis*-PtCl₂(amine)₂ causes a large change in tumour specificity.

[†] *L1210/0:* Sensitive to most types of platinum compounds.

[‡] *L1210/DDP:* Resistant to platinum compounds with the ethylenediamine (en) carrier ligand but sensitive to those with the diaminocyclohexane (dach) ligand.

[ſ] *L1210/DACH:* Resistant to dach-Pt compounds but sensitive to en-Pt compounds.

1.5.2 Bi-functional Platinum Centres

The synthesis of multi-nuclear complexes was initially based upon the linking of two cisplatin like centres as shown in *Figure 1.10*.[60-66] The first complex developed $(2,2/c,c)^{\dagger}$ (1) was a simple cisplatin derivative with two cisplatin units linked by a flexible diamine chain.[46,64] This was in keeping with the traditional structure activity rule, of a neutral complex consisting of a square planar platinum with two *cis*-chloro ligands and with at least one amine group. The replacement of the chloro ligands with malonate (2) to improve water solubility, resulted in a series of 2,2/c,c complexes with good activity in cisplatin resistant cancer cell lines. Whilst these complexes are capable of binding DNA in a manner similar to that of cisplatin, GpG intrastrand cross-links, they were also capable of forming longer-range intra- and interstrand adducts.[46] Mechanistic studies have demonstrated that the 2,2/c,c complexes produce a high percentage of interstrand adducts.[46]
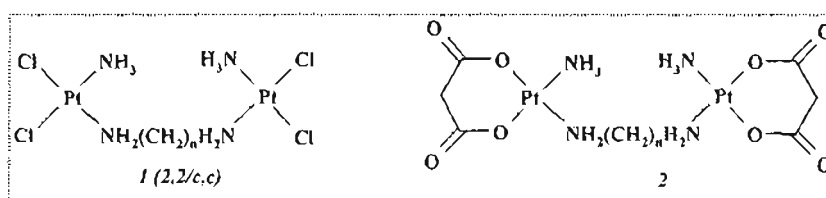
Figure 1.10: **Dinuclear platinum complexes containing two linked cisplatin centres, where n = 2-6.**

An approach similar to this was adopted by Broomhead[61-63] and coworkers, who linked two cisplatin centres together with a 4,4'-dypyrazolylmethane (dpzm) ligand. A series of double bridged dinuclear complexes with either a square planar or octahedral structure have been synthesized and tested for anticancer activity, both in vitro and in vivo (*Figure 1.11*, 3-7).[61-63] This series was thereafter extended to single bridged dinuclear complexes, with either two chloro/DMSO ligands present on each platinum centre (*Figure 1.12*, 8-11).[67-69]

---

† *System of abbreviations adopted whereby the numbers represent the number of chloride leaving groups on each platinum centre, whilst the lettering refers to the geometry of the leaving group with respect to the nitrogen on the bridging diamine.*

1-20
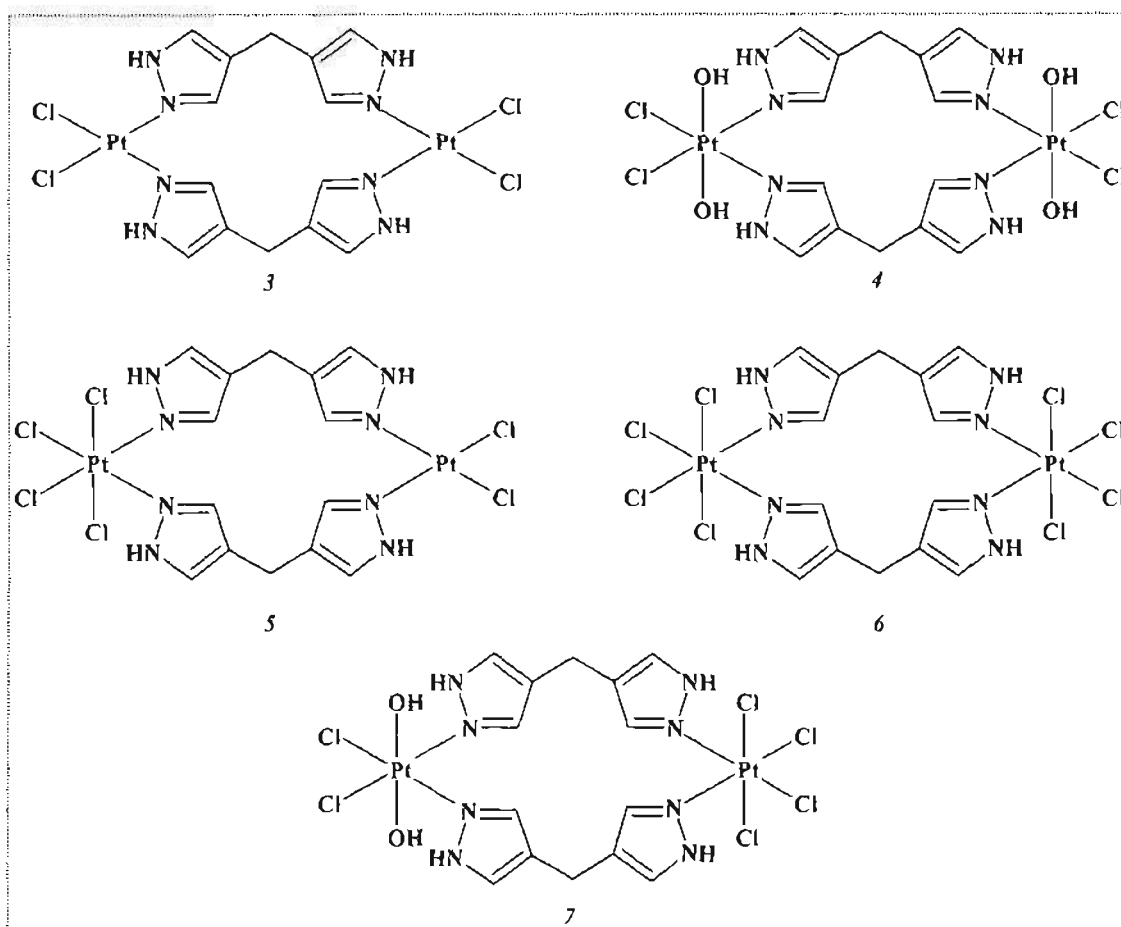
Figure 1.11: <u>*Double bridged, multi-nuclear platinum complexes linked by the 4,4'-dipyrazolylmethane (dpzm) ligand synthesized by Broomhead*</u>[61-63] <u>*and co-workers.*</u>
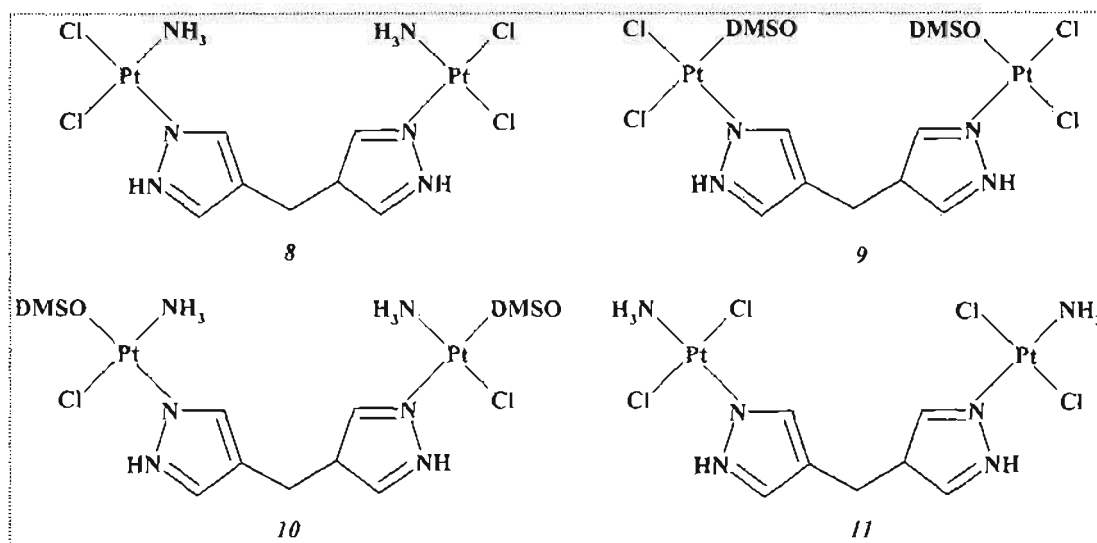
Figure 1.12: *Singularly bridged, multi-nuclear platinum complexes linked by the 4,4'-dipyrazolylmethane (dpzm) ligand.*[61-63]

1.5.3 Mono-functional Platinum Centres

Whilst the synthesis of dinuclear complexes with two bi-functional centres resulted in complexes that could bind to DNA in a different manner than cisplatin, the most important development was the subsequent synthesis of dinuclear complexes that contained mono-functional platinum centres (*Figure 1.13*, 12-16).[46,70-82] The first complexes called 1,1/t,t (12) and 1,1/c,c (13) represented a truly new class of metal-based anticancer compound, as these were cationic complexes containing one chloro leaving group on each platinum centre.

The 1,1/t,t series, for example BBR3005 (14), was identified as having the most promising pattern of antitumour activity as well as DNA binding. Complexes with improved DNA affinity for long range cross-linking were also accomplished through the incorporation of a third platinum centre with the alkane diamine chain such as BBR3464 (16). The overall charge of 4$^+$ combined with the presence of at least two platinum coordination units capable of binding to DNA, and the consequence of such DNA binding is a remarkable departure from the cisplatin structural prototype. BBR3464 (16) represents a highly promising agent, where in preclinical studies, it exhibited a complete lack of cross-

resistance to cisplatin resistant cell lines.[83,84] It is also more potent than cisplatin *in vitro* in an osteosarcoma cell line.[85]

$$12\ (1,1/t,t)$$ $$13\ (1,1/c,c)$$ $$14\ (1,2/t,c)$$ $$15\ (1,2/c,c)$$ $$16\ (1,0,1/t,t/t)$$
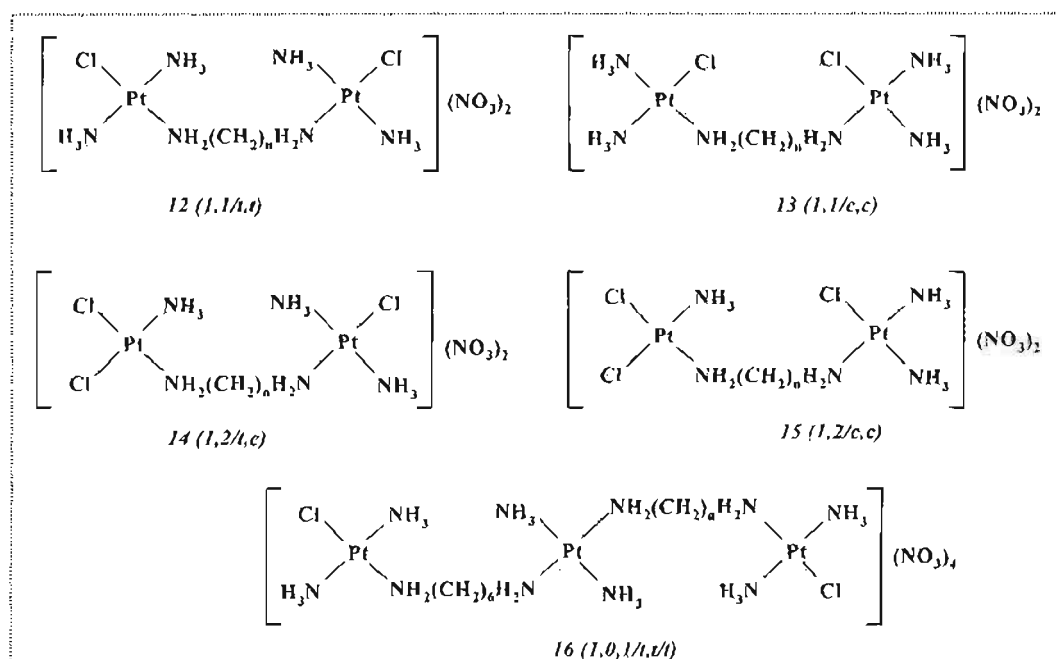
Figure 1.13: **The range of dinuclear platinum complexes synthesized by Farrell and co-workers[65], that contain charged mono-functional platinum centres.**

The DNA binding profiles of the multinuclear compounds differ significantly from that of cisplatin with both the 1,1/t,t (**12**) and 1,1/c,c (**13**) complexes showing some differences amongst themselves (*Figure 1.14*).[86] The limiting modes of reaction of bis-platinum complexes are highly dependent on the structure of the complex. Upon initial monodentate binding, further reaction may result in a series of structurally distinct adducts including:

- DNA (Pt, Pt) interstrand cross-links by binding of one of Pt atom to each strand of DNA;[87]
- (Pt, Pt) intrastrand cross-links by binding of the two Pt atoms to the same strand;[88]
- *cis*-DDP-like intrastrand cross-links from one bidentate unit of a bis(Pt) complex as well as DNA-protein crosslinks.

(Pt,Pt) Intrastrand Cross-link   (Pt,Pt) Interstrand Cross-link
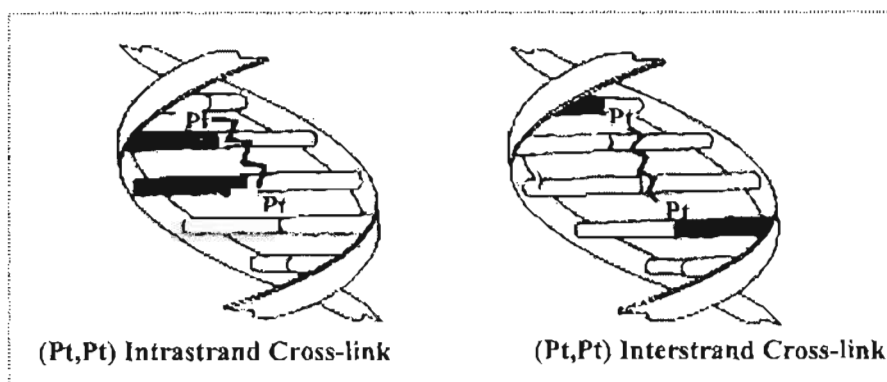
Figure 1.14: *Schematic binding modes for dinuclear bifunctional DNA-binding compounds. The 1,1/t,t geometry forms both types of adducts whereas the 1,1/c,c geometry forms only interstrand cross-links.*[86]

In a different approach, Komeda *et al.*,[81,82] produced a series of pyrazole linked complexes (*Figure 1.15*, **17-19**). These pyrazole linked complexes were synthesized to mimic cisplatin binding without the major DNA kinking. The distance between the two platinum centres is similar to the distance between two sequential G bases in B-type DNA. These complexes were synthesized in the hope that upon binding to DNA the DNA helix would remain intact.
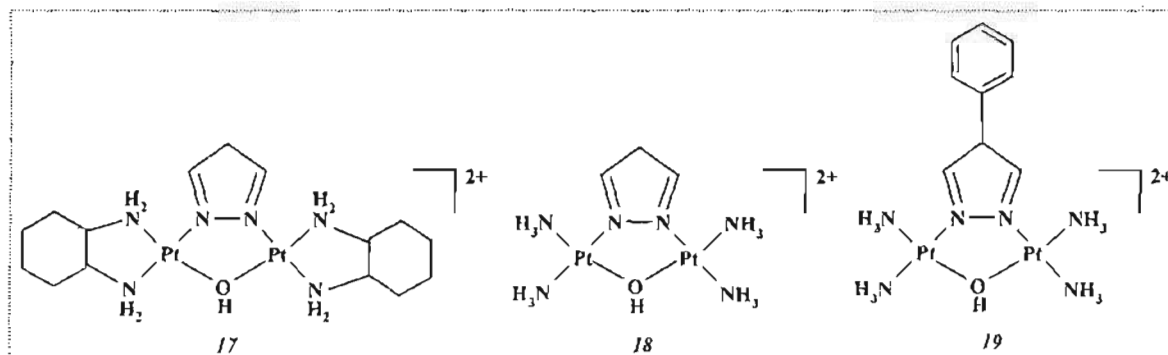
Figure 1.15: *The dinuclear pyrazole linked complexes of Komeda* [81,82] *et al., designed to mimic the binding of cisplatin to sequential G bases of DNA.*

1-24

1.5.4 Complexes Incorporating Cationic and Hydrogen-Bonding Linking Ligands.

The development of trinuclear as well as dinuclear complexes linked with polyamine ligands that incorporate charge and hydrogen-bonding functionality into the bridging ligand further increased the multinuclear series (*Figure 1.16*, **20-22**).[46,64,65] The amine groups of the polyamine linkers, or the central platinum centre, provide groups capable of hydrogen bond formation with DNA atoms such as the O6 or O3 of guanine and thymine respectively. These complexes exhibit excellent water solubility, which is good for the administration of the drug. More importantly whilst the dinuclear complexes shown in *Figure 1.13* exhibit cytotoxicity at micromolar concentrations, some of these complexes (**20-22**) are active at nanomolar concentrations.[60]

20 (BBR3464)

21 (BBR3571)

22 (BBR3610)
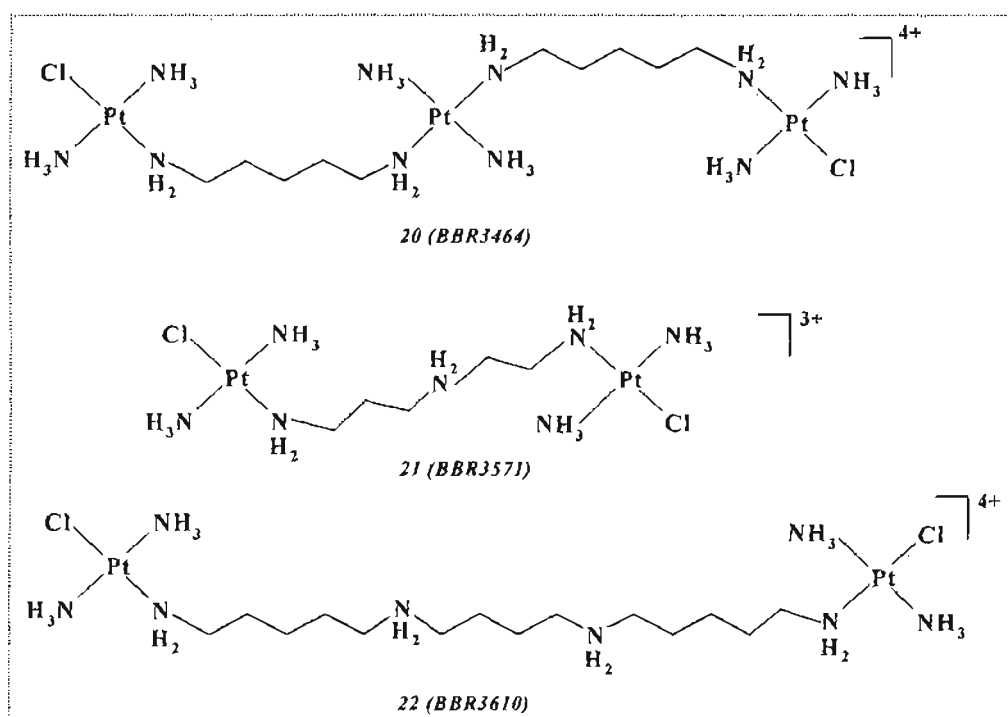
Figure 1.16: *A selection of multi-nuclear platinum complexes, synthesized by Farrell and co-workers[46], that incorporate hydrogen-bonding capacity and charge into the linker.*

1-25

1.6   DNA Interactions of Bis(Platinum) Complexes

Upon initial monofunctional binding, further reaction of the second platinum site may lead to a series of structurally distinct adducts including:

-   DNA (Pt, Pt) interstrand cross-links by binding of one Pt atom to each strand DNA;
-   (Pt, Pt) intrastrand cross-links by binding of the Pt atoms to the same strand as well as DNA-protein cross-links.

The DNA binding modes shown in *Figure 1.17* are minimal in the sense that they require only leaving group (chloride) on each Pt atom. A fully reacted bis(platinum) complex with *cis*-DDP like coordination spheres are in fact tetrafunctional. In situations of this nature, the second step of binding to DNA is important because a competition arises between the formation of (Pt, Pt) interstrand cross-links or a cisplatin-like intrastrand adduct by preferential reaction of one *cis*-Pt unit (*Figure 1.18*). A summary of the binding preferences and conformational changes in bis-(Pt)-DNA interactions are presented hereafter.

(Pt, Pt) Intrastrand
Cross-link

(Pt, Pt) Interstrand
Cross-link

(Pt, Pt) DNA-Protein
Cross-link

(Pt, Pt) DNA-Protein
Cross-link
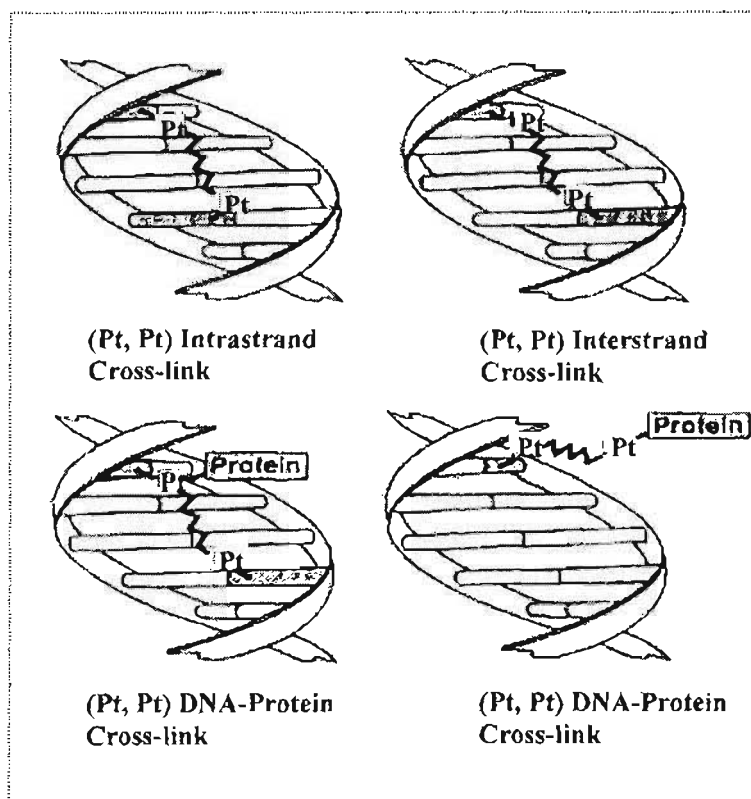
Figure 1.17: *Schematic limiting modes for possible DNA-DNA and DNA-protein cross-linking induced by dinuclear platinum complexes.*[89]

— Monodentate
--- Intrastrand (cis-Pt)
····· Interstrand (Pt,Pt)
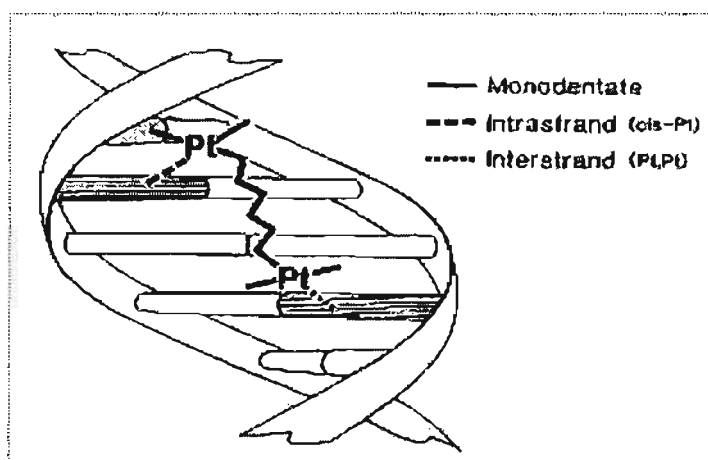
Figure 1.18: *Schematic demonstration of competitive binding of a dinuclear platinum complex containing bifunctional coordination spheres. Formation of the first Pt-purine bond, results in a competition being set up between the cis-DDP like intrastrand cross-link formation and the (Pt, Pt) interstrand cross-link. Suitable modification of coordination sphere or backbone may affect the reaction pathways.*[89]

1.6.1 Kinetics of Binding of Bis(Platinum) Complexes

Early studies have indicated that bis(platinum) complexes react faster than *cis*-DDP with DNA.[90] Sequencing studies have also shown binding to alternating purine-pyramidine GCGC runs.[46] The initial rates of reaction of bis(platinum) complexes with self complementary oligonucleotides 5′-aTATAGCGCATATAT-3′ (GCGC) and 5′-ATATATGGCCATATAT-3′ (GGCC) were calculated in order to determine the kinetic preferences between the two sequences. The GGCC oligonucleotide reacted faster than its GCGC counterpart with both the mononuclear and dinuclear platinum complexes. The bis(platinum) complexes are nevertheless, much more reactive with GCGC sequences than *cis*-DDP.[91] The presence of GCGC runs in many promoter sequences of DNA suggests that dinuclear complexes may be designed to specifically modify such regions. The kinetic results obtained indicate that the differences in antitumour activity between dinuclear and monomeric platinum complexes are dictated primarily by the nature of adducts formed within a similar sequence (*i.e.* GGCC) rather than different sequence specificity.

Recently, the kinetics and mechanism of formation of both the inter- and intrastrand cross-links formed by dinuclear complex [{*trans*-PtCl$_2$(NH$_3$)$_2$}$_2$-H$_2$N(CH$_2$)$_6$NH$_2$]$^{2+}$ was investigated[92] using [^{1}H, ^{15}N] HSQC NMR spectroscopy. It is taken that aquation is usually the rate determining step in the binding of Pt^{II} ammine complexes to DNA and the aqua ligands are more labile to substitution than hydroxo ligands, therefore it is important to understand the speciation profile of dinuclear complexes in aqueous solution. A generalized reaction scheme for the dinuclear complex is shown in *Scheme 1.1*.

CI/CI $\xrightleftharpoons{\;K_1,\;-Cl^-+H_2O\;}$ CI/H_2O $\xrightleftharpoons{\;K_2,\;-Cl^-+H_2O\;}$ H_2O/H_2O $\xrightleftharpoons{\;-2H^+\;}$ OH/OH

1 *2* *3* *6*

K_{a1} $\searrow\!\!\nearrow$ $-H^+$

K_{a2} $\searrow\!\!\nearrow$ $-H^+$ $-H^+$ $\nearrow\!\!\nwarrow$ K_{a3}

CI/OH

4

OH/H_2O

5
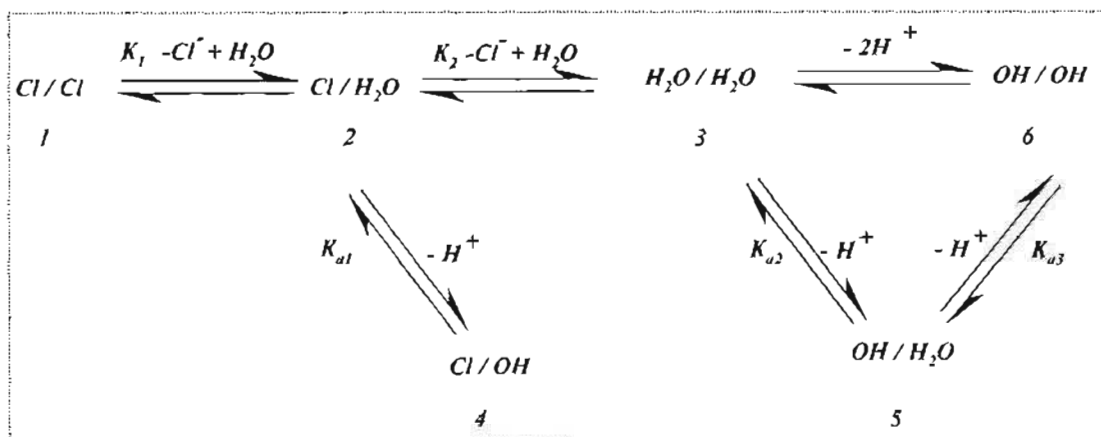
Scheme 1.1: *Schematic representation of mono- and di- aquation of [{trans-PtCl$_2$(NH$_3$)$_2$}$_2$-H$_2$N(CH$_2$)$_6$NH$_2$]$^{2+}$*

The study conducted using [^{1}H, ^{15}N] HSQC NMR spectroscopy could not distinguish between the {PtON$_3$} group of the aqua / chloro complex **2** as well as the diaqua complex **3**. However, given that the positively charged {PtN$_3$} groups are separated by a six carbon chain linker, it is reasonable to assume that the two platinum centres act independently of one another and the equilibrium constant for the second aquation step (K_2) will be similar to that of the first aquation step (K_1).[92]

1.6.2 *The (Pt, Pt) Intrastrand Cross-Link*

Studies detailing the (Pt, Pt) intrastrand cross-link were conducted using a combination of NMR studies on model dinucleotides, sequencing on oligonucleotides of defined sequence, and protein recognition of bis(platinum)-damaged DNA.

1.6.2.1 *NMR Studies on Model Dinucleotides*

The formation of a unique macrochelate formed by the reaction of d(GpG) and [{*trans*-PtCl(NH$_3$)$_2$}$_2$-H$_2$N(CH$_2$)$_6$NH$_2$]$^{2+}$ (1,1/t,t, n = 6)[88] has been reported and characterized using NMR spectroscopy. This structure represents a model for the (Pt, Pt) intrastrand cross-link and is the direct dinuclear analogue of the major intrastrand adduct of *cis*-DDP with DNA. The important features are a separation of 1.8 Hz for the two independent (5´ and 3´) H8 protons and a complicated NMR pattern for the H1 protons of

the sugar groups. Kinetic studies have shown that the rate of formation of the chelate is dependent on the chain length with n = 6 > 4 >2. The H(8) separation is also dependent on the chain length.[88]

1.6.2.2 *Sequencing of Bis(Pt)-DNA Lesions*

The assignment of intrastrand and interstrand cross-links produced by platinum complexes was aided by the development of a new assay taking advantage of the fact that $3' \rightarrow 5'$ exonuclease digestion of randomly platinated DNA produces a pool of fragments of different length.[93] Farrell *et al*[93] reasoned that termination of exonuclease activity prior to an interstrand cross-linking site would leave a fragment with complementary base pairs at the cross-linking site, which may act as a primer template for extension upon subsequent treatment with a DNA polymerase. Alternatively, degradation of intrastrand adducts will not produce fragments with complementary base pairs and the fragments will not act as templates for DNA replication. Using the properties of Pt-DNA adducts allowed for intrastrand links to be distinguished from the interstrand cross-linked fragments, and the formation of the (Pt, Pt) intrastrand cross-link in a 49-bp (base pair) duplex DNA was confirmed.[37]

1.6.2.3 *Conformational Changes Due to the (Pt, Pt) Intrastrand Cross-Link*

How similar is the (Pt, Pt) intrastrand cross-link to that of *cis*-DDP? A principle feature of the *cis*-DDP intrastrand cross-link is a kink or bend of the double helix toward the major groove.[94] Recent studies have implicated this conformational change as responsible for the recognition of *cis*-DDP-damaged DNA by the family of HMG proteins.[95,96] Molecular modeling has shown that the (Pt, Pt) intrastrand cross-links results in kinking due to the relative orientations of the two guanine bases. Interestingly enough, HMG proteins recognize DNA damaged by bis(platinum) complexes but not as efficiently as for *cis*-DDP-damaged DNA.[97] This protein recognition implies that the bisplatinum complexes induce the conformational changes similar to those that are induced by cisplatin.

1.6.3 *The (Pt, Pt) Interstrand Cross-Link*

cis-DDP, and indeed most alkylating agents, give rise to only 1,2-interstrand cross-links. In contrast, the sequencing work described above and in previous studies[93,98] suggests that both the length and flexibility of the diamine chain in dinuclear complexes allow the targeting of much larger DNA sequences for cross-link formation. For binding between guanines on opposite strands, in addition to 1,2 cross-links, 1,3 together with 1,4-DNA interstrand cross-links may also be formed.[93]

1.6.3.1 *Conformational Changes Due to the (Pt,Pt) Interstrand Cross-Link*

The differences between mononuclear and dinuclear complexes can further be illustrated if one considers the stabilization of Z-form DNA. Bis(platinum) complexes, more especially [{*trans*-PtCl(NH$_3$)$_2$}$_2$-H$_2$N(CH$_2$)$_6$NH$_2$]$^{2+}$, are particularly efficient at inducing the B → Z transition at poly(dG.dC)-poly(dG.dC).[99] The effect of different adduct structures on conformational changes within a similar sequence may be appreciated by the fact that *cis*-DDP stabilizes B-form poly (dG.dC)-poly(dG.dC).[100,101] Studies with a series of dinuclear complexes have delineated the mechanistic scheme for Z-DNA formation shown in *Figure 1.19*.[91,99] Of interest to note is that bifunctional binding is not a prerequisite for the B → Z transition. Instead, bifunctional binding or interstrand cross-linking "locks" the DNA in the left-handed conformation. In accordance with this, ethidium bromide does not reverse the Z-conformation caused by the interstrand cross-linking agents.

Pt—Pt + B—DNA $\xrightarrow{\text{(i)}}$ [Pt—Pt] [DNA] $z\ddot{u}$

| (ii)
↓

Pt\
 | >DNA $\xleftarrow{\text{(iii)}}$ Pt—Pt—DNA
Pt/

ziii   zii
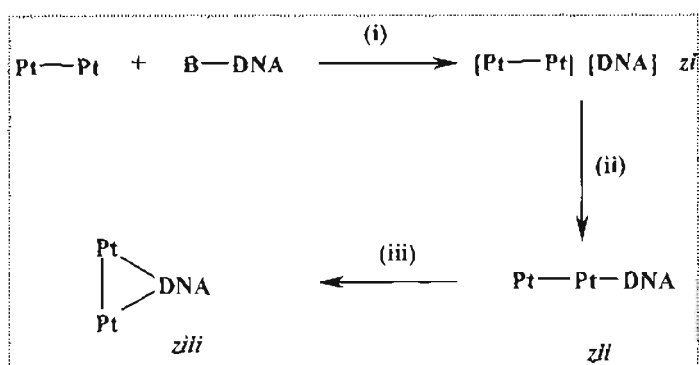
Figure 1.19:   *Proposed mechanism of Z-form DNA induction by dinuclear complexes. Z_i, Z_{ii} and Z_{iii} refer to different forms of left-handed DNA. Z_i is induced by purely electrostatic interactions from tetra-amine bis(platinum) cations and Z_{ii} is induced by monofunctional binding from only one Pt unit of a bis(platinum) complex and Z_{iii} is caused by covalent binding of the second Pt unit resulting in bifunctional binding on the polynucleotide. The cross-linked form Z_{iii} is irreversible.*[98]

1.6.4 Cross-Linking of Platinated DNA to Repair Proteins

The excision repair UVrABC complex[87,102] also recognizes bis(Pt)-DNA adducts formed either by tetrafunctional (2,2/c,c) or bifunctional (1,1/t,t) complexes. The polyfunctional nature of the bis(platinum) complexes suggests that the availability of multiple coordination sites   (> 2) could be used to induce covalent cross-linking of protein to platinated DNA. This possibility was confirmed for both the homodinuclear (Pt, Pt) and heterodinuclear (Pt, Ru) complexes using a radiolabeled 49 bp DNA fragment combined with native and polyacrylamide gel electrophoresis.[87] The DNA lesion responsible for efficient protein-DNA cross-linking is in all probability a DNA-DNA interstrand cross-link in which each metal atom is coordinated with one strand of the DNA helix as depicted in *Figure 1.20*. The cross linking efficiency is significantly greater than for mononuclear complexes such as *cis* and *trans*-DDP and suggests novel ways for designing specific DNA-protein cross-linking agents. The formation of ternary DNA-protein adducts could play an important role in the development of "suicide" agents capable of activating repair proteins as well as in the isolation of DNA-bound proteins from cells.
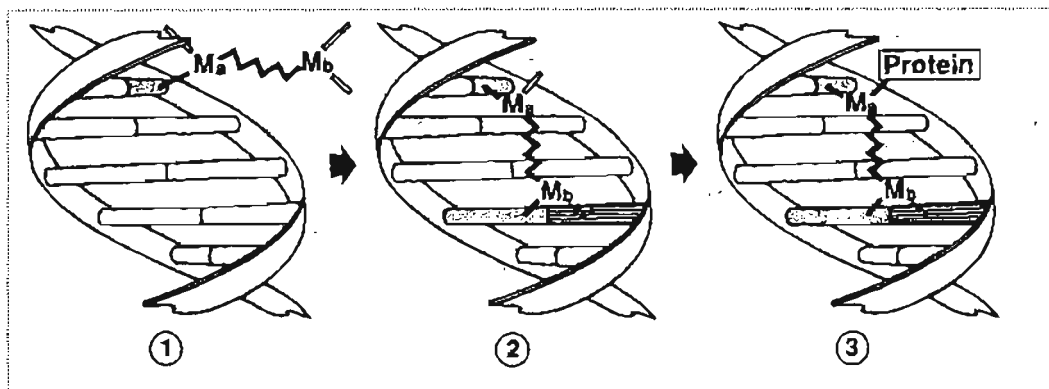
Figure 1.20:   *Scheme for formation of ternary Pt-DNA-protein cross-links. Cross-linking of*
          UvrAB proteins probably occurs via a pre-formed DNA-DNA interstrand cross-
          links (1 → 2 → 3). This mode of DNA-protein cross-linking is only available
          through a polyfunctional complex, such as the dinuclear complexes.[87,102]

1.7 Objectives of the Current Study

Multinuclear platinum complexes comprising of either di- or trinuclear platinum centres linked by variable length diamine chains constitute a new and discrete class of platinum-based anticancer agents.[103] Development of these complexes were driven by the hypothesis that complexes with distinctly different DNA binding mechanisms may exhibit unique biological activity in comparison to the current mononuclear clinically used agents.

Di- or trinuclear compounds exemplified by the structures presented in *Figure 1.21*, represent only one structurally distinct subclass of polynuclear platinum compounds, they are bifunctional platinating agents because only two Pt-Cl bonds are present. Their intrinsic difference are dictated by the separation between the two platinating centres and the overall charge on the molecule, that is caused by the presence of the extra "noncoordinating" tetraammineplatinum moiety.[92,103] These structures display biological activity that differs substantially from that of cisplatin.
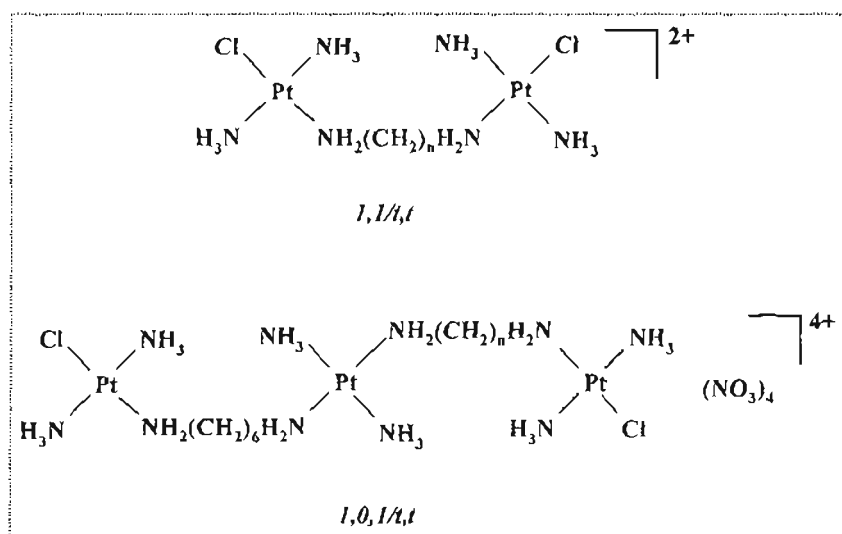
Figure 1.21: <u>General structure diagram for di- and trinuclear Pt complexes.</u>

There are several aspects of the DNA binding profiles of these complexes that are remarkably different to that found for cisplatin and other mononuclear platinum[II] complexes. Firstly, these compounds are capable of forming bifunctional DNA adducts that are structurally different to that of cisplatin, especially long-range (Pt, Pt) interstrand

cross-links.[103,104] These cross-links represent a new class of DNA adducts of anticancer agents, situated in the major groove by virtue of guanine N7 binding. In principle, the bifunctional DNA binding modes of dinuclear complexes may be manipulated by geometry of the complex, especially with regard to the relationship of the leaving groups to the diamine bridge, and the nature of the diamine bridge itself as well as the other ligands present within the platinum coordination sphere.[92]

The flexibility of the bridging group allows for the formation of a number of different cross-links, while classically bifunctional mononuclear compounds are restricted in the number and type of cross-links they can form.[103,105,106] Depending on sequence, both A- and Z- form DNA are induced by binding to DNA of polynuclear platinum complexes.[107] Further, 1,3- and 1,4- (Pt, Pt)-interstrand cross-links formed by the 1,1/t,t compounds do not significantly bend DNA and thus are not recognized by HMGI proteins.[108] Such protein recognition is postulated to be an important aspect of the antitumour activity of cisplatin[109-111] and lends support to the hypothesis that structurally unique DNA adduct structures may lead to different "downstream" effects which may result in a significantly different profile of antitumour activity.[112]

An interesting aspect in the chemistry of bis(platinum) complexes containing two platinum centres linked by a diamine bridge is their mode of substitution. Bis(platinum) complexes with two identical coordination spheres are equally likely to react at either metal centres. In a substitution reaction this equivalence is broken upon reaction of Pt centre. There now exists a competition between the two non-equivalent platinum centres and the final product will therefore be dependant on the incoming ligand.

Comprehensive studies on the role of DNA binding properties and product formation have been conducted on bis(platinum) complexes, with the results being interpreted in terms of charge, hydrogen bonding, length and flexibility of the bridging ligand.[1] However, there is limited information available with regard to the reactivity and thermodynamic properties of the two platinum centres. Such data is only available for the complexes shown in *Figure 1.22*, and suggests that the reactivity and properties of the first platinum centre is independent of the state of the second and *vice versa*.[113,114] Data available in literature is insufficient to formulate a relationship between the reactivity of the two platinum centres and the nature of the bridging ligand.

In an effort to gain more insight into the role of the bridging diamine linker, the following study was undertaken whereby the influence of four different bridges on the reactivity of each of the platinum centres was investigated. The variation of the bridging diamine spacer enabled a systematic study of the influence of chain length, flexibility and hybridisation of the bridge on the thermodynamic and kinetic properties of the two platinum centres (*Figure 1.22*). A similar study was conducted by Hofmann and van Eldik[114](*Figure 1.23*), whereby four different bridges on the reactivity of each of the platinum centres was investigated.
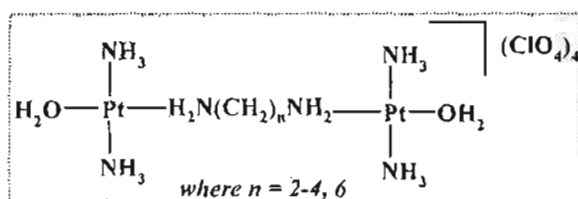
Figure 1.22: *Structures of the complexes synthesized for the purposes of this work.*
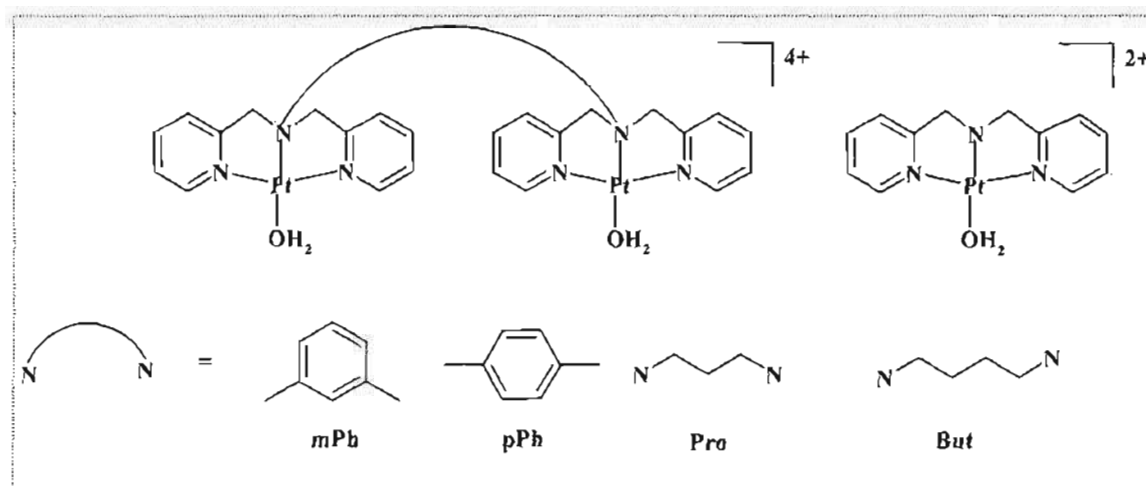
Figure 1.23: *Structures of the complexes investigated by Hofmann and van Eldik.[114]*

1-36

References

1. Belluco, U., *Organometallic and Coordination Chemistry of Platinum*, Academic Press, London, **1974**, pp 1-20.

2. Sherman, S.E. & Lippard, S.J., *Chem. Rev.*, *87*, **1987**, 1153.

3. Rosenburg, B., van Camp, L., Krigass, T., *Nature*, *205*, **1965**, 698.

4. Rosenburg, B., van Camp, L., Trosko, J.E., Mansour, V.H., *Nature*, *222*, **1969**, 385.

5. Lippert, B., *Cisplatin: The Chemistry and Biochemistry of a Leading Anticancer Drug*, Wiley-VCH, Weinheim, **1999**, pp 3-39, 479.

6. Rosenburg, B., *Plat. Met. Rev.*, *15*, **1971**, 42.

7. Lippard, S.J., *Acc. Chem. Res.*, **1978**. 211.

8. Jakupec, M.A., Galanski, M., Keppler, B.K., *Rev. Physiol. Biochem. Pharmoc.*, *146*, **2003**, 1

9. Cleare, M.J & Hoeschele, J.D., *Plat. Met. Rev.*, *17*, **1973**, 2

10. Cleare, M.J & Hoeschele, J.D., *Bioinorg. Chem.*, *2*,**1973**, 187.

11. Lebhowl, D & Canatta, R., *Eur. J. Cancer.*, *34*, **1998**, 1522.

12. Ho, Y.P., Steve, C.F., Au-Yeung., Kenneth, K.W.To., *Med. Res. Revs.*, *23*, **2003**,633.

13. Chu, G., *J. Biol. Chem.*, *269*, **1994**, 787.

14. Pera, M.F., Zook, B.C., Harder, H.C., *Can. Res.*, *39*, **1979**, 1269.

15. Ozols, R.F., Corden, B.J., Collins, J., Young, R.C., *Platinum Coordination Complexes in Cancer Chemotherapy*, Martinu-Nijhoff Publ., Boston, **1984**, pp 321-329.

16. Ozols, R.F., Corden, R.J., Isash, J., Wesley, M.N., Otscahga, Y., Young, R.C., *Ann. Intern. Med.*, *100*, **1984**, 19.

17. Schaefer, S.D., Post, J.D., Close, L.G., Wright, C.G., *Cancer*, *56*, **1985**, 1934.

18. Goren, M.P., Wright, R.K., Horowitz, M.E., *Cancer. Chemother. Pharmocol.*, *18*, **1986**, 69.

19. Alberts, D.S. & Noel, J.K., *Anticancer Drugs*, *6*, **1995**, 369.

20. Borch, R.F., Bedon, P.C., Gringeri, A., Montin, T.J., Nicolini, M., (Ed.), *Platinum and other Coordination Compounds in Cancer Chemotherapy*, Martinus Nijhoff Publ., Boston, **1988**, pp 207-215.

21. Douple, E.B., *Pharmac. Ther.*, *25*, **1984**, 297.

22. Eastman, A., Schulte, N., Sheibani, N., Sorenson, C.M., Nicolini, M (Ed.), *Platinum and other Coordination Compounds in Cancer Chemotherapy*, Martinus Nijhoff Publ., Boston, **1988**, pp 178-196.

23. Reedjik, J., Fichtinger-Schepmann, A.M.J., van Oosterom, A.T., van de Putte, P., *Structure Bonding*, *67*, **1987**, 53.

24. Sherman, S.E., Lippard, S.J., *Chem. Rev.*, *87*, **1987**,1153.

25. Hambley, T.W., *J. Chem. Soc. Dalton Trans.*, **2001**, 2718.

26. Farrell, N., *Transition Metal Complexes as Drugs and Chemotherapeutic Agents*, Kluwer, Dordrecht, **1989**, pp 46-49, 67-90.

27. Sorenson, C.M. & Eastman, A., *Cancer Res.*, *48*, **1988**, 4484.

28. Simonian, P.L., Grillot, D.A.M., Nunez, G., *Blood*, *90*, **1997**, 1208.

29. Eastman A., Lippert, B (Ed.)., Cisplatin, *Chemistry and Biochemistry of a Leading Anticancer Drug*, Wiley-VCH, **1999**, pp 111-134.

30. Johnson, S.W., Shen, D.W., Pastan, I., Gottesman, M.M., Hamilton, T.C., *Exp. Cell Res.*, *226*, **1996**, 133.

31. Akiyama, S-I., Chen, Z-S., Sumizawa, T., Furukawa, T., *Anticancer Drug Design*, *14*, **1999**, 143.

32. Kleland, L.R., *Drugs*, *59*, **2000**, 1.

33. Andrews, P.A.& Howell, S.B., *Cancer Cells*, *2*, **1990**, 35.

34. Mistry, P., Kelland, L.R., Abel, G., *Br. J. Cancer*, *64*, **1991**, 215.

35. Chaney, S.G.& Vaisman, A., J. *Inorg. Biochem.*, *77*, **1999**, 71.

36. Wyllie, A.H., Kerr, J.F.R., Currie, A.R., *Int. Rev. Cytol.*, *68*, **1980**, 251.

37. Searle, J., Kerr, J.F.R., Bishop, C.L., *Pathol. Annu.*, *17*, **1982**, 229.

38. Hickman, J.A., *Cancer Metastasis Rev.*, *11*, **1992**, 121.

39. Chu, G., *J. Biol. Chem.*, *269*, **1994**, 787.

40. Calvert, A.H., et.al., *Cancer Chemother. Pharmocol.*, *9*, **1982**, 140.

41. Evans, B.D., Raju, K.S., Calvert, A.H., Harland, S.J., Wiltshaw, E., *Cancer Treat Rep.*, *67*, **1983**, 997.

42. Ruckdeschel, J.C., *Semin. Onco.*, *21*, **1994**, 114.

43. Harrap, K.R., *Cancer Treat Rev.*, *12*, **1985**, 1855.

44. Rixe, O., Ortuza, W., Alvarez, M., *Biochem. Pharmocol.*, *52*, **1996**, 1855.

45. Farrell, N., *Cancer Investigation*, *11*, **1993**, 578.

46. Farrell, N., Qu, Y., Feng, L., van Houten. B., *Biochemistry*, *29*, **1990**, 9522.

47.   Farrell, N., Tam, T.B., Ha Souchard, J-P., Wimmer, F.L., Cros, S., Johnson, N.P., *J. Med. Chem.*, *32*, **1989**, 2240.

48.   Farrell, N., Kiley, D.M., Schmidt, W., Hacker, M.P., *Inorg. Chem.*, *29*, **1990**, 397.

49.   Hollis, L.S., Amundsen, A.R., Stern, E.W., *J. Med. Chem.*, *32*, **1989**, 128.

50.   Skov, K.A., Adomat, H., Chaplin, D.J., Farrell, N.P., *Anticancer Drug Design*, *5*, **1990**, 121.

51.   Johnson, N.P., Lapetoule, P., Razake, H., Villani, G., McBrien D.C.H (Ed.), *Biochemical Mechanisms of Platinum Antitumour Drugs*, IRL Press, Oxford, **1986**, pp 1-28.

52.   Roberts, J.J & Friedlos, F., *Cancer Res.*, *47*, **1987**, 31.

53.   Ciccarelli, R.B., Solomon, M.J., Varshavsky, A., Lippard, S.J., *Biochemistry*, *24*, **1985**, 7533.

54.   Eastman, A., Jennerwein, M.M., Nagel, D.L., *Chem. Biol. Inter.*, *67*, **1988**, 71.

55.   van de Veer, J.L., Ligtvoet, G.J., van den Eist, H., van der Marel, G.A., Reedjik, J., *J. Amer. Chem. Soc.*, *108*, **1986**, 3860.

56.   Gibson, D. & Lippard, S.J., *Inorg. Chem.*, *26*, **1987**, 2275.

57.   Eastman, A. & Barry, M.A., *Biochemistry*, *26*, **1987**, 3303.

58.   Bancroft, D.P., Lepre, C.A., Lippard, S.J., *J. Amer. Chem. Soc.*, *112*, **1990**, 6860.

59.   Farrell, N., Kelland, L.R., Roberts, J.D., *Cancer Res.*, *52*, **1992**, 5065.

60.   Wheate, N.J & Collins, J.C., *Coord. Chem. Rev.*, *241*, **2003**, 133.

61.   Broomhead, J.A., Rendina, L.M., Sterns, M., *Inorg. Chem.*, *31*, **1991**, 1880.

62.   Broomhead, J.A., Rendina, L.M., Webster, L.K., *J. Inorg. Biochem.*, *49*, **1993**, 221.

63.   Broomhead, J.A., Lynch, M.J., *Inorg. Chim. Acta.*, *240*, **1995**, 13.

64.   Farrell, N. & Qu, Y., *Inorg. Chem.*, *28*, **1989**, 3416.

65.   Qu, Y., Appleton, T.G., Hoescele, J.D., *Inorg. Chem.*, *32*, **1993**, 2591.

66.   Farrell, N., Qu, Y., Hacker, M.P., *J. Med. Chem.*, *33*, **1992**, 930.

67.   Chen, Y., Guo, Z., Parsons, S., Saddler, P.J., *Chem. Eur. J.*, *4*, **1998**, 672.

68.   Holford, J., Raynaud, F., Murrer, B.A., Grimaldi, K., Hartley, J.A., Abrams, M., Kelland, L.R., *Anticancer Drug Design*, *13*, **1998**, 1.

69.   Holford, J., Sharp, S.Y., Murrer, B.A., Abrams, M., Kelland, L.R., *Br. J. Cancer*, *77*, **1998**, 366.

70.   Qu, Y. & Farrell, N., *Inorg. Chem.*, *31*, **1992**, 930.

71.   Qu, Y. & Farrell, N., *J. Amer. Chem. Soc.*, *113*, **1991**, 4851.

72.   Hoeschele, J.D., Kraker, A.J., Qu, Y., van Houten, B., Farrell, N., Pullman, B., Jortner, J (Eds.)., *Chemistry, Antitumour Activity and DNA-Binding: Molecular Basis and Specificity in Nucleic Acid-Drug Interactions*, Kluwer Academic, Dordrecht, 1990, p 301.

73.   Qu, Y., Rauter, R., Soares-Fontes, A.P., Bandarage, R., Kelland, L.R., Farrell, N., *J. Med. Chem.*, *43*, 2000, 3189.

74.   Jansen, B.A.J., van der Zwan., J., den Dulk, H., Brouwer, J., Reedjik, J., *J. Med. Chem.*, *44*, 2001, 245.

75.   Jansen, B.A.J., Brouwer, J., Reedjik, J., *J. Inorg. Biochem.*, *89*, 2002, 197.

76.   Qu, Y., Fitzgerald, J.A., Rauter, H., Farrell, N., *Inorg. Chem.*, *40*, 2001, 6324.

77.   Zhao, G., Lin, H., Zhu, S., Sun, H., Chen, Y., *Anticancer Drug Design*, *13*, 1998, 769.

78.   Wheate, N.J., Cullinane, C., Webster, L.K., Collins, J.G., *Anticancer Drug Design*, *16*, 2001, 91.

79.   Jansen, B.A.J., van der Zwan, J., Reedjik, J., den Dulk, H., Brouwer, J., *Eur. J. Inorg. Chem.*, 1999, 1429.

80.   Bierbach, U., Roberts, J.D., Farrell, N., *Inorg. Chem.*, *37*, 1998, 717.

81.   Komeda, S., Lutz, M., Spek, A.L., Chikuma, M., Reedjik, J., *Inorg. Chem.*, *39*, 2000, 4230.

82.   Komeda, S., Lutz, M., Spek, A.L., Yamanka, Y., Sato, T., Chikuma, M., *J. Amer. Chem. Soc.*, *124*, 2002, 4738.

83.   Di Blasi, P., Bernareggi, A., Beggiolin, G., Piazzoni, L., Menat, E., Formneto, M.L., *Anticancer Res.*, *18*, 1998, 3113.

84.   Perego, P., Gatti, L., Caserini, C., Supino, R., Colangelo, D., Leon, R., Spinelli, S., Farrell, N., Zunino, F., *J. Inorg. Biochem.*, *77*, 1999, 59.

85.   Perego, P., Caserini, C., Gatti, L., *et al.*, *Mol Pharm.*, *55*, 1999, 528.

86.   Farrell, N. & Spindelli, S., *Royal Soc. of Chem.*, 1999, 124.

87.   Roberts, J.D., van Houten, B., Qu, Y., Farrell, N.P., *Nucleic Acid. Res.*, *17*, 1989, 9719.

88.   Bloemink, M.J., Reedjik, J., Farrell, N., Qu, Y., Stetsenko, A.I., *J. Chem. Soc. Chem. Commun.*, 1992, 1002.

89.   Farrell, N., *Comments Inorg. Chem.*, *16*, 1995, 373.

90.   Farrell, N.P., de Almeida, S.G., Skov, K.A., *J. Amer. Chem. Soc.*, *110*, 1988, 5018.

91.   Wu, P.K., Qu, Y., van Houten, B., Farrell, N., *J. Inorg. Biochem.*, *54*, 1994, 207.

92. Cox, J.W., Berners-Price, S.J., Davies, M.S., Qu, Y., Farrell, N.P., *J. Amer. Chem. Soc.*, *123*, 2001, 1316

93. Zou, Y., van Houten, B., Farrell, N., *Biochemistry*, *22*, 1994, 5404.

94. Rice, J.A., Crothers, D.M., Pinto, A.L., Lippard, S.J., *Proc. Natl. Acad. Sci. USA.*, *85*, 1988, 4158.

95. Billings, P.C., Davis, R.J., Engelsberg, B.N., Skov, K.A., Hughes, E.N., *Biochem. Biophys. Res. Commun.*, *188*, 1992, 1286.

96. Pil, P.M. & Lippard, S.J., *Science*, *256*, 1992, 234.

97. Skov, K.A., Adomat, H., Farrell, N.P., Marples, B., Matthews, J., Walter, P., Qu, Y., Zhou, H., *Proc. AACR.*, 34, 1993, 2571.

98. Gruff, E.S. & Orgel, L.E., *Nucl. Acid. Res.*, *19*, 1991, 6849.

99. Johnson, A., Qu, Y., van Houten, B., Farrell, N., *Nucl. Acid. Res.*, 20, 1992, 1697.

100. Malfoy, B., Hartmann, B., Leng, M., *Nucl. Acid. Res.*, *9*, 1981, 5659.

101. Ushay, M., Santella, R.M., Grunberger, D., Lippard, S.J., *Nucl. Acid. Res.*, *10*, 1982, 3573.

102. van Houten, B., Illenye, S., Qu, Y., Farrell, N., *Biochemistry*, *32*, 1994, 11794.

103. Farrell, N.P., Qu, Y., Bierbach, U., Valsecchi, M., Menta, E., Lippert, B (Ed); *Cisplatin: Chemistry and Biochemistry of a Leading Anticancer Drug*, Wiley-VCH, New York, 1999, pp 479-496.

104. Zaludova, R., Zavoska, A., Kasparkova, J., et al., *Eur. J. Biochem.*, *246*, 1997, 508.

105. Kasparkova, J., Mellish, K.J., Qu, Y., Brabec, V., Farrell, N., *Biochemistry*, *38*, 1996, 16705.

106. Brabec, V., Kasparkova, K., Vrana, O., Novakova, O., Cox, J.W., Qu, Y., Farrell, N., *Biochemistry*, *38*, 1999, 6781.

107. McGregor, T.D., Balcarova, Z., Qu, Y., Tran, M-C., Zaludova, R., Brabec, V., Farrell, N., *J. Inorg. Biochem.*, *77*, 1999, 43.

108. Kasparkov, J., Farrell, N., Brabec, V., *J. Biol. Chem.*, *275*, 2000, 15789.

109. Ohndorf, U-M., Rould, M.A., He, Q., Pabo, C.O., Lippard, S.J., *Nature*, *399*, 1999, 708.

110. Ohndorf, U-M., Whitehead, J.P., Raju, N., Lippard, S.J., *Biochemistry*, *36*, 1999, 14807.

111. Jamieson, E.R., Lippard, S.J., *J. Chem. Reviews*, *99*, 1999, 2467.

112. Davies, M.S., Cox, J.W., Berners-Price, S.J., Barklage, W., Qu, Y., Farrell, N., *Inorg. Chem.*, *39*, **2000**, 1710.

113. Davies, M.S., Thomas, D.S., Hegmans, A., Berners-Price, S.J., Farrell, N., *Inorg. Chem.*, *41*, **2002**, 1101.

114. Hofmann, A. & van Eldik, R., *J. Chem. Soc. Dalton Trans.*, **2003**, 2979.

Chapter 2

Substitution Reactions

Chapter 2

Substitution Reactions

2.1 General Considerations

A substitution reaction may best be described as a process whereby a ligand in the coordination shell is replaced by another ligand from the environment.[1-3] If there is no temporary change in the oxidation state of the reaction centre the process can be referred to as a simple substitution reaction.[1]

In the act of a simple substitution a bond is made and a bond is broken, so the reaction centre must undergo a temporary change in coordination number.[1-4] There are two important parts to the description of a single act of ligand substitution. The first concerns the changes in electron distribution that occur as the acts of bond making and bond breaking take place. The second deals primarily with the timing of the bond making as well as the bond-breaking processes.[1]

In the seminal work of Ingold[5] and Hughes, substitution reactions at the carbon were classified in terms of the mode of the breaking of the bond between the reaction centre and the leaving group, which could either be homolytic or heterolytic and, if heterolytic it could further be subdivided according to whether electrons of the bond remain with the reaction centre or depart with the leaving group. These modes of bond breaking may be represented as follows:[1,6]

$$A : B \longrightarrow A^{\cdot} + B^{\cdot} \qquad \text{Homolysis} \qquad\qquad 2.1$$

$$A : B \longrightarrow A^{+} + :B^{-} \qquad \text{Nucleophilic Heterolysis} \qquad 2.2$$

$$A : B \longrightarrow A:^{-} + B^{+} \qquad \text{Electrophilic Heterolysis} \qquad 2.3$$

However, this method of classification was limited, in that it worked well only for carbon centres and therefore could not be extended to incorporate inorganic systems.

2.2 Classification of Substitution Mechanisms

In 1965 an operational approach, first formulated by Langford and Gray[7,8], was used to classify reaction mechanisms in relation to the type of information the kinetic studies of various types can provide. It delineates what can be said about the mechanism on the basis of the observations from certain types of experiments. The mechanism can be classified by two properties, *viz.* its stoichiometric character and its intimate character.

Reactions may be classified into one of three groups based on their stoichiometric mechanisms:[6-8]

- Associative (A): A process that involves an intermediate of increased coordination number.

- Dissociative (D): A process that involves an intermediate of decreased coordination number.

- Interchange (I): A process whereby there is no evidence of an intermediate being formed.

The *intimate* mechanism can be thought of as a process by which the stoichiometric interchange mechanism is further classified and can be divided into two classes:[1,6]

1) Dissociative Activation (I_d) whereby the reaction mechanism is more sensitive to changes in the leaving group and,

2) Associative Activation (I_a) where the reaction rate is more sensitive to changes in the entering group.

True examples of pure D and A mechanisms are quite rare with most substitution reactions proceeding via an I mechanism. Transition states and intermediates often resemble known species; mechanisms requiring unusual or unknown postulated species are unlikely.

The distinguishing features of these mechanisms will be dealt with in greater detail below (see *Section 2.2.1 - 2.2.3*). The relationship that exists as one progresses from a dissociative mechanism to an associative mechanism can be pictorially summarized in *Figure 2.1*.
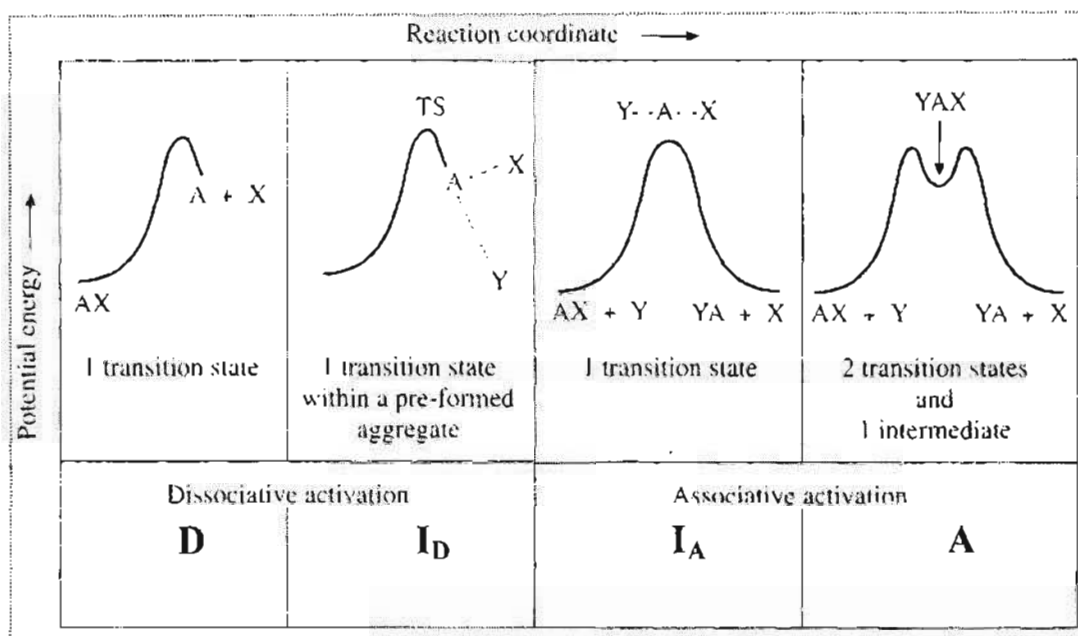
Figure 2.1: **The relationship between the mechanism of substitution, and its corresponding energy profile, in terms of the Langford-Gray nomenclature.**[1]

2.2.1 *The Dissociative Mechanism*

Let us consider the replacement of X by Y in a metal complex where our primary concern is with the bond breaking and bond making between the metal centre, M and ligands X and Y respectively.

$$M\text{-}X + Y \rightleftharpoons M\text{-}Y + X \qquad\qquad 2.4$$

$$M\text{-}X \overset{Y}{\rightleftharpoons} M + X \qquad\qquad 2.5$$

$$M + Y \longrightarrow M\text{-}Y \qquad\qquad 2.6$$
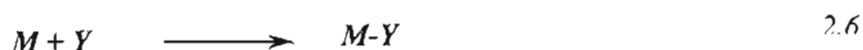
The overall reaction (*2.4*) proceeds in two steps (*2.5*) and (*2.6*) respectively. The energy profile for the dissociative (**D**) mechanism can be seen in *Figure 2.2*. The reaction step *2.5* is a slow dissociation. In the transition state the M···X bond is practically broken. The entering ligand Y, does not participate in the transition state, which is the highest energy barrier. Therefore, the reaction rate does not depend on the nature of the entering ligand (with the exception of effects that might be due to solvation). The reaction intermediate M, has a reduced coordination number, and its relative stabilization is due to solvation.[1]

Formation of the secondary transition state (TS₂) requires relatively little energy, which is mainly required for the elimination of the bound solvent. In this way, the location for new coordination is freed and the weak $M\cdots Y$ bond is established. As can be seen from *Figure 2.2*, the reaction is exothermic. The reaction product M-Y is stable as a result of the reverse reaction requiring a relatively large Gibbs free energy.[6]
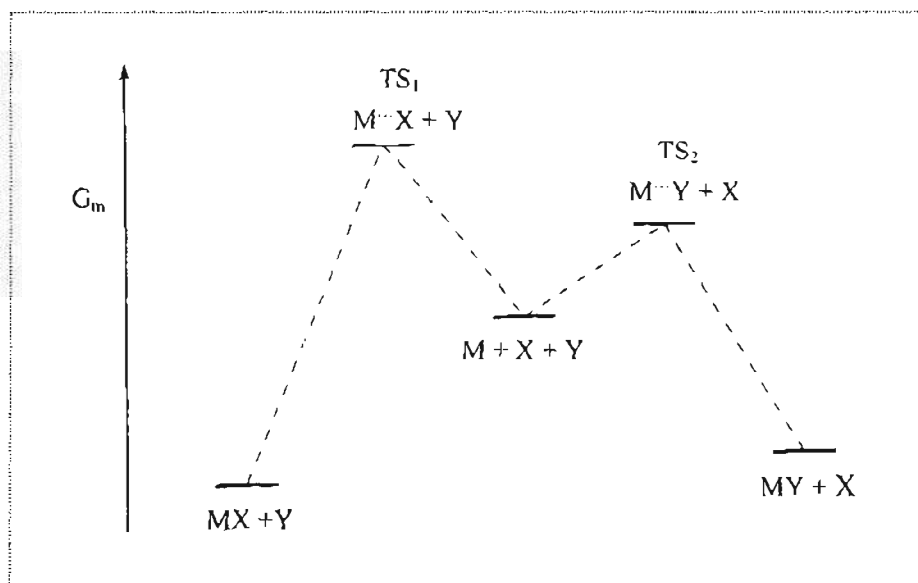
Figure 2.2: <u>*Activation profile for a dissociative (D) type reaction.*</u>[6]

In conclusion, one can say, that for a D mechanism, the intermediate has a reduced coordination number. The bond between the metal and the leaving ligand is virtually broken in the transition state and the bond with the incoming ligand has not yet been established.

2.2.2 *The Associative Mechanism*

If the reaction mechanism proceeds via an associative mechanism, then the reaction scheme can be represented as follows:

$$M - X + Y \Leftrightarrow [Y\cdots M\cdots X] \rightarrow M - Y + X \qquad\qquad 2.7$$
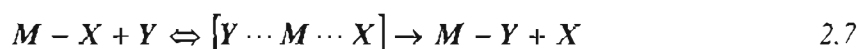
The reactions energy profile can be seen in *Figure 2.3*.
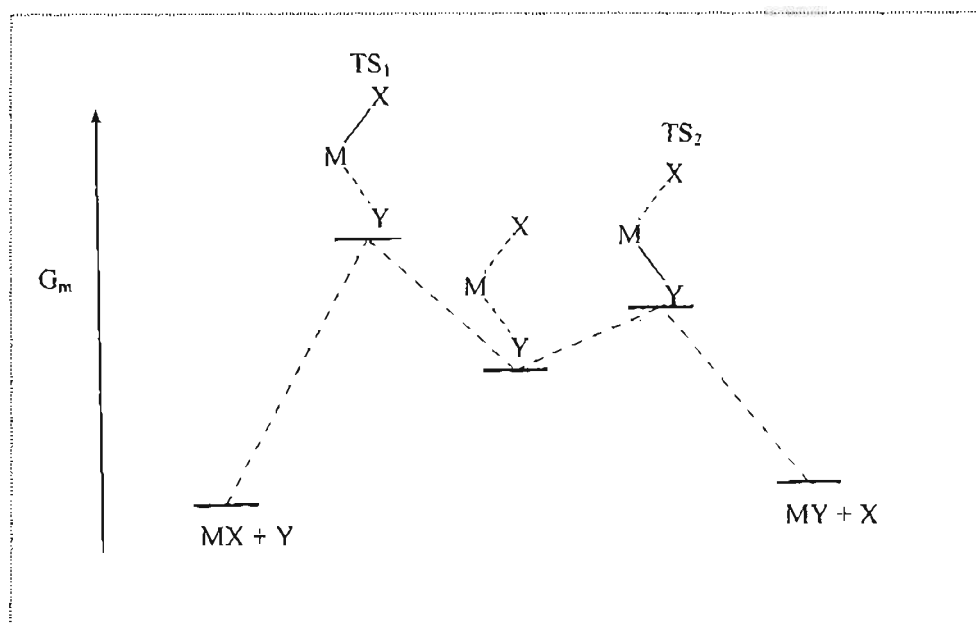
Figure 2.3: *Activation profile for an associative (A) type reaction.*[6]

If a reaction proceeds via an A mechanism, then the intermediate will have an increased coordination number. In the transition state (TS_1), the bond between the metal and the incoming ligand is largely established, whilst the bond between the metal and the leaving ligand is not essentially weakened. The rate of the reaction depends strongly on the nature of the incoming ligand, because Y participates in the transition state.[1,6,9]

2.2.3 The Interchange Mechanism

Interchange mechanisms, or "concerted" mechanisms, are the interchanges of ligands X and Y between the inner and outer coordination spheres of the metal. These mechanisms can involve different transition states, where I_d or I_a are extreme border cases.[6]

In a dissociative interchange (I_d) mechanism, there is no evidence of an intermediate being formed. In the transition state there is a large degree of bond breaking to the leaving group and a small amount of bond making to the entering group. The rate is more sensitive to the leaving group.

In an associative interchange (I_a), there is also no evidence of an intermediate being formed. However, there is some bond breaking between the metal and the leaving group and an increased degree of bond formation between the metal and the entering ligand.[6,7]

2.3   The Substitution Reactions of Square Planar Complexes

Square-planar complexes are most common for metal ions having a d^8 configuration e.g. Pt^{II}, Pd^{II}, Ni^{II} and Au^{II}. Such square planar complexes are invariably spin paired (diamagnetic).[6,9] By far the most stable square planar complexes are those of Pt^{II}, and as such the synthesis and reactions of these compounds have long been the subject of intensive research. During the past decade more quantitative studies have been conducted on these systems and an appreciable effort has been devoted to investigations of the kinetics and mechanisms of their reactions. [10-13]

Theoretically it would appear that square planar substitution would involve a bimolecular displacement mechanism. For both steric and electronic reasons, substitution reactions in these systems would proceed most readily by an expansion of coordination number to include the entering ligand. The metal is exposed to attack above and below the plane, as there are no ligands perpendicular to the plane to obstruct the approach of the ligand, and coordination numbers of greater than four are commonplace. Furthermore, these low spin d^8 systems have a vacant p_z orbital of relatively low energy that can help accommodate the pair of electrons donated by the entering ligand.[12,14]

The substitution in square planar complexes is indeed bimolecular and this is supported by the following criteria:[14]

- the fact that substitution occurs with steric retention;
- the isolation of many five and six-coordinated d^8 systems;
- the dependence of the rate of a reaction on the entering reagent and
- steric effects on rates.

A large number of reactions of *cis*- and *trans*-PtA$_2$LX with Y to yield PtA$_2$LY have been studied and without exception the *cis* and *trans* conformations yield *cis* and *trans* products respectively.[7,13] That there is complete retention of configuration requires a mechanism having a high degree of stereospecificity. This would be unlikely for a dissociative process, because the three-coordinated species involved, may at times, have a nearly regular (angles at 120°) planar structure. Thus, depending on whether Y enters PtA$_2$L adjacent to L or opposite to L, the product PtA$_2$LY can be either the *cis* or *trans* isomer respectively. Stereospecific displacement can best take place via a nucleophilic attack through a trigonal bipyramidal structure as shown in *Figure 2.4*.
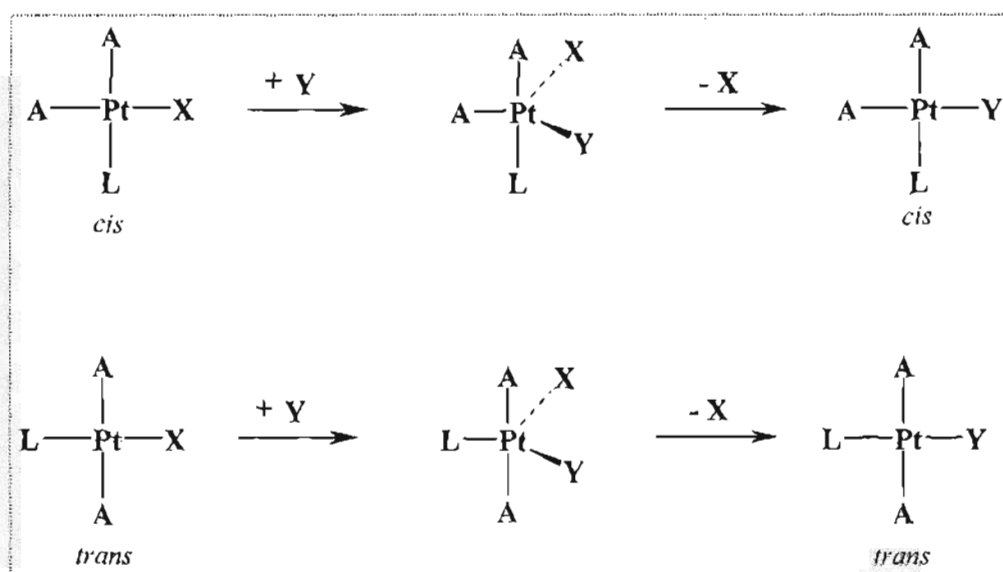
Figure 2.4: *Stereochemistry of square planar substitution via a trigonal bipyramidal structure which proceed with retention of stereochemistry.*[1,14]

2.3.1 The Kinetics and Mechanism of Substitution

There is a large amount of kinetic data on the substitution reactions of square planar complexes, all of which can best be described in terms of a bimolecular displacement mechanism.[14] For reactions of the following type:

$$MA_3X^{n+} + Y \xrightarrow{\ H_2O\ } MA_3Y^{n+} + X \qquad\qquad 2.8$$
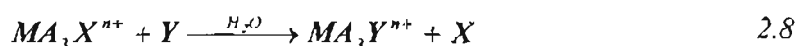
In aqueous solution, a two-term rate law is generally followed,

$$Rate = k_1[MA_3X^{n+}] + k_2[MA_3X^{n+}][Y] \qquad\qquad 2.9$$

where k_1 and k_2 are first and second-order rate constants respectively.

Under pseudo first-order conditions containing an excess of Y, the experimental first-order rate constant, k_{obs}, is related to the individual rate constants as shown by *Equation 2.10.*

$$k_{obs} = k_1 + k_2[Y] \qquad\qquad 2.10$$

This is frequently referred to as " the typical rate law for square-planar substitution". It is of course, only typical in coordinating solvents. Hence, a plot of k_{obs} versus [Y] will be linear with an intercept of k_1 for the reagent-independent path and a slope of k_2 for the reagent-dependent path. Plots of this type are common for the substitution reactions of square planar complexes, an example of which is shown in *Figure 2.5* for the reaction of *trans*-Pt(py)$_2$Cl$_2$ with a series of different nucleophiles.[15]

The value for k_1 is normally constant for different nucleophiles, whilst k_2 on the other hand is sensitive to the nature of the entering ligand, Y. One should also consider the fact that a positive intercept as indicated by *Figure 2.5*, may not always be attributed to k_1, and may reflect the rate constant for the reverse reaction instead.[16,17]
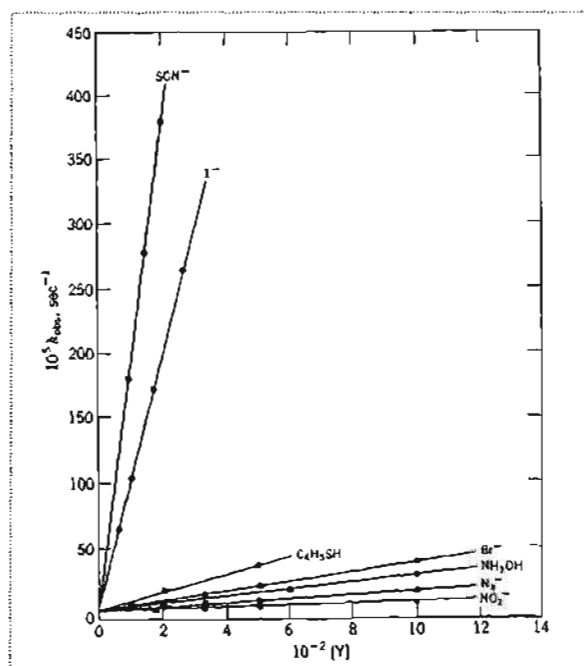
Figure 2.5: *Rates of reaction of trans-Pt(py)₂Cl₂ in methanol as a function of concentration of different nucleophiles.*[15]

The two-term rate law (*Equation 2.9*) requires a two-path reaction mechanism. Kinetic studies detailing the substitution behaviour of Pt^{II} complexes are largely conducted in the presence of coordinating solvents[18], *e.g.* water or methanol. In cases whereby the contribution of the reverse reaction is negligible, the k_1 term may be attributed to the solvolysis pathway. Experimental evidence overwhelmingly supports the mechanism shown in *Figure 2.6*.
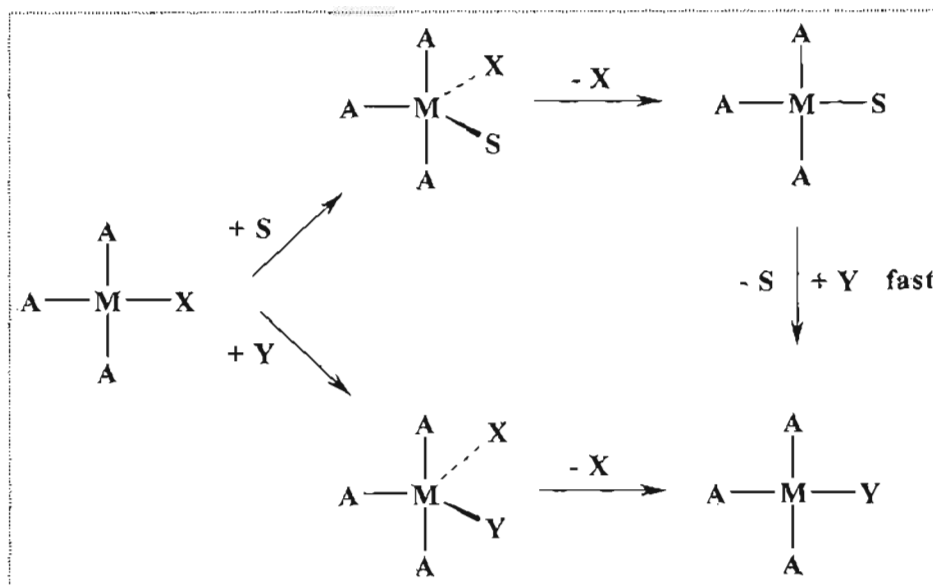
Figure 2.6: *Two-path mechanism proposed for the reaction of a square planar complex, MA₃X, with Y to yield MA₃Y. The upper path represents the solvolytic pathway and the lower one the direct pathway, represented by k_s and k_y, respectively, in Equation 2.11.*

The rate constant k_1 is due to the slow displacement of X by the solvent, which is then rapidly displaced by Y. A direct nucleophilic displacement of X by Y is responsible for k_2. It therefore becomes convenient to designate the rate constant for the solvent pathway k_1 as k_s and the rate constant for the reagent pathway k_2 as k_Y, so that *Equation 2.10* becomes

$$k_{obs} = k_s + k_Y [Y]$$

2.11

Evidence presented suggests that the transition state for Pt^{II} substitution reactions is six-coordinated. This implies that the five-coordinated species is an active intermediate, and hence the energy-reaction profile may be represented by *Figure 2.7*. The alternative would be that the five-coordinated species represents the transition state. However, the existence of the stable five-coordinated species mentioned earlier, makes this unlikely.
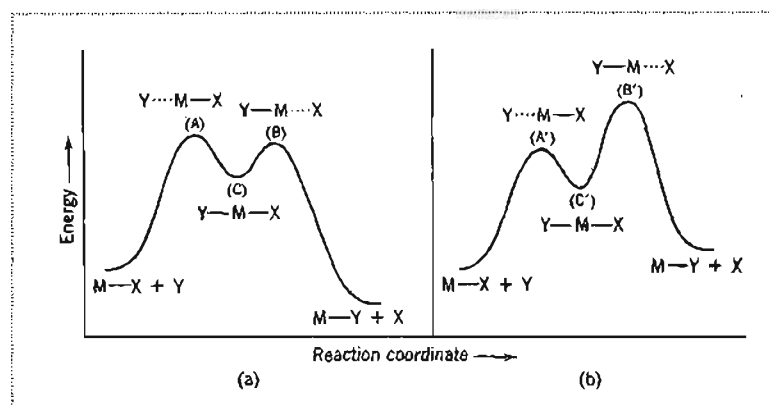
Figure 2.7:   Reaction profiles for a displacement mechanism involving a reactive

intermediate, C or C'. For (a) the activation energy involves transition state A,

M⋯Y bond formation, whereas for (b) it is the transition state B' or M⋯X bond

rupture that is important.[15]

In the situation represented by *Figure 2.7(a)*, the rate-determining step is the addition of the nucleophile accompanied by structural rearrangement. However, the bond to the leaving group remains intact and the mechanism falls under the associative category. For the reaction represented by *Figure 2.7(b)*, the addition of the nucleophile is reversible and the rate step is equal to the loss of the nucleophile, followed by rearrangement. The mechanism is a typical associative mechanism, since both bond-making and bond-formation occur. In either scenario, the rates would show the characteristic behaviour of a displacement mechanism in that the nature and concentration of the incoming nucleophile would exert a major effect on the rates of the reaction.

2.4   *Factors Affecting the Rate of Substitution*

2.4.1   *The Effect of the Non-Labile Group*

The ability of certain ligands to promote substitution reactions *trans* to themselves was initially observed by Werner at the beginning of the 20th century.[19,20] However, this observation was not generally utilized until after 1926, at which time Chernyaev introduced the concept of the *trans* effect to correlate many reactions of Pt^{II} complexes. Chernyaev called attention to the general phenomenon that a negative ligand such as Cl⁻ has a greater labilizing effect on a group *trans* to it than it does on groups present in the *cis* positions. Furthermore, this labilizing effect is generally larger for a negative ligand than it is for a non π-bonding neutral group, *e.g.* NH_3.

The usefulness of the *trans* effect becomes apparent if one considers a few reactions of Pt^{II} complexes. The *trans* effect has often been used as a guide in the synthesis of desired isomeric Pt^{II} complexes. Examples of the empirical *trans* effect rule can be applied to the synthesis of *cis* and *trans* isomers of $Pt(NH_3)_2Cl_2$ (*Equations 2.12-2.13*) and $Pt(NH_3)(NO_2)Cl_2$ (*Equations 2.14-2.15*).
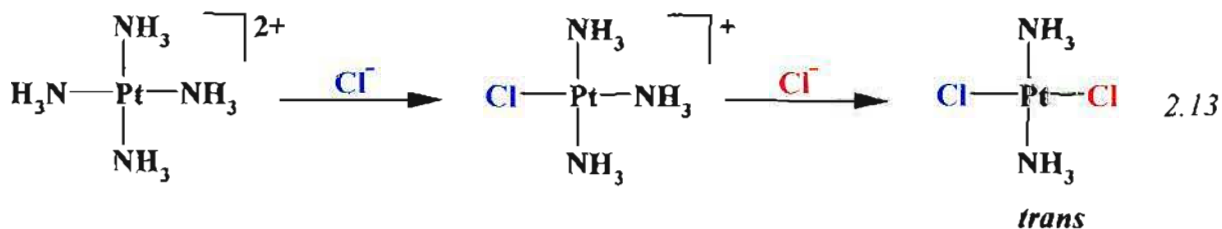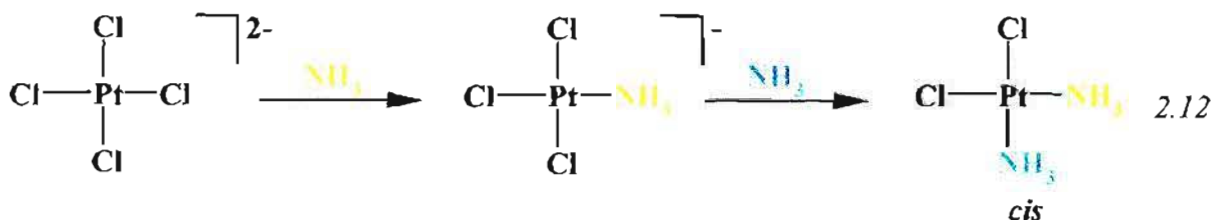
The *cis* isomer of $Pt(NH_3)_2Cl_2$ is prepared by reaction of the tetrachloro complex with ammonia, with the success of the reaction depending on the chloride ion having a larger *trans* directing influence than ammonia thus ensuring that the second ammonia enters a *cis* position. This is an indication that the least reactive chloro group in $PtNH_3Cl_3^-$ is the one opposite the ammonia group. The *trans* isomer of $Pt(NH_3)_2Cl_2$ is conveniently prepared by heating the tetraamine complex, showing in the second stage that the chloride ion replaces the most labile ammonia in $Pt(NH_3)_3Cl^+$, which is the group opposite to that of the chloride ion. This results in the *trans*-$Pt(NH_3)_2Cl_2$ complex being formed.

The synthesis of *cis*- and *trans*- isomers of $[Pt(NH_3)(NO_2)Cl_2]$[21] can be performed simply and elegantly by reversing the order of substituting groups.

$$
\begin{array}{ccccc}
\left[\begin{array}{c} Cl \\ | \\ Cl\!-\!Pt\!-\!Cl \\ | \\ Cl \end{array}\right]^{2-}
& \xrightarrow{NH_3} &
\left[\begin{array}{c} Cl \\ | \\ Cl\!-\!Pt\!-\!NH_3 \\ | \\ Cl \end{array}\right]^{-}
& \xrightarrow{NO_2^-} &
\left[\begin{array}{c} NO_2 \\ | \\ Cl\!-\!Pt\!-\!NH_3 \\ | \\ Cl \end{array}\right]^{-} \\
& & & & cis
\end{array}
\qquad 2.14
$$

$$
\begin{array}{ccccc}
\left[\begin{array}{c} Cl \\ | \\ Cl\!-\!Pt\!-\!Cl \\ | \\ Cl \end{array}\right]^{2-}
& \xrightarrow{NO_2^-} &
\left[\begin{array}{c} NO_2 \\ | \\ Cl\!-\!Pt\!-\!Cl \\ | \\ Cl \end{array}\right]^{2-}
& \xrightarrow{NH_3} &
\left[\begin{array}{c} NO_2 \\ | \\ Cl\!-\!Pt\!-\!Cl \\ | \\ NH_3 \end{array}\right]^{-} \\
& & & & trans
\end{array}
\qquad 2.15
$$
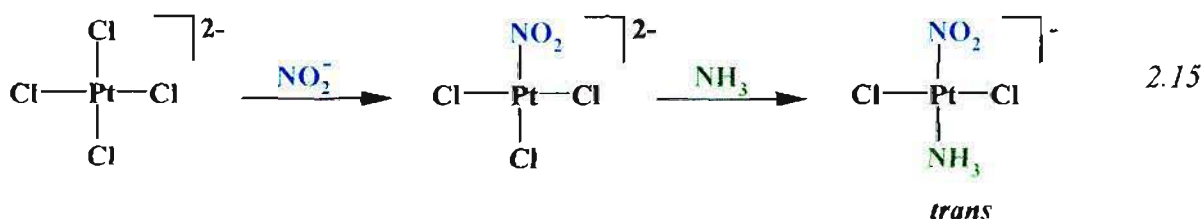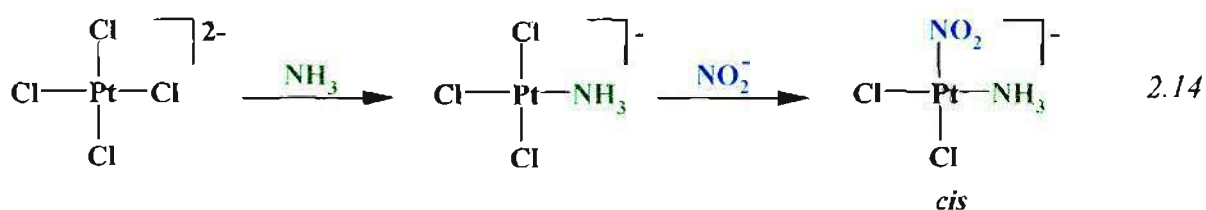
For the above reactions, the order of *trans*-labilizing effectiveness is $NO_2^- > Cl^- > NH_3$.

Additional examples illustrating the usefulness of the *trans* effect are shown in *Equations 2.16-2.19*.

For example, the *trans*-elimination[14] step may be designated as a two-step process for the following reaction:

$$
\begin{array}{ccccc}
\left[\begin{array}{c} py \\ | \\ py\!-\!Pt\!-\!NH_3 \\ | \\ NH_3 \end{array}\right]^{2+}
& \xrightarrow{+\,Cl^-} &
\left[\begin{array}{c} py \\ | \\ Cl\!-\!Pt\!-\!NH_3 \\ | \\ NH_3 \end{array}\right]^{+}
& \xrightarrow{+\,Cl^-} &
\left[\begin{array}{c} py \\ | \\ Cl\!-\!Pt\!-\!Cl \\ | \\ NH_3 \end{array}\right]
\end{array}
\qquad 2.16
$$
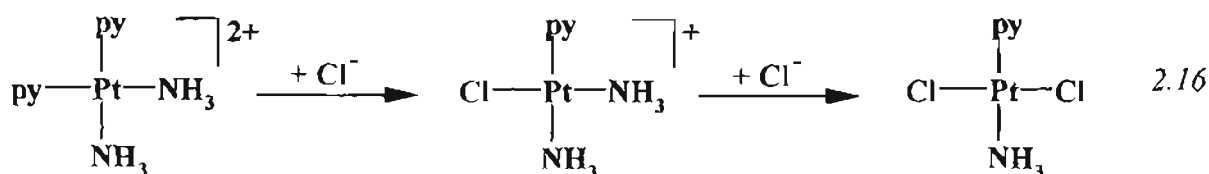
Once the first chloride ion has entered the complex, the second chloride ion replaces the ligand *trans* to the first Cl⁻ since this position is now labilized. The chloride ion has a larger *trans* labilizing effect than either pyridine or ammonia.

Three possible geometrical isomers of Pt(py)(NH₃)(Cl)(Br)[14] can be prepared by observing the order Br⁻ > Cl⁻ > py > NH₃.

$$
\left[\begin{array}{c} Cl \\ | \\ Cl-Pt-NH_3 \\ | \\ Cl \end{array}\right]^- \xrightarrow{\ Br^-\ } \left[\begin{array}{c} Br \\ | \\ Cl-Pt-NH_3 \\ | \\ Cl \end{array}\right]^- \xrightarrow{\ py\ } \begin{array}{c} Br \\ | \\ Cl-Pt-NH_3 \\ | \\ py \end{array} \quad 2.17
$$

$$
\left[\begin{array}{c} Cl \\ | \\ Cl-Pt-py \\ | \\ Cl \end{array}\right]^- \xrightarrow{\ Br^-\ } \left[\begin{array}{c} Br \\ | \\ Cl-Pt-py \\ | \\ Cl \end{array}\right]^- \xrightarrow{\ NH_3\ } \begin{array}{c} Br \\ | \\ Cl-Pt-py \\ | \\ NH_3 \end{array} \quad 2.18
$$

$$
\left[\begin{array}{c} Cl \\ | \\ Cl-Pt-py \\ | \\ py \end{array}\right] \xrightarrow{\ NH_3\ } \left[\begin{array}{c} NH_3 \\ | \\ Cl-Pt-py \\ | \\ py \end{array}\right]^+ \xrightarrow{\ Br^-\ } \begin{array}{c} NH_3 \\ | \\ Cl-Pt-Br \\ | \\ py \end{array} \quad 2.19
$$
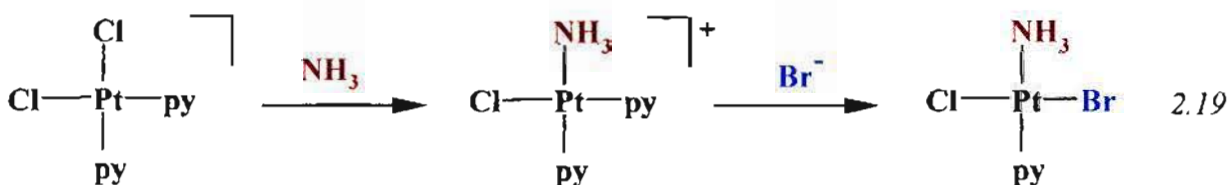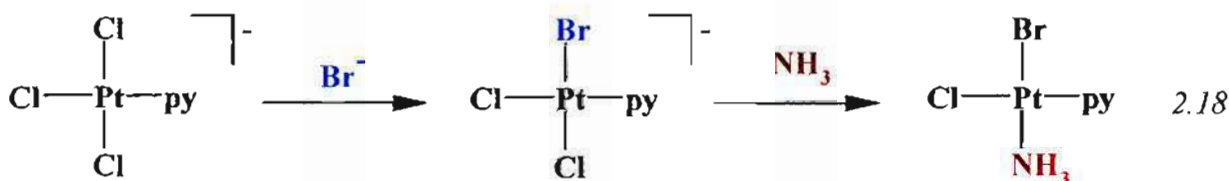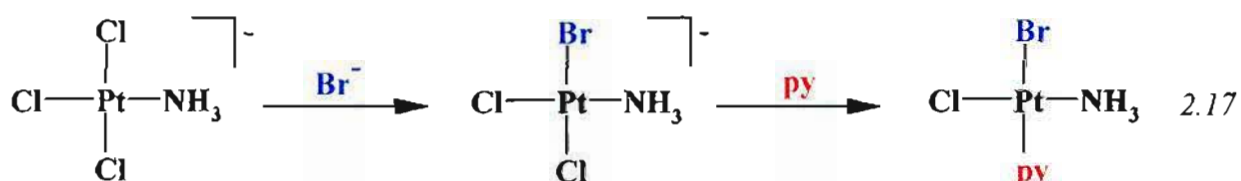
The success of these reactions depends upon the greater *trans* effect of Br⁻ and Cl⁻ ligands in comparison to the py and NH₃ ligands, and also on the fact that the Pt-N bond strength is greater than that of the Pt-Cl bond strength. This serves as an indication that the metal-ligand bond strength has to be considered as well as the labilizing influence of the *trans* group.

The chemistry involved in the synthesis of Pt^{II} complexes has made extensive use of the role of the *trans* effect. These observations have provided qualitative information regarding the *trans*-directing influence of various ligands. The approximate order of decreasing *trans* effect is as follows:[7,9]

$$CO, \ CN^-, \ C_2H_4 > PR_3, \ H^- > CH_3^- > SC(NH_2)_2 > C_6H_5^-, \ NO_2^-, \ I^-,$$

$$SCN^- > Br^-, \ Cl^- > py, \ NH_3, \ OH^-, \ H_2O.$$
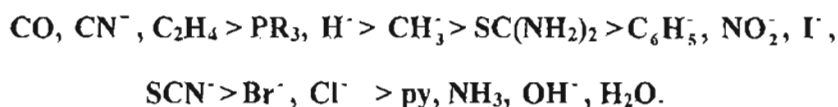
An interesting point to note is that kinetically this effect can be large. A factor of 10^6 or more in rates is found between a complex containing a good *trans* labilizing ligand as opposed to one with a ligand that lies low in the *trans* effect series. This effect is surely the most dramatic on the rates of substitution reactions in metal complexes.[14]

The *trans* effect is a well-established concept in Pt^{II} chemistry and several explanations have been offered. Basolo and Pearson[14] defined the *trans* effect as the "effect of a coordinated group upon the rate of substitution reactions of ligands opposite to it in a metal complex". Perhaps the best explanation considers both the σ-donating and π-accepting capabilities of the ligand. Strong σ-donation from a ligand, giving a weaker *trans* bond (*i.e.* a high ground state *trans*-influence), increases the rate of substitution. Charge delocalization in the transition state helps to stabilize it and thus to increase the rate. Strong π-acceptors typically give this kind of stabilization, and therefore have high *trans* effects.[22,23]

2.4.2 The π-Bonding Theory

This theory deals only with ligands that have π-bonding abilities *viz.* C_2H_4, PR_3 and CO, and suggests that these ligands are high in the *trans*-effect series due to the fact that they tend to stabilize the transition state for a reaction. Pauling first introduced the idea of π-bonding to account for the short Ni-C bond distance within the $Ni(CO)_4$ complex and also for the large stability of the cyanide complexes of transition metals as compared to non-transition metals. The existence and significance of such double bonding are now generally recognized. A schematic diagram of the double bond in $Pt = PR_3$ is shown in *Figure 2.8*.
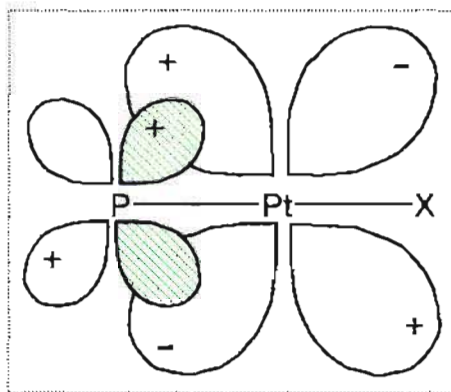
Figure 2.8: *Schematic representation of the R_3P-Pt double bond. If ligands PR_3 and X are in the xy plane, then the d orbitals shown are either d_{xy} or d_{yz}* [14.21]

The donation of a pair of electrons from phosphorous towards platinum results in a σ bond being formed. A corresponding π- bond is formed by the overlap of a filled *d* orbital of platinum and a vacant *d* orbital of phosphorous.

The removal of electrons from the metal due to π-bonding should result in the strengthening of the other ligands in general, the *trans* ligand in particular. Evidence suggests that the **Pt-X** bond is weakened in almost all cases where **L** is a good *trans* activator, the only exception being olefins, which do not always result in bond weakening. This holds true even if **L** is a π-bonding ligand. Thus, it is quite evident that even for these ligands, electron donation within the σ bond is more important than electron removal in the π-bond.

It is not clear whether or not bond weakening within the ground state is always sufficient to account for the effect of good *trans* activators, the increased rate of reaction should result from a stabilization of the transition state for the reaction. Chatt and Orgel independently proposed a π-bonding stabilization of the activated complex in order to explain the *trans* effect, whereby the activated state is assumed to have a trigonal bipyramidal structure as shown in *Figure 2.9*.
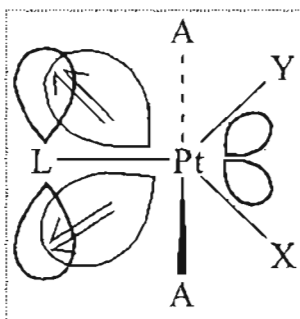
Figure 2.9: *Stabilization of a 5-coordinate transition state by a good trans-activating ligand.*[1,14,21]

Chatt *et al.*[24] placed emphasis on the fact that the removal of charge from Pt^{II} by π-bonding of *L*, allows the addition of *Y* to become more favourable and hence a faster reaction rate. Orgell[25] stated that an increased stability of the transition state as a result of π-bonding was mainly accounted for by the fact that the electron density along the *Pt-X* and *Pt-Y* directions were reduced. Such an activated complex will allow for retention of configuration and predicts that the properties of *Y* and *L* will influence the rate of the reaction in a similar manner.

2.4.3 *The Molecular Orbital Theory for σ- and π- trans Effect*

a) *σ-trans effect*

A simplified molecular orbital (M.O) diagram for the complex $PtCl_4^{2-}$ is shown in *Figure 2.10*. The most stable are the σ bonding orbitals, which are located primarily on the four chlorine molecules. The next in order of stability are the π-bonding orbitals, followed by the antibonding partners of the σ- and π-bonding molecular orbitals. These are derived from the 5*d* atomic orbitals of Pt^{II} and comprise of four relatively stable M.O.'s in the following order:

$$\pi_{xz}^{*}, \pi_{yz}^{*}, \sigma_{z^2}^{*}, \pi_{xy}, \text{ and the relatively unstable } \sigma_{x^2-y^2}^{*}$$

The p_z valence orbital, which is not involved in σ-bonding as well as the antibonding orbitals, σ_s^{*}, σ_x^{*} σ_y^{*} are found at higher energy levels.
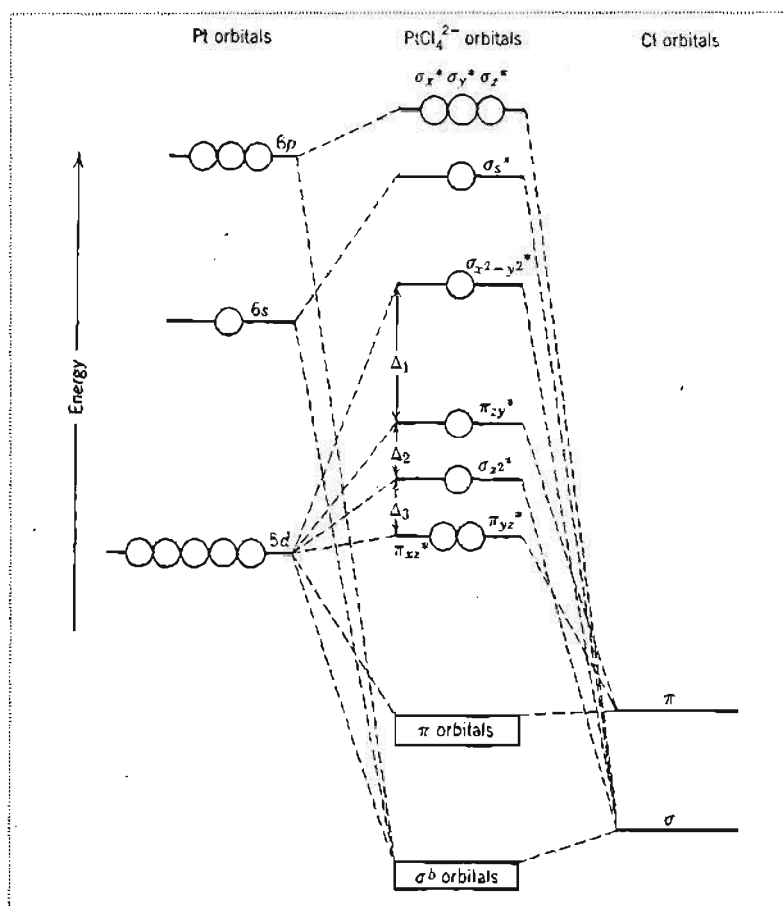
Figure 2.10: Relative orbital energies in $PtCl_4^{2-}$

Using this type of bonding allows one to account for the large *trans* effect for strong σ bonding ligands such as H^- and CH_3^-. If one considers the geometries of the atomic orbitals, it can be seen that of the four valence orbitals of the metal $(d_{x^2-y^2}^2, s, p_x \text{ and } p_y)$ participating in σ- bonding, only the p-orbitals possess *trans* directional properties. This is an indication that both the *trans* ligand L and the leaving group X in *trans*-PtA$_2$LX must share the same σ_x-orbital. It follows that a strong σ-bonding ligand L has a larger share in the bonding σ_x orbital than X. This results in the Pt-X bond being weakened. Irrespective of the mechanism involved in substitution, this would ultimately lead to an increased rate of replacement of X.

Langford and Gray developed a simple and easily visualized model, whereby the *trans* ligands compete for use of the appropriate p-orbital. (See *Figure 2.11*)
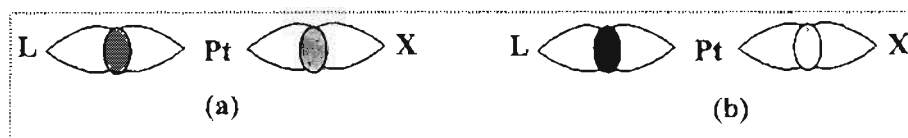
Figure 2.11: *The σ bonding of L-Pt-X, using the σ_x MO. (a) the σ-bond strengths of L and X are about equal. (b) The σ-bond strength of L is much greater than that of X.*[14]

Whilst only one p-orbital is used for bonding of the L-Pt-X on the x axis of the square planar complex, the addition of the entering group Y from the xy-plane, causes the X ligand to move out of the plane, resulting in a five-coordinate transition state.

Good σ-bonding ligands such as H^- and CH_3^- that use extra p character to firm up the σ structure in the trigonal bypyramid will have high *trans* effects.

b) The π-trans Effect

For ligands that form strong π-bonds, *e.g.* C_2H_4, CO and CN, and are good *trans* activators, the effect has been explained in terms of the π-bonding theory described earlier in *Section 2.4.2*. This effect may be expressed in terms of M.O. theory and can now be referred to as the *π-trans effect*. Of the five d-orbitals in a square planar complex, only three orbitals have the correct symmetry for π-interaction, *viz.*, d_{xy}, d_{xz} and d_{yz}. Upon addition of the entering group Y and subsequent formation of the trigonal bipyramidal structure, four d-orbitals meet the symmetry requirements for π interaction. Of importance is the fact that all these orbitals are shared in π bonding with the three ligands, L, X and Y in the trigonal plane. Thus the trigonal bipyramidal activated state will be stabilized if L is capable of bonding to the π^* orbitals. Electronic charge is delocalized to the ligands resulting in the energy of the system being lowered. Thus, the net effect of a good π acceptor ligand L is to lower the overall activation energy for a reaction.

Attempts have been made to assess the σ- and π- *trans* effects of numerous ligands, and the qualitative results are given in *Table 2.1*. It appears that ligands that are good *trans* activators may fall in one of three categories *viz.*:

- strong σ-bonding such as H⁻ and CH₃⁻,

- strong π-bonding such as C_2H_4 and CO and

- moderate σ- and π- bonding e.g. I⁻ and $SC(NH_2)_2$.

Table 2.1: **Estimated relative σ- and π- trans effects of some ligands.** [a]

Ligand	σ effect[a]	π effect[a]
C_2H_4	W	VS
CO	M	VS
CN	M	S
$SnCl_3$	W[b]	S[b]
PR_3	S	M
H	VS	VW
$SC(NH_2)_2$	M	M
NO_2	W	M
I	M	M
CH_3	S	VW
-SCN	M	M
C_6H_5	M	W
Br	M	W
Cl	M	VW
Pyridine	W	W
NH_3	W	VW
OH	VW	VW

[a] VS, very strong; S, strong; M, medium; W, Weak; VW, very weak

[b] Assumed on the basis of NMR data relative to analogous CN compound.

2.4.4 The cis- Effect

The ligands in the *cis*-position to the leaving ligand (*X*) exhibits a small electronic effect and consequently a small replacement rate effect.[26,27] The reactions of *cis*-Pt(PEt₃)₂LCl illustrate the magnitude expected and data obtained for the chloride exchange reaction is given in *Table 2.2*.

$$cis - Pt(PEt_3)LCl + py \rightarrow cis - Pt(PEt_3)_2 L(py) + Cl^-$$
2.21

In general, the *cis* effect is small and the order is variable, unless steric factors are involved. Steric factors provide one of the best means of differentiating between a dissociative and associative mechanism. An increase in the rate of a reaction is usually observed for a dissociative mechanism with increasing steric interactions and is known as *steric acceleration*. The opposite holds true for an associative mechanism, which involves an increase in coordination number, whereby increasing steric size would result in a decrease in the reaction rate.

Table 2.2:   *Rate constants observed for substitution of Cl⁻ by pyridine in the cis and trans complexes of Pt(PEt)₃LCl.[26,28]*

Complex	k_{obs}, s⁻¹
cis-Pt(PEt₃)₂LCl	
L = phenyl	8.0×10^{-2}
L = *o*-tolyl	2.0×10^{-4}
L = mesityl	1.0×10^{-6}
trans-Pt(PEt₃)₂LCl	
L = phenyl	1.2×10^{-4}
L = *o*-tolyl	1.7×10^{-5}
L = mesityl	3.4×10^{-6}

The data shown in *Table 2.2* provides excellent confirmation of the associative nature of Pt^II complexes and illustrates several points of interest. An increase in the size of the ligands dramatically slows the rate of substitution reactions. The orientation of the aromatic aryl ligand is perpendicular to the plane of the molecule with the substituents

occupying positions above and below the plane of the molecule, effectively blocking the site of attack. This is shown in *Figure 2.12*.
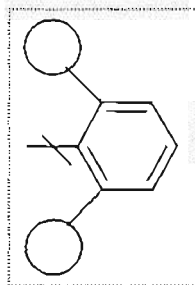
Figure 2.12: *Geometry of an aryl square-planar complex showing the ortho substituents blocking the site of attack.*

cis ligands occupy axial sites in the intermediate and interact with the entering and leaving groups at 90° angles. Therefore an increased effect on the rate by the *cis* ligands is observed.

2.4.5 The trans- and cis-Influence

The *trans* and *cis* influences are two thermodynamic phenomena observed for square planar platinum[II] complexes. The *trans* influence[29,30] is the tendency of a ligand to weaken the bond *trans* to itself in the ground state of a metal complex. Experimental evidence and theoretical rationale have been thoroughly reviewed.[31] Most information obtained supports the theory that a rehybridization of metal σ orbitals occurs whereby the ligand that exhibits a strong *trans* influence competes more effectively for the platinum 6s orbital than do the other ligands, resulting in a weakening of the bond in the *trans* position. The net transfer of electron density from ligand to metal is also of importance. However certain circumstances, *e.g.* π-bonding may outweigh the degree of metal rehybridization.

The *trans* influence may be determined by any one of the following *viz*.:

-   comparing bond lengths determined by X-ray crystallography[32] for similar compounds;

-   by nuclear magnetic resonance (NMR) chemical shifts and coupling constants since these parameters reflect the hybridization of a metal ion[31,32];

- by infrared spectroscopy[31] (since these parameters are a reflection of the hybridization of a metal ion) and

- in the case of complexes having Pt-I bonds, Mossbauer parameters, which reflects differences between s character and overall σ and π interactions in the metal-iodide bond.[33]

Although the *trans* influence is partially dependent upon the total composition of a complex, the following trends have been observed:[34]

For neutral ligands : $PF_3 > PEt_3 > C_2H_4 > CO > H_2S > NH_3 > H_2O$

For anionic ligands: $H^- > SiH_3^- > CN^- > CH_3^- > I^- > Cl^- > OH^- > NO_2^-$

A comparison of the equilibrium constants corresponding to ground-state energy differences of Pt^{II}–DMSO complexes has shown the *trans* influence to vary as $NH_3 >$ DMSO $\approx C_2H_4 >$ $Br^- \approx Cl^- \approx H_2O$ with factors relative to H_2O of $10(NH_3)$: $4(DMSO)$: $3(C_2H_4)$: $1(Br^-, Cl^-)$.[35] In the case of σ-bonding ligands, there appears to be a correlation between the *trans* influence and the kinetic *trans* effect. For π-bonding ligands however, no correlation between these two phenomena is observed, presumably owing to differences in their origin.

There exists some degree of disagreement over the relative importance of the *cis* influence in square planar complexes. Molecular orbital calculations[34] performed have indicated the *cis* influence to be of comparable magnitude to the *trans* influence. For a series of Pt^{II}-I complexes it was calculated that the *cis* influence is highest for ligands having empty, low lying d orbitals.[34] The order of *cis* influence on a $PtLI_3^-$ complex was as follows:

L is neutral: $PF_3 > PEt_3 > C_2H_4 > H_2S > NH_3 > H_2O > CO$

L is anionic: $SiH_3^- > CH_3^- > OH^- > I^- > CN^- > H^- > Cl^- > NO_2^-$

The experimental evidence for the *cis* influence is much lower than that of the corresponding *trans* influence. The *cis* influences of Pt^{II}-DMSO compounds were found to be $NH_3 > H_2O \approx Cl^- \approx Br^- > C_2H_4 >$ DMSO   with factors relative to H_2O of

1-2(NH_3): 1(Br^-, Cl^-) : 0.3 (C_2H_4) : 0.1 (DMSO).[35] These values are considerably lower than those obtained for the corresponding *trans* influence factors.

2.4.6 *Effect of the Entering Nucleophile*

For a reaction that would involve attack of the entering ligand, one should certainly expect a dependence on the nucleophilicity of the entering ligand. In order to discuss the nucleophilicity of a ligand, the species interacting with the nucleophile must be defined. The nucleophilic reactivity order observed for Pt^{II} substitution reactions is as follows:[8,9]

$$PR_3 > I^-, SCN^-, N_3^- > NO_2^- > Br^- > Py > NH_3, Cl^- > H_2O > OH^-$$
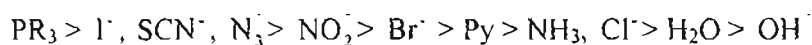
and a striking feature is that the nucleophilic character of the reagents does not correlate with their base strength.

It is generally taken that ligand nucleophilicity is influenced by various factors:[6]

a) *Basicity* -   the basicity of an entering ligand is characterized by its pK_a value, which correlates very well with ligand nucleophilicity towards the central metal atom.

b) *Polarizability* -   the *polarizability* or *softness* of a nucleophile is an important consideration. Soft nucleophiles have a preference for soft substrates whereas, *hard* (*nonpolarizable*) ligands prefer hard substrates. The observation that larger donors are effective nucleophiles toward Pt^{II} indicates that Pt^{II} is a soft centre.

c) *Oxidability* -   Ligands that undergo oxidation quickly are good nucleophiles. This ability is characterized by their standard reduction potentials or alternatively by polographic half-wave potentials.

d) _Solvating Energy_ - it is expected that better solvated ligands will be weaker nucleophiles, because in order to be bonded to a metal, a nucleophile must be freed of the bonded solvent, a process that requires energy.

e) _Metal centre_ - this factor limits the general applicability of nucleophilicity scales in inorganic chemistry since most show a marked dependence on the nature of the metal centre.

These factors mentioned above are generally difficult to define and as such the nucleophilicity scales are used much less in inorganic chemistry than in organic chemistry. In general, if the nature of the nucleophile is to be described, then a correlation of the reactivity with other properties of the ligand is required. This type of correlation is a linear free relationship (LFER). Experimental data that has been collected for the displacement of chloride from _trans_-PtL_2Cl_2 are presented in _Table 2.3_.

$$trans - PtL_2Cl_2 + Y \rightarrow trans - PtL_2ClY + Cl^- \qquad 2.22$$
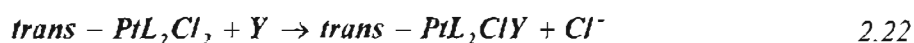
Table 2.3:   Effect of the entering nucleophile on the substitution reactions of trans-PtL$_2$Cl$_2$[a]

Y	L = Py	L = Pet$_3$	n^c_{Pt}
Cl$^-$	0.45	0.029	3.04
NH$_3$	0.47	-	3.07
NO$_2^-$	0.68	0.027	3.22
N$_3^-$	1.55	0.2	3.58
Br$^-$	3.7	0.93	4.18
I$^-$	107	236	5.46
SCN$^-$	180	371	6.65
PPh$_3$	249 000	-	8.93

[a] _Entries are 10^3 k with units of $M^{-1}s^{-1}$._

It can clearly be seen that the ligand dependence is not on the basicity toward a proton. The parameter, n°_{Pt}, defined for each ligand, is called the *nucleophilic reactivity constant*. This constant is defined as

$$\log\left[\frac{k_Y}{k_s}\right] = n^{\circ}_{Pt} \qquad\qquad 2.23$$

where k_Y and k_s represent the rate constant for the reaction of an entering nucleophile, Y, with $Pt(Py)_2Cl_2$ and the rate constant for attack by solvent (CH_3OH) on the complex respectively.

This constant is a measure of the reactivity of a nucleophile toward Pt and is useful for correlation with other ligand properties. Also, plots of k_Y for other Pt^{II} complexes versus n°_{Pt} are observed to be linear. Examples of these plots are shown in *Figure 2.13*.
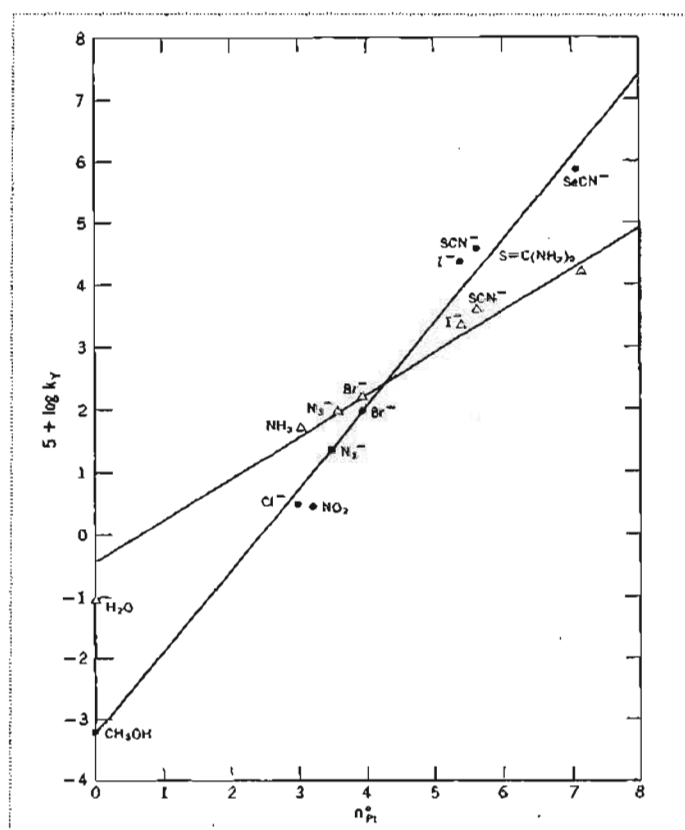
Figure 2.13:   <u>*Correlation of the rates of reaction of Pt^{II} complexes with the standard trans-*</u> <u>*$Pt(py)_2Cl_2$ for the different nucleophiles:* • = *trans-[Pt(PEt_3)_2Cl_2 in methanol at*</u> <u>*30 °C;* ▲ = *[Pt(en)Cl_2] in water at 35 °C.*[9]</u>

An LFER is given by the following equation;

$$\log k_Y = s n_{Pt}^* + \log k_s$$ 2.24

and is found to hold for a variety of Pt^{II} complexes and solvents. The constant s, which is referred to as the *nucleophilic discriminating factor*, is a measure of the sensitivity of the metal centre to the nucleophilicity of the entering ligand. A large value is an indication that the rate is very sensitive to changes in nucleophilic character.

The comparison of the complexes $Pt(dien)X^+$ (where $X = Br^-$, Cl^-, H_2O) offers confirmation of an often-stated postulate. The complex that is most reactive (*i.e.* it has the best leaving group) is least discriminating in its reactions (*i.e.* a small value of s).

2.4.7 *Effect of the Leaving Nucleophile*

Studies of substitution reactions should logically include the assessment of the ease of replacement of different groups from closely analogous substrates. The $Pt(dien)X^+$ complexes have provided excellent information with regard to leaving group effects. In this complex the three other coordination positions are kept constant by using the inert dien ligand, and the entering ligand in all cases is pyridine (py). The only variable is X, and therefore its effect on the rate of the reaction was investigated.[9]

In dissociation reactions a large dependence on the nature of the leaving group is expected, due to the bond between the metal and the leaving group being broken. However, for associative reactions the effect of the leaving group depends primarily on the extent of bond breaking in the transition state. Data for the reaction

$$Pt(dien)X^+ + py \rightarrow Pt(dien)py + X^{2+}$$ 2.25
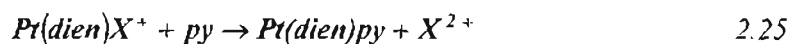
are summarized in *Table 2.4*.

Table 2.4: *The effect of leaving groups on the rates of substitution for the reaction of Pt(dien)X$^+$ with py.*[36,37]

X	k_{obs} / s^{-1}
NO$_3^-$	Very fast
H$_2$O	1900
Cl$^-$	35
Br$^-$	23
I$^-$	10
N$_3^-$	0.83
SCN$^-$	0.30
NO$_2^-$	0.050
CN$^-$	0.017

The data shows a decreasing rate for changes in X in the order:

$$NO_3^- > H_2O > Cl^- > Br^- > I^- > N_3^- > SCN^- > NO_2^- > CN^-$$
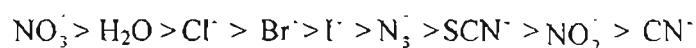
The spread in rates of approximately 10^6 in this series indicates that a substantial amount of bond breaking occurs within the transition state. This does not demand a dissociation process, but merely requires that the Pt-X bond breaking make a contribution comparable to that of the Pt-py bond forming.

It is significant that with only X changing in these systems, the order of labilities of the complexes does not parallel their order of instabilities. Hence, the complex Pt(dien)Cl$^+$ reacts 2000 times faster than the more stable Pt(dien)CN$^+$ complex. Furthermore the leaving groups high in the *trans* effect series are slowly replaced. This is in accord with the combined σ and π-*trans* effect theory, which states that good *trans* activators are strongly bonded to the metal. The reverse, that a poor *trans* activator is readily replaced, need not be true. Both NH$_3$ and OH$^-$ are low in the *trans* effect series, but they are very difficult to replace in a Pt^{II} complex.

This lack of coordination of the bond strength with *trans* effect is not surprising since the amount of covalent bonding into the σ_x orbital must be relatively small for electronegative ligands such as NH_3 and OH^-, because of the high energy of the 6_p orbital of platinum. Hence, the bond strength is largely determined by non-stereospecific σ_s and σ_d bonds and by ionic interactions.

2.4.8 *Solvent Effects*

There is considerable evidence supporting the fact that the solvent path for planar substitution involves a direct displacement by the solvent. Therefore it is expected that the contribution made by this path to the overall rate of a reaction would increase with increasing coordinating ability of the solvent. This is best shown by the experimental data (*Table 2.5*) obtained for the solvent effect on the rate of $^{36}Cl^-$ exchange with *trans*-$Pt(py)_2Cl_2$.

$$trans - [Pt(py)_2Cl_2] + {}^{36}Cl^- \longrightarrow trans - [Pt(py)_2Cl(^{36}Cl)] + Cl^- \qquad 2.26$$

Table 2.5:   *Effect of solvent on the rate of $^{36}Cl^-$ exchange with trans-Pt(py)$_2$Cl$_2$ at 25 °C.*[38]

Solvents[a]	$k / 10^{-5} \, s^{-1}$	Solvents[b]	$k / M^{-1}s^{-1}$
DMSO	380	CCl_4	10^4
H_2O	3.5	C_6H_6	10^2
CH_3NO_2	3.2	$t\text{-}C_4H_9OH$	10^{-1}
C_2H_5OH	1.4	EtOAc	10^{-2}
$n\text{-}C_3H_7OH$	0.42	$(CH_3)_2CO$	10^{-2}
		DMF	10^{-3}

Under experimental conditions of moderately low $^{36}Cl^-$ concentrations, the solvents were divided into two groups. The first of these containing the good coordinating solvents (*i.e.* a) provided a purely solvolytic pathway for exchange ($k_s >> k_{Cl}[^{36}Cl^-]$). The poor coordinating solvents (*i.e.* b) such as benzene, carbon tetrachloride, and sterically hindered alcohols, contribute little to the overall rate of the reaction. The exchange takes place with

^{36}Cl$^-$ acting as the nucleophile (k_{Cl}[^{36}Cl$^-$] >> k_s). For good coordinating solvents, an interesting point to note is that the values of k_s increase in the following order:

$$ROH < H_2O < CH_3NO_2 < DMSO$$

This is a strong indication that bond formation between the metal and the solvent in the transition state is important. Since the sulfur ligand is a better nucleophile than oxygen towards Pt^{II} it follows that DMSO is a better reagent as compared to water. It is known that Pt^{II} forms stable complexes with DMSO and that the mode of bonding is Pt-S. However, if the role of the solvent were to primarily solvate the departing ^{36}Cl$^-$, then H$_2$O rather than DMSO would be the more efficient solvent for the reaction. This would be the case if bond-breaking were of primary importance and hence the experimental results would argue against this.[13]

2.4.9 Steric Effects

A classical way of obtaining information on the molecularity of a substitution reaction is to investigate the steric effect on its rate of reaction. If a bimolecular displacement is involved an increase in steric hindrance causes a corresponding decrease in the rate, whereas steric accelerations is generally observed for a dissociative process.

Reactivity is very sensitive to the electron displacement properties of the ligand *trans* to the leaving group and insensitive to variations in its bulk whilst the opposite is true for the *cis* ligands. It is easy to see how steric hindrance exerts a much greater effect from the *cis* position by using models of *cis* and *trans* isomers containing a selection of bulky ligands. An increase in the cone angle of the *trans* ligand or the introduction of bulky ligands adjacent to the donor atoms will increase the non-bonding repulsions between this ligand and its *cis* partners, but this is not a drastic change on going from the ground state to the transition state. Conversely, an increase in the bulk of the ligands *cis* to the leaving group results in further crowding when the number of *cis* partners changes from two to three in the trigonal bipyramidal state.

A classic example of steric hindrance is the way in which the reactivity of complexes of the type [Pt(PEt$_3$)$_2$RCl] changes with increasing *ortho*-methyl substitution in the aryl group, R, along the sequence R = phenyl, 2-methylphenyl, 2,5,6-trimethylphenyl (*Table 2.6*).[1,39] The absence of any significant response to changes in the nature of the substituent in the 4-position shows that this effect is steric in origin and the much greater response when R is *cis* to the leaving groups is fully evident in both the values for k_1, the solvolytic pathway and k_2 for the reactions of the strong nucleophile CN$^-$. This was one of the earliest indications that the transition state for substitution of square-planar complexes was trigonal bipyramidal.

Table 2.6: *The steric cis effect of ortho-methylation of an aryl ligand. Rate constants for the reactions 1[†] and 2[††] are k_1 and k_2 respectively.*

R	phenyl	p-tolyl	o-tolyl (CH₃)	o-ethylphenyl (CH₂CH₃)	2,4,6-trimethylphenyl	phenyl	o-tolyl (CH₃)	2,4,6-trimethylphenyl
X	cis-Br	cis-Br	cis-Br	cis-Br	cis-Br	trans-Cl	trans-Cl	trans-Cl
$10^3 k_1$ (s⁻¹)	6000	4200	54.4	16.2	0.19	40.0	2.29	0.405
k_2 (M⁻¹s⁻¹)	21400	-	2460	-	0.312	34.8	0.90	0.043

[†] Reaction 1 - $[Pt(PEt_3)_2 RX]$ + MeOH → $[Pt(PEt_3)_2 R(MeOH)]^+$ + X⁻

[††] Reaction 2 - $[Pt(PEt_3)_2 RX]$ + CN⁻ → $[Pt(PEt_3)_2 R(CN)]^-$ + X⁻

Although the effects of varying the electron displacement properties of the *cis* ligands upon the reactivities of the substrates are small compared with *trans* effects they can still be seen. Due to the effect being relatively small, they become difficult to systematize and it is not easy to distinguish a site-specific phenomenon from a general effect. A proper study of the effect that a *cis* ligand might exert would include means of anchoring the ligand *trans* to the site of variation; otherwise one has no control over the choice of leaving group.[40-43]

A study of this nature was conducted by Jaganyi *et al.*[44], whereby the substitution behaviour of terdendate Pt[II] complexes of the type [Pt(N-N-N)] or [Pt(N-N-C)] (*Figure 2.14*) with varying substituents on the central pyridine moiety by a series of nucleophiles, the results of which are shown in *Table 2.7*, was investigated.
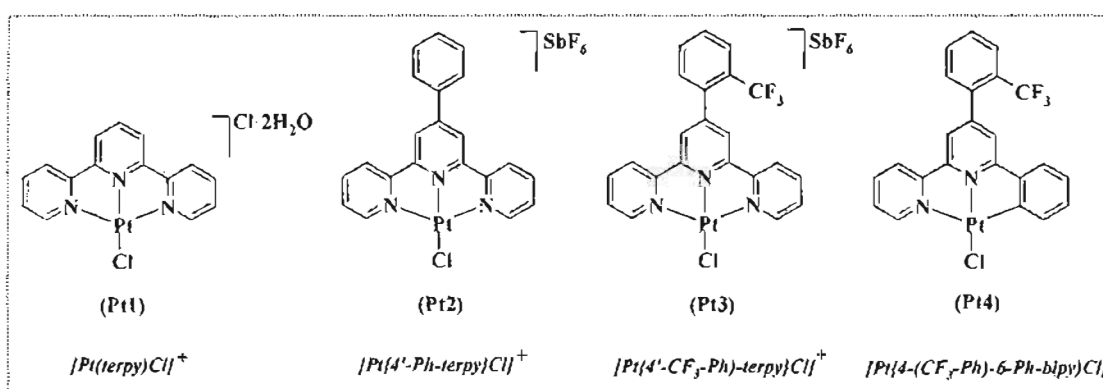
Figure 2.14: *Structural formula of the complexes investigated by Jaganyi et al.*[44]

Table 2.7: *Summary of rate constants for the substitution of Cl⁻ by TU, DMTU, TMTU in methanol at 25 °C.*[44]

Nucleophile	k_2, $M^{-1}s^{-1}$			
	Pt 1	Pt 2	Pt 3	Pt 4
TU	1494 ± 10	1258 ± 13	1933 ± 32	123.0 ± 0.3
DMTU	448 ± 10	377 ± 7	662 ± 3	72.0 ± 0.6
TMTU	82 ± 4	100 ± 3	144 ± 1	29.0 ± 0.5
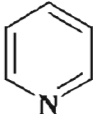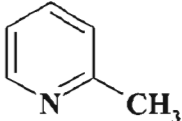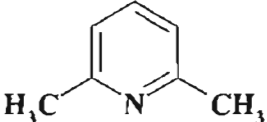
The role of the *cis* σ- effect was established by comparing the reactivities of complexes, Pt 3 and Pt 4. The data obtained (*Table 2.7*) suggests that the introduction of the Pt-C bond in the *cis* position to the leaving group (*i.e.* Cl⁻) reduces its lability by a factor of sixteen if the

entering nucleophile is TU, and similar retardations on the rates of substitution were observed for DMTU and TMTU. The accumulation of electron density at the platinum centre results in the corresponding decrease in reactivity for **Pt 4**. The *cis* effect of the carbon atom was shown to decrease the lability of complexes whose reactivity is enhanced by the presence of strong π-electron withdrawing backbone.

An interesting point to note is that the *cis* and *trans* effects have opposite net effects and influence the lability of the leaving group in a different manner. The latter enhances the rate of substitution through ground state destabilization whilst the former slows down the process by an accumulation of electron density on the metal centre.

The rate constants (*Table 2.8*) obtained for the hydrolysis of *cis*-[PtClL(PEt₃)₂] complexes further illustrates the effects of steric hindrance.

Table 2.8:   <u>*Rate Constants for Substitution of Cl⁻ by H₂O in cis-[PtClL(PEt₃)₂] at 25 °C.*</u>[45]

L	k / s^{-1}
	8×10^{-2}
	2.0×10^{-4}
	1.0×10^{-6}

The methyl group adjacent to the N donor atom greatly decreases the rate in the 2-methylpyridine complex, as they block the positions either above or below the plane. In the 2,6-dimethylpyridine both the positions above and below the plane are blocked (*Figure 2.15 (a)*). Therefore, along the series the attack by H₂O is hindered by the presence of the methyl groups. This effect is seen to be small if **L** is *trans* to **Cl**. This difference is explained by the methyl groups being further away from the entering and leaving ligands

in the trigonal-bipyramidal activated complex, if the pyridine ligand is in the trigonal plane (*Figure 2.15 (b)*).
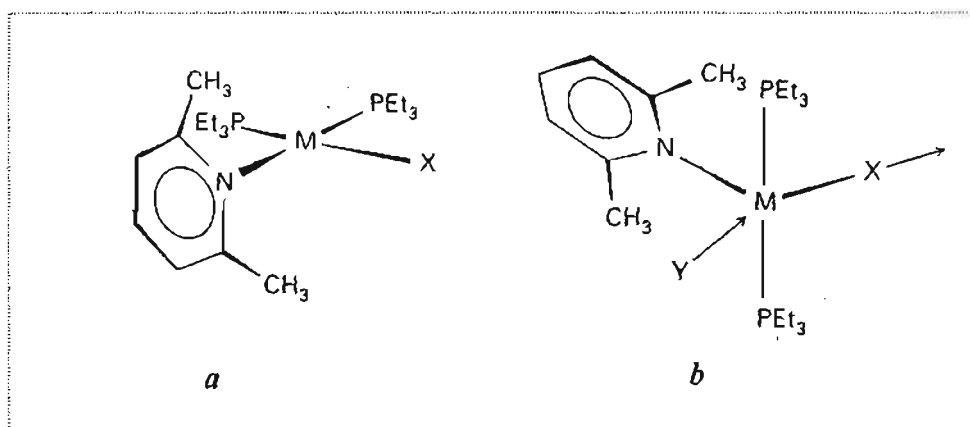
Figure 2.15: *The effect of steric crowding on the cis and trans position.*[45]

2.5 Dissociative Mechanism for Substitution in Four-Coordinate Planar Metal Complexes

As a result of the ready availability of the pathway for associative activation, it has long been of considerable interest to find out just how dominant this pathway can be in the substitution reactions of four-coordinate planar d^8 metal complexes. The approach to be taken in order to favour a dissociative mechanism should bear in mind the following:[46]

- high electron density at the metal which would prevent the approach of an axially incoming nucleophile,

- bond weakening at the leaving group due to the *trans* influence of strong σ-donors and,

- the stabilization by the remaining set of three interplane ligands of a three coordinated 14-electron intermediate without changing the singlet ground state.

These factors however, do not apply in the presence of ligands that have π-accepting capabilities. This can be seen in the complex *cis*-[PtPh$_2$(CO)(SEt$_2$)], whereby the relief of electron density at the metal by the carbon monoxide and the presence of the low lying LUMO, π-delocalised over the Pt-C-O atoms, facilitates a changeover of mechanism from a dissociative one to an associative pathway of activation.[47]

A consequence of a mechanistic changeover for the substitution reactions of square planar complexes is the stereochemistry that is formed. The dissociation of a ligand from a square planar complex gives rise to a three-coordinate, T-shaped intermediate (*Figure 2.16*). The first convincing evidence for the presence of a three-coordinate, 14-electron species as a key intermediate in nucleophilic substitution reactions comes from the kinetic study of complexes having a set of donor atoms of the type cis-[Pt(C,C)(S,S)] (where C is a strong σ-donor carbon group and S a thioether or a sulfoxide).[46,48]
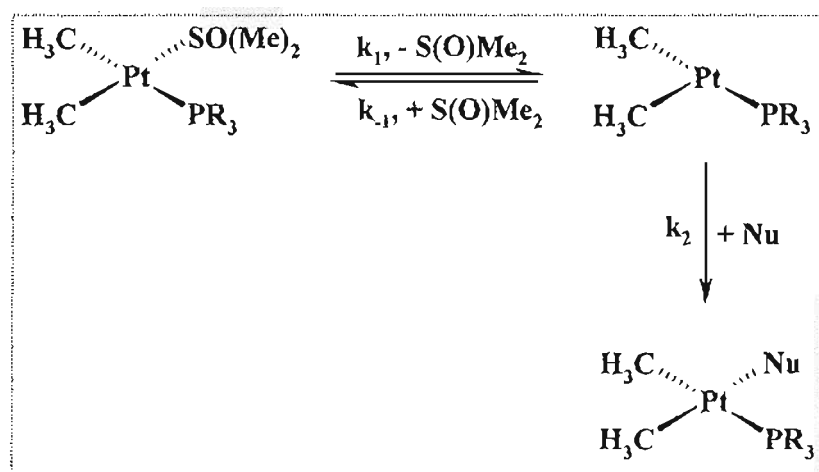
Figure 2.16: *Diagrammatic representation of the non-stereospecificity resulting in intramolecular rearrangements during the substitution reaction of the cis-[PtMe₂(Me₂SO)(PR₃) complex following a dissociative pathway.*[46]

2.6 *The Substitution Reactions of Dinuclear Pt^{II} Complexes*

Following Rosenburg's discovery of the anti-tumour properties of cis-[Pt(Cl₂(NH₃)₂] (cisplatin) in 1969[49], thousands of Pt complexes have been synthesized and evaluated as potential anti-tumour drugs. Promising candidates among these complexes are bridged dinuclear or trinuclear Pt^{II} complexes, which can form DNA adducts that are not accessible to mononuclear Pt^{II} complexes, such as 1,3- and 1,4- GG interstrand cross-links.[50-52] The nature of the bridging ligand varies significantly.

Although the role of the bridge on the DNA binding properties and product formation has been investigated intensively and the results have been interpreted in terms of charge,

hydrogen bonding, length and flexibility of the bridging ligand[53], there is less data regarding the influence of the bridging ligand on the reactivity and thermodynamic properties of the two platinum centres. Such data is available for the trinuclear complex $[\{trans\text{-}PtCl(NH_3)_2\}_2\text{-}\{\mu\text{-}trans\text{-}Pt(NH_3)_2(NH_2(CH_2)_6NH_2\}]^{4+}$ (BBR3464), which is currently being used in clinical trials and its corresponding dinuclear complex, $[\{trans\text{-}PtCl(NH_3)_2\}_2\text{-}\mu\text{-}NH_2(CH_2)_6NH_2]^{2+}$. It is suggested that the reactivity and properties of the first platinum centre is independent of the state of the second and *vice versa*.[54,55] However an interaction between the two platinum centres has been observed in some cases.[56] Data present in literature is insufficient to formulate a relationship between the reactivity of the two platinum centres and the nature of the bridging ligand.[57]

Studies conducted to date, have investigated the influence of four different bridges on the reactivity of each of the platinum centres of the dinuclear complex and thereafter compared to the corresponding mononuclear complex. The following dinuclear complexes were investigated by Hofmann and van Eldik[57]; $[Pt_2(N,N,N',N'\text{-tetrakis})2\text{-}pyridylmethyl)benzene\text{-}1,3\text{-}diamine)(H_2O)_2]^{4+}$ **(mPh)**, $[Pt_2(N,N,N',N'\text{-tetrakis})2\text{-}pyridylmethyl)benzene\text{-}1,4\text{-}diamine)(H_2O)_2]^{4+}$ **(pPh)**, $[Pt_2(N,N,N',N'\text{-tetrakis})2\text{-}pyridylmethyl)1,3\text{-}propanediamine)(H_2O)_2]^{4+}$**(Pro)** and $[Pt_2(N,N,N',N'\text{-tetrakis})2\text{-}pyridylmethyl)1,4\text{-}butanediamine)(H_2O)_2]^{4+}$ **(But)** (*Figure 2.17*) as a function of concentration and temperature, the results of which are shown in *Table 2.9*.

The variation of the bridging diamine spacer enabled a systematic study of the influence of chain length, flexibility and hybridization of the bridge (aliphatic or aromatic backbone) to be conducted, and thereafter study the effects on the thermodynamic and kinetic properties of the two platinum centres.
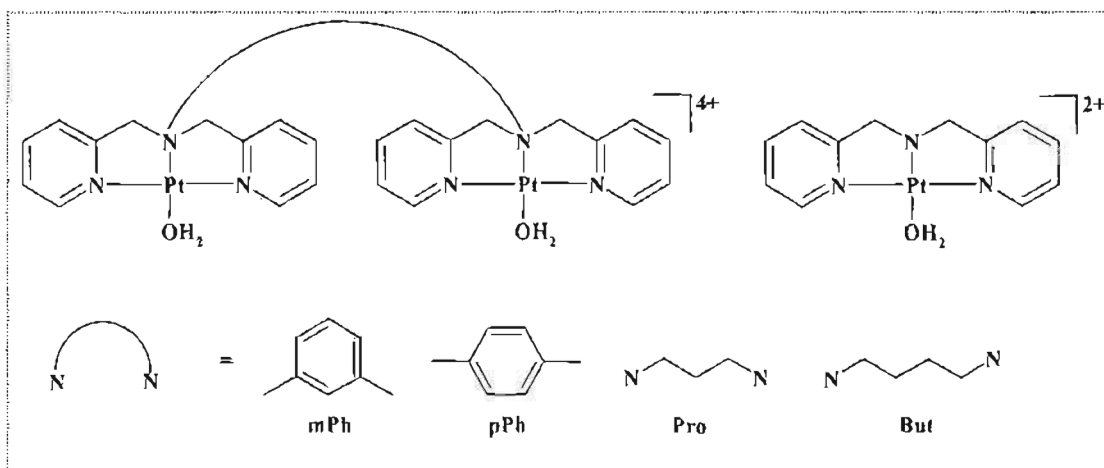
Figure 2.17: _Schematic structures and abbreviations used for the investigated complexes._[57]

Table 2.9: _Summary of second-order rate constants and corresponding activation parameters for the displacement of water by chloride and pKa values for the first and second deprotonation steps of the aqua complexes._[57]

	Mononuclear	mPh	pPh	Pro	But
pK_{a1}	5.5	3.33	3.34	4.36	3.94
pK_{a2}	-	4.76	4.46	6.07	5.46
k_1/ M^{-1}s^{-1}	19.1 ± 0.1	312 ± 6	265 ± 7	649 ± 38	249 ± 11
k_2/ M^{-1}s^{-1}	-	24.4 ± 0.2	88 ± 1	132 ± 6	40 ± 1
$\Delta H^{\#}_1$/ kJ mol^{-1}	64.5 ± 0.1	55.1 ± 1.3	61.1 ± 1.8	63.8 ± 0.7	57.8 ± 0.8
$\Delta H^{\#}_2$/ kJ mol^{-1}	-	60.5 ± 0.9	60.5 ± 1.5	60.0 ± 0.8	57.7 ± 1.5
$\Delta S^{\#}_1$/J K^{-1} mol^{-1}	-3.5 ± 1	-12 ± 4	5 ± 6	22 ± 2	-6 ± 3
$\Delta S^{\#}_1$/J K^{-1} mol^{-1}	-	-15 ± 3	-6 ± 3	-4 ± 3	-21 ± 5

It has been shown recently that the pK_a value of a water molecule coordinated to Pt^{II} can be used as a measure of the electrophilicity of the metal centre.[58,59] Electron withdrawing π-acceptor effects stabilize the electron rich hydroxo species in comparison to the aqua complex and as a result lead to lower pK_a values. Contrary to this, the pK_a value increases if the σ-donor capacity of the *trans* ligand is enhanced. It is widely acknowledged that the pK_a value of anilines is lower than that of tertiary amines, with the higher basicity suggesting that amines are better σ-donor than anilines. This would account for the fact

that the pK_a values of the aniline bridged complexes (mPh and pPh) are lower than those of the corresponding, stronger σ-donating aliphatic diamine bridged complexes Pro and But.

The pK_a values obtained for all the dinuclear complexes were at least 1.1 units lower than those obtained for the corresponding mononuclear complexes. Similar effects have been observed for the following dinuclear complexes synthesized by Farrell et al., trans-{PtCl(NH$_3$)$_2$}$_2$-{μ-trans-Pt(NH$_3$)$_2$(NH$_2$(CH$_2$)$_6$NH$_2$}]$^{4+}$(1,0,1/,t,t) and trans-[{PtCl(NH$_3$)$_2$}$_2$- μ -NH$_2$(CH$_2$)$_6$NH$_2$]$^{2+}$ (1,1/t,t)[54,55] whereby the values are about 0.4 units lower than for the corresponding mononuclear complex [Pt(NH$_3$)$_3$OH$_2$]$^{2+}$. This observation could be related to the length of the bridging ligand and the overall charge of the complex.

An interesting point to note, is that the complexes investigated by Hofmann and van Eldik, display a second deprotonation step, whereas the complexes investigated by Farrell et al.[54,55], the pK_a values for the first and second deprotonation step could not be separated. This could be attributed to the fact that the distance between the two platinum centres is shorter in complexes investigated by Hoffmann and van Eldik, as opposed to the (1,0,1/,t,t) and (1,1/t,t) complexes. An important point to note, is that it is the average distance between the two Pt^{II} centres that is important and not the maximum possible distance as a number of conformers can exist with shorter Pt-Pt distance as a result of the higher flexibility of the bridging ligand.[57]

Substitution reactions studies conducted on the mononuclear complex with various nucleophiles have shown that the mononuclear complex follows an associative mechanism. The observed activation parameters for the mPh, pPh, Pro and But were also shown to be associative in nature, with the exception being the first reactions steps for pPh and Pro. There were no significant differences obtained for the enthalpy values for both steps in all four complexes. In all cases the lability of the dinuclear bridged complexes was shown to differ markedly from that of the corresponding mononuclear complex. This can be attributed to the enhanced nucleophilicity of the dinuclear Pt^{II} centres. The reactivity of one Pt^{II} centre was shown to be dependent on the state of the other Pt^{II} centre, which leads to different thermodynamic as well as kinetic properties for the first and second reaction steps respectively. The interactions between the two Pt^{II} centres depend on the Pt-Pt distance; the

closer the proximity of the two metal centres, the larger the interaction between them. These observations have led to the suggestion that the observed interaction does not result from an electronic effect mediated by the bridging ligand, since a larger difference between the behaviour of the aromatic (sp^2) and aliphatic (sp^3) bridged complexes would be expected.[48]

However, in order to fully understand the influence of the aliphatic chain length on the dinuclear complexes in terms of their folding abilities or the average Pt-Pt distance and interactions, a wider range of bridging ligands will have to be studied.

References

1. Tobe, M.L. & Burgess, J., *Inorganic Reaction Mechanisms*, Addison Wesley Longman Ltd., Essex, **1999**, p30-43, 70,112.

2. Wilkins, R.G., *Kinetics and Mechanism of Reactions at Transition Metal Complexes*, 2nd Ed., VCH, Weinheim, **1991**, p 199-201, 232-242.

3. Tobe, M.L., *Comprehensive Coord. Chem.*, **1987**, *1*, Ch 7.1.

4. Henderson, R.A., *The Mechanisms of Reactions at Transition Metal Sites*, Oxford University Press, Oxford, **1993**, p 2-21.

5. Ingold, C.K., *Structure and Mechanism in Organic Chemistry*, 2nd Ed., Cornell University Press, Ithaca, NY, **1969**, p 241.

6. Asperger, S., *Chemical Kinetics and Inorganic Reaction Mechanisms*, 2nd Ed., Kluwer Academic/ Plenum Publishers, NY, **2003**, p 38-40.

7. Jordan, R.B., *Reaction Mechanisms of Inorganic and Organometallic Systems*, Oxford University Press, **1991**, p 29-63.

8. Langford, C.H. & Gray, H.B., *Ligand Substitution Processes*, Benjamin Inc., NY, **1965**.

9. Atwood, J.D., *Inorganic & Organometallic Reaction Mechanisms*, 2nd Ed., Wiley-VCH, **1997**, pp 43-61.

10. Basolo, F., *Coordination Chem. Reviews*, **1996**, *154*, 151.

11. Cross, R.J., *Chem. Soc. Reviews*, **1985**, *14*, 197.

12. Catallini, L., *Progress Inorg.Chem.*, **1970**, *13*, 263.

13. Cross, R.J., *Advance. Inorg. Chem.*, **1989**, *34*, 219.

14. Basolo, F. & Pearson, R.J., *Mechanisms of Inorganic Reactions*, John Wiley & Sons., NY, **1967**.

15. Banerjea, D., Basolo, F., Pearson, R.J., *J. Amer. Chem. Soc.*, *79*, **1957**, 4055.

16. Haake, P., Chan, S.C., Jones, V., *Inorg. Chem.*, **1970**, *9*, 1925.

17. Beattie, J.K., *Inorg. Chim. Acta.*, **1983**, *76*, L69.

18. Peloso, A., *Coord. Chem. Reviews*, *56*, **1973**, 2179.

19. Pearson, R.J., *J. Amer. Chem. Soc.*, *85*, **1963**, 3533.

20. Pearson. R.J., *J. Chem. Edu.*, *64*, **1987**,561.

21. Belucco, U., *Organometallic and Coordination Chemistry of Platinum*, Academic press, London, **1974**, pp 138-160.

22. Kuznik, N. & Wendt, O.F., *J. Chem. Soc. Dalton Trans.*, **2002**, 3074.

23. Plutino, M., Otto, S., Roodt, A., Elding, L.I., *Inorg. Chem.*, *38*, **1999**, 1233.

24. Chatt, J., Duncanson, A., Venanzi, L.M., *J. Chem. Soc.*, **1955**, 4456.

25. Orgell, L.F., *J. Inorg. Nucl. Chem.*, *2*, **1956**, 137.

26. Basolo, F. & Pearson, R.J., *Mechanisms of Inorganic Reactions*, John Wiley & Sons., New York, **1968**, pp 369-410.

27. Burdett, J.K., *Inorg Chem.*, *15*, **1976**, 2349.

28. Basolo, F., Chatt, J., Gray, H.B., Pearson, R.J., Shaw, B.L., *J. Chem. Soc.*, **1961**, 2201.

29. Siegel, H., *Metal Ions in Biological Systems: Metal Complexes as Anticancer Agents*. *Vol 11*, Marcel Dekker Inc., NY, **1980**, pp 79-81.

30. Pidcock, A., Richards, R.E., Venanzi, L.M., *J. Chem. Soc., A.*, **1966**, 1707.

31. Appleton, T.G., Clark, H.C., Manzer, L.E., *Coord. Chem. Reviews*, *10*, **1973**, 335.

32. Manaljovic-Muir, L.J., Muir, K.W., *Inorg. Chim. Acta.*, *10*, **1974**, 47.

33. Bancroft, G.M. & Butler, K.D., *J. Amer. Chem. Soc.*, *96*, **1974**, 7208.

34. Armstrong, D.R., Foryune, R., Perkins, P.G., Dickinson, R.J., Parish, R.V., *Inorg. Chim. Acta.*, *17*, **1976**, 73.

35. Elding, L.I. & Groning, O., *Inorg. Chem.*, *17*, **1978**, 1872.

36. Mellor, D.P., *Chem. Reviews*, *33*, **1943**, 137.

37. Basolo, F., Gray, H.B., Pearson, R.J., *J. Amer. Chem. Soc.*, *82*, **1960**, 4200.

38. Pearson, R.J., Gray, H.B., Basolo, F., *J. Amer. Chem. Soc.*, *82*, **1960**, 787.

39. Romeo, R., Minniti, D., Trozzi, M., *Inorg. Chem.*, *15*, **1976**, 1134.

40. Jaganyi, D., Hofmann A., van Eldik, R., *Agnew. Chem., Int. Ed.*, *40*, **2001**, 1680.

41. Hofmann, A., Jaganyi, D., Munro, O.Q., Liehr, L., van Eldik, R., *Inorg. Chem.*, *42*, **2003**, 1688.

42. Braddock, P.D., Romeo, R., Tobe, M.L., *J. Chem. Soc. Dalton Trans.*, **1993**, 233.

43. Cattalini, L., Guidi, F., Tobe, M.L., *J. Chem. Soc. Dalton Trans.*, **1992**, 3021.

44. Jaganyi, D., Reddy, D., Gertenbach, J.A., Hofmann, A., van Eldik, R., *J. Chem. Soc. Dalton Trans.*, **2004**, 299.

45. Shriver, D.F. & Atkins, P.W., *Inorganic Chemistry*, 3rd Ed., Oxford University Press, **1999**, p 474.

46. Romeo, R., Monsu Scolaro, L., Plutino, M.R., *et al.*, *Inorganica Chimica Acta.*, *350*, **2003**, 143.

47. Romeo, R., Grassi, A., Monsu-Scolaro, L., *Inorg. Chem.*, *31*, **1992**, 4383.

48. Plutino, M.R., Monsu-Scolaro, A., Romeo, R., Grassi, A., *Inorg. Chem.*, *39*, **2000**, 2712.

49. Rosenburg, B., Van Champ, L., Trosko, E., Mansour, V.H., *Nature*, *22*, **1969**, 385.

50. Farrell, N., *Comments Inorg. Chem.*, *16*, **1994**, 373.

51. Zou, Y., Van Houten, B., Farrell, N., *Biochemistry*, *33*, **1994**, 5404.

52. Farrell, N., Appleton, T.G., Qu, Y., Roberts, J.D., Soares-Fontes, A.P., Skov, K.A., Zou, Y., *Biochemistry*, *34*, **1995**, 13840.

53. Farrell, N., Qu, Y., Bierbach, U., Valsecchi, M., Menat, E., *Cisplatin: Chemistry and Biochemistry of a Leading Anticancer Drug*, Wiley-VCH., Weinheim, **1999**, p 479.

54. Davies, M.S., Cox, J.W., Berners-Price, S.J., Barklage, W., Qu, Y., Farrell, N., *Inorg. Chem.*, *39*, **2000**, 1710.

55. Davies, M.S., Thomas, D.S., Hegmans, A., Berners-Price, S.J., Farrell, N., *Inorg. Chem.*, *41*, **2002**, 1101.

56. Kortes, R.A., Geib, S.J., Lin, T., Shepherd, R.E., *Inorg. Chem.*, *38*, **1999**, 5045.

57. Hofmann, A. & van Eldik, R., *J. Chem. Soc. Dalton Trans.*, **2003**, 2979.

58. Hofmann, A., Jaganyi, D., Munro, O.Q., Liehr, G., van Eldik, R., *Inorg. Chem.*, *42*, **2003**, 1688.

59. Jaganyi, D., Hofmann, A., van Eldik, R., *Angew. Chem. Int. Ed.*, *40*, **2001**, 1680.

Chapter 3

Kinetic Theory & Techniques

Chapter 3

Kinetic Theory & Techniques

3.1 Introduction

A reaction rate may be defined as a measure of how quickly a reaction occurs. A precise, quantitative definition must therefore relate the quantities of reactants and products to time, or more accurately, relate changes in quantities to changes in time. Therefore it is logical to express reaction rates in terms of time derivatives of concentration.[1] Changing one of several factors can enhance this rate. These factors include:-[2]

1. Concentration - the rate of a reaction is proportional to the number of collisions experienced by the molecules of reactant. Thus, the number of collisions experienced increases proportionally with an increase in reactant concentration.

2. Solvent properties - there are various factors that have an effect on the reaction rates and these include: solvent polarity, viscosity and donor number. Buffer components may change a reaction rate as well as added electrolytes.

3. Physical conditions - temperature and pressure affect reaction rates, but both are normally kept constant in a given determination.

4. Intensity of absorbed radiation - there are certain reactions *e.g.* photosensitive reactions that are influenced by the amount of light available to it. The light level that is present within an optical spectrophotometer that utilizes monochromatic light may not pose any problems, however, continuous exposure of the sample to white light may have an adverse effect on the rate of a photosensitive reaction.

Among the factors mentioned above, the most important variable is the concentration, as this can be used to determine the rate law whilst other variables are held constant. Therefore a kinetic study would involve the collection of data of concentration versus time for a reactant or product. This may be achieved by studying the time dependence of a

variable that is proportional to the concentration, such as absorbance. The concentration-time data is thereafter fitted to an appropriate model that allows for the determination of the rate constant.

A summary of some of the integrated rate laws as well as some of the experimental techniques that are applicable to the study conducted, are presented in this chapter.

3.2 *Rate Laws*

The rate of a reaction is expressed in terms of time derivatives of concentration.

$$Rate = \frac{-d[reactant]}{dt} = \frac{d[product]}{dt}$$ 3.1

The units of rate are expressed in molarity per second (M s^{-1}). The rate law describes the rate of a reaction in terms of the concentrations of all species affecting the rate and a general way of expressing this can be described as:

$$Rate = -k\prod_i [A_i]^{\alpha_i} [X_j]^{\beta_i}$$ 3.2

where A_i is the reactants, k is the rate constant, and X_j are the other species that may have an effect on the term.

The reaction order can therefore be defined as

$$Reaction\, Order = \sum_i \alpha_i$$ 3.3

The units of the rate constant k are therefore dependent upon the rate order.[3]

3.3 Integrated Rate Equations

3.3.1 First-Order Reactions

Most reactions are either first-order or are carried out under conditions that approximate first-order. For a first order reaction of the type,

$$A \xrightarrow{k_1} C \qquad \qquad 3.4$$

the rate of the reaction is as follows

$$Rate = k_1 [A]_1 = \frac{-d[A]}{dt} \qquad \qquad 3.5$$

which yields on rearrangement

$$\frac{-d[A]}{[A]_1} = k_1 dt \qquad \qquad 3.6$$

Integrating from $t = 0$ ($[A]_0$) to $t = t$ ($[A]_t$) gives

$$\int_{[A]_o}^{[A]_t} \frac{d[A]}{[A]_1} = -\int_o^t k_1 dt \qquad \qquad 3.7$$

$$ln\frac{[A]}{[A]_o} = -k_1 t \qquad \qquad 3.8$$

Equivalent forms of the integrated first-order rate *Equation 3.8* are shown below (*Equation 3.9-3.10*)

$$ln[A]_1 = -k_1 t + ln[A]_o \qquad \qquad 3.9$$

or

$$[A]_1 = [A]_o e^{-k_1 t} \qquad \qquad 3.10$$

Thus for a first-order reaction, a plot of $ln[A]_1$ versus t should be linear, with the first order rate constant being represented by the slope. The dimension of a first-order rate constant is time^{-1}, usually represented as s^{-1}.[1-5]

3.3.2 *Reversible First-Order Reactions*

In principle, all reactions are reversible and although simple considerations suggest ways of driving many reactions in one direction only, there are systems where reversibility cannot be ignored. The simplest of these is the reversible, first-order reaction.

$$A \underset{k_b}{\overset{k_f}{\rightleftharpoons}} B \qquad\qquad 3.11$$

Recognizing that loss of a reagent corresponds to a negative rate and gains to a positive rate, the rate law applicable to this system is:

$$Rate = \frac{d[B]}{dt} = -\frac{d[A]}{dt}$$

$$= k_f[A]_t - k_b[B]_t \qquad\qquad 3.12$$

At time $t = 0$, $[B]_0 = 0$, and $[A]_t = [A]_o$, consequently at any given time

$$[B]_t = [A]_o - [A]_t \qquad\qquad 3.13$$

Substitution of *3.13* into *3.12* gives

$$-\frac{d[A]}{dt} = k_f[A]_t - k_b([A]_o - [A]_t) \qquad\qquad 3.14$$

No net reaction occurs at equilibrium, and hence

$$-\frac{d[A]}{dt} = 0 \qquad\qquad 3.15$$

Applying *Equation 3.15* to *3.12* and *3.14* affords the following equilibrium expression

$$k_f[A]_{eq} = k_b[B]_{eq} = k_b([A]_o - [A]_{eq}) \qquad\qquad 3.16$$

which implies that

$$[A]_o = \frac{k_f + k_b}{k_b}[A]_{eq} \qquad\qquad 3.17$$

Substitution of *3.17* into *3.14* affords the following term

$$-d\frac{[A]}{dt} = (k_f + k_b)[A]_t - (k_f + k_b)[A]_{eq} \qquad\qquad 3.18$$

Subsequent separation of variables

$$\frac{d[A]}{([A]_t - [A]_{eq})} = -(k_f + k_b)\,dt \qquad\qquad 3.19$$

Integration of *3.19* gives

$$\int_{[A]_0}^{[A]_t} \frac{d[A]}{([A]_t - [A]_{eq})} = -(k_f + k_a)\int_0^t dt \qquad\qquad 3.20$$

which affords

$$ln\left(\frac{[A]_o - [A]_{eq}}{[A]_t - [A]_{eq}}\right) = -(k_f + k_b)t \qquad\qquad 3.21$$

An equivalent form of *Equation 3.21* is shown in *Equation 3.22*

$$ln([A]_t - [A]_{eq}) = -(k_f + k_b)t + ln([A]_o - [A]_{eq}) \qquad\qquad 3.22$$

A plot of $ln([A]_t - [A]_{eq})$ versus time should give a straight line with a slope that corresponds to $-(k_f + k_b)$.

Evaluation of the equilibrium constants allows one to determine the individual rate constants k_f and k_b respectively.

$$K_{eq} = \frac{[B]_{eq}}{[A]_{eq}} = \frac{k_f}{k_b} \qquad\qquad 3.23$$

With the observed rate constant, k_{obs}.

$$k_{obs} = (k_f + k_b) \qquad\qquad 3.24$$

The most difficult problem encountered in treating reversible first-order reactions is in accurately measuring $[A]_{eq}$.[1-5]

3.3.3 *Second-Order Reactions*

Second-order reactions can be divided into two types. The first type is that when the rate is second order with respect to one of the reactants and zero order with respect to the second reactant. The second type that will be analyzed in further detail is that whereby the second-order reaction is first order with respect to each reagent.

For the reaction

$$A \;\; + \;\; B \xrightarrow{\;\;k_2\;\;} C \qquad\qquad 3.25$$

the rate equation can be written as

$$\frac{d[C]}{dt} = -\frac{d[A]}{dt} = -\frac{d[B]}{dt} = k_2[A]_t[B]_t \qquad\qquad 3.26$$

Separation of variables leads to

$$\frac{d[A]}{[A]_t[B]_t} = -k_2\, dt \qquad\qquad 3.27$$

By substituting $\dfrac{1}{[A]_t[B]_t}$ in *Equation 3.27* with $\dfrac{1}{([A]_o - [B]_o)}\left\{\dfrac{1}{[B]_t} - \dfrac{1}{[A]_t}\right\}$, the *Equation*

3.27 can now be expressed as

$$\frac{1}{([A]_o - [B]_o)}\left\{\frac{1}{[B]_t} - \frac{1}{[A]_t}\right\} d[A] = -k_2 dt \qquad\qquad 3.28$$

Integration of *3.28* leads to

$$\frac{1}{([A]_o - [B]_o)} ln\frac{[B]_o[A]_t}{[A]_o[B]_o} = -k_2\, t \qquad\qquad 3.29$$

In order to evaluate the second-order rate constant k_2 ($M^{-1}.s^{-1}$) for the reaction, one needs to know the concentrations of both A and B, both initially and at any time t, *i.e.* $[A]_o$, $[B]_o$, $[A]_t$, and $[B]_t$. However, this presents a complicated and time-consuming process for most kinetic experiments. As a result of this, these experiments are often conducted with either reactant A or B in large excess, *i.e.* $[B] >> [A]$ (at least a 10-fold excess). Under these conditions the concentration of B remains relatively constant throughout the course of the

reaction, and the reaction may be treated as a first-order reaction. These conditions whereby one reactant is present in a large excess over the other are commonly referred to as pseudo *first-order conditions*.

Therefore *Equation 3.26* may be written as

$$-\frac{d[A]}{dt} = k_2[A]_t[B]_t$$
$$= (k_2[B]_o)[A]_t$$
$$= k_{obs}[A]_t$$

3.30

where k_{obs} is the observed rate constant with units s^{-1}.

A plot of $\ln[A]_t$ vs. time will result in a straight line with a slope equal to k_{obs}. Monitoring the reactions for several concentrations of *B*, whilst simultaneously ensuring that *B* is in a large excess over A, generates a series of k_{obs} for different [*B*]. With reference to *Equation 3.30*, $k_{obs} = k_2[B]_o$, and a plot of k_{obs} vs. [*B*]$_o$ will be linear with a slope of k_2 having units of $M^{-1}s^{-1}$.[1-5]

3.3.4 *Reversible Second-Order Reactions*

Reactions may not go to completion at times, instead an equilibrium between the reactants maybe reached. These types of reactions may be represented as follows:

$$A + B \underset{k_b}{\overset{k_f}{\rightleftharpoons}} C$$

3.31

Assuming that the reverse reaction is first-order, whilst the forward reaction is second-order. Due to this the reaction in general exhibits mixed-order behaviour. Pseudo first-order conditions are often selected for the forward reaction, *i.e.* [*B*]$_o$ >> [*A*]$_o$, so as to eliminate the complexity of the problem. This results in the equation now being treated as if it were a reversible first-order reaction.

The rate of formation of *C* can be written as

$$-\frac{d[A]}{dt} = -\frac{d[B]}{dt} = \frac{d[C]}{dt} = k_f[A]_t[B]_t - k_b[C]_t$$

3.32

Application of the mass balance gives:

At any time t

$$[A]_t = [A]_o - [C]_t$$

and
$$[B]_t = [B]_o - [C]_t \qquad\qquad 3.33$$

At equilibrium

$$[A]_{eq} = [A]_o - [C]_{eq} \text{ and } [B]_{eq} = [B]_o - [C]_{eq} \qquad 3.34$$

The rates of the two opposing reactions at equilibrium are equal, *i.e.*

$$-\frac{d[A]}{dt} = k_f [A]_{eq}[B]_{eq} - k_b[C]_{eq} = 0 \qquad 3.35$$

This implies that

$$k_f [A]_{eq}[B]_{eq} = k_b[C]_{eq} \qquad\qquad 3.36$$

However, $[C]_t = [A]_o - [A]_t$ and $[C]_{eq} = [A]_o - [A]_{eq}$ and *Equation 3.36* may now be written as

$$k_f [A]_{eq}[B]_{eq} = k_b([A]_o - [A]_{eq}) \qquad 3.37$$

Resulting in

$$k_b[A]_o = k_f [A]_{eq}[B]_{eq} + k_b[A]_{eq} \qquad 3.38$$

Substituting $[C]_t = [A]_o - [A]_t$ and *Equation 3.38* into *3.32* results in

$$-\frac{d[A]}{dt} = k_f [A]_t[B]_t - k_b[A]_{eq}[B]_{eq} - k_b[A]_{eq} + k_b[A]_t \qquad 3.39$$

Since $[B]_o \gg [A]_o$, *Equation 3.39* can be expressed as

$$-\frac{d[A]}{dt} = k_f [A]_t[B]_o - k_f [A]_{eq}[B]_o - k_b[A]_{eq} + k_b[A]_t$$

$$= (k_f [B]_o + k_b)([A]_t - [A]_{eq}) \qquad 3.40$$

Separation of variables and integration gives

$$\int_{[A]_o}^{[A]_t} \frac{d[A]}{([A]_t - [A]_{eq})} = -(k_f [B]_o + k_b)\int^{t} dt \qquad 3.41$$

3-8

which results in

$$ln\left(\frac{[A]_t - [A]_{eq}}{[A]_o - [A]_{eq}}\right) = -(k_f[B]_o + k_b)t$$

$$= -k_{obs}t \qquad\qquad 3.42$$

with $k_{obs} = k_f[B]_o + k_b$.

For a second-order reversible reaction a plot of k_{obs} versus $[B]_o$ will be linear with a slope equal to k_f and an intercept equal to k_b. The equilibrium constant K^* can be obtained from the ratio of k_f / k_b and may also be determined thermodynamically.[1-5]

3.3.5 *Consecutive First-Order Reactions*

Frequently a product of one reaction becomes a reactant in a subsequent reaction. This is true in multi-step reaction mechanisms. A simple case involving two consecutive irreversible first-order reactions is represented by *Equation 3.43*.

$$A \xrightarrow{k_1} B \xrightarrow{k_2} C \qquad\qquad 3.43$$

The rates of change of [A], [B] and [C] are as follows:

$$\frac{d[A]}{dt} = -k_1 dt \qquad\qquad 3.44$$

$$\frac{d[B]}{dt} = k_1[A] - k_2[B] \qquad\qquad 3.45$$

$$\frac{d[C]}{dt} = k_2[B] \qquad\qquad 3.46$$

Since B is formed by the first reaction and is destroyed by the second reaction, the expression for $\frac{d[B]}{dt}$ has two terms.

Let only A be present in the system at $t = 0$:

$$[A]_o \neq 0, \qquad [B]_o = 0, \qquad [C]_o = 0 \qquad\qquad 3.47$$

We have three coupled equations and *Equation 3.44* can be represented as

$$[A] = [A]_o e^{-k_1 t}$$ 3.48

Substitution of *Equation 3.48* into *Equation 3.45* affords

$$\frac{d[B]}{dt} = k_1 [A]_o e^{-k_1 t} - k_2 [B]$$ 3.49

Integration of *3.49* yields

$$[B] = \frac{k_1 [A]_o}{k_2 - k_1} (e^{-k_1 t} - e^{-k_2 t})$$ 3.50

Using conservation of matter enables one to determine $[C]$. The total number of moles present is constant with time, so $[A] + [B] + [C] = [A]_o$. Using *Equations 3.48* and *3.50* gives

$$[C] = [A]_o \left(1 - \frac{k_2}{k_2 - k_1} e^{-k_1 t} + \frac{k_1}{k_2 - k_1} e^{-k_2 t} \right)$$ 3.51

3.3.6 Pre-Equilibrium with Parallel Reactions (one Acid-Base Equilibrium)

Reactions are often conducted in solution, most of them being aqueous in nature. Therefore, the reaction rates are often pH dependant. The changing of the rate with varying pH is a direct result of the presence of different species having different reactivities. A plot of the observed or intrinsic rate constant versus pH resembles the profile for an acid-base titration curve. Typical examples of these types of reactions are the aqua and hydroxo bound complexes. The general reaction scheme can be represented as follows.
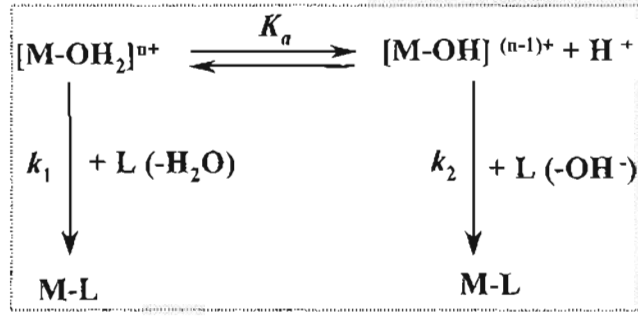
Scheme 3.1: *A general representation of a one-acid base equilibrium.*

It follows from *Scheme 3.1* that

$$\frac{d[M \text{ - } L]}{dt} = -\frac{d[M \text{ - } OH_2]}{dt} = -\frac{d[M \text{ - } OH]}{dt} = k_1[M \text{ - } OH_2][L] + k_2[M \text{ - } OH][L]$$

$$= -\frac{d[M \text{ - } OH_2 + M \text{ - } OH]}{dt} = k_1[M \text{ - } OH_2][L] + k_2[M \text{ - } OH][L] \qquad 3.52$$

Applying the law of mass balance gives

$$K_a = \frac{[M \text{ - } OH][H^+]}{[M \text{ - } OH_2]} \qquad 3.53$$

$$[M \text{ - } OH_2] = \frac{([M \text{ - } OH_2] + [M \text{ - } OH][H^+])}{[H^+] + K_a} \qquad 3.54$$

$$[M \text{ - } OH] = \frac{([M \text{ - } OH_2] + [M \text{ - } OH])}{[H^+] + K_a} \qquad 3.55$$

When *Equations 3.54* and *3.55* are substituted into *3.52* it affords

$$-\frac{d[M \text{ - } OH_2 + M \text{ - } OH]}{dt} = \left\{ \frac{k_1[H^+] + k_2 K_a}{[H^+] + K_a} \right\}[L]([M \text{ - } OH_2] + [M \text{ - } OH]) \qquad 3.56$$

therefore

$$k_{obs} = \left\{ \frac{k_1[H^+] + k_2 K_a}{[H^+] + K_a} \right\}[L] \qquad 3.57$$

The $[H^+]$ limits Equation 3.57

At low $[H^+]$

$$k_{obs} = k_2[L]$$ 3.58

At high $[H^+]$

$$k_{obs} = k_1[L]$$ 3.59

3.4 Activation Parameters

Although the mechanism of a reaction may be assigned using the rate law, it is often useful to have other data available. Among these are activation parameters, which may be obtained from the temperature or pressure dependence of a reaction's rate constant.

Using the theory of absolute reaction rates a relationship may be formulated between a reaction's activation parameters and its rate law. However, empirical relationships are now, more commonly utilized.

3.4.1 The Arrhenius Equation

Arrhenius is believed to be the first to empirically find that rate constants have temperature dependence similar to that of equilibrium constants. These were then described by the following exponential or logarithmic forms:[3,4]

$$k = A e^{-\frac{E_a}{RT}}$$ 3.60

$$i.e. \ \ln k = \ln A - \frac{E_a}{RT}$$ 3.61

where A = Arrhenius pre-exponential factor (having the same units as k);

E_a = is the Arrhenius Activation Energy (with units of J/mol);

R = gas constant (equal to 8.315 $J.K^{-1}mol^{-1}$) and

T = temperature (having units of K).

k can be determined by appropriate experiments at several temperatures, and a plot of ln k versus $1/T$ has a slope of $-E_a/RT$. The rate constant is predicted to increase with increasing temperature.

The Arrhenius equation is still widely used in certain aspects of kinetics and more especially for complex systems where the measured rate constant is thought to be a complex composite of specific rate constants.[4]

3.4.2 *The Transition-State Theory*

Since orientation and other effects cannot be treated satisfactorily via a modification of hard-sphere collision theory, an alternative approach to the problem resulted in the development of the transition-state theory. According to Henry Eyring and Michael Polyani, many reactions proceed *via* a pre-equilibrium mechanism, which can be represented as in *Equation 3.62*.[1,3]

$$A \longrightarrow B \underset{}{\overset{K^{\neq}}{\rightleftharpoons}} \{A \text{---} B\} \xrightarrow{k_2} A + B$$

Activated Complex or Transition State

3.62

The rate of the reaction can be expressed as

$$\frac{-d[A]}{dt} = \frac{k_b T}{h}[A - B]$$

$$= \frac{k_b T}{h} K^{\neq}[A][B] \qquad\qquad 3.63$$

where k_b = Boltzman's constant $(1.38 \times 10^{-23} \ J.K^{-1})$ and

h = Planck's constant $(6.626 \times 10^{-34} \ J.s^{-1})$

$K^{\neq}$ = Equilibrium constant.

The second-order rate constant, k_2, can be equated to

$$k_2 = \frac{k_b T}{h} K^{\neq} \qquad\qquad 3.64$$

But, ΔG^{*}, the free energy of activation may be expressed in terms of enthalpy of activation, ΔH^{*} and entropy of activation, ΔS^{*}, as follows:

$$\Delta G^{*} = -RT \ln K^{*} = \Delta H^{*} - T\Delta S^{*}$$
3.65

Rearranging *Equation 3.65* and substituting for K^{*} in *Equation 3.64* in terms of ΔS^{*} affords:

$$k_2 = \frac{k_b T}{h} \exp\left(-\frac{\Delta G^{*}}{RT}\right)$$

$$= \frac{k_b T}{h} \exp\left(-\frac{\Delta H^{*}}{RT}\right) \exp\left(\frac{\Delta S^{*}}{R}\right)$$
3.66

Equation 3.66 can be expressed in a linear form as

$$\ln\left(\frac{k_2}{T}\right) = -\frac{\Delta H^{*}}{RT} + \left[\ln\left(\frac{k_b}{h}\right) + \frac{\Delta S^{*}}{R}\right]$$

$$= -\frac{\Delta H^{*}}{RT} + \left(23.8 + \frac{\Delta S^{*}}{R}\right)$$
3.67

The activation parameters, ΔH^{*} (enthalpy of activation) and ΔS^{*} (entropy of activation) can be determined from a plot of $\ln (k_2/T)$ versus $1/T$, with the slope being equal to $\Delta H^{*}/R$ and the intercept being equal to $23.8 + \Delta S^{*}/R$. This plot is commonly referred to as the *Eyring Plot*.

3.4.3 *The Dependence of the Rate Constant on Pressure*

It is much more difficult to study the effect of pressure on a solution phase reaction than it is to study the effect of temperature.[6] The reaction rate is comparatively insensitive to changes in pressure and very substantial pressures (up to several kilobars), must be applied before reasonably large changes can be observed. The major reasons for studying such pressure dependence is its usefulness in providing insight into the mechanism of the reactions.

Variable pressure measurements allows the determination of an activation volume, $\Delta V^{\neq}$, which can be used as a supplementary parameter for mechanistic assignment.[7-9]

The thermodynamic equation[3]

$$dG = SdT + VdP \qquad\qquad 3.68$$

when subjected to partial derivitization at constant temperature the following is obtained: [3]

$$\left(\frac{\partial \Delta G^{o}}{\partial P}\right)_{T} = \Delta V^{o} \qquad\qquad 3.69$$

van't Hoff's[4] equation can be described using the same partial derivative of ΔG^{o} with respect to pressure:

$$\left(\frac{\partial lnK^{\neq}}{\partial P}\right)_{T} = \left(\frac{-\partial\left(\frac{\Delta G^{o}}{RT}\right)}{\partial P}\right)_{T} = -\frac{\Delta V^{o}}{RT} \qquad\qquad 3.70$$

where ΔV^{o} represents the difference in partial molar volume between the reactants and the products.

Therefore the variation of k_{f} with P can be expressed by *Equation 3.71*[4], since the equilibrium constant, $K^{\neq} = \dfrac{k_{f}}{k_{b}}$.

$$\left(\frac{\partial lnk_{f}}{\partial P}\right)_{T} = -\frac{\Delta V^{\neq}}{RT} \qquad\qquad 3.71$$

where $\Delta V^{\neq}$ is the volume of activation, for the forward step of the reaction and is equal to the difference between the partial molar volumes of the transition state and that of the reactant.

$\Delta V^{\ddagger}$ is normally assumed to be independent of pressure, therefore, by integrating between the limits of P = 0 to P, and $k_f = (k_f)_0$ gives rise to the following equation:[3]

$$\ln k_f = \ln(k_f)_0 - \frac{\Delta V^{\ddagger}}{RT} P \qquad\qquad 3.72$$

where $\ln (k_f)_0$ is the value at ambient pressure.

A plot of $\ln k_f$ versus P should be linear with a slope of $-\frac{\Delta V^{\ddagger}}{RT}$. In general $\Delta V^{\ddagger}$ (volume of activation) values are more reliable than $\Delta S^{\ddagger}$ (entropy of activation) values that are obtained as the y-intercept from the extrapolation of the *Eyring Plot*. The values of $\Delta V^{\ddagger}$ and $\Delta S^{\ddagger}$ both depend on the reaction mechanism. A negative value for $\Delta S^{\ddagger}$ is indicative of an associative mechanism, whereas a positive $\Delta S^{\ddagger}$ value indicates a dissociative mechanism. This is also true for $\Delta V^{\ddagger}$.

3.5 *Experimental Techniques*

The essential feature of all methods of studying the chemical kinetics of a reaction is to determine the time dependence of concentrations of reactants and/or products. Certain reactions are so fast that special techniques have to be employed in order for this to be achieved. Examples of these types of reactions are proton transfers, enzymatic reactions and non-covalent complex formation.

There are two reasons why conventional techniques are not suitable for rapid reactions:[10,11]

1.   The time that it usually takes to mix reactants, or to bring them to a specified temperature, may be significant in comparison to the half-life of the reaction. This would result in an appreciable error being made, since the initial time cannot be determined accurately.

2.   The time taken to make a measurement of a concentration is significant compared to the half-life of the reaction.

The methods that are used in the study of rapid reactions falls into two main classes *viz.* flow methods and pulse methods.

A summary of reaction techniques used for the study of chemical kinetics is shown in *Figure 3.1*.

Reactions involving
breaking of bonds

Combinations of free
radicals in the gas phase

CHEMICAL
REACTIONS

Photochemical
isomerization

Photoionization:
photodissociation

Diffusion-controlled reactions in solution
(e.g., combinations of free radicals)

Molecular
rotation

Molecular
vibration

PHYSICAL
PROCESSES

Intramolecular energy redistribution

Solute-solvent collisions:
solvent redistribution

Time/s 10^3 1 10^{-3} 10^{-6} 10^{-9} 10^{-12} 10^{-15}
                                   (1 ms)   (1 μs)   (1 ns)   (1 ps)   (1 fs)
Corresponding   Long   Short   Long   IR   UV
spectral region   radio   radio   micro-   Visible
                                   waves   waves   waves

Conventional
methods
Flow methods 1887

Ultrasonic methods 1960

Pressure-jump, shock waves 1954

Temperature-jump 1954   TECHNIQUES

NMR methods

Line-shape analysis 1960   Correlation times 1980

Microsecond flash photolysis 1950

Nanosecond flash photolysis 1970

Picosecond flash photolysis 1976

Subpicosecond flash photolysis 1980

Figure 3.1: *Summary of reaction techniques and their corresponding time scales.*[8]

There exists a number of other techniques that are currently available for the study of chemical kinetics. These include infrared spectroscopy (IR), nuclear magnetic resonance spectroscopy (NMR) and pulse methods. The study undertaken here made use of UV/Visible absorption spectroscopy and stopped-flow methods. These two methods will be discussed in greater detail.

3.5.1 Flow Methods

Flow methods are the best way of following fast reactions in which the reagents cannot be prematurely mixed. All fast flow methods are based on the pioneering work of Hartridge and Roughton.[12,13] These methods may be used to study reactive intermediates that are too unstable to be isolated as well as to follow rapid changes involving stable reactants.[14] Flow reactors are also widely used for industrial processes because of the ease of handling large quantities of reactants in a limited reactors space and because of the possibility of continuous operation. This is particularly advantageous for reactions involving solid catalysts, where emptying and filling operations may alter the activity of the catalyst.

For the measurement of reaction rates, mixtures of reactants of known initial concentration flow through a region of known volume at a constant rate. The mixture is thereafter analyzed after it has passed through the reaction space or at fixed points in some space. Complete mixing of the reactants before they enter the zone of reaction is assumed. Specially designed mixing chambers just upstream of the reaction space are usually employed.[12]

Flow methods function within a time range of *ca.* 1×10^{-3}–10 s. Unlike relaxation kinetics and NMR, it is possible to use flow methods for the study of irreversible reactions.[5] The continuous flow method operates in a manner whereby solutions of both reactants are forced by pistons into the mixing chamber, whose design contributes to rapid mixing. The mixed solution thereafter flows into an observation chamber, where detection takes place via spectroscopy. A schematic diagram of a continuous flow system is shown in *Figure 3.2.*[2]
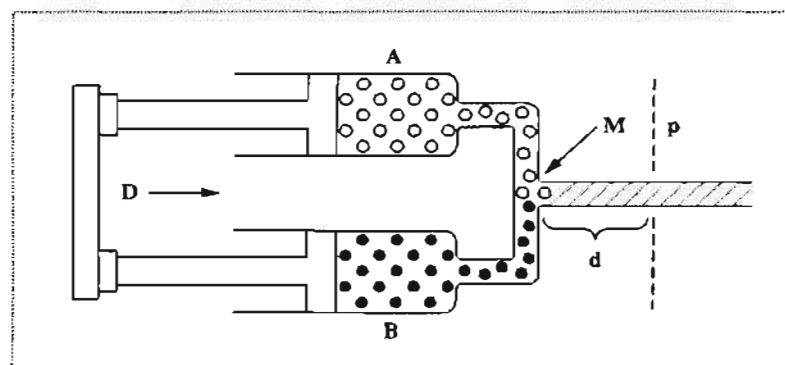
Figure 3.2:   *Schematic diagram of a continuous flow kinetic system.*[2]

One of the most frequently used rapid kinetics techniques is stopped-flow. Stopped-flow techniques are frequently used for monitoring reactions with a half-life ranging from $10^0 - 10^3$ seconds. A schematic diagram of the stopped-flow apparatus is shown in *Figure 3.3*.
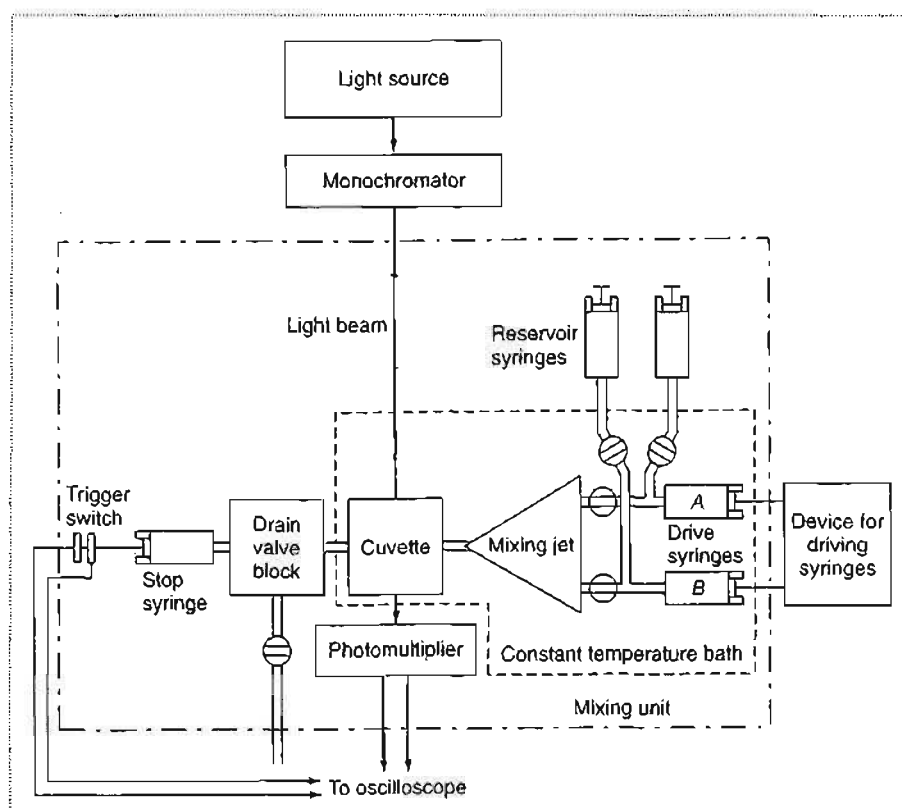
Figure 3.3: ___Schematic diagram of a stopped-flow instrument.___[11]

The stopped-flow principle of operation allows small volumes of solutions to be driven from high performance syringes to a high efficiency mixer just before passing into a measurement flow cell. As the solutions flow through, a steady-state equilibrium is established and the resultant solution is only a few milliseconds old as it passes through the cell. The mixed solution then passes into a stopping syringe, which then allows the flow to be instantaneously stopped. Some of the resultant solution will then be trapped in the flow cell and as the reaction proceeds, the kinetics can be followed using the appropriate measurement technique. The most common method of following the kinetics is by absorbance or fluorescence spectrometry, and in these cases the measurement cell is an appropriate spectrometer flow cell.

3.5.2 *UV/ Visible Spectrophotometry*

UV-Visible spectroscopy is a sensitive technique that can detect samples of low concentrations and is usually applied to molecules and inorganic ions or complexes in solution. The key components of a spectrophotometer (shown in *Figure 3.4*) are:

- a source that generates a broad band of electromagnetic radiation;
- a dispersion device that selects from the broadband radiation of the source;
- a particular wavelength (a waveband);
- a sample area and,
- one or more detectors to measure the intensity of the radiation.

The light source is usually a hydrogen or deuterium lamp for UV measurements and a tungsten lamp for visible measurements. The wavelengths of these continuous light sources are selected with a wavelength separator such as a prism or grating monochromator. Prisms used are dependant on the region in which they absorb, with glass prisms being used for the UV/ Visible region.[15]
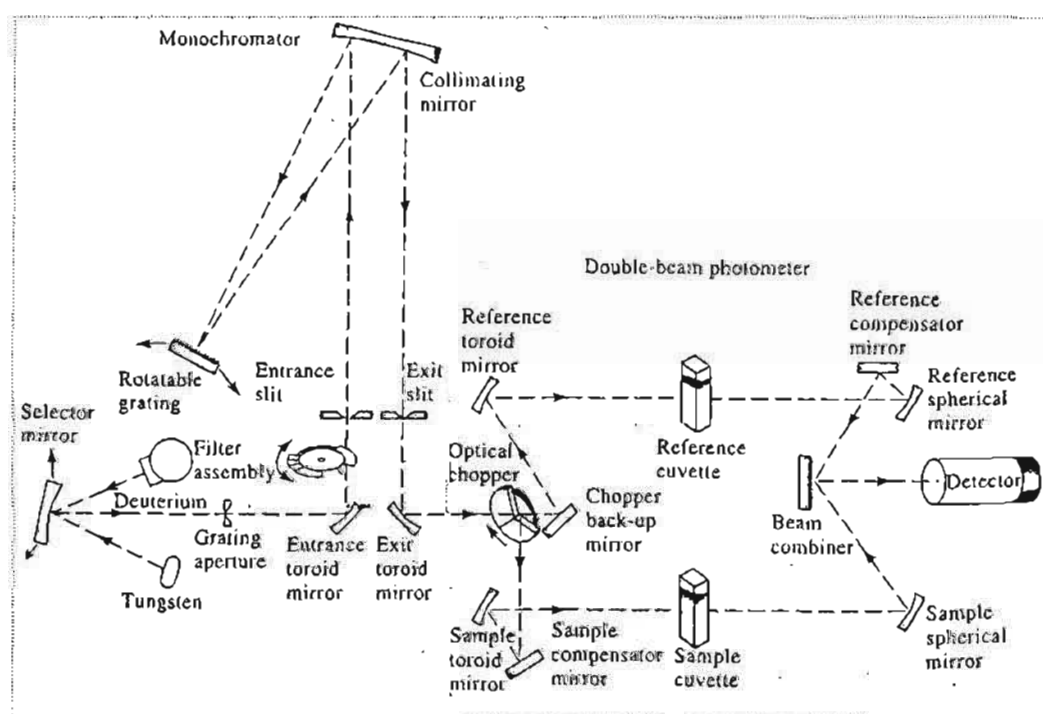
Figure 3.4: *A schematic diagram showing the different components of a UV-Visible spectrophotometer.*[15]

When light passes through or is reflected from a sample, the amount of light absorbed is the difference between the incident radiation (I_o) and the transmitted radiation (I). The amount of light absorbed is expressed as either transmittance or absorbance. Transmittance usually is given in terms of a fraction of 1 or as a percentage and is defined as follows:

$$T = I / I_o \text{ or } \% T = (I / I_o * 100) \qquad 3.73$$

Absorbance is defined as follows:

$$A = - \log T \qquad 3.74$$

For most applications, absorbance values are used since the relationship between absorbance and both concentration and path length normally is linear. The concentration of the analyte in solution can be determined by measuring the absorbance at a specific wavelength, and then applying the Beer-Lambert Law.

$$A = \varepsilon CL \qquad 3.75$$

where
- A = optical absorbance
- ε = molar extinction coefficient
- C = concentration of the chromophore in mol / dm^3
- L = path length in cm

For a simple first-order reaction

$$X \xrightarrow{\ k_1\ } Y$$
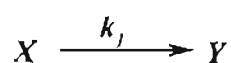
The absorbance at any time t will be expressed as follows

$$A_t \quad = \quad \varepsilon_X[X] + \varepsilon_Y[Y] \qquad 3.76$$

Where A_t = absorbance at any time, t.

$\varepsilon_X, \varepsilon_Y$ = molar extinction coefficient of X and Y.

the absorbance of the reaction upon completion would be given by

$$A_\infty \quad = \quad \varepsilon_X[X]_o + \varepsilon_Y[Y]_o \qquad 3.77$$

where A_∞ = absorbance at the end of a reaction while $[X]_o$ and $[Y]_o$ = initial concentration of X and Y respectively.

The term required for kinetic analysis is represented purely by absorbances and is given by

$$\ln\frac{[X]_o}{[X]_t} = \ln\left(\frac{A_o - A_\infty}{A_t - A_\infty}\right) = k_j t \qquad\qquad 3.78$$

Figure *3.5* shows the reaction profile for the substitution of H_2O from [{trans-Pt(H_2O)(NH_3)_2}_2-H_2N(CH_2)_4NH_2](ClO_4)_4 by TMTU (see *Chapter 5*), which has been monitored over the wavelength range 330-460 nm. The rate constant for the reaction can then be calculated using the least-squares fit of an observed absorbance versus time trace at a specific wavelength where the largest change in absorbance over a period of time can be seen. Temperature dependence data can be obtained by monitoring reactions at various temperatures by thermostatting of the instrument.
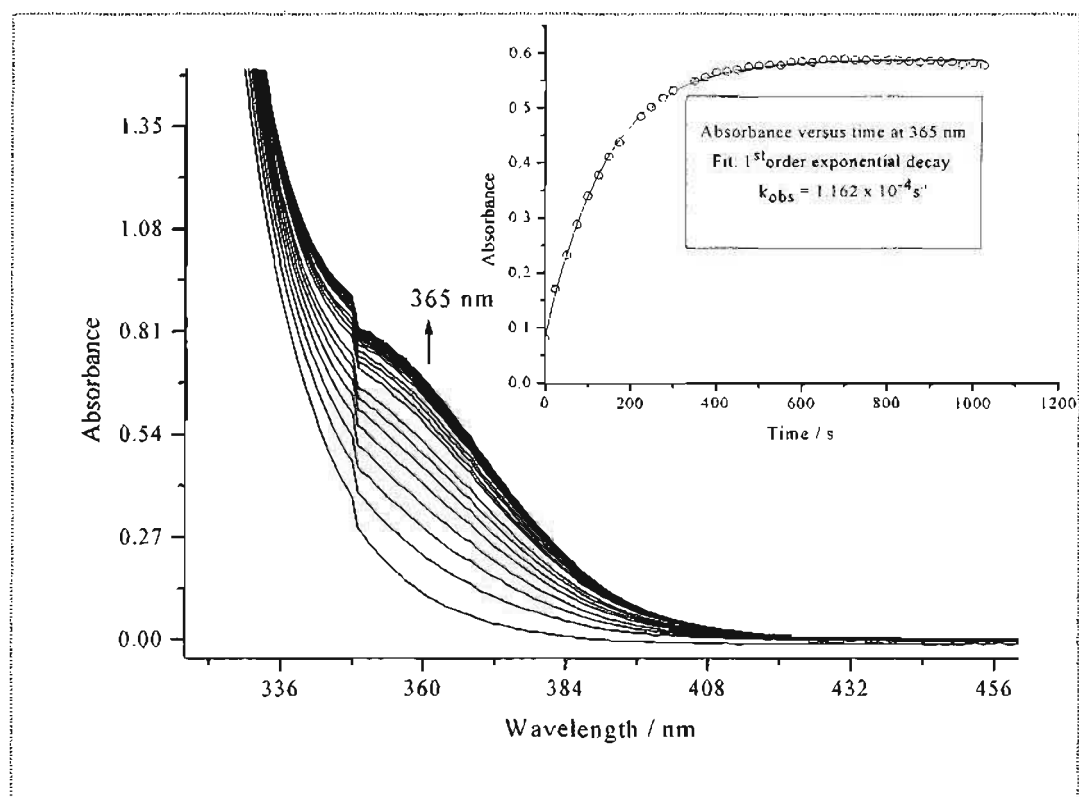
Figure 3.5: UV/ Visible spectra for the substitution of H_2O from [{trans-Pt(H_2O)(NH_3)_2}_2- $H_2N(CH_2)_4NH_2](ClO_4)_4 by TMTU. [Pt] = 0.689 mM, [TMTU] = 68.9 mM, I = 0.2 M (NaClO_4). Inset: The kinetic trace of absorbance versus time at 365 nm and the corresponding 1st order exponential decay curve, with the rate constant being calculated as the inverse of t_j.

References

1. Asperger, S., *Chemical Kinetics and Inorganic Reaction Mechanisms*, 2nd Ed., **2003**, pp 7-20

2. Espenson, J.H., *Chemical Kinetics and Reaction Mechanisms*, 2nd Ed., McGraw-Hill, New York, **1995**, pp 1-80, 253-256

3. Atwood, J.D., *Inorganic and Organometallic Reaction Mechanisms*, 2nd Ed., Wiley-VCH, New York, **1997**, pp 1-32.

4. Jordan, R.B., *Reaction Mechanisms in Inorganic and Organometallic Systems*, Oxford University Press, New York, **1991**, pp 1-16.

5. Connors, K.A., *Chemical Kinetics: The Study of Reaction Rates in Solution*, Wiley-VCH, New York, **1990**, pp 17-26

6. Helm, L. & Merbach, A., *J. Chem. Soc. Dalton Trans.*, **2002**, 633.

7. Jaganyi, D., Hofmann, A. & van Eldik, R., *Agnew. Chem. Int. Ed.*, **2001**, *40*, 1680.

8. Hofmann, A., Jaganyi, D., Munro, O.Q., Liehr, G. & van Eldik, R., *Inorg. Chem.*, **2003**, *42*, 1688.

9. Jaganyi, D., Reddy, D., Gertenbach, J.A., Hofmann, A. & van Eldik., *J. Chem. Soc. Dalton Trans.*, **2004**, 299.

10. Pilling, M.J. & Seakins, P.W., *Reaction Kinetics*, Oxford Science Publications, Oxford, **1995**.

11. Laidler, K.J. & Meiser, J.H., *Physical Chemistry*, 3rd Ed., Houghton Mifflin, Boston, **1999**, pp 379.

12. Moore, J.W. & Pearson, R.G., *Kinetics and Mechanism*, 3rd Ed., John Wiley & Sons, New York, **1981**, pp 12-36.

13. Hartridge, H. & Roughton, F.J.W., *Proc. R. Soc.*, London, **A104**, **1923**, 376

14. Chance, B., *"Rapid Flow Methods,"* in *Investigations of Rates and Mechanisms of Reactions*, Part II, Wiley-Interscience, **1974**.

15. Skoog, D.A, West, D.M. & Holler, J.R., *Fundamentals in Analytical Chemistry*, 7th Ed., Hartcourt College Publishers, Fort Worth, **1997**, pp 564.

Chapter 4

Experimental: Synthesis & Kinetic Analysis of Dinuclear Platinum^{II} Diamine-Bridged Complexes

Chapter 4

Experimental: Synthesis & Kinetic Analysis of Dinuclear Platinum[II] Diamine-Bridged Complexes

All the reactions involving synthesis of the dinuclear platinum[II] diamine-bridged complexes were performed in air unless otherwise stated. Characterization of these complexes was achieved through the use of nuclear magnetic resonance (NMR) spectroscopy, infrared (IR) spectroscopy and elemental analysis. ^1H NMR spectra were recorded on a Varian Gemini 500 spectrometer at 25 °C, referenced to the proton signal of the solvent using transmitter presaturation of H_2O resonance. Infrared spectra were recorded as KBr discs on a Perkin Elmer Spectrum One FTIR spectrometer. Elemental analysis was performed at the Institute for Inorganic Chemistry, University of Erlangen-Nürnberg, Ergelandstr. 1, Erlangen, Germany.

pK_a determinations were performed using a Jenway 4330 Conductivity and pH meter fitted with a Micro 4.5 diameter glass electrode. All kinetic measurements were conducted under pseudo first-order conditions. The wavelengths that were suitable for kinetic analysis were initially determined using a Varian Cary 100 Bio Spectrophotometer with an attached temperature-control unit. Subsequent kinetic measurements were performed using either a Varian Cary 100 Bio Scanning Kinetic Utility or an Applied Photophysics SX.18MV (v 4.33) stopped-flow system, both coupled to a temperature control unit and an online data acquisition system. All data obtained was analysed using the software package, Origin 7.5[®].

4.1 Synthesis of Dinuclear Platinum[II] Diamine-Bridged Complexes

The following reagents were used in the synthesis of the dinuclear platinum[II] complexes. trans-diamminedichloroplatinum[II] (99%) was purchased from Strem Chemicals and used as supplied. The following diamines; 1,2-ethanediamine (99%), 1,4-butanediamine (99%)

and 1,6-hexanediamine (98%) were all purchased from Aldrich and used without further purification. 1,6-hexanediamine was stored in a dessicator when not in use. 1,3-propanediamine (97%) was purchased from Fluka and used without purification. Silver nitrate (AgNO$_3$, 99.99%) was obtained from Aldrich and stored under nitrogen. N,N-Dimethylformamide (DMF, Saarchem) and ethanol (EtOH, Merck) were purified via standard methods prior to use.[1] Ultrapure water (Modulab systems) was used for all aqueous reactions. All other reagents used were of the highest purity and used as supplied.

4.1.1 *Synthesis of [{ trans-PtCl(NH$_3$)$_2$}$_2$-H$_2$N(CH$_2$)$_n$NH$_2$]Cl$_2$ (where n = 2-4)*

The complexes [{*trans*-PtCl$_2$(NH$_3$)$_2$}$_2$-H$_2$N(CH$_2$)$_2$NH$_2$]Cl$_2$ (**1**), [{*trans*-PtCl$_2$(NH$_3$)$_2$}$_2$-H$_2$N(CH$_2$)$_3$NH$_2$]Cl$_2$ (**2**) and [{*trans*-PtCl$_2$(NH$_3$)$_2$}$_2$-H$_2$N(CH$_2$)$_4$NH$_2$]Cl$_2$ (**3**) were all synthesized following the same general procedure adopted from literature.[2,3]

where n = 2-4
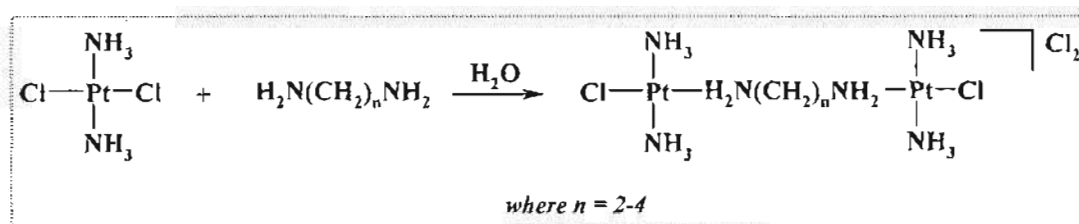
To a stirred suspension of *trans*-diamminedichloroplatinum[II] (0.500 g, 1.67 mmol) in H$_2$O (50 ml) was added dropwise, a half-equivalent of the appropriate diamine, *viz.* 1,2-ethanediamine (0.050g, 0.837 mmol), 1,3-propanediamine (0.062 g, 0.832 mmol) and 1,4-butanediamine (0.0734 g, 0.833 mmol). The resulting solution was then heated to *ca.* 50-60 °C for three hours whilst stirring, during which time all the *trans*-diamminedichloroplatinum[II] dissolves. The pale yellow solution was thereafter left to stir overnight at room temperature. The resulting solution was filtered and concentrated *in vacuo* to *ca.* 2 ml. A large excess of ethanol was added to the filtrate to precipitate the product as an off-white solid. The crude product was thereafter recrystallised by dissolving it in a minimum amount of hot water and thereafter adding a large excess of ethanol to precipitate the product. This process was repeated 2-3 times, until the product was found to be pure.

Table 4.1: *Characterization Data for Chloro-Substituted Complexes 1-3*

	1 $C_2H_{20}N_6Cl_4Pt_2$	2 $C_3H_{22}N_6Cl_4Pt_2$	3 $C_4H_{24}N_6Cl_4Pt_2$
Yield	0.367 g (66%)	0.347 g (62%)	0.389 g (68%)
Elemental Analysis			
% C			
Calculated	3.62	5.34	6.98
Found	3.98	5.84	7.44
% H			
Calculated	3.04	3.29	3.50
Found	3.13	3.46	3.47
% N			
Calculated	12.63	12.46	12.21
Found	12.69	12.51	12.20
IR (KBr)[†] cm^{-1}			
ν(NH)	3300, 3159, 3087	3098 (br), 3162	3093, 3172
ν(Pt-Cl)	340	320	337
NMR (H$_2$O:D$_2$O)[‡] ppm			
^{1}H NMR	3.07 (m)	2.78, 2.11	2.74, 1.79
^{195}Pt	- 2415	- 2421	-2436.7

[†] *Designation: br = broad*
[‡] *Ratio: 90% H$_2$O : 10 % D$_2$O*

4.1.2 Synthesis of [{trans-PtCl(NH₃)₂}₂-H₂N(CH₂)₆NH₂](NO₃)₂ (5) [3-5]
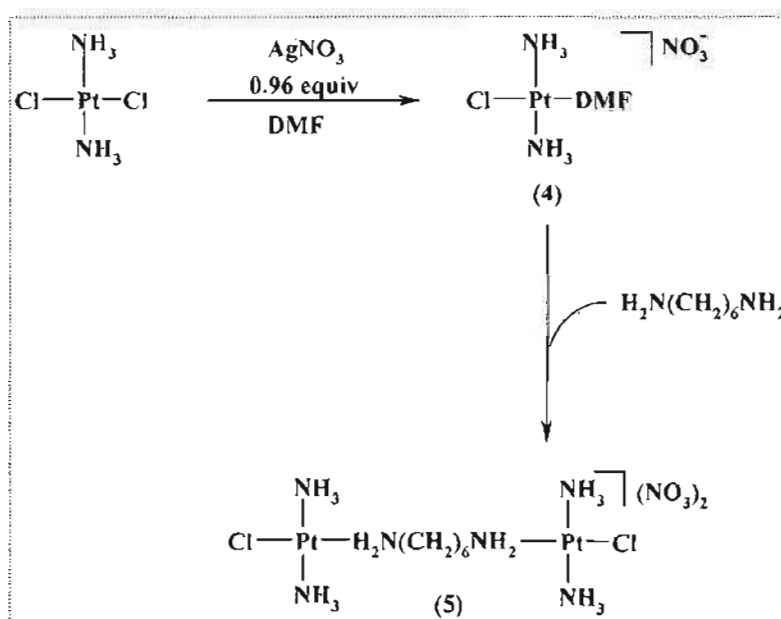
To a stirred solution of *trans*-diamminedichloroplatinum[II] (0.300 g, 1.000 mmol) in *N,N*-dimethylformamide (DMF, 17 ml) at room temperature in the dark, was added dropwise over three hours, a solution of silver nitrate (AgNO₃, 0.165 g, 0.970 mmol) in DMF (3 ml). Stirring was maintained for a period of eighteen hours and the resulting AgCl precipitate was thereafter filtered through a 0.45 μm nylon membrane filter using a Millipore filtration apparatus. The resulting pale yellow solution (4) was used as the starting material for the preparation of (5). Hexamethylenediamine (0.0581 g, 0.500 mmol) was added to (4) and the solution was allowed to stir overnight at room temperature in the dark. The resulting solution was thereafter filtered and taken to dryness on a rotary evaporator. The complex was dissolved in water and filtered to remove any unreacted starting material and recrystallized from H₂O/ acetone 3-times until the product was pure.

Yield   :   0.254g (66%)

Elemental Analysis:

     Calc. for $C_4H_{24}N_6Cl_4Pt_2$:   % C, 9.37, % H, 3.67, % N, 14.56

     Found   :   % C, 9.69, % H, 3.22, % N, 14.56

IR   : ν(NH) 3220, 3278 cm⁻¹

                                         ν(Pt-Cl) 320 cm⁻¹

NMR   : ^{1}H :   2.68, 1.69, 1.38 ppm
                               ^{195}Pt : -2416 ppm

4.2 Preparation of Complex and Nucleophile Solutions for Kinetic Analysis and pK$_a$ Determinations

The neutral nucleophiles, thiourea (TU, 99%), 1,3-dimethyl-2-thiourea (DMTU, 99%) and 1,1,3,3-tetramethyl-2-thiourea (TMTU, 98%) were purchased from Aldrich and used without further purification. Silver perchlorate (AgClO$_4$, 99.998 %) was also purchased from Aldrich and stored under nitrogen prior to use. Perchloric acid (HClO$_4$, 10.6 M) and sodium hydroxide (NaOH) were obtained from Saarchem and used without further purification. Buffer solutions of pH 4, 7 and 10 were purchased from BDH chemicals.

4.2.1 Preparation of the Aqua-Metal Complexes

where n = 2-4
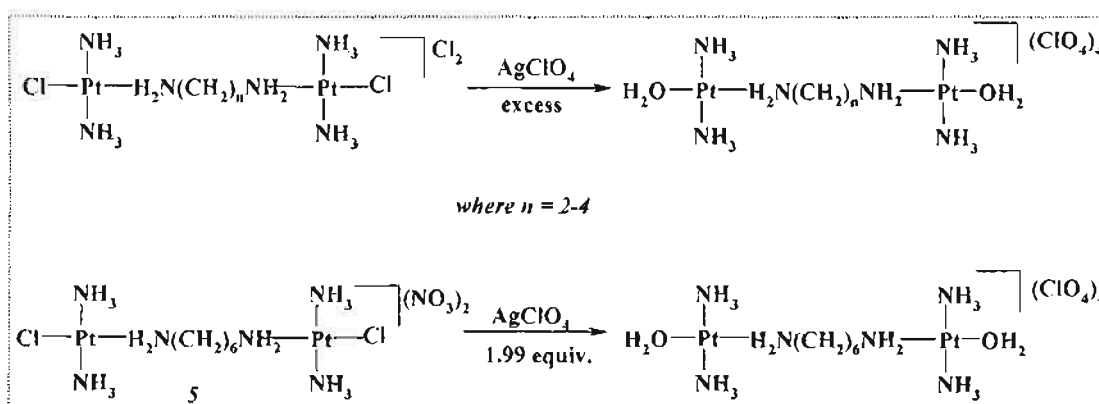
Solutions of the aqua complexes were prepared by dissolving a known amount of the chloro complex (1, 2 and 3) in 0.001 M perchloric acid and then adding a stoichiometric excess (with respect to chloride) of AgClO$_4$ (150-200%).[6] The mixture was then stirred overnight at 40-50 °C. The precipitated silver chloride was removed by filtration through a 0.45 μm nylon membrane filter using a Millipore filtration apparatus. The pH of the solution was thereafter adjusted to ca 10-11 via the careful addition of 0.1 M NaOH. This process resulted in the precipitation of a gelatinous brown solid, Ag$_2$O, which was then separated from the mixture by filtering it through a 0.45 μm nylon membrane. This

procedure was repeated to ensure that the removal of the brown Ag_2O precipitate had been achieved. The pH of the resulting solution was adjusted to 2 by the careful addition of perchloric acid (10.6 M). The colourless solution was thereafter diluted with 0.01 M $HClO_4$ solution to afford the desired complex concentration of 0.998 mM, 1.330 mM and 1.378 mM for the aqua analogues of complexes 1, 2 and 3 respectively.

A method used by Bugarčič et al.[7] was used to prepare the aqua analogue of complex (5). This entailed reacting a known amount of the chloro complex with 1.99 equivalents of $AgClO_4$ in the presence of 0.01 M $HClO_4$. The solution was then heated to 40-50 °C, and the temperature maintained for a period of 24 hours. The precipitated AgCl was removed by filtration through a 0.45 μm nylon membrane filter using a Millipore filtration apparatus, and the resulting solution made up to 0.991 mM using 0.01 M $HClO_4$. For all investigations to be carried out the pH of the complex solutions were maintained at 2.0 and the ionic strength was adjusted to 0.1 M by adding $NaClO_4$. The use of an acidic medium ensured that only the aqua species were present in solution and not a mixture of both the aqua and hydroxo species.

4.2.2 pK_a Determinations

UV-Vis spectra for the determination of the pK_a values were recorded on a Varian Cary 100 Bio Spectrophotometer. The pH of the solutions were recorded using a Jenway 4330 Conductivity / pH meter fitted with a Micro 4.5 mm diameter glass electrode. Calibration of the electrode was achieved through the use of buffers of pH 4, 7 and 10 at 25 °C.

Preparation of the aqua complexes is described in *Section 4.2.1*. The starting concentration of the complexes was 1.010 mM, 1.009 mM and 0.998 mM for the aqua analogues of complexes 1, 2 and 3 respectively. Spectrophotometric pH titrations of the aqua complex solutions, from pH 2-10 were performed using NaOH as the base. A large volume (100 ml) of the complex solution was used so as to avoid absorbance changes due to dilution effects. Initially, crushed pellets of NaOH were used to obtain a pH change from 2-3. All subsequent pH measurements were obtained by dipping a needle into a saturated solution of NaOH and thereafter into the complex solution. To avoid precipitation of $KClO_4$ within the electrode the KCl solution was replaced with a 3 M NaCl solution. It was found that if

the pH electrode was dipped into the test solution for a long period of time, it resulted in the formation of the chloro complex. It was therefore necessary to take 0.6 ml aliquots from the complex solution, which was then transferred into narrow vials for the pH measurements. These were then discarded after each measurement.

The reversibility of the titration was also tested using aqueous solutions of perchloric acid. The pK_a values were thereafter determined using *Equation 4.1* to fit the points.

$$Abs = \left(K - \frac{[H^+]K}{K_a + [H^+]} \right)\alpha + \left(\frac{[H^+]K}{K_a + [H^+]} \right)\beta$$

<div align="right">4.1</div>

where H = *the concentration of protons and can be expressed as 10^{-pH}.*

K_a = *the acid dissociation constant and may be written as 10^{-pK_a}.*

K = *the fraction of [H^+] and [OH^-] in solution with a maximum value of 1 and*

α, β = *the upper and lower limits of the absorbance values at the chosen wavelength*

4.2.3 *Preparation of Nucleophile Solutions for Kinetic Analysis*

Solutions of the nucleophiles *viz.* TU, DMTU and TMTU, were prepared by dissolving an appropriate amount of the nucleophile in a solution of constant ionic strength, 0.2 M NaClO$_4$. This solution was prepared by dissolving sodium perchlorate monohydrate (NaClO$_4$.H$_2$O, 56.2 g, 0.400 mmol) in 2 L of ultrapure water to afford a solution with a final concentration of 0.2 M. The ClO$_4^-$ anion does not coordinate to Pt^{II}, therefore, the substitution reactions of platinum complexes was not going to be affected by the presence of this ion.

The nucleophile solutions were prepared by dissolving a known quantity of the appropriate nucleophile in 100 ml of the constant ionic strength solution (*i.e.* 0.2 M NaClO$_4$) to afford a concentration that was approximately 100 times greater than that of the metal complex. Subsequent dilution of the stock nucleophile solution at constant ionic strength afforded a series of concentrations, in the order of 20, 40, 60, 80 times the concentration of the metal complex. These concentrations were chosen so as to maintain pseudo *first-order* conditions, and the concentration of the nucleophile was in at least ten-fold excess with respect to each of the platinum-bonded chlorides.

4.3 Preliminary Kinetic Investigations

Initial studies using UV/Visible spectrophotometry were conducted, in order to ascertain the wavelength at which kinetic analysis could be performed. Equal volumes of both the complex and nucleophile solution were injected into separate compartments of a tandem quartz cuvette. Care was taken to prevent premature mixing of the solutions. The solutions was thereafter allowed to equilibrate at 25 °C in the spectrophotometric chamber for a period of 10 minutes, prior to the initial spectrum being recorded over a wavelength range of 190-800 nm. A second spectrum was recorded once the solutions were thoroughly mixed. Subsequent scans were recorded at three-minute intervals until no further changes could be observed in the absorption spectra. This was an indication that the reaction had reached completion. The preliminary study allowed for the determination of the wavelength at which kinetic studies could be performed in the stopped-flow and also provides an indication of the time scale for the reactions. Reactions that reached completion in sixteen minutes or less were within the stopped-flow range, whilst those requiring more than sixteen minutes to reach completion were performed using the Cary 100 Bio Scanning Kinetics Application.

4.4 Kinetic Study using Stopped-Flow Spectrophotometry

The rate constants and activation parameters for substitution reactions requiring less than sixteen minutes to reach completion were determined using a stopped-flow apparatus. This was followed for the reaction involving [{$trans$-Pt($H_2O)_2$($NH_3)_2$}$_2$-$H_2N(CH_2)_2NH_2$]($ClO_4)_4$ with TU as the nucleophile.

The instrument lamp (150W Xenon Arc Lamp) was allowed to warm for an hour prior to analysis. Sample syringes and the reaction chamber were rinsed thoroughly with water and 0.1 M $NaClO_4$ solution. Once washing was complete, both sample syringes were then filled with 0.1 M $NaClO_4$ solution and allowed to equilibrate at 25 °C, and the instrument subsequently blanked at the chosen wavelength where the absorbance change was most noticeable. The sample syringes were then rinsed with the appropriate solutions (i.e. either the metal complex or the nucleophile solution) and allowed to equilibrate at the desired temperature.

The substitution reactions were initiated by injecting equal volumes of the metal complex and appropriate nucleophile solution, into a mixing chamber using nit rogen pressure (800 kPa) to drive the syringe pistons. The progress of the reaction was monitored spectrophotometrically. Once an accurate time-scale for the completion of each reaction had been established, consecutive measurements were automatically performed; the number of runs performed were dependant on the reproducibility of the data obtained. In all cases, all reported rate constants represent an average value of at least eight kinetic runs for each experimental condition.

All kinetic measurements were best described using a single exponential equation (with the exception of the reaction between **DiPtEn-Aqua** + Tu which exhibited second order kinetics, hence a second order fit was used to calculate the observed rate constant, k_{obs}.

The observed pseudo first-order rate constant, k_{obs}, was calculated using the online non-linear least-squares fit of exponential data to *Equation 4.2*.

$$A_t = A_\infty + (A_0 - A_\infty)exp(-k_{obs}t) \qquad\qquad 4.2$$

where A_∞, A_t and A_0 represent the absorbance of the reaction mixture initially, at time t and at the end of the reaction respectively.

The dependence of the rate constant on the concentration of the incoming nucleophile was performed in this manner for all concentrations, whilst maintaining the temperature at 25 °C. The rate constant, k_2, for the reaction of each metal complex with a particular nucleophile was obtained from the linear regression of a plot of k_{obs} versus concentration of the nucleophile using Origin 7.0®, a graphical analysis software package.

A similar approach was used to determine the dependence of the rate constant on temperature, with the nucleophile concentration been held constant at 100 times the concentration of the metal complex, whilst varying the temperature from 20-40 °C in 5 °C intervals. Studies conducted for the concentration dependence study revealed no reverse reaction with water, since all plots of k_{obs} versus nucleophile concentration were found to pass through zero, therefore a single nucleophile concentration at 50 times that of the metal complex was chosen for the temperature dependence study. Application of the *Eyring*

equation to values obtained from the slope and intercept of a plot of ln (k_2/ T) versus $1/T$ (where $k_2 = k_{obs}/[\text{Nu}]$) afforded the activation parameters $\Delta H^{\ast}$ and $\Delta S^{\ast}$ respectively.

4.5 *Kinetic Study using UV/Visible Spectrophotometry*

Substitution reactions reaching completion after sixteen minutes *viz.* ***trans-[{Pt(H$_2$O)$_2$(NH$_3$)$_2$}$_2$-H$_2$N(CH$_2$)$_2$NH$_2$](ClO$_4$)$_4$*** + Nu (where Nu = DMTU and TMTU) and ***trans[{Pt(H$_2$O)$_2$(NH$_3$)$_2$}$_2$-H$_2$N(CH$_2$)$_n$NH$_2$](ClO$_4$)$_4$*** (**where n = 3, 4 and 6**) + Nu (where Nu = TU, DMTU and TMTU) were spectrophotometrically monitored using a Cary 100 Bio UV/Visible spectrophotometer, equipped with a Varian Peltier temperature controller and coupled to an on-line kinetics application.

An approximate time of one hour was allowed for the instrument lamps, *i.e.* UV deuterium (D$_2$) lamp and a Visible QI lamp, to warm up. The instrument was thereafter blanked using an appropriate blanking solution (*i.e.* 0.1 M NaClO$_4$) at 25°C at the wavelength where the most noticeable change in absorbance was observed (see *Section 4.3*). Equal volumes of the metal complex and the nucleophile solution were injected into two separate compartments of the tandem quartz cuvette (*Path Length = 0.8 cm*), with precaution taken to prevent premature mixing of the solutions. The solution was then allowed to equilibrate at the required temperature for a period of approximately ten minutes. The substitution reactions were then monitored for the time-period that had already been established during the preliminary investigations, and were initiated by thorough mixing of the solutions of the metal complex and nucleophile solution before the on-line timer reached 0.00 s. The on-line timer system, allows the user a maximum of 120 s to mix the solutions thoroughly, *i.e.* the metal complex and the nucleophile, before acquiring an initial scan.

Kinetic parameters, *viz.* k_2 $\Delta H^{\ast}$ and $\Delta S^{\ast}$ were calculated using the same procedure as outlined in *Section 4.4*.

References

1. Perrin, D.D., Armarego, W.L.F, Perrin, D.R., *Purification of Laboratory Chemicals*, 2nd Ed., Pergamon, Oxford, **1980**, pp 229, 249.

2. Farrell, N., Qu, Y., Feng, L., van Houten, B.; *Biochemistry*, *29*, **1990**, 9522.

3. Farrell, N. & Qu,Y., *Inorg. Chem.*, *31*, **1992**, 930.

4. Farrell, N., *Comments Inorg. Chem.*, *16*, **1995**, Part 6, 373.

5. Rauter, H., Di Domenico, R., Menta E., Oliva, A., Qu, Y., Farrell, N., *Inorg. Chem.*, *36*, **1997**, 3919.

6. Hoffmann, A. & van Eldik, R., *J. Chem. Soc. Dalton Trans.*, **2003**, 2979.

7. Bugarčič, Z.D., Petrović, B.V., Jelić, R., *Trans. Met. Chem.*, *26*, **2001**, 668.

Chapter 5

Results and Discussion

Chapter 5

Results and Discussion

5.1 Synthesis and Characterization of the Dinuclear Platinum^{II} Complexes

The complexes [{trans-PtCl$_2$(NH$_3$)$_2$}$_2$-H$_2$N(CH$_2$)$_2$NH$_2$]Cl$_2$ (1), [{trans-PtCl$_2$(NH$_3$)$_2$}$_2$-H$_2$N(CH$_2$)$_3$NH$_2$]Cl$_2$ (2), [{trans-PtCl$_2$(NH$_3$)$_2$}$_2$-H$_2$N(CH$_2$)$_4$NH$_2$]Cl$_2$ (3) and [{trans-PtCl(NH$_3$)$_2$}-H$_2$N(CH$_2$)$_6$NH$_2$}(NO$_3$)$_2$ (5) (*Figure 5.1*), hereafter referred to as **DiPtEn-Chloro, DiPtProp-Chloro, DiPtBut-Chloro** and **DiPtHex-Chloro** respectively, were readily synthesized using established literature procedures.[1-4]

Where

n = 2 (*DiPtEn-Chloro*); 3 (*DiPtProp-Chloro*); 4 (*DiPtBut-Chloro*) and 6 (*DiPtHex-Chloro*)
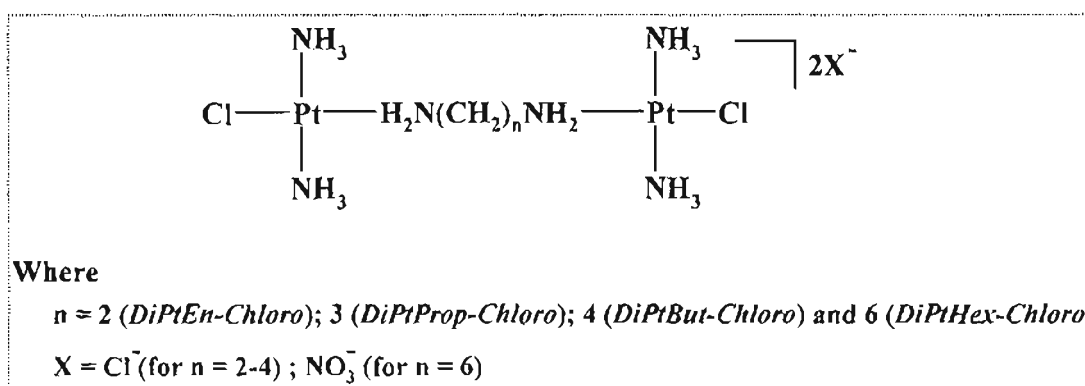
X = Cl$^-$(for n = 2-4) ; NO$_3^-$ (for n = 6)

Figure 5.1: *Structural formula of the complexes utilized in the current study.*

The complexes, **DiPtEn-Chloro, DiPtProp-Chloro** and **DiPBut-Chloro** were synthesized following the method of Farrell *et al.*[1,2], whereby the reaction of one equivalent of *trans*-dichlorodiammineplatinum^{II} with a half equivalent of the respective diammines at 50-60 °C afford the title complexes in moderate yields (50-60 %). These complexes precipitated as off-white solids and were collected by filtration and thereafter recrystallised using water/ethanol.

Characterization of these complexes was achieved through the aid of infrared spectroscopy, nuclear magnetic spectroscopy and elemental analysis. The IR spectra, recorded as KBr discs, showed strong v(N–H) stretching bands in the 3300 – 3100 cm^{-1}

region, for **DiPtEn-Chloro**, **DiPtProp-Chloro** and **DiPtBut-Chloro**. $v(Pt-Cl)$ stretching bands were also observed at 340, 320, 337 cm^{-1} for **DiPtEn-Chloro**, **DiPtProp-Chloro** and **DiPBut-Chloro** respectively. Elemental analysis for carbon, hydrogen and nitrogen were found to correlate well with the expected values.

The synthesis of **DiPtHex-Chloro** was achieved using a slightly different approach.[2-4] One equivalent of *trans*-dichlorodiammineplatinum^{II} in dimethyl formamide (DMF) was treated with 0.99 equivalents of silver nitrate (AgNO$_3$) to afford the intermediate species, *trans*-[PtCl(NH$_3$)$_2$(DMF)](NO$_3$). The DMF moiety was then selectively displaced upon the addition of 0.45 equivalents of 1,6-hexanediamine to afford the desired diplatinum complex, [{*trans*-PtCl(NH$_3$)$_2$}$_2$-H$_2$N(CH$_2$)$_6$NH$_2$](NO$_3$)$_2$ (**DiPtHex-Chloro**). The complex precipitated as an off-white solid and was collected by filtration and thereafter recrystallised using water/acetone. **DiPtHex-Chloro** was characterized using infrared spectroscopy, nuclear magnetic resonance spectroscopy and elemental analysis. Data obtained from the infrared spectra showed stretching frequencies in the 3100 – 3300 cm^{-1} region assigned to the $v(N-H)$ stretching frequency and at 320 cm^{-1} assigned to the $v(Pt-Cl)$ stretching band. Elemental analysis was found to be in good agreement with the calculated values.
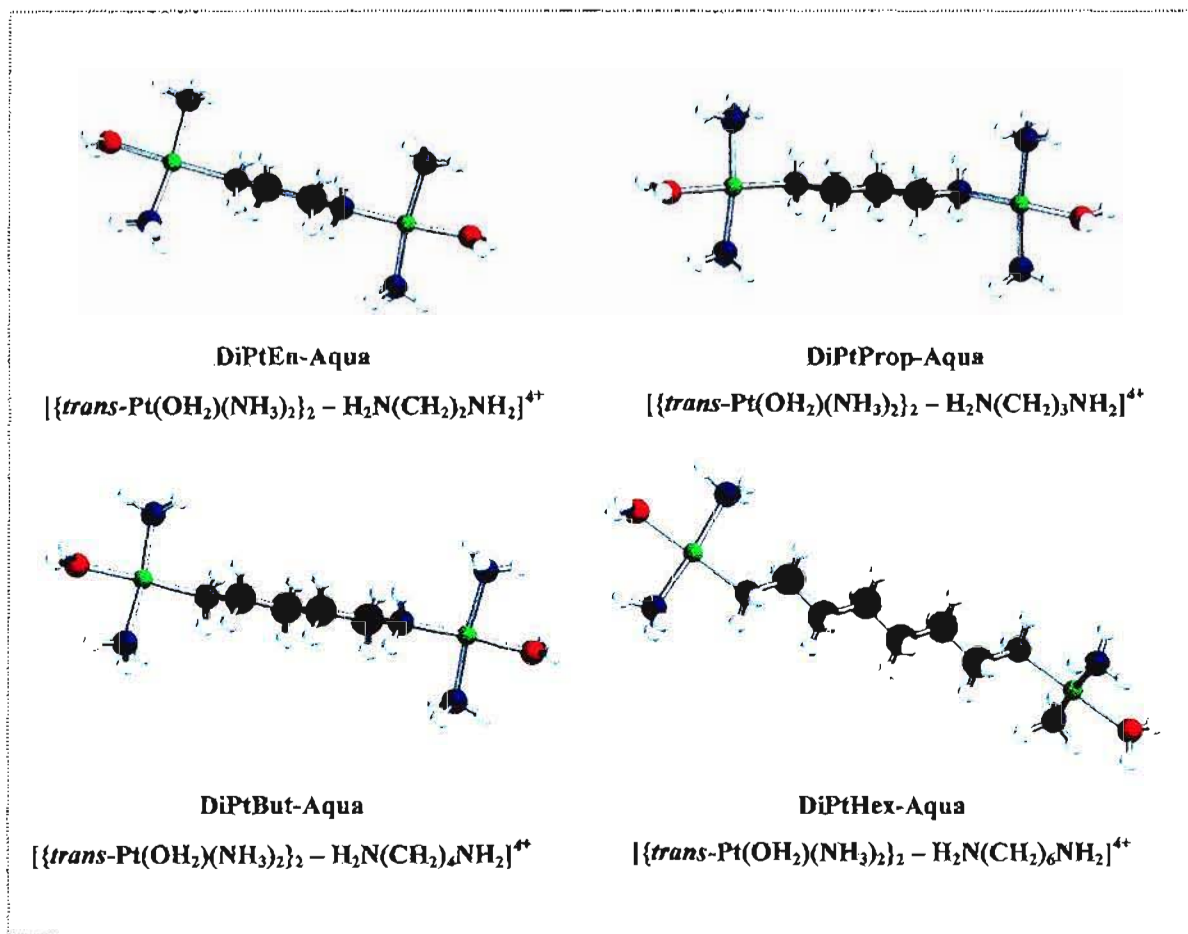
The aqua analogues of the **DiPtEn-Chloro**, **DiPtProp-Chloro** and **DiPBut-Chloro** complexes, hereafter referred to as **DiPtEn-Aqua**, **DiPtProp- Aqua** and **DiPBut- Aqua** respectively, were easily achieved using the method of Hofmann and van Eldik.[5] A known amount of the chloro complex was dissolved in 0.001 M perchloric acid and reacted with a stoichiometric excess (with respect to chloride) of AgClO$_4$ (150-200 %) at 40-50 °C for a period of twenty-four hours. The precipitated silver chloride was removed by filtration through a 0.45 µm nylon membrane filter using a Millipore filtration apparatus. The pH of the solution was adjusted to *ca* 10-11 through the addition of 0.1 M NaOH, resulting in the precipitation of brown Ag$_2$O, which was removed from the solution by filtration. The pH of the solution was adjusted to 2 by the careful addition of concentrated perchloric acid (10.6 M). The procedure was twice repeated to ensure complete removal of excess silver. The clear, colourless filtrate was thereafter made up to the desired concentrations with 0.01 M perchloric acid. The use of an acidic solvent (HClO$_4$, 0.01 M, pH = 2) was necessary to ensure that only the aqua complex, and not a mixture of both the aqua and hydroxo species was present in solution.

The aqua analogue of **DiPtHex-Chloro** was prepared using the procedure outlined by Burgarčič et al.[6] One equivalent of the chloro complex was reacted with 1.98 equivalents of silver perchlorate (AgClO$_4$) in 0.01 M HClO$_4$. The resulting solution was warmed to approximately 40-50 °C and maintained at this temperature whilst stirred for a period of twenty-four hours after which time the resulting white precipitate of AgCl was removed by filtration, through a 0.45 µm nylon membrane filter using a Millipore filtration apparatus. The resulting clear, colourless solution of **DiPtHex-Aqua** was thereafter made to the required concentration with 0.01 M HClO$_4$. The use of an acidic medium ensured that only the aqua species were present in solution and not a mixture of both the aqua and hydroxo species.

5.2 *Computational Analyses*

The investigated complexes, **DiPtEn-Aqua**, **DiPtProp-Aqua**, **DiPtBut-Aqua** and **DiPtHex-Aqua**, were modeled using computational techniques in order to assist in explaining any kinetic trends that would be observed and to determine how the molecular structures of the complexes are likely to influence the reactivity of the metal centres.
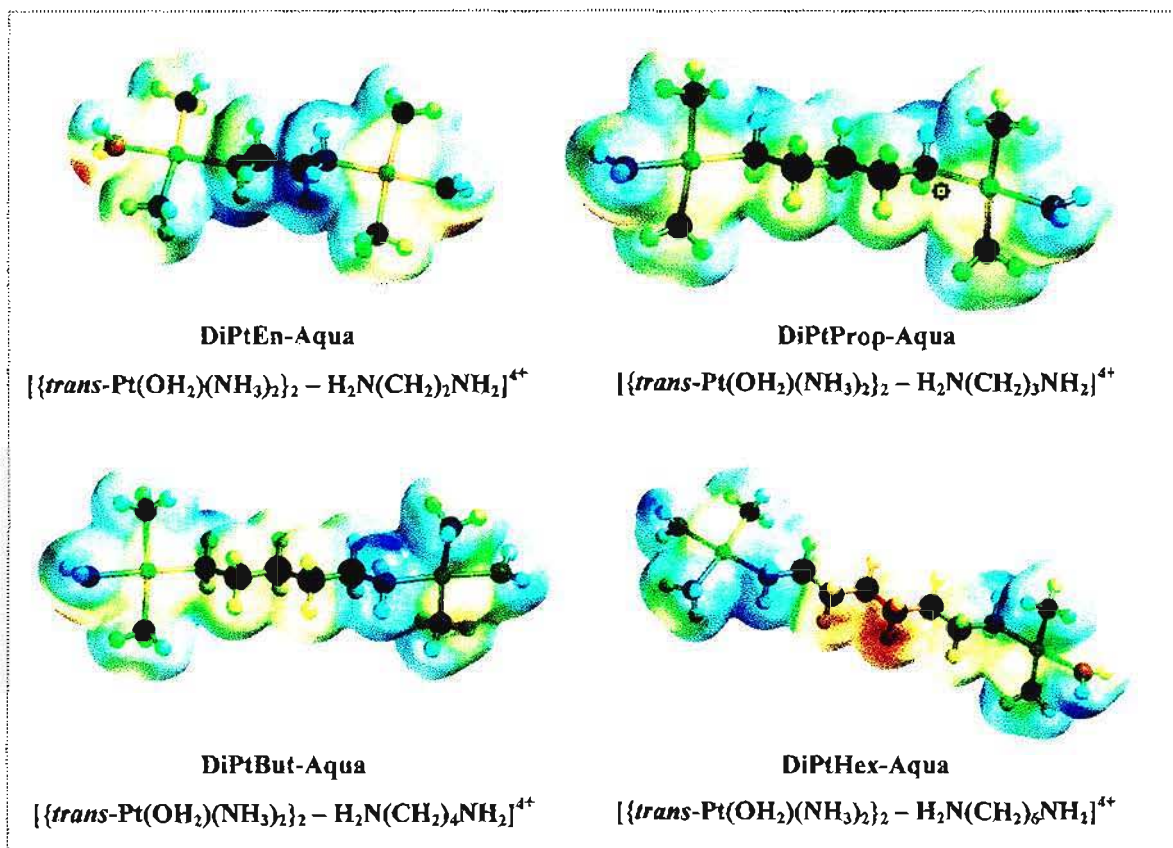
The complexes were all modeled as cations with a +4 charge using the computational software package Spartan® '04 for Windows® using B3LYP density functional method (DFT) and the LACVP+** pseudopotential basis set. The geometry-optimised structures are shown in *Figure 5.2*.

DiPtEn-Aqua

$[\{\mathit{trans}\text{-Pt}(OH_2)(NH_3)_2\}_2 - H_2N(CH_2)_2NH_2]^{4+}$

DiPtProp-Aqua

$[\{\mathit{trans}\text{-Pt}(OH_2)(NH_3)_2\}_2 - H_2N(CH_2)_3NH_2]^{4+}$

DiPtBut-Aqua

$[\{\mathit{trans}\text{-Pt}(OH_2)(NH_3)_2\}_2 - H_2N(CH_2)_4NH_2]^{4+}$

DiPtHex-Aqua

$[\{\mathit{trans}\text{-Pt}(OH_2)(NH_3)_2\}_2 - H_2N(CH_2)_6NH_2]^{4+}$

Figure 5.2: *Geometry optimised structures of complexes DiPtEn-Aqua, DiPtProp-Aqua, DiPtBut-Aqua and DiPtHex-Aqua.*

The electron density distribution about the complexes was also plotted and is shown in *Figure 5.3.*

DiPtEn-Aqua

$[\{trans\text{-}Pt(OH_2)(NH_3)_2\}_2 - H_2N(CH_2)_2NH_2]^{4+}$

DiPtProp-Aqua

$[\{trans\text{-}Pt(OH_2)(NH_3)_2\}_2 - H_2N(CH_2)_3NH_2]^{4+}$

DiPtBut-Aqua

$[\{trans\text{-}Pt(OH_2)(NH_3)_2\}_2 - H_2N(CH_2)_4NH_2]^{4+}$

DiPtHex-Aqua

$[\{trans\text{-}Pt(OH_2)(NH_3)_2\}_2 - H_2N(CH_2)_6NH_2]^{4+}$

Figure 5.3: ***Electron density distribution about each of the investigated complexes. The blue regions indicate the most electropositive areas whilst the red regions indicate the most electronegative areas.***

From the modeled structures, bond lengths and bond angles were obtained and are given in *Table 5.1*. In addition the HOMO (*Figure 5.4*) and LUMO (*Figure 5.5*) structures of the complexes were determined and their energies calculated (*Table 5.2*).

Table 5.1: ***Summary of selected bond lengths and bond angles for each of the investigated complexes obtained from geometry optimization studies using the B3LYP/LACVP+*** *level of theory.*
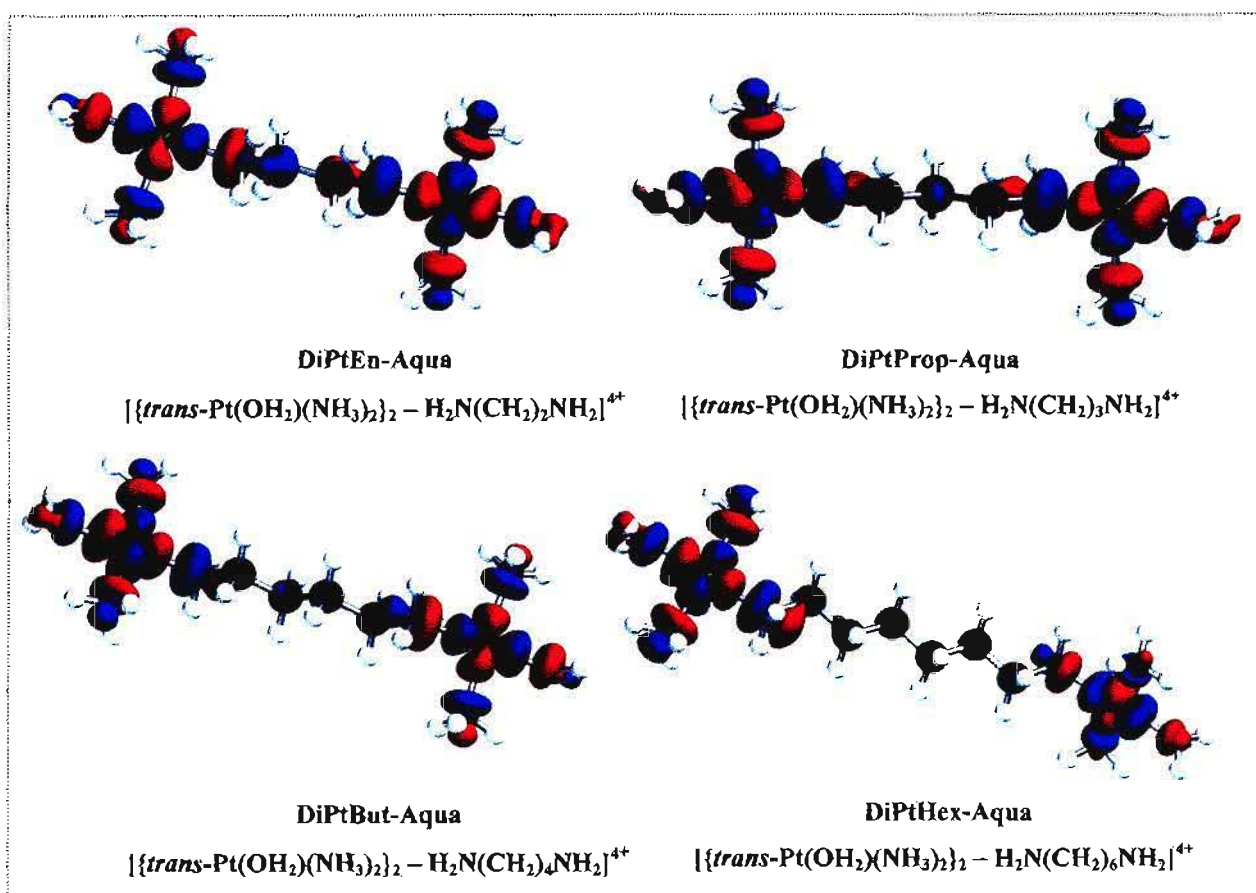
	Dinuclear Platinum^{II} Complexes			
	DiPtEn-Aqua	DiPtProp-Aqua	DiPtBut-Aqua	DiPtHex-Aqua
Pt – OH$_2$ / Å	2.107	2.117	2.124	2.134
Pt – *trans* N† / Å	2.125	2.105	2.093	2.084
Pt – *cis* N†† / Å	2.109	2.107	2.101	2.105
cis N –Pt – *cis* N$^{|}$ / °	172.73	173.57	174.01	174.60

† *trans to the leaving group, i.e. OH$_2$;* †† *cis to the leaving group, i.e. OH$_2$*

$^{|}$ *on the side of H$_2$O*

DiPtEn-Aqua

[{*trans*-Pt(OH$_2$)(NH$_3$)$_2$}$_2$ – H$_2$N(CH$_2$)$_2$NH$_2$]$^{4+}$

DiPtProp-Aqua

[{*trans*-Pt(OH$_2$)(NH$_3$)$_2$}$_2$ – H$_2$N(CH$_2$)$_3$NH$_2$]$^{4+}$

DiPtBut-Aqua

[{*trans*-Pt(OH$_2$)(NH$_3$)$_2$}$_2$ – H$_2$N(CH$_2$)$_4$NH$_2$]$^{4+}$

DiPtHex-Aqua

[{*trans*-Pt(OH$_2$)(NH$_3$)$_2$}$_2$ – H$_2$N(CH$_2$)$_6$NH$_2$]$^{4+}$
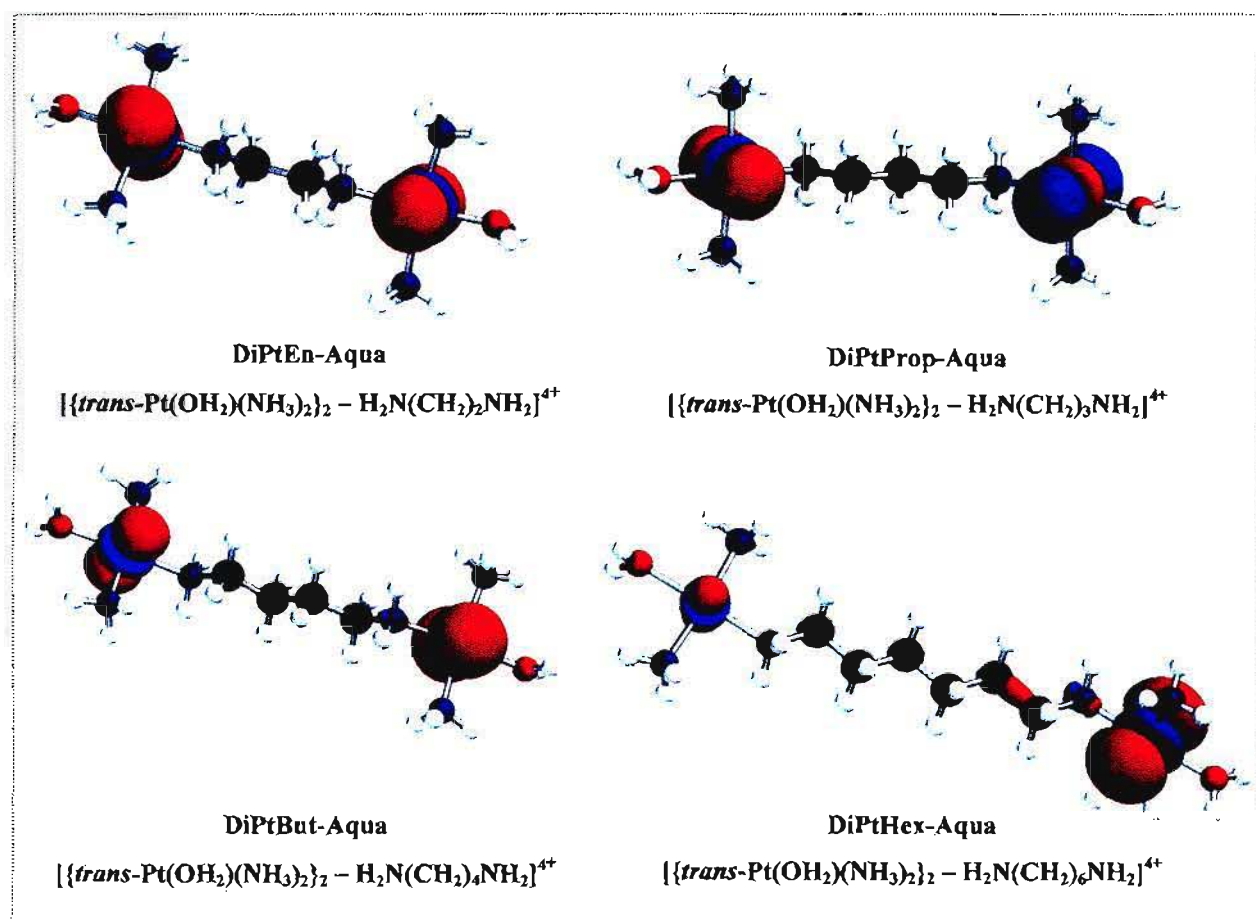
Figure 5.4: ***DFT-calculated (B3LYP/LACVP**) HOMO's for the investigated complexes.***

DiPtEn-Aqua

$[\{trans\text{-}Pt(OH_2)(NH_3)_2\}_2 - H_2N(CH_2)_2NH_2]^{4+}$

DiPtProp-Aqua

$[\{trans\text{-}Pt(OH_2)(NH_3)_2\}_2 - H_2N(CH_2)_3NH_2]^{4+}$

DiPtBut-Aqua

$[\{trans\text{-}Pt(OH_2)(NH_3)_2\}_2 - H_2N(CH_2)_4NH_2]^{4+}$

DiPtHex-Aqua

$[\{trans\text{-}Pt(OH_2)(NH_3)_2\}_2 - H_2N(CH_2)_6NH_2]^{4+}$

Figure 5.5:   *DFT-calculated (B3LYP/LACVP** LUMO's for the investigated complexes.*

To understand the importance of the HOMO-LUMO gap, energy level diagrams showing the interactions are illustrated in *Figure 5.6*.
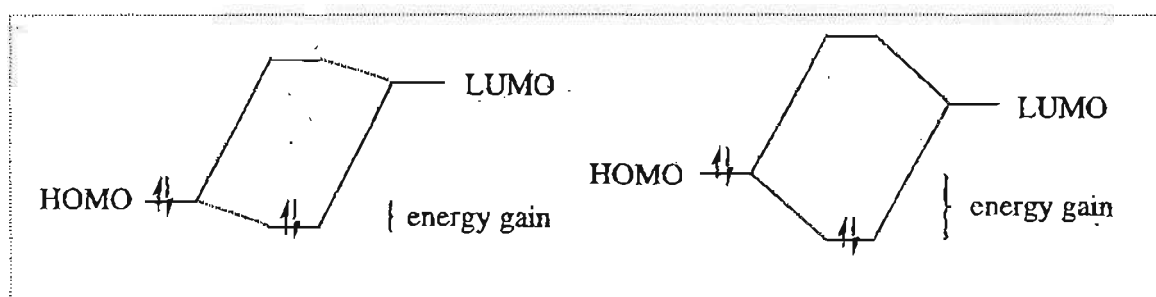
Figure 5.6:   *Energy level diagrams illustrating the interactions between the HOMO and LUMO orbitals.*

The diagrams show two interactions that result into two different energy gaps. The smaller the gap the greater the interaction between the orbitals. This energy gap was determined for the complexes investigated and the outcome is tabulated in *Table 5.2*.

Table 5.2: *Summary of the HOMO and LUMO values obtained for each of the investigated complexes from geometry optimization studies using the B3LYP/LACVP+** level of theory.*

| Complex	HOMO / eV	LUMO / eV	ΔE / eV
DiPtEn-Aqua	-19.62	-14.74	4.88
DiPtProp-Aqua	-19.06	-14.04	5.02
DiPtBut-Aqua	-18.58	-13.49	5.09
DiPtHex-Aqua	-17.90	-12.76	5.14

Figure 5.7 shows the linear correlation between chain length and the energy gap between HOMO and LUMO orbitals. The only complex that does not adhere to this correlation is **DiPtEn-Aqua**, which is probably a result of the stronger interaction between the metal centres due to the shortness of the backbone chain joining them.
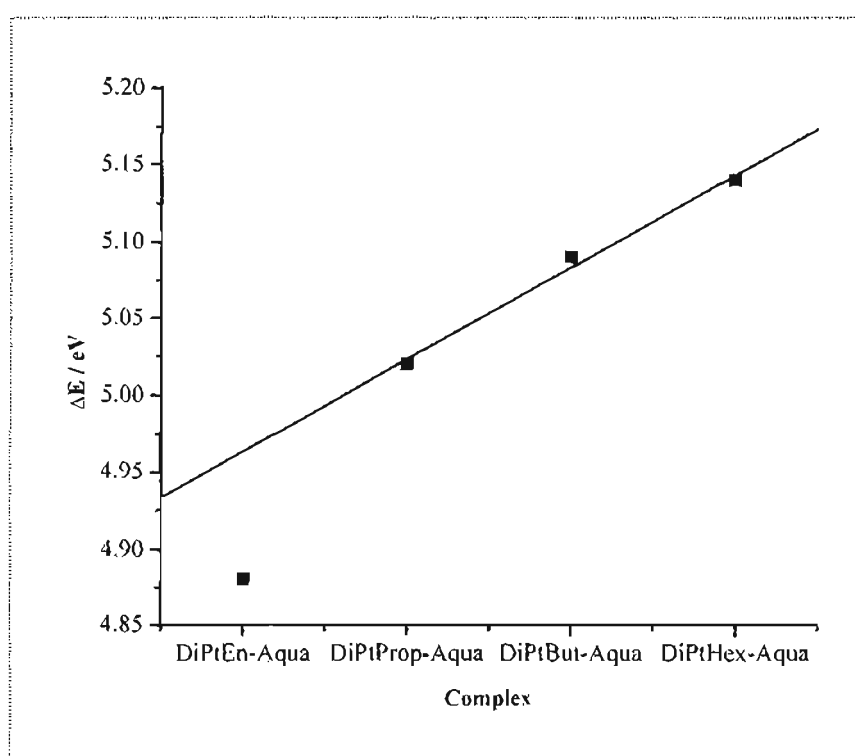
Figure 5.7: *The linear correlation between chain length and the energy gap between HOMO and LUMO orbitals.*

From the data tabulated in *Table 5.1*, it can be observed that upon increasing the length of the diamine chain, the Pt-OH$_2$ and Pt-*trans* N bond lengths are most affected, with the bond lengths increasing and decreasing respectively. The process of increasing the chain length increases the electron density around the *trans*-atom to the platinum through the inductive process, which is equal in both directions. This is supported by an equal decrease and increase of the bonds at the platinum centre. The increase in σ-donor capacity at the *trans*-donor atom results in the shortening of the Pt-N bond length *trans* to the H$_2$O molecule, and consequently a lengthening of the Pt-H$_2$O bond length.

The frontier orbital energies in *Table 5.2* show a clear increasing trend along the series as shown in *Figure 5.8*. This results in the energy gap (E_{HOMO}-E_{LUMO}) increasing from **DiPtEn-Aqua** to **DiPtHex-Aqua**.
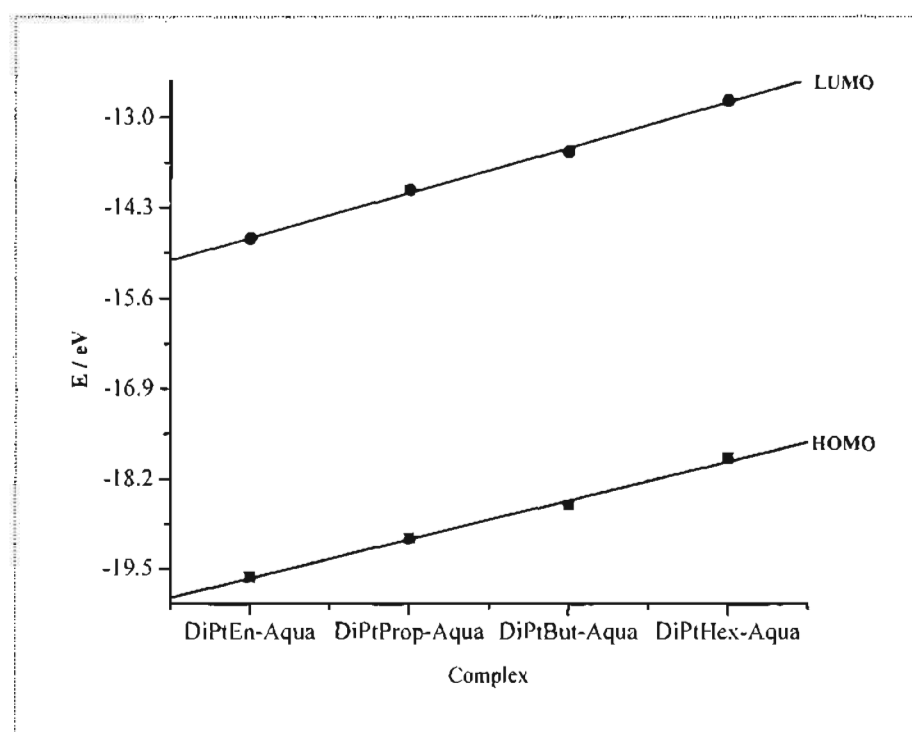
Figure 5.8: *The energy values of the HOMO and LUMO orbitals for the dinuclear platinum complexes.*

The increase in energy is in line with the expectation, since electron donating groups are known to raise the energy of a molecular orbital, unlike electron withdrawing groups[7-10], which lowers the energy. This means as one increases the CH$_2$ groups, the substitution reactions should be expected to be slower due to the increasing energy gap. [7-10]

5.3 *Kinetic Analyses*

The complexes, DiPtEn-Aqua, DiPtProp-Aqua, DiPtBut-Aqua and DiPtHex-Aqua, were synthesized largely in an effort to determine the manner in which the bridging diamine linker might influence the reactivity of the metal centre.

Prior to any nucleophilic substitution processes being investigated, the pK_a of each of the coordinated water moieties were initially determined. This not only served as a means of determining pH conditions for subsequent kinetic analyses, but also provided initial clues in determining how the increased chain length of the diamine linker might affect the substitution processes at the metal centres.

5.3.1 *pK_a Determinations*

The pH titrations of the complexes were carried out in aqueous solution over the pH range of 2-10 as described in *Section 4.2.2* at 25 °C. The initial concentrations and the corresponding pK_a values obtained for the complexes are given in *Table 5.3.*

Table 5.3:   *Summary of the pK_a values obtained for the investigated dinuclear platinum[II] complexes.*

Complex	Initial Concentration (mM)	pK_a
DiPtEn-Aqua	1.01	4.98 ± 0.09
DiPtProp-Aqua	1.01	5.30 ± 0.12
DiPtBut-Aqua	1.00	5.50 ± 0.02
[†]*DiPtHex-Aqua*[11,12]	5.45	5.62 ± 0.03

[†]   *Data obtained from literature.*

A typical example of the spectral changes observed during the pH titration is shown in *Figure 5.9* and the overall process involving the dissociation of the aqua complex may be represented by *Scheme 5.1*.
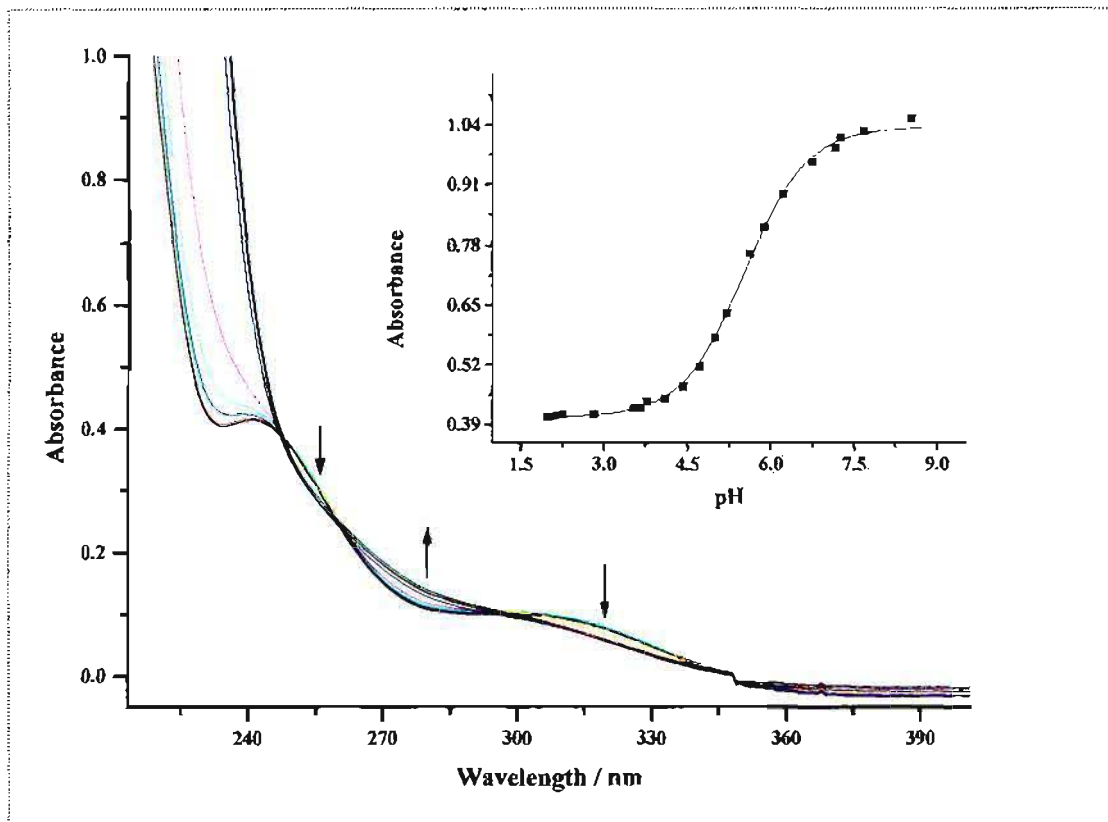
Figure 5.9: *UV/Vis Spectra obtained for DiPtBut-Aqua as a function of pH in the range 2-10 at 25 °C. Inset: Corresponding pKₐ graph at 280 nm.*

$$[H_2O\text{-}Pt_1\text{-}L\text{-}Pt_2\text{-}OH_2]^{4+} + 2\ H_2O$$

$$K_{a1}$$

$$[HO\text{-}Pt_1\text{-}L\text{-}Pt_2\text{-}OH_2]^{3+} + H_2O + H_3O^{+}$$

$$K_{a2}$$

$$[HO\text{-}Pt_1\text{-}L\text{-}Pt_2\text{-}OH]^{2+} + 2\ H_3O^{+}$$
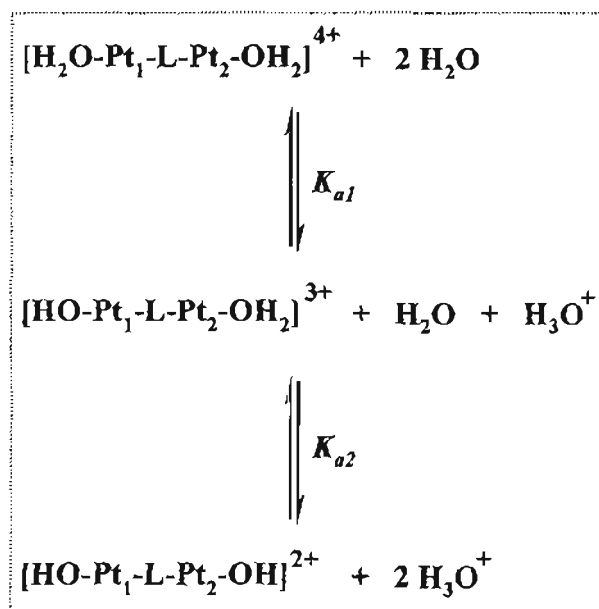
Scheme 5.1: *A general representation of an acid-base equilibria.*

The observation of isosbestic points during the titration is a clear indication that both the hydroxo and aqua species were present in solution. The reversibility of the titration was also tested using aqueous solutions of perchloric acid. The pK_a values were thereafter determined by the fit of *Equation 4.1 (Section 4.2.2)* to the data obtained.

For the complexes, **DiPtEn-Aqua**, **DiPtProp-Aqua** and **DiPtBut-Aqua**, only one pK_a value was obtained, similar to that obtained by Davies *et al.*[11,12] for **DiPtHex-Aqua**. From the results obtained, it can be observed that the pK_a value increases with increasing diamine chain length. This phenomenon is in total agreement with the computational calculation. The lengthening of the chain increases the electron density around the platinum centre through an inductive effect. The net result is the shortening of the bond length *trans* to the H_2O molecule. Since the electron density around the Pt atom increases with increasing chain length, the σ-bond interaction between the Pt-OH_2 becomes weaker resulting in the Pt-O bond length becoming longer *i.e.* the H_2O becomes more labile. This means that the O-H bonds become increasingly more difficult to break resulting in higher pK_a's. This observation is in agreement with what is in literature.[7,13]

It has been shown that the pK_a value obtained for the coordinated water moiety at the platinum[II] centre is a good indicator of the electrophilicity of the metal centre.[7,8] Electron withdrawing π-acceptor effects tends to stabilize the electron rich hydroxo species in comparison to the aqua species and result in lower pK_a values.[7,8] Alternatively, the pK_a value increases if the σ-donor capacity of the ligand *trans* to the aqua moiety is enhanced.[12] Thus, as the length of the bridging diamine chain increases from 2 to 6, so too does the effective σ-donor capacity due to the greater number of CH_2 groups resulting in an increase in the pK_a value as already explained.

Interestingly, the dinuclear complexes studied by Hofmann and van Eldik[5] *(Section 2.6)*, displayed two deprotonation steps whereas in the case of the **1,1/t,t** and **1,1,0/t,t** complexes *(Section 1.6, Figure 1.21)*[11,12], no differentiation between the pK_a value of the first and second deprotonation steps could be made. In addition the order of magnitude of the pK_a values in this study is opposite to that reported in literature[5] when comparing only the propane and butane chains. This difference is likely to be due to the ligand system around the platinum metal.

5.3.2 *Nucleophilic Substitution Reactions*

The rate of substitution of the coordinated aqua moieties from the dinuclear platinum[II] complexes, **DiPtEn-Aqua, DiPtProp-Aqua, DiPBut-Aqua** and **DiPtHex-Aqua** by a series of neutral nucleophiles (*Figure 5.10*), *viz.* thiourea (TU), 1,3-dimethyl-2-thiourea (DMTU) and 1,1,3,3-tetramethyl-2-thiourea (TMTU) was investigated as a function of concentration and temperature under pseudo first-order conditions by monitoring the substitution reactions using either conventional stopped-flow techniques or UV/Visible spectrophotometry.
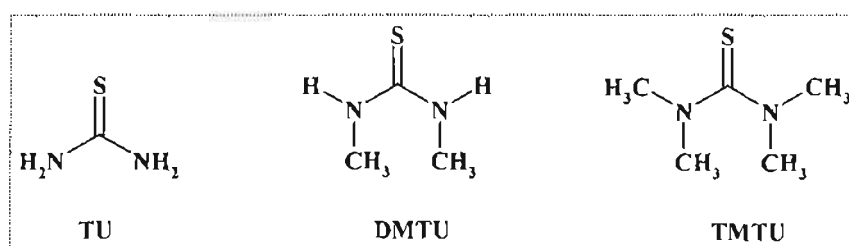
Figure 5.10: *Structural formulae of the nucleophiles utilized in the study viz. thiourea (TU), 1,3-dimethyl-2-thiourea (DMTU) and 1,1,3,3-tetramethyl-2-thiourea (TMTU).*

Reactions involving **DiPtEn-Aqua** were fast enough to be monitored using stopped-flow techniques whilst the other reactions involving the other complexes were followed using the UV-Visible spectrophotometer. The kinetic traces obtained using these two methods are shown in *Figures 5.11* and *5.12* respectively.
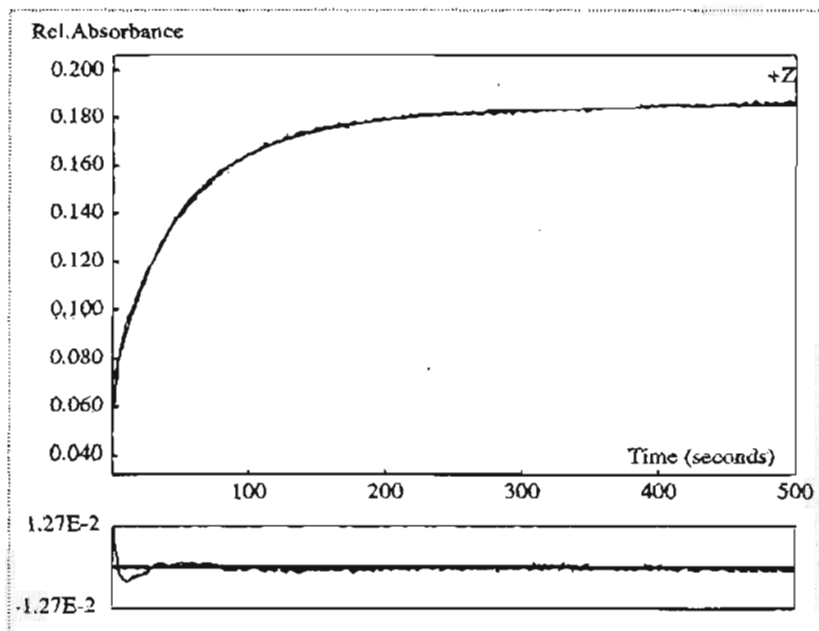
Figure 5.11: *Fit of a double exponential and residuals for the reaction of DiPtEn-Aqua (0.499 mM) with thiourea (50 X, 49.90 mM) followed at 340 nm, I = 0.2 M NaClO₄, T = 298.15 K.*
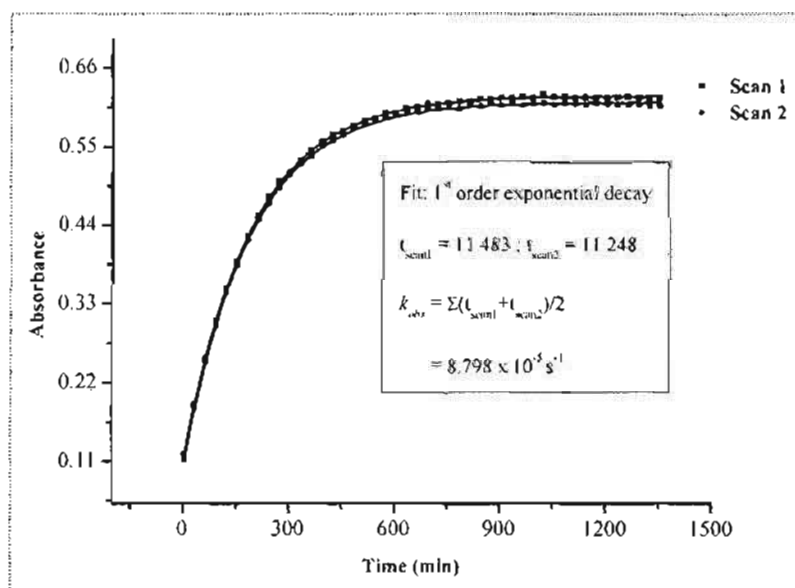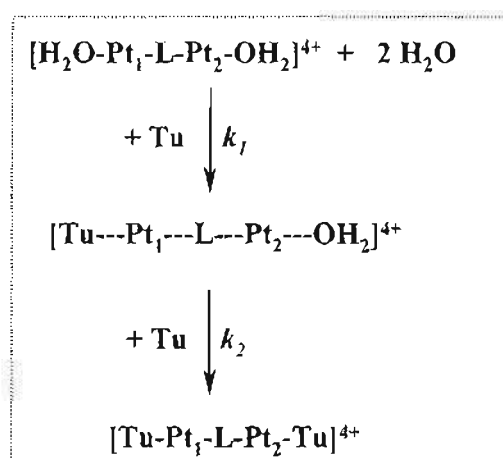

Figure 5.12: *Fit of a first-order exponential decay for the reaction of DiPtBut-Aqua (0.689 mM) with 1,1,3,3-tetramethyl-2-thiourea (TMTU) (40 X, 55.12 mM) followed at 365 nm, I = 0.2 M (NaClO₄), T = 298.15 K.*

It was initially anticipated that the complexes investigated would all exhibit second-order kinetics due to the presence of the two labile aqua moieties. As such, all kinetic traces obtained were initially fitted using a non-linear curve fit on Origin $7.5^{\circledR}$ using a second-order exponential decay function (*Equation 5.1*).

$$y = y_o + A_1 e^{(-(x-x_o))} + A_2 e^{(-(x-x_o)/t_2)} \qquad\qquad 5.1$$

It was found however that only the reaction between **DiPtEn-Aqua** + TU exhibited second-order kinetics and a double exponential fit (*Scheme 5.2*) had to be used to fit the observed time dependant spectra (*Figure 5.13*).

$$[H_2O-Pt_1-L-Pt_2-OH_2]^{4+} + 2\,H_2O$$

$$+\,Tu \quad \bigg\downarrow k_1$$

$$[Tu{-}{-}{-}Pt_1{-}{-}{-}L{-}{-}{-}Pt_2{-}{-}{-}OH_2]^{4+}$$

$$+\,Tu \quad \bigg\downarrow k_2$$

$$[Tu-Pt_1-L-Pt_2-Tu]^{4+}$$

Scheme 5.2: ***Reaction scheme illustrating the mode of substitution of the aqua species from the dinuclear platinum^{II} species exhibiting second-order kinetics.***
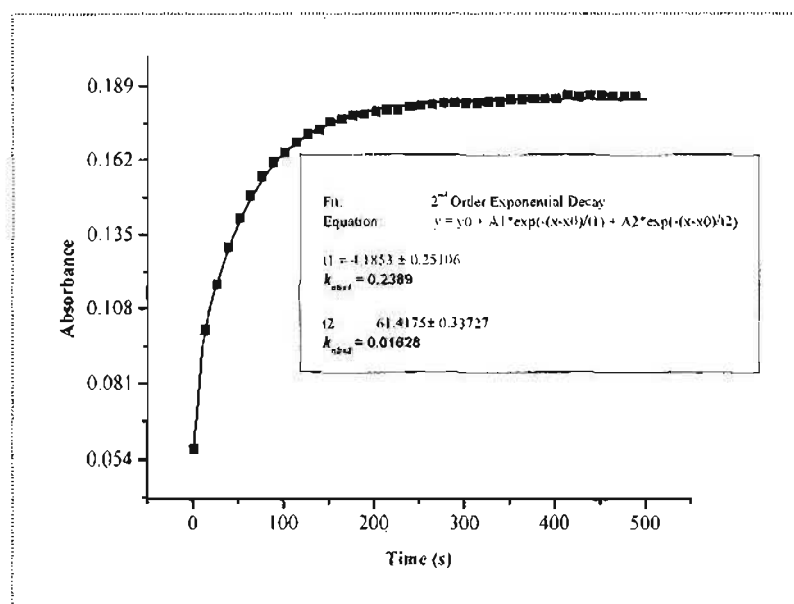
Figure 5.13: __Fit of a second-order exponential for the reaction of DiPtEn-Aqua (0.499 M) with thiourea (50 X, 49.90 mM) followed at 340 nm, I = 0.2 M NaClO₄, T = 298.15 K.__

The observed rate constants, $k_{obs(1,2)}$ obtained hereafter were plotted against the concentration of the entering nucleophile (TU). A linear dependence on the nucleophile concentration was observed for this reaction. The corresponding plot obtained for the reaction of **DiPtEn-Aqua** + Tu is shown in *Figure 5.14* for k_{obs1} and k_{obs2}. The results obtained imply that $k_{obs(1,2)}$ may be expressed as follows:

$$k_{obs(1,2)} = k_{(1,2)}[\text{Nu}]$$

5.2

where $k_{(1,2)}$ represents the second-order rate constants.
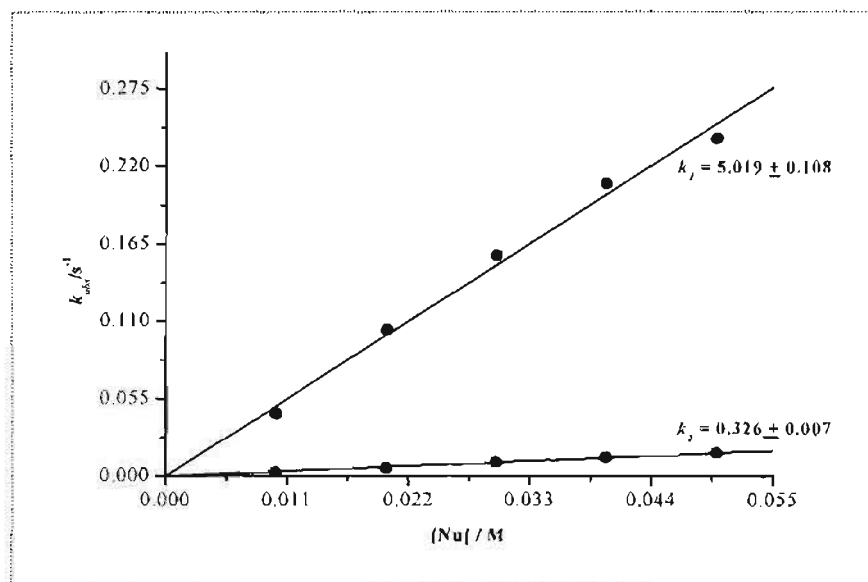
Figure 5.14: *Plots of $k_{obs(1,2)}$ versus [Nu] for the reaction of DiPtEn-Aqua (0.499 mM) with TU at 298.15 K.*

Since no meaningful intercept was obtained, it was concluded that the reverse reaction involving water was too slow to make a significant contribution on the $k_{obs(1,2)}$ values or was completely absent. A difference of approximately 15 times was observed between the values of the second-order rate constants, k_1 and k_2 obtained. This distinction between k_1 and k_2 was however, only observed for the reaction of **DiPtEn-Aqua** with TU as the nucleophile.

Reactions of the remaining complexes, **DiPtProp-Aqua**, **DiPtBut-Aqua** and **DiPtHex-Aqua** with all nucleophiles and **DiPtEn-Aqua** with the DMTU and TMTU were found to be first-order with respect to the incoming nucleophiles and gave excellent fits to a single exponential, a process that can be represented by *Scheme 5.3*.

$$[H_2O\text{-}Pt_1\text{-}L\text{-}Pt_2\text{-}OH_2]^{4+} \ + \ 2\,Tu$$

$$\Big\downarrow k_1$$

$$[TU\text{---}Pt_1\text{---}L\text{---}Pt_2\text{---}TU]^{4+} \ + \ 2\,H_2O$$
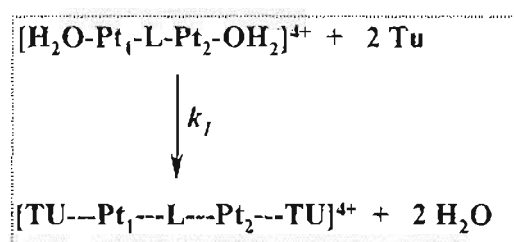
Scheme 5.3: *Reaction scheme illustrating the mode of substitution of the aqua species from the dinuclear platinum^{II} species exhibiting first-order kinetics.*

5-17

The pseudo first-order rate constants k_{obs}, was plotted against the concentration of the incoming nucleophiles. Once again, a linear dependence with no meaningful intercept was obtained. Therefore, k_{obs} can be represented by *Equation 5.3*.

$$k_{obs} = k_2[\text{Nu}]$$
5.3

Representative plots of the second-order rate constants, k_2 obtained from those reactions exhibiting first-order kinetics are shown in *Figure 5.15*. The values of the second-order rate constants, k_2, which results from the direct attack of the nucleophile were obtained from the slopes of these plots at 298.15 K and are summarized in *Table 5.4*.
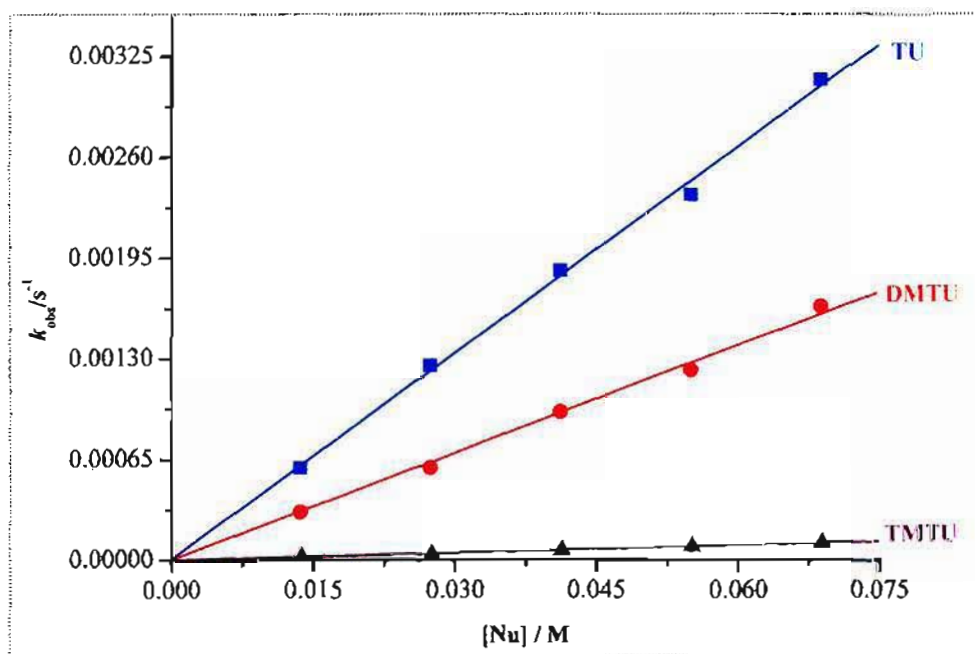
Figure 5.15: *Plots of k_{obs} versus [Nu] for the reaction of DiPtBut-Aqua (0.689 mM) with a series of nucleophiles viz. TU, DMTU and TMTU at 298.15 K.*

Table 5.4: *Summary of rate constants and their corresponding standard deviations for the displacement of the coordinated water molecules by TU, DMTU and TMTU; I = 0.2 M (NaClO₄), T = 298.15 K.*

Nucleophile	$k_2 / 10^{-3} M^{-1}s^{-1}$			
	DiPtEn-Aqua	DiPtProp-Aqua	DiPtBut-Aqua	DiPtHex-Aqua
TU	5029.24 ± 0.01 $(335.6 ± 7.5)^{\dagger}$	70.1 ± 1.0	44.4± 0.6	31.2 ± 0.2
DMTU	131.78 ± 0.01	33.7 ± 0.1	23.1 ± 0.4	17.1 ± 0.1
TMTU	7.23 ± 0.12	2.33 ± 0.02	1.61 ± 0.02	1.01 ± 0.02

The temperature dependence of the rate constant, k_2 was studied over the range of 15-35 °C or 20-40 °C depending on the reactivity of the complex. A typical plot obtained is illustrated in *Figure 5.16*. The corresponding activation parameters were calculated using the Eyring equation (*Chapter 3, Equation 3.76*) and are tabulated in *Table 5.5*.

---

†   *Second-order rate constant, k_2, calculated for the second substitution step.*

Figure 5.16: <u>Plots of ln(k_2/T) versus 1/T for the reaction of DiPtHex-Aqua with a series of nucleophiles viz. TU, DMTU and TMTU at various temperatures, whilst keeping the nucleophile concentration constant at ca. 50 X greater than that of the metal complex.</u>

Table 5.5: **Summary of activation parameters and the corresponding standard deviations for the displacement of the coordinated water molecules by TU, DMTU and TMTU; I = 0.2 M (NaClO₄).**

Complex	Nucleophile	$\Delta H^{\neq}$ (kJ mol^{-1})	$\Delta S^{\neq}$ (J K^{-1} mol^{-1})
DiPtEn-Aqua	TU	48.7 ± 6.1 (48.7 ± 1.1)[†]	-67.6 ± 19.9 (-69.4 ± 3.8)[†]
	DMTU	45.8 ± 2.5	-108 ± 8.4
	TMTU	59.9 ± 2.8	-82.1 ± 9.5
DiPtProp-Aqua	TU	38.2 ± 1.5	-138 ± 5
	DMTU	38.7 ± 2.2	-144 ± 7
	TMTU	54.6 ± 2.3	-113 ± 8
DiPtBut-Aqua	TU	49.1 ± 1.6	-107 ± 5
	DMTU	55.7 ± 1.5	-90.5 ± 4.9
	TMTU	60.6 ± 1.7	-95.6 ± 5.6
DiPtHex-Aqua	TU	56.5 ± 0.6	-84.6 ± 1.8
	DMTU	61.6 ± 0.5	-72.4 ± 1.7
	TMTU	64.1 ± 1.1	-87.5 ± 3.6

[†] *Calculated activation parameters ($\Delta H^{\neq}$ and $\Delta S^{\neq}$) for the second substitution step.*

5.4 *Discussion*

What has the study achieved? It has shown that the pK_a value for the coordinated water increased with increasing length of the diamine linker as seen in *Table 5.3*. This trend is supported by the computational calculations on the $Pt\text{-}OH_2$ bond length, which were also found to increase as the distance between the two platinum atoms was increased. One can infer from this that the water molecule becomes more labile with the increase of the diamine linker.

The lengthening of the $Pt\text{-}OH_2$ bond can be accounted for, by looking at the bond *trans* to the water molecules. The theoretical calculation shows a decrease in length of this bond. It can therefore be concluded that there is a net increase in σ-donicity toward the platinum centre *i.e.* the well-known *trans*-effect is influencing the basicity of the complex by promoting ground-state destabilization. This is manifested in the elongation of the $M\text{-}OH_2$ bonds *trans* to the σ-bound nitrogen atom of the diamine linker. This observation is probably the same with that observed for metal-halide and metal-water *trans* to the σ-bound carbon atom.[13,14]

The reactivity of these di-platinum complexes were determined and found to be dependent on the length of the diamine linker as well. Looking at the pK_a values and the HOMO-LUMO energy gap, it is reasonable to expect the reactivity of these complexes to decrease from **DiPtEn-Aqua** to **DiPtHex-Aqua**.[9,10] This was indeed found to be the case. From the bond length of $M\text{-}OH_2$ one would have expected the trend to be in the opposite direction due to the lability of the water molecules as indicated by the theoretical calculation. However, this is contrary to the result obtained. The interpretation of this is that, whilst the *trans*-effect is operational in these molecules and increases from the **En** to the **Hex** ligand, it does not appear to be the controlling factor. It is obvious, that the rate of substitution increases due to either ground-state destabilization or transition state destabilization. In this case destabilization of the ground-state does occur as supported by the computational calculations of the $M\text{-}OH_2$ bond lengths which have been shown to increase with an increase in the length of the linking chain. In addition to this effect, the shortening of the Pt-N bond in the *trans* position to the water molecules results in destabilization of the transition state. This is thought to be due to the increase in σ-donicity to the metal centre.

5-22

This decreases the electrophilic character of the metal centre with a net effect of repelling the incoming nucleophile. In this case it is most likely that the two effects play a simultaneous role, with the latter probably being more dominant.

The retardation on the rate of substitution from **DiPtEn-Aqua** to **DiPtHex-Aqua** can also be attributed to steric hindrance around the Pt centre. Analysis of the geometry-optimized structures tends to suggest that as the chain length of the diamine linker increases, so too does the flexibility of the complex. It would appear that as the CH_2 groups are increased, the number of rotations about these bonds increases leading to a greater number of possible conformers for the diplatinum complexes. This increased flexibility consequently leads to a greater degree of steric influence and in all probability do directly influence the path that the incoming nucleophile adopts in approaching the metal centre. If it is assumed that these complexes from **DiPtProp- Aqua** can form curvature in solution, it becomes obvious that the axial attack from one side will be greatly reduced. It is most likely that this steric hindrance by itself may account for a bigger percentage of the factors influencing the reactivity of these complexes.

In comparing the reactivity of the aqua complexes in *Table 5.4*, it can be summarized that the substitution behaviour of the complexes clearly depends on the length of the diamine linker. The increasing of the CH_2 group increases the σ-donicity around the platinum centre, as reflected by the shortening of the Pt-N bond length and higher pK_a for the ionisation of the aqua ligand. This results in a net decrease in the electrophilicity at the metal centre. In addition, increasing of the CH_2 unit increases the flexibility of the complexes, resulting in increased steric hindrance. Both these factors contribute towards the decrease in the rate of substitution of the coordinated water molecule.

Substitution reactions with sterically less hindered thiourea (Tu) is about 10^2 times faster for **DiPtEn-Aqua** when compared to the other complexes. The reason for the observed trend across the complexes has been accounted for, what requires explanation is the big difference between **DiPtEn-Aqua** and the other complexes. The reason for this enhanced reactivity is due to the interaction between the two Pt^{II} centres, apart from all other factors, which are also operational. This is strongly supported by the fact that this was the only complex where absolute values of k_1 and k_2 could be differentiated. The findings compare well with Farrell's[11] study involving 1,1/t,t where there was no measurable difference in

the coordinated water and decreases the electrophilicity of the metal centre. Other factors that slow down the rate of substitution is the increasing steric hindrance due to the flexibility of the complexes as the chain becomes longer. It is also observed that when $n \geq 3$, the Pt···Pt interactions diminishes, and it is not possible to distinguish the two rate constants. The associative substitution mechanism remains operational in all the systems investigated. This study has shed some light in trying to understand the influence of the linker backbone on the binuclear complexes with regards to folding abilities, Pt···Pt distance and interactions.

References

1. Farrell, N., Qu, Y., Feng, L., van Houten, B., *Biochemistry*, *29*, **1990**, 9522.

2. Farrell, N. & Qu. Y., *Inorg. Chem.*, *31*, **1992**, 930.

3. Farrell, N., *Comments Inorg. Chem.*, *16*, **1995**, Part 6, 373.

4. Rauter, H., Di Domenico, R., Menta E., Oliva, A., Qu, Y., Farrell, N., *Inorg. Chem.*, *36*, **1997**, 3919.

5. Hofmann, A. & van Eldik, R., *J. Chem. Soc. Dalton Trans.*, **2003**, 2979.

6. Bugarčič, Z.D., Petrović, B.V.; Jelić, R., *Trans. Met. Chem.*, *26*, **2001**, 668.

7. Hofmann, A., Jaganyi, D., Munro, O.Q., Liehr, G., van Eldik, R., *Inorg. Chem.*, *42*, **2003**, 1688.

8. Jaganyi, D., Hofmann, A., van Eldik, R., *Agnew. Chem., Int. Ed.*, *40*, **2001**, 1680.

9. Otto, S., Elding, L.I., *J. Chem. Soc. Dalton Trans.*, **2002**, 2354.

10. Romeo, R., Plutino, M.R., Scolaro, L.M., Stoccoro, S., Minghetti, G., *Inorg. Chem.*, *39*, **2000**, 4749.

11. Davies, M.S., Cox, J.W., Berners-Price, S.J., Barklage, W., Qu, Y., Farrell, N., *Inorg. Chem.*, *39*, **2000**, 1710.

12. Davies, M.S., Thomas, D.S., Hegmans, A., Berners-Price, S.J., Farrell, N., *Inorg. Chem.*, *41*, **2002**, 1101.

13. Ryabov, A.D., Kazankov, G.M., Yatsimirky, A.K., et.al., *Inorg. Chem.*, *32*, **1992**, 3083.

14. Castan., P., Laud, J., Wimmer, S., Wimmer, F.L., *J. Chem. Soc. Dalton Trans.*, **1991**, 1155.

15. Jaganyi, D. & Tiba, F., *Trans. Met. Chem.*, *28*, **2003**, 803.

16. Romeo, R., Monsu-Scolaro, L., Plutino, M.R., et al., *Inorganica Chimica Acta.*, *350*, **2003**, 143.

17. Romeo, R., Grassi, A., Monsu-Scolaro, L., *Inorg. Chem.*, *31*, **1992**, 4383.

Appendix A

Supporting Information

Appendix A

Table A1:   Summary of the pK_a values obtained for the deprotonation of the aqua complexes of **DiPtEn-Aqua, DiPtProp-Aqua** and **DiPtBut-Aqua**.

	Complex		
	DiPtEn-Aqua	**DiPtProp-Aqua**	**DiPtBut-Aqua**
pK_a	4.98	5.30	5.50
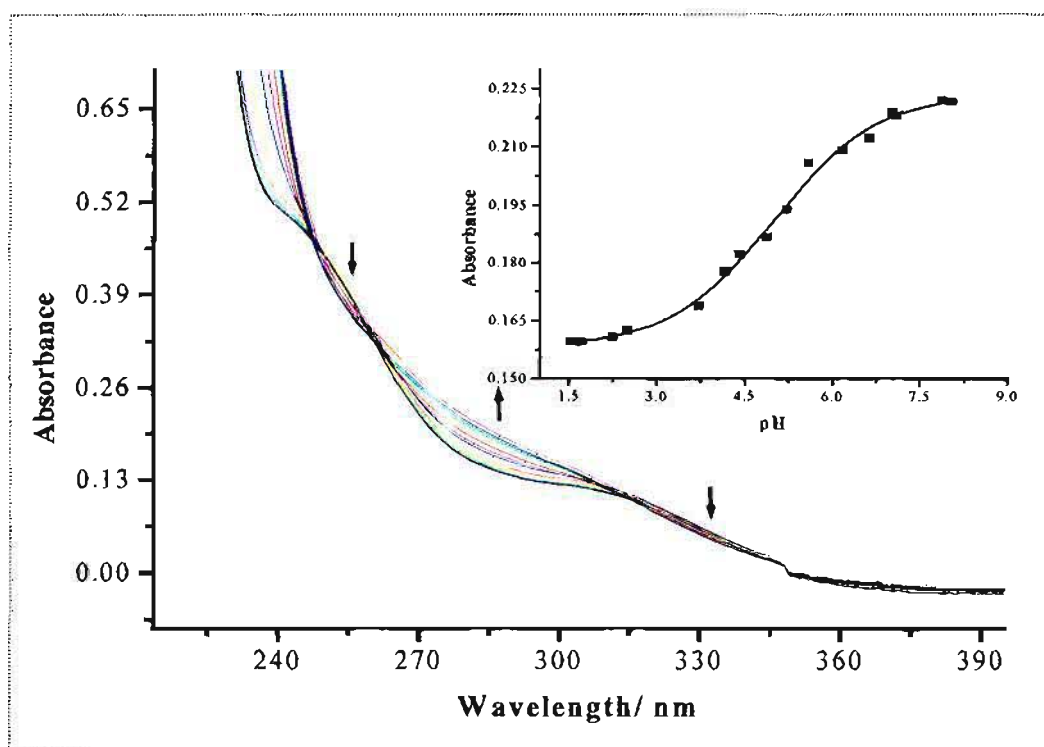
Figure A1:   UV/Vis Spectra obtained for **DiPtEn-Aqua** as a function of pH in the range 2-10 at 25 °C. *Inset: Corresponding pK_a graph at 280 nm.*
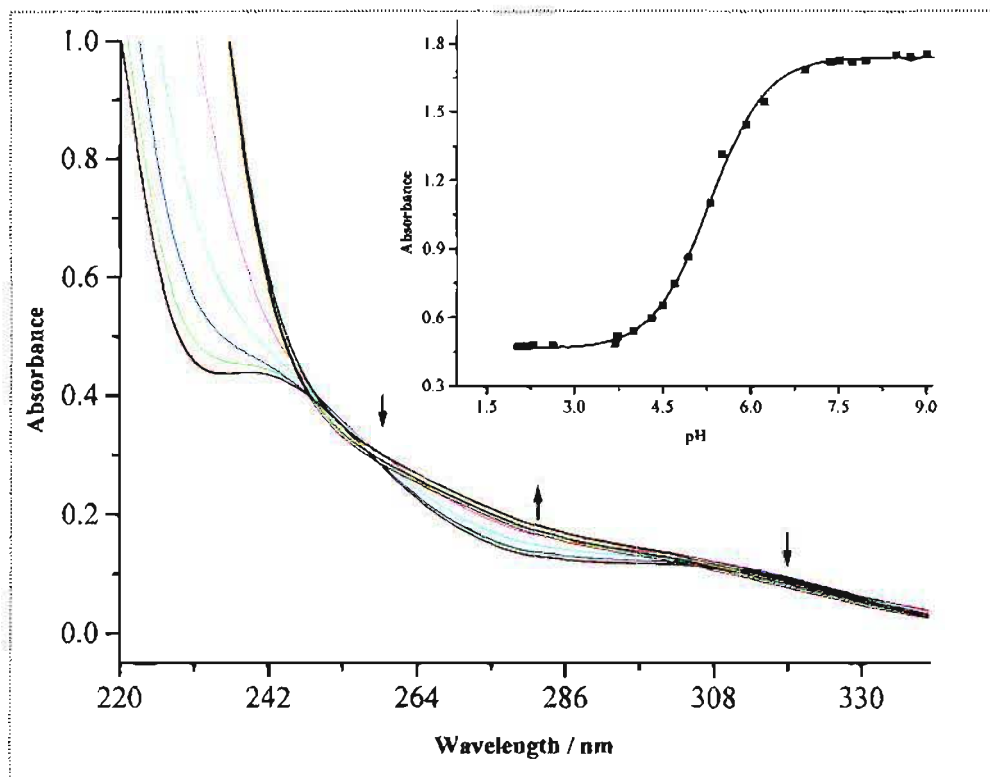
Figure A2: UV/Vis Spectra obtained for **DiPtProp-Aqua** as a function of pH in the range 2-10 at 25 °C. *Inset: Corresponding pK$_a$ graph at 280 nm.*
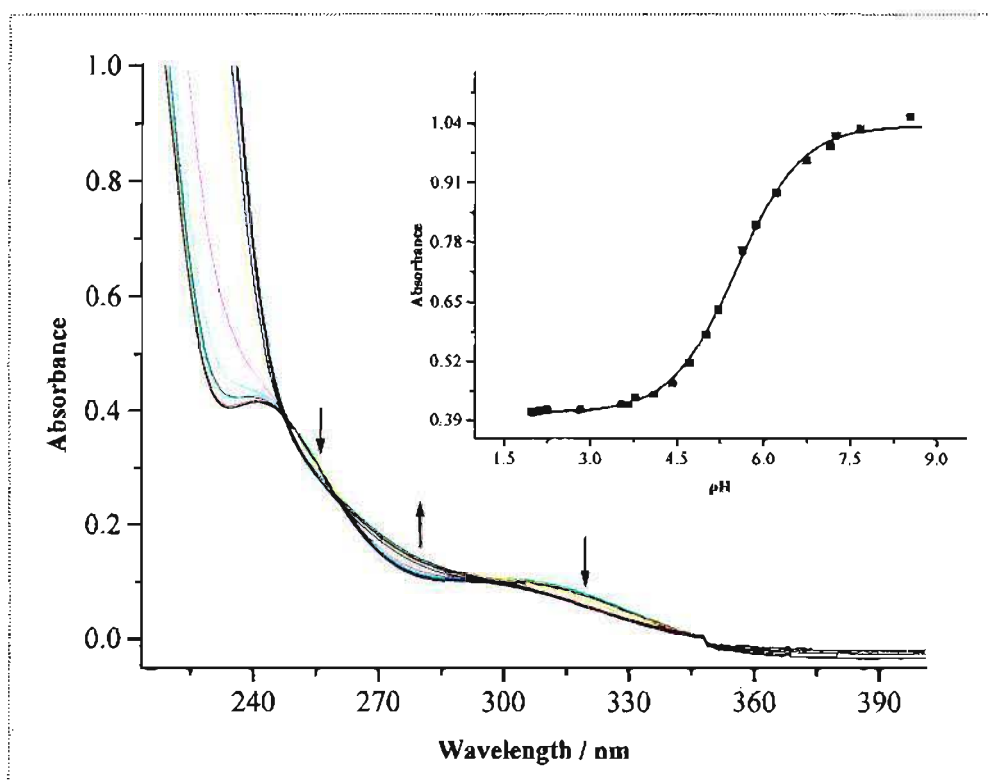
Figure A3: UV/Vis Spectra obtained for **DiPtBut-Aqua** as a function of pH in the range 2-10 at 25 °C. *Inset: Corresponding pK$_a$ graph at 280 nm.*

Table A2:   Summary of Selected Wavelengths (nm) used in Kinetic Measurements.

Complex				
Nucleophile	**DiPtEn-Aqua**	**DiPtProp-Aqua**	**DiPtBut-Aqua**	**DiPtHex-Aqua**
TU	340	340	338	338
DMTU	295	340	338	338
TMTU	365	360	365	360

Table A3:   Average observed rate constants, k_{obs}, at 25 °C, for the reactions of **DiPtEn-Aqua** (0.499 mM) with a series of nucleophiles at different concentrations.

[TU]/ mM	k_{obs}, s^{-1}	[DMTU]/ mM	k_{obs}, s^{-1}	[TMTU]/ mM	k_{obs}, s^{-1}
9.983	4.476×10^{-2} $2.567 \times 10^{-3\dagger}$	9.983	1.460×10^{-3}	7.260	7.559×10^{-5}
19.97	1.070×10^{-1} $5.750 \times 10^{-3\dagger}$	19.97	2.825×10^{-3}	14.52	1.545×10^{-4}
29.95	1.570×10^{-1} $9.864 \times 10^{-3\dagger}$	29.95	4.309×10^{-3}	21.78	2.177×10^{-4}
39.93	2.080×10^{-1} $1.341 \times 10^{-3\dagger}$	39.93	4.869×10^{-3}	29.04	2.973×10^{-4}
49.91	2.399×10^{-1} $1.629 \times 10^{-3\dagger}$	49.91	6.567×10^{-3}	36.30	3.486×10^{-4}

[Pt] = 0.363 mM for the reaction with TMTU.

$\dagger$ k_{obs} calculated for the second substitution step.

Table A4: Average observed rate constants, k_{obs}, at 25 °C, for the reactions of DiPtProp-Aqua (0.665 mM) with a series of nucleophiles at different concentrations.

[TU]/ mM	k_{obs}, s^{-1}	[DMTU] / mM	k_{obs}, s^{-1}	[TMTU] / mM	k_{obs}, s^{-1}
13.30	1.040×10^{-3}	13.30	4.988×10^{-4}	13.30	3.284×10^{-5}
26.60	1.960×10^{-3}	26.60	9.439×10^{-4}	26.60	6.431×10^{-5}
39.90	2.660×10^{-3}	39.90	1.294×10^{-3}	39.90	9.486×10^{-5}
53.20	3.720×10^{-3}	53.20	1.646×10^{-3}	53.20	1.224×10^{-4}
66.50	4.750×10^{-3}	66.50	2.353×10^{-3}	66.50	1.541×10^{-4}

Table A5: Average observed rate constants, k_{obs}, at 25 °C, for the reactions of DiPtBut-Aqua (0.689 mM) with a series of nucleophiles at different concentrations.

[TU] / mM	k_{obs}, s^{-1}	[DMTU] / mM	k_{obs}, s^{-1}	[TMTU] / mM	k_{obs}, s^{-1}
13.78	5.989×10^{-4}	13.78	3.115×10^{-4}	13.78	2.303×10^{-5}
27.56	1.259×10^{-3}	27.56	6.015×10^{-4}	27.56	4.195×10^{-5}
41.34	1.869×10^{-3}	41.34	9.595×10^{-4}	41.34	6.418×10^{-5}
55.12	2.338×10^{-3}	55.12	1.226×10^{-3}	55.12	8.798×10^{-5}
68.9	3.104×10^{-3}	68.9	1.640×10^{-3}	68.9	1.136×10^{-4}

Table A6: Average observed rate constants, k_{obs}, at 25 °C, for the reactions of DiPtHex-Aqua (0.496 mM) with a series of nucleophiles at different concentrations.

[TU] / mM	k_{obs}, s^{-1}	[DMTU] / mM	k_{obs}, s^{-1}	[TMTU] / mM	k_{obs}, s^{-1}
9.91	2.885×10^{-4}	9.91	1.564×10^{-4}	9.91	9.329×10^{-6}
19.82	6.185×10^{-4}	19.82	3.385×10^{-4}	19.82	1.899×10^{-5}
29.73	9.013×10^{-3}	29.73	5.056×10^{-4}	29.73	2.795×10^{-5}
39.64	1.238×10^{-3}	39.64	6.770×10^{-4}	39.64	4.097×10^{-5}
49.55	1.559×10^{-3}	49.55	8.553×10	49.55	5.061×10^{-5}

Table A7: Average observed rate constants, k_{obs}, at 25 °C, for the reactions of **DiPtEn-Aqua** (0.499 mM) at varied temperatures, whilst maintaining nucleophile concentration constant at $\approx$ 30x **[DiPtEn-Aqua]**.[Tu], [DMTU] were 29.95 mM.

T / K	TU, k_{obs} (s^{-1})	DMTU, k_{obs} (s^{-1})	TMTU, k_{obs} (s^{-1})
283.15	8.923 x 10^{-2} 4.521 x 10$^{-3\dagger}$	2.100 x 10^{-3}	-
288.15	1.082 x 10^{-1} 6.450 x 10$^{-3\dagger}$	2.738 x 10^{-3}	1.521 x 10^{-4}
293.15	1.778 x 10^{-1} 9.864 x 10$^{-3\dagger}$	4.310 x 10^{-3}	2.177 x 10^{-4}
298.15	2.042 x 10^{-1} 1.374 x 10$^{-2\dagger}$	5.708 x 10^{-3}	3.565 x 10^{-4}
303.15	3.682 x 10^{-1} 2.124 x 10$^{-2\dagger}$	7.445 x 10^{-3}	5.182 x 10^{-4}

Table A8: Average observed rate constants, k_{obs}, at 25 °C, for the reactions of **DiPtProp-Aqua** (0.665 mM) at varied temperatures, whilst maintaining nucleophile concentration constant at $\approx$ 50x **[DiPtProp-Aqua]**. [Tu], [DMTU] and [TMTU] were 66.50 mM.

T / K	TU, k_{obs} (s^{-1})	DMTU, k_{obs} (s^{-1})	TMTU, k_{obs} (s^{-1})
288.15	3.503 x 10^{-3}	1.597 x 10^{-3}	9.656 x 10^{-3}
293.15	4.802 x 10^{-3}	2.353 x 10^{-3}	1.542 x 10^{-3}
298.15	6.294 x 10^{-3}	2.999 x 10^{-3}	2.300 x 10^{-3}
303.15	8.353 x 10^{-3}	5.699 x 10^{-3}	3.217 x 10^{-3}
308.15	1.007 x 10^{-2}	7.286 x 10^{-3}	4.327 x 10^{-3}

[Pt] = 0.363 mM, [TMTU] = 21.78 mM
† k_{obs} calculated for the second substitution step.

Table A9: Average observed rate constants, k_{obs}, at 25 °C, for the reactions of **DiPtBut-Aqua** (0.689 mM) at varied temperatures, whilst maintaining nucleophile concentration constant at $\approx$ 50x [**DiPtBut-Aqua**]. [Tu], [DMTU] and [TMTU] were 68.90 mM.

T / K	TU, k_{obs} (s^{-1})	DMTU, k_{obs} (s^{-1})	TMTU, k_{obs} (s^{-1})
288.15	2.104 x 10^{-3}	9.820 x 10^{-4}	7.004 x 10^{-5}
293.15	3.104 x 10^{-3}	1.654 x 10^{-3}	1.136 x 10^{-4}
298.15	4.361 x 10^{-3}	2.169 x 10^{-3}	1.552 x 10^{-4}
303.15	6.243 x 10^{-3}	3.263 x 10^{-3}	2.513 x 10^{-4}
308.15	8.042 x 10^{-3}	4.379 x 10^{-3}	3.707 x 10^{-4}

Table A10: Average observed rate constants, k_{obs}, at 25 °C, for the reactions of **DiPtHex-Aqua** (0.496 mM) at varied temperatures, whilst maintaining nucleophile concentration constant at $\approx$ 50x [**DiPtHex-Aqua**]. [Tu], [DMTU] and [TMTU] were 49.55 mM.

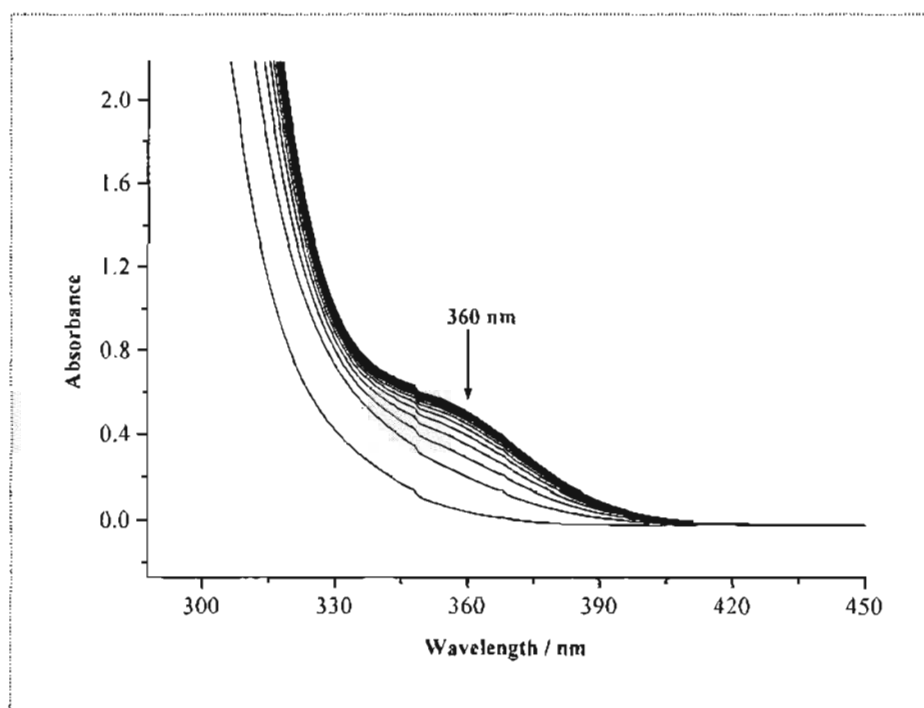| T / K	TU, k_{obs} (s^{-1})	DMTU, k_{obs} (s^{-1})	TMTU, k_{obs} (s^{-1})
288.15	1.041 x 10^{-3}	5.437 x 10^{-4}	3.257 x 10^{-5}
293.15	1.558 x 10^{-3}	8.553 x 10^{-4}	5.061 x 10^{-5}
298.15	2.308 x 10^{-3}	1.327 x 10^{-3}	7.613 x 10^{-5}
303.15	3.440 x 10^{-3}	1.982 x 10^{-3}	1.215 x 10^{-4}
308.15	4.837 x 10^{-3}	2.992 x 10^{-3}	1.855 x 10^{-4}

Figure A4: Observed change in absorbance for the reaction of **DiPtEn-Aqua** + TMTU at 25 °C.
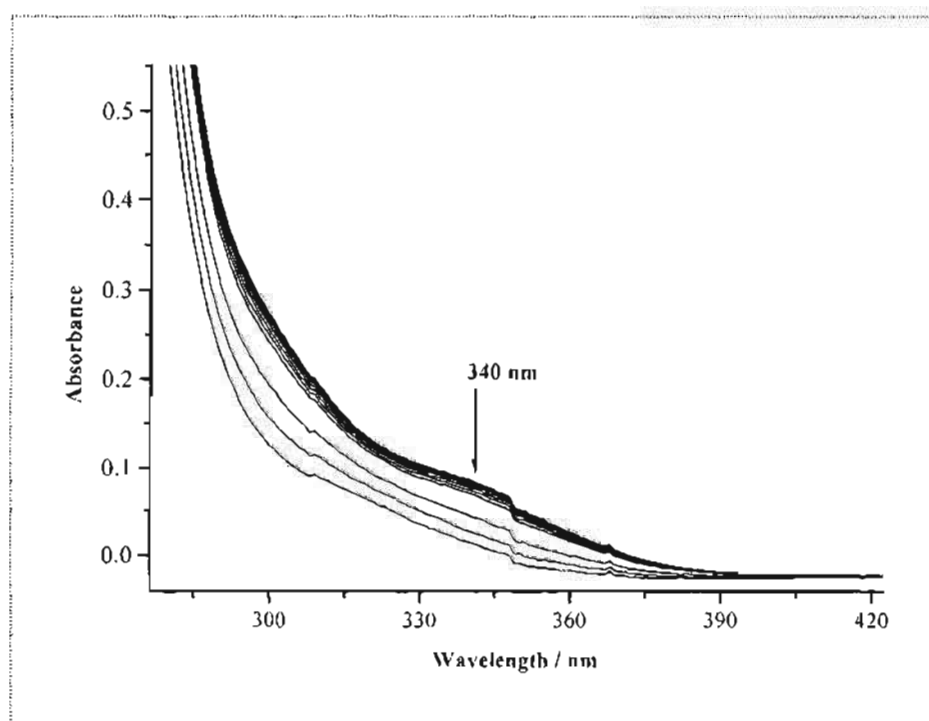

Figure A5: Observed change in absorbance for the reaction of **DiPtProp-Aqua** + DMTU at 25 °C.
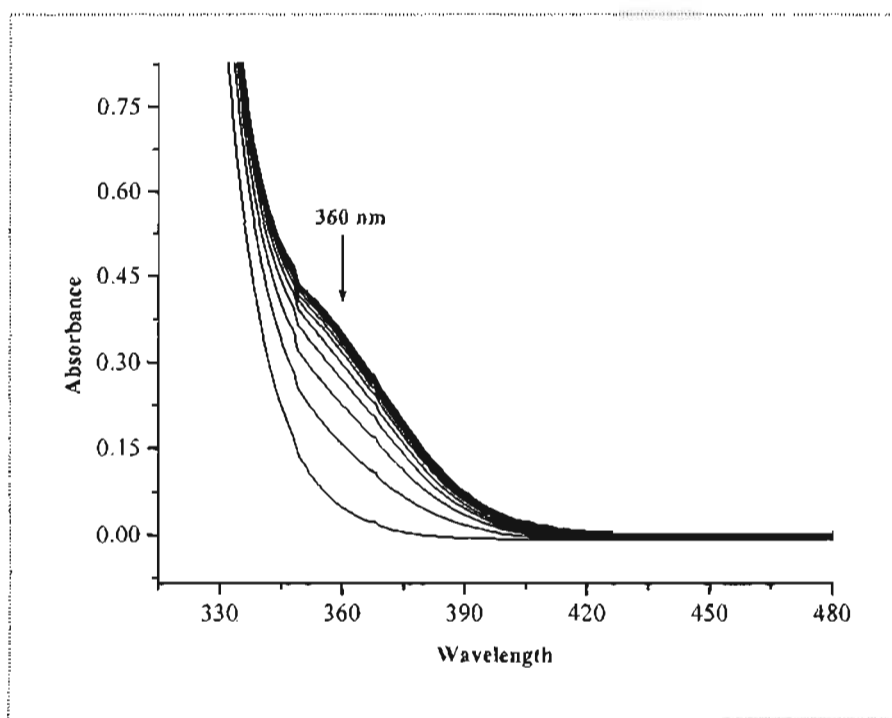
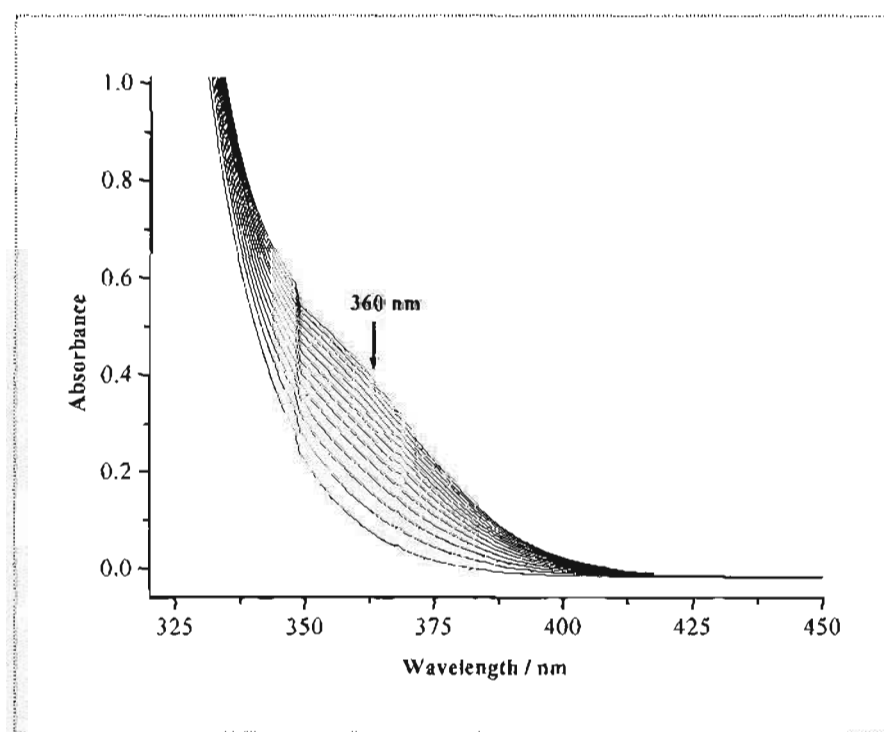**Figure A6:** Observed change in absorbance for the reaction of **DiPtProp-Aqua** + TMTU at 25 °C.

Figure A7: Observed change in absorbance for the reaction of **DiPtHex-Aqua** + TMTU at 25 °C.
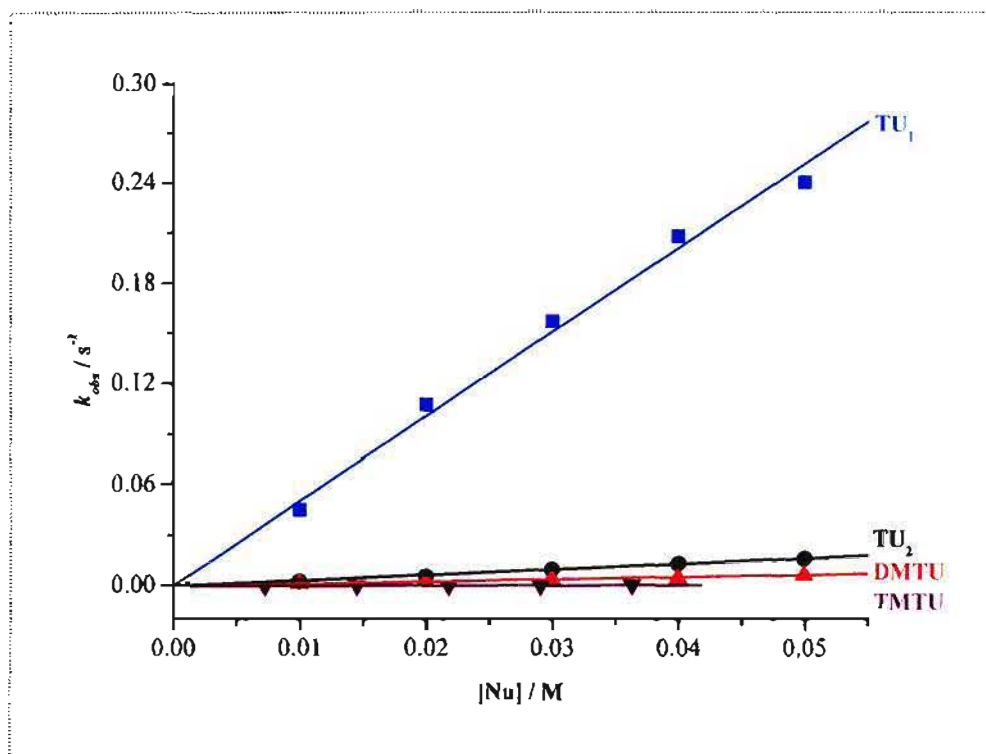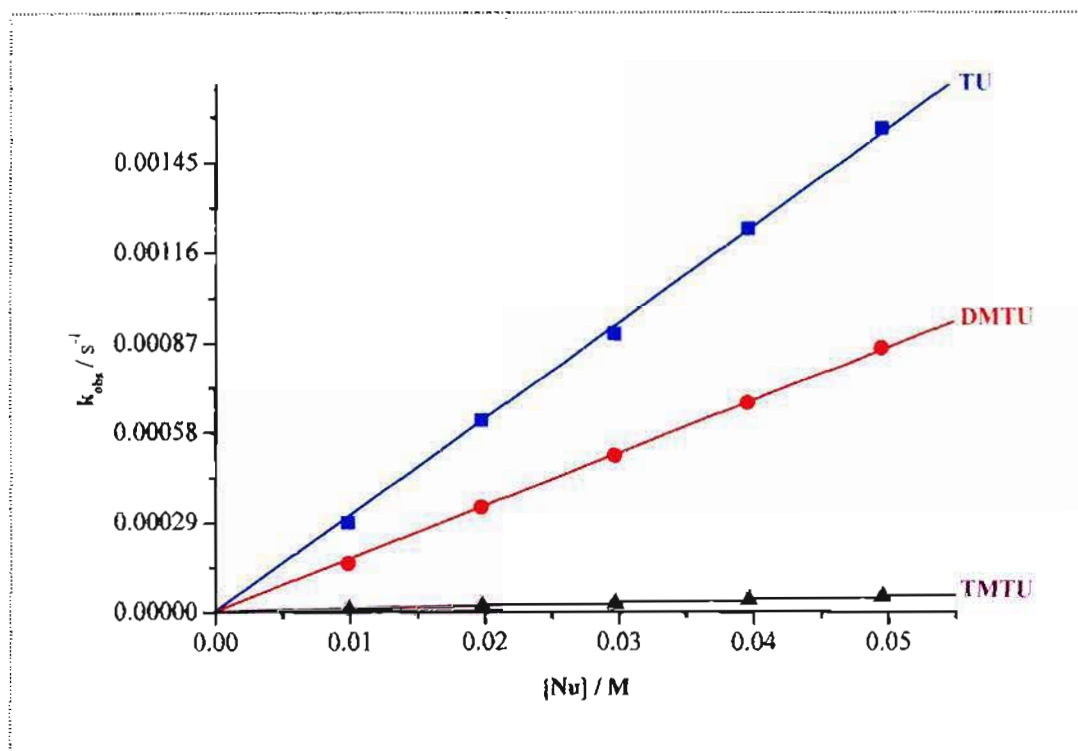
Figure A8: Graph of k_{obs} vs [Nu] for the reaction of **DiPtEn-Aqua** with a series of three nucleophiles at 25.0 °C.
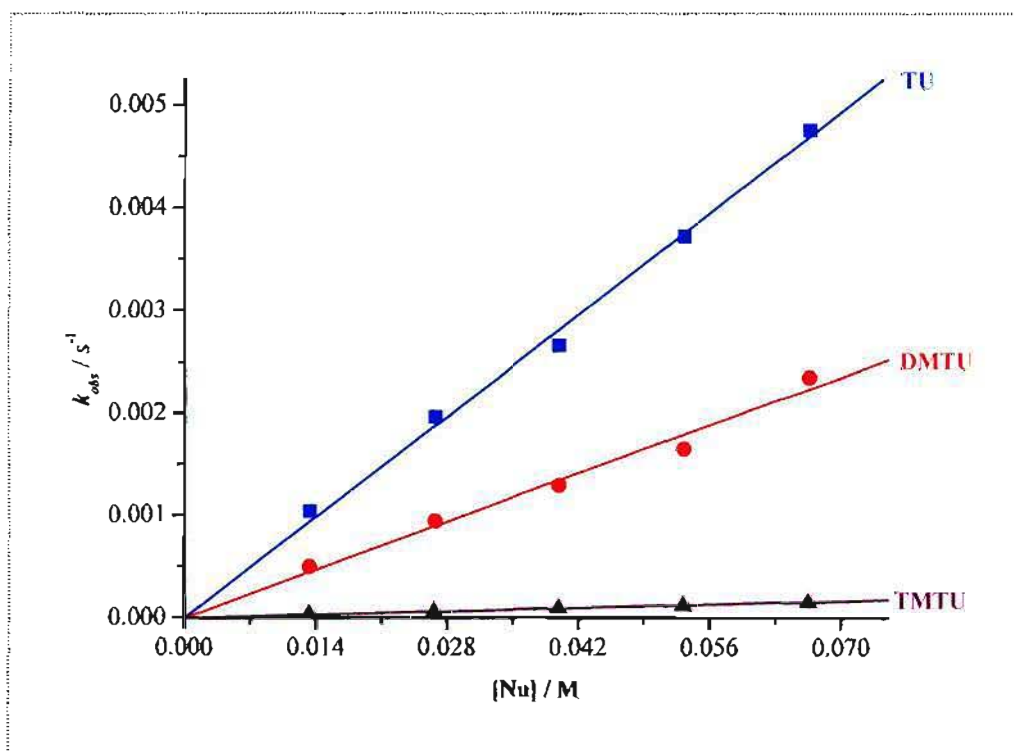
Figure A9: Graph of k_{obs} vs [Nu] for the reaction of **DiPtProp-Aqua** with a series of three nucleophiles at 25.0 °C.
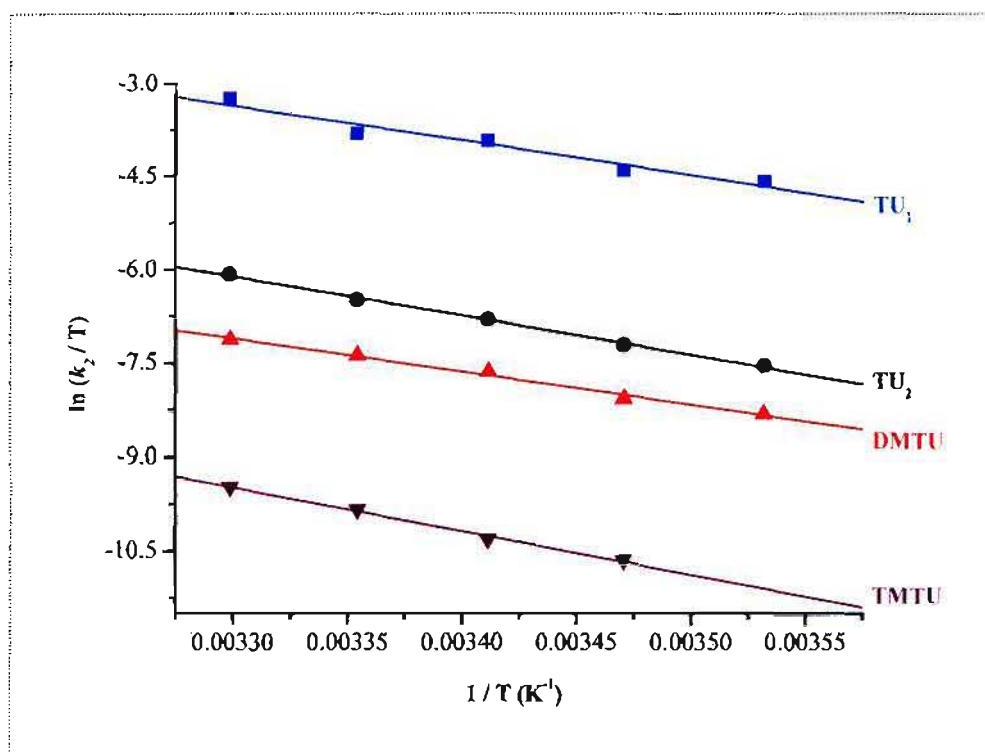
A-9
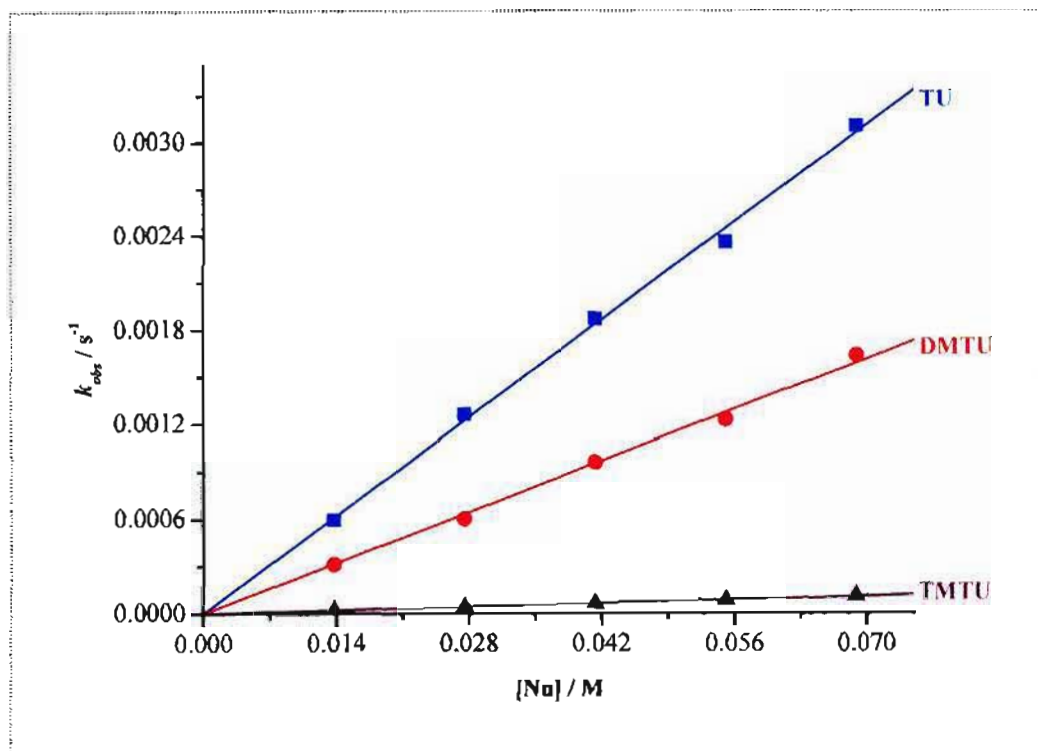
Figure A10:   Graph of k_{obs} vs [Nu] for the reaction of **DiPtBut-Aqua** with a series of three nucleophiles at 25.0 °C.

Figure A11:   Graph of k_{obs} vs [Nu] for the reaction of **DiPtHex-Aqua** with a series of three nucleophiles at 25.0 °C.

Figure A12: Graph of ln (k_2/T) vs (1/T) for the reaction of **DiPtEn-Aqua** with a series of different nucleophiles at varying temperatures.
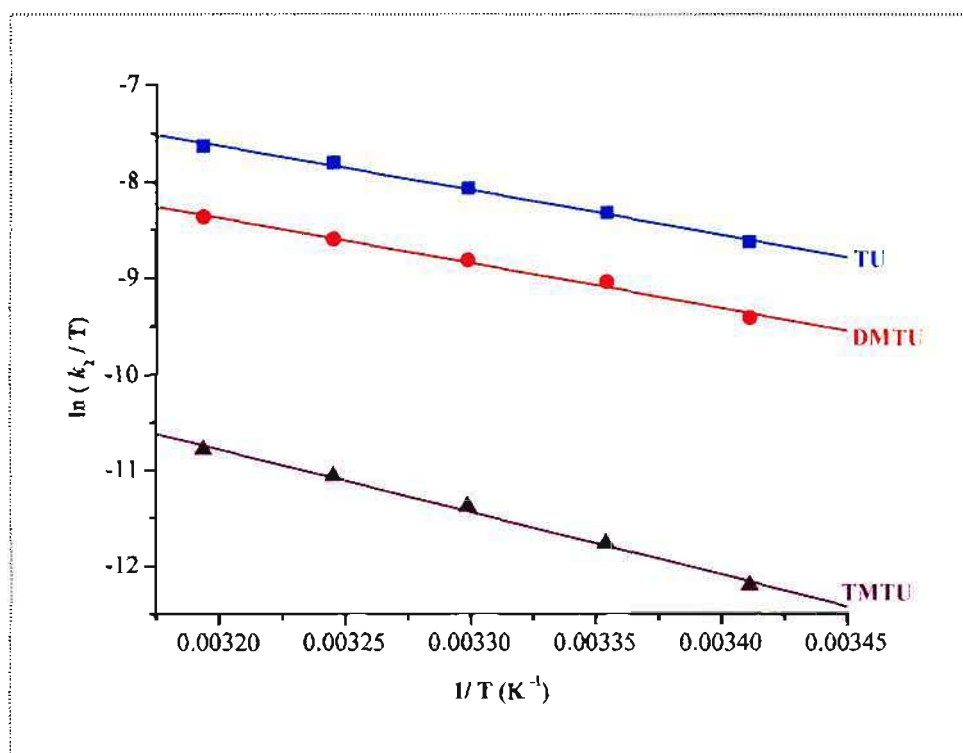

Figure A13: Graph of ln (k_2/T) vs (1/T) for the reaction of **DiPtProp-Aqua** with a series of different nucleophiles at varying temperatures.
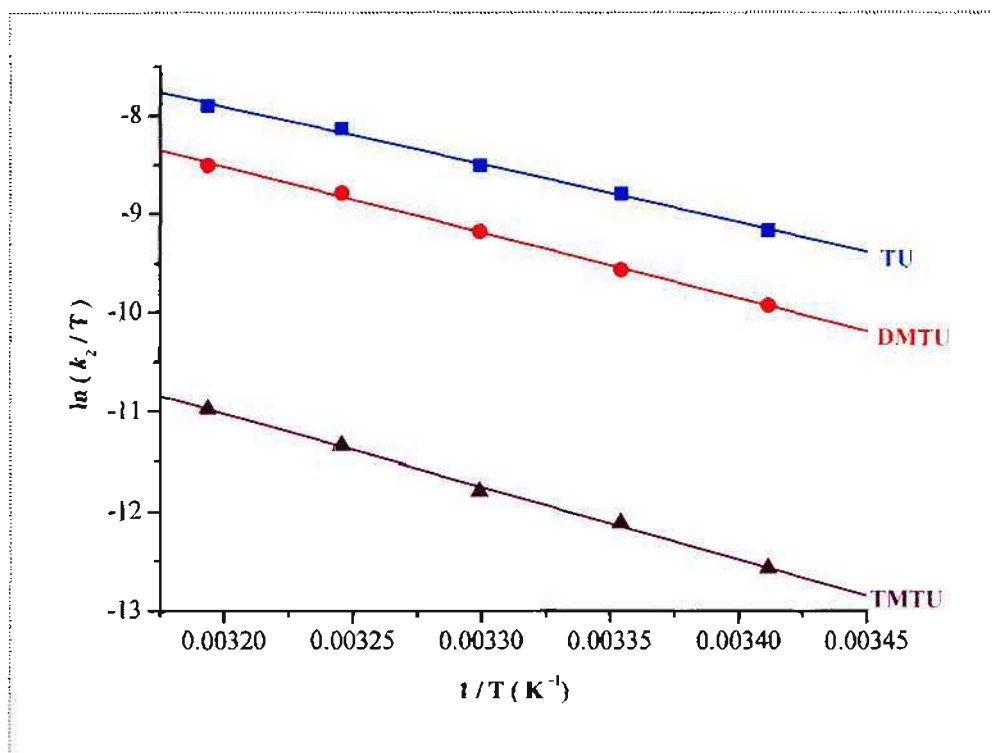
Figure A14: Graph of ln (k_2/T) vs $(1/T)$ for the reaction of **DiPtBut-Aqua** with a series of different nucleophiles at varying temperatures.
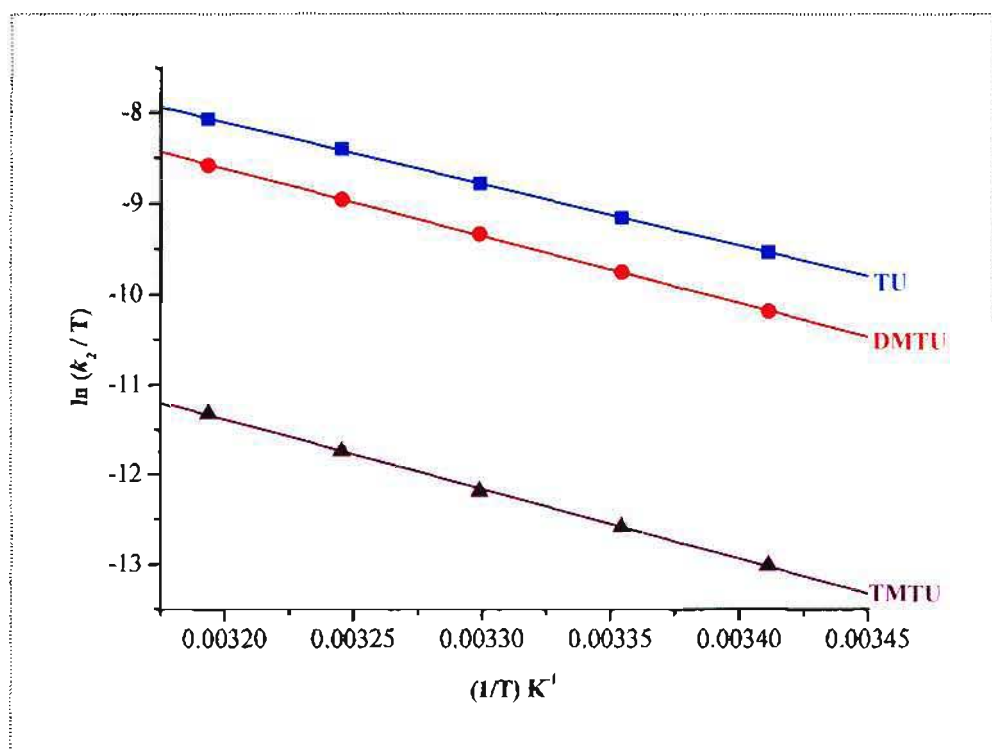

Figure A15: Graph of ln (k_2/T) vs $(1/T)$ for the reaction of **DiPtHex-Aqua** with a series of different nucleophiles at varying temperatures.
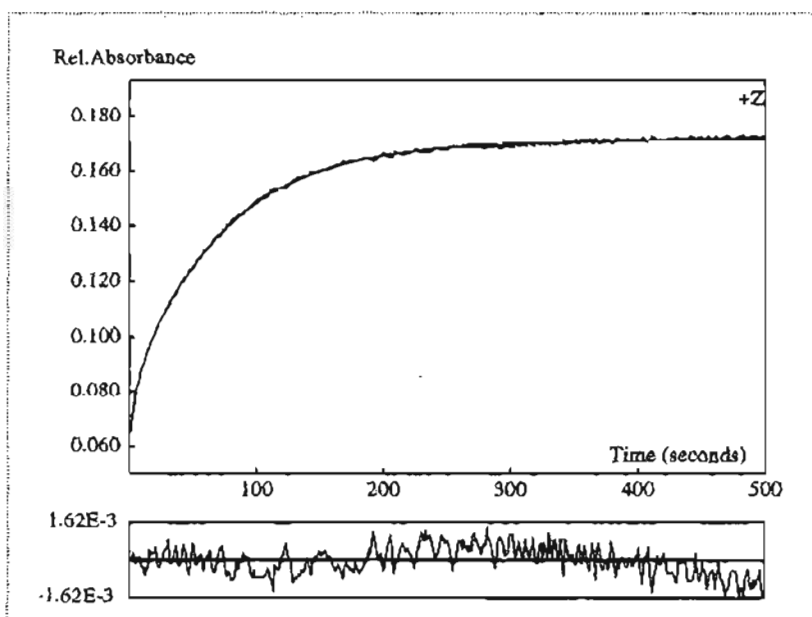
A-12

Figure A16: Representative Stopped-flow Scan obtained for the reaction of **DiPtEn-Aqua** (0.499 mM) and TU (40 X, 39.92 mM) at 25 °C shown with a double exponential fit. λ = 340 nm, I = 0.2 M $NaClO_4$.
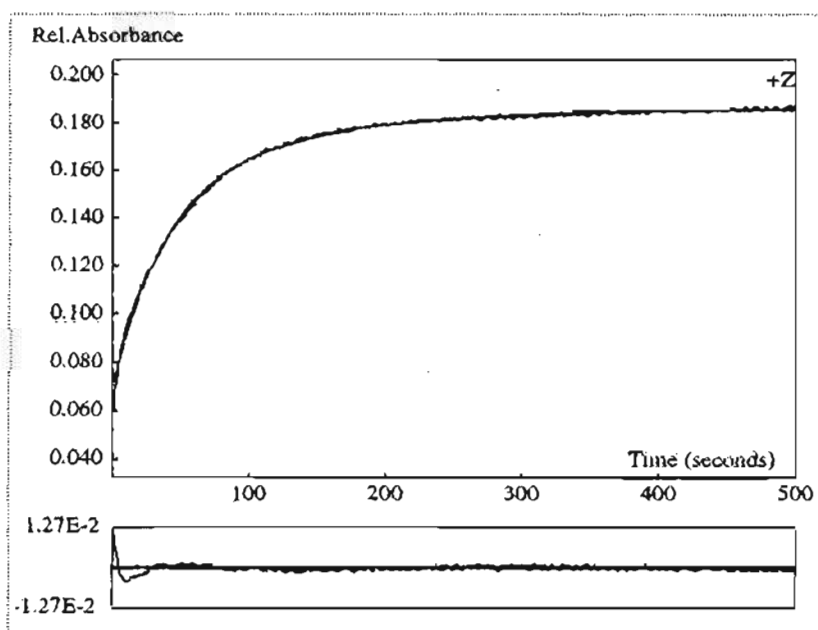

Figure A17: Representative Stopped-flow Scan obtained for the reaction of **DiPtEn-Aqua** (0.499 mM) and TU (50 X, 49.90 mM) at 25 °C shown with a double exponential fit. λ = 340 nm, I = 0.2 M $NaClO_4$.
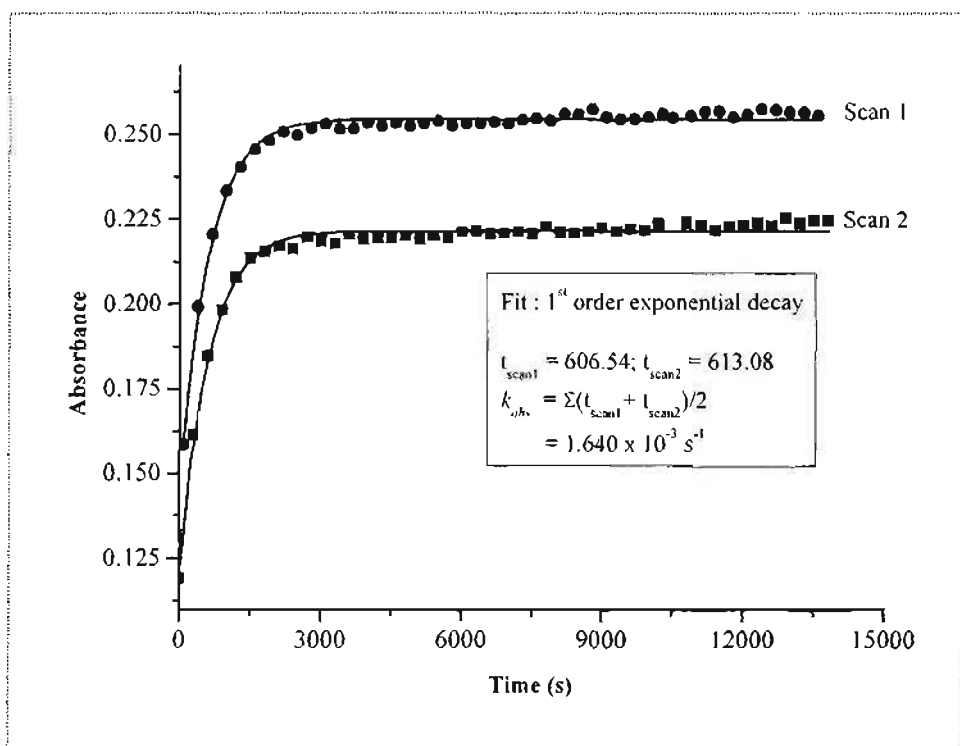
Figure A18: Plots of Absorbance versus Time for the reaction of DiPtBut-Aqua (0.689 mM) and DMTU (50 X, 68.9 mM) at 25 °C.
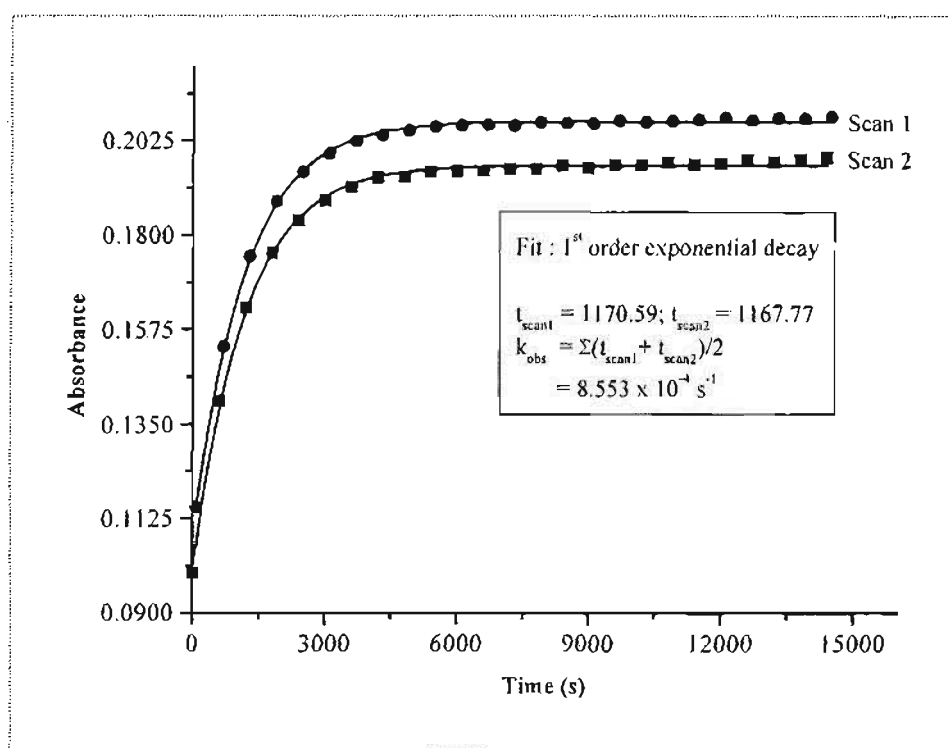

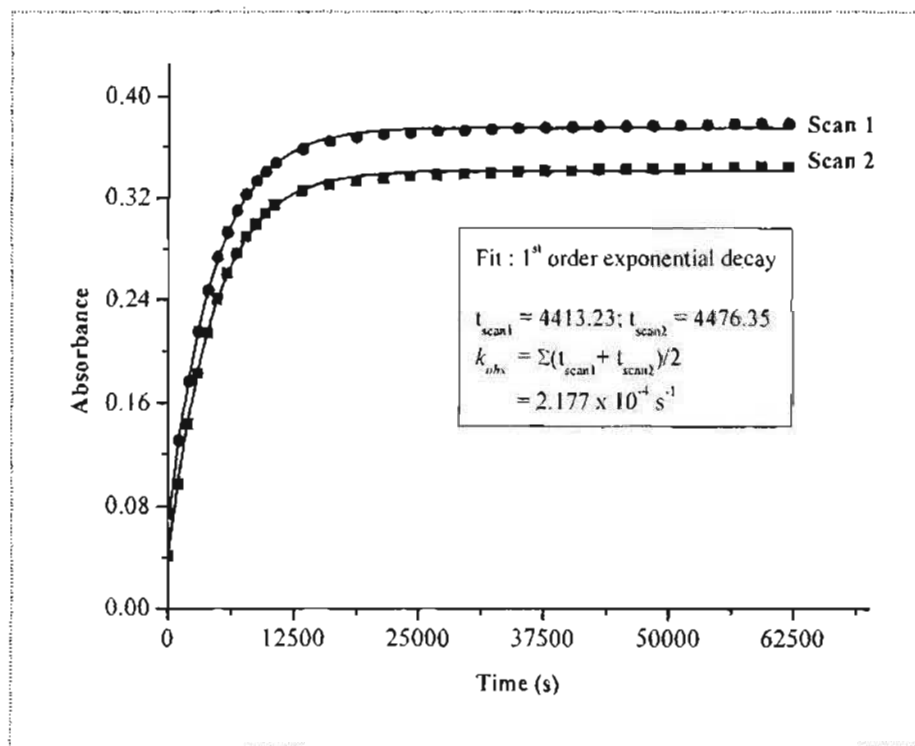**Figure A19:** Plots of Absorbance versus Time for the reaction of DiPtHex-Aqua (0.496 mM) and DMTU (50 X, 49.55 mM) at 25 °C.

Figure A20: Plots of Absorbance versus Time for the reaction of **DiPtEn-Aqua** (0.499 mM) and **TMTU** (30 X, 21.78 mM) at 25 °C.

Figure A21: Plots of Absorbance versus Time for the reaction of **DiPtProp-Aqua** (0.655 mM) and **TMTU** (50 X, 66.5 mM) at 25 °C.
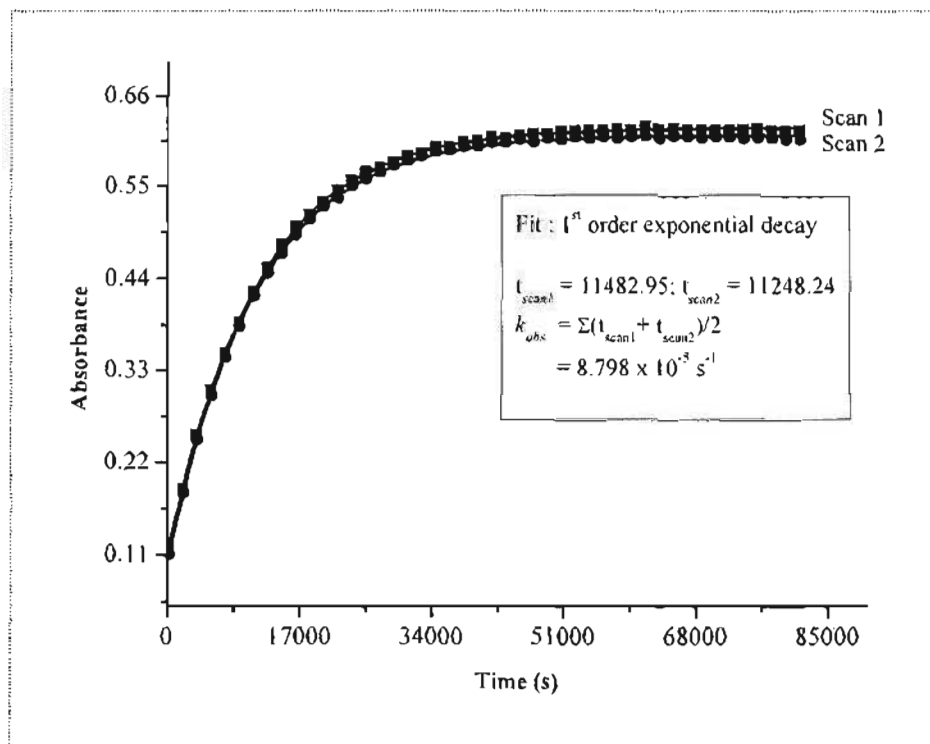
Figure A22: Plots of Absorbance versus Time for the reaction of **DiPtBut-Aqua (0.689 mM)** and **TMTU (40 X, 68.9 mM)** at 25 °C.
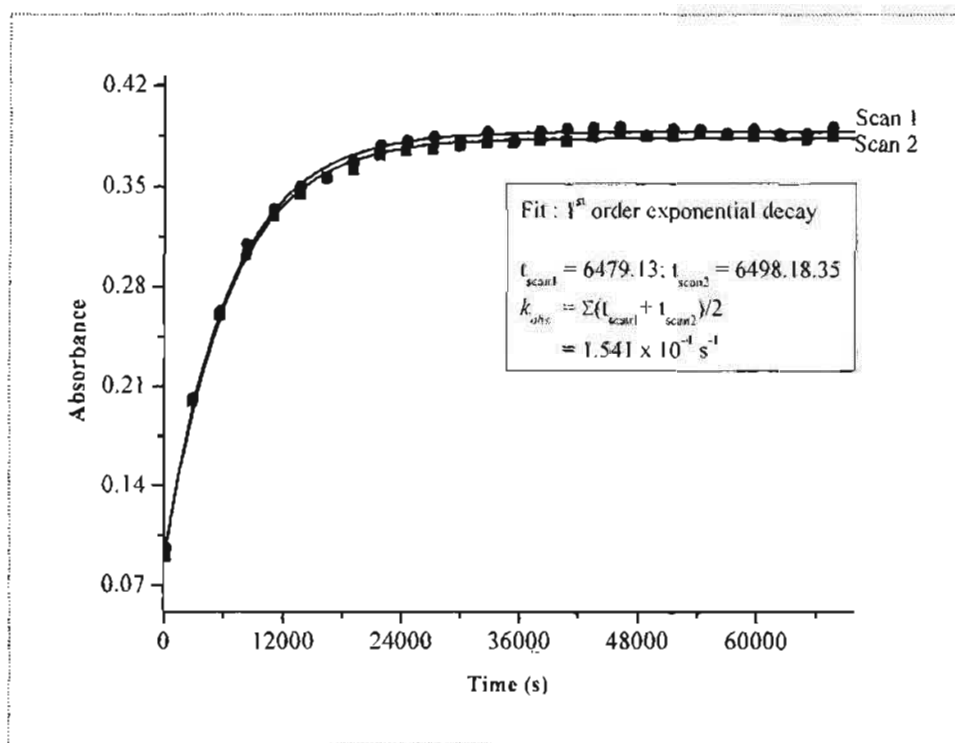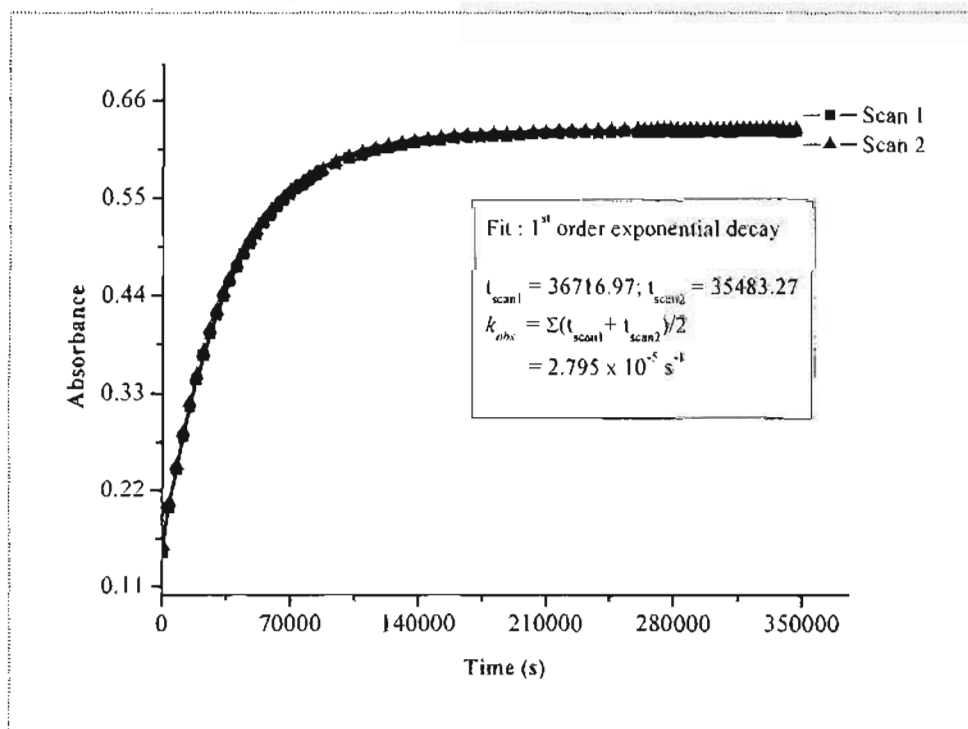

Figure A23: Plots of Absorbance versus Time for the reaction of **DiPtHex-Aqua (0.496 mM)** and **TMTU (30 X, 29.73 mM)** at 25 °C.

Figure A24:   Infrared Spectrum of [{trans-PtCl(NH₃)₂}₂-H₂N(CH₂)₂NH₂]Cl₂ [**DiPtEn-Chloro**] in KBr.
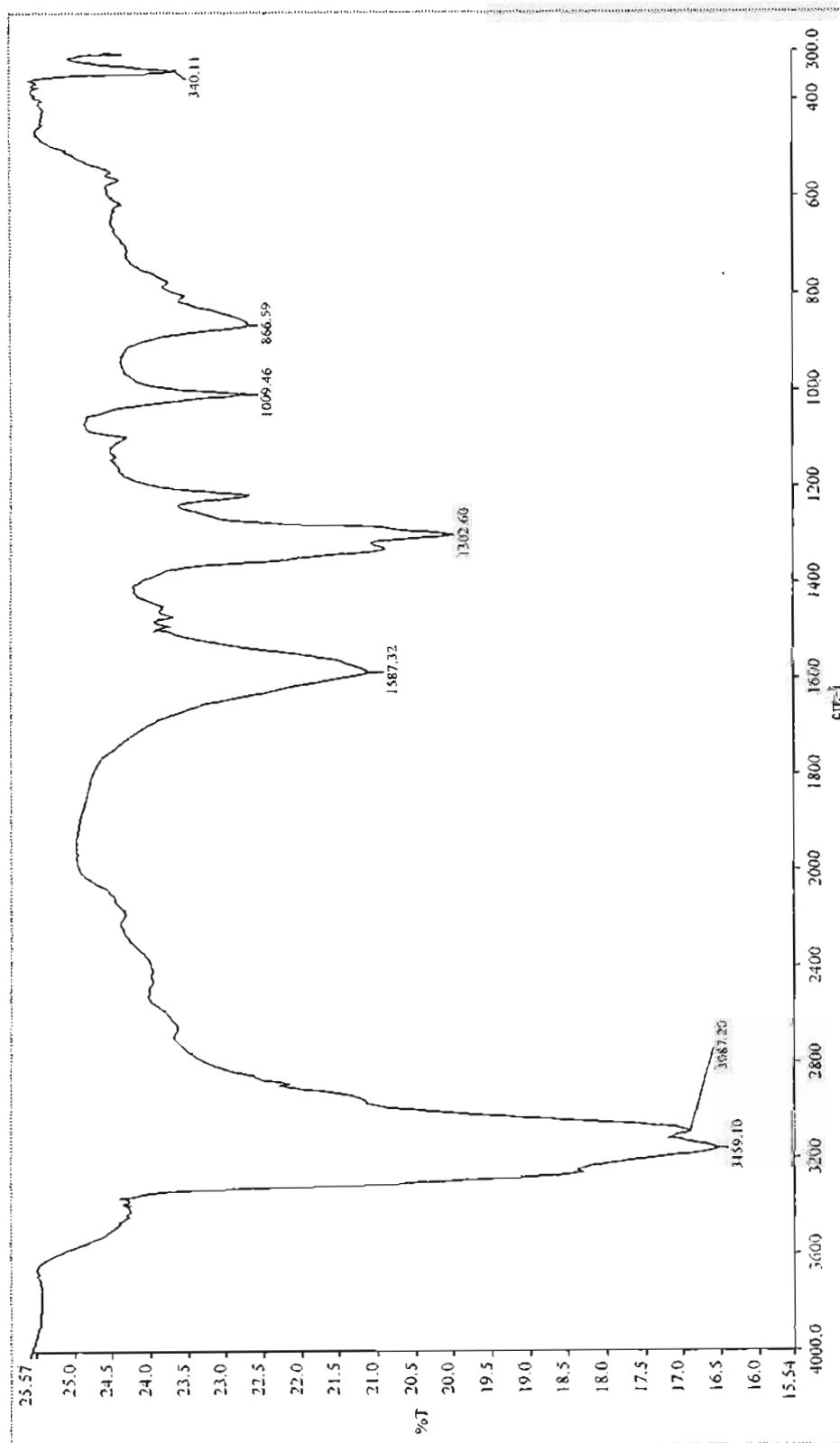
Figure A25:   Infrared Spectrum of [{trans-PtCl(NH₃)₂}₂-H₂N(CH₂)₃NH₂]Cl₂ [DiPtProp-Chloro] in KBr.
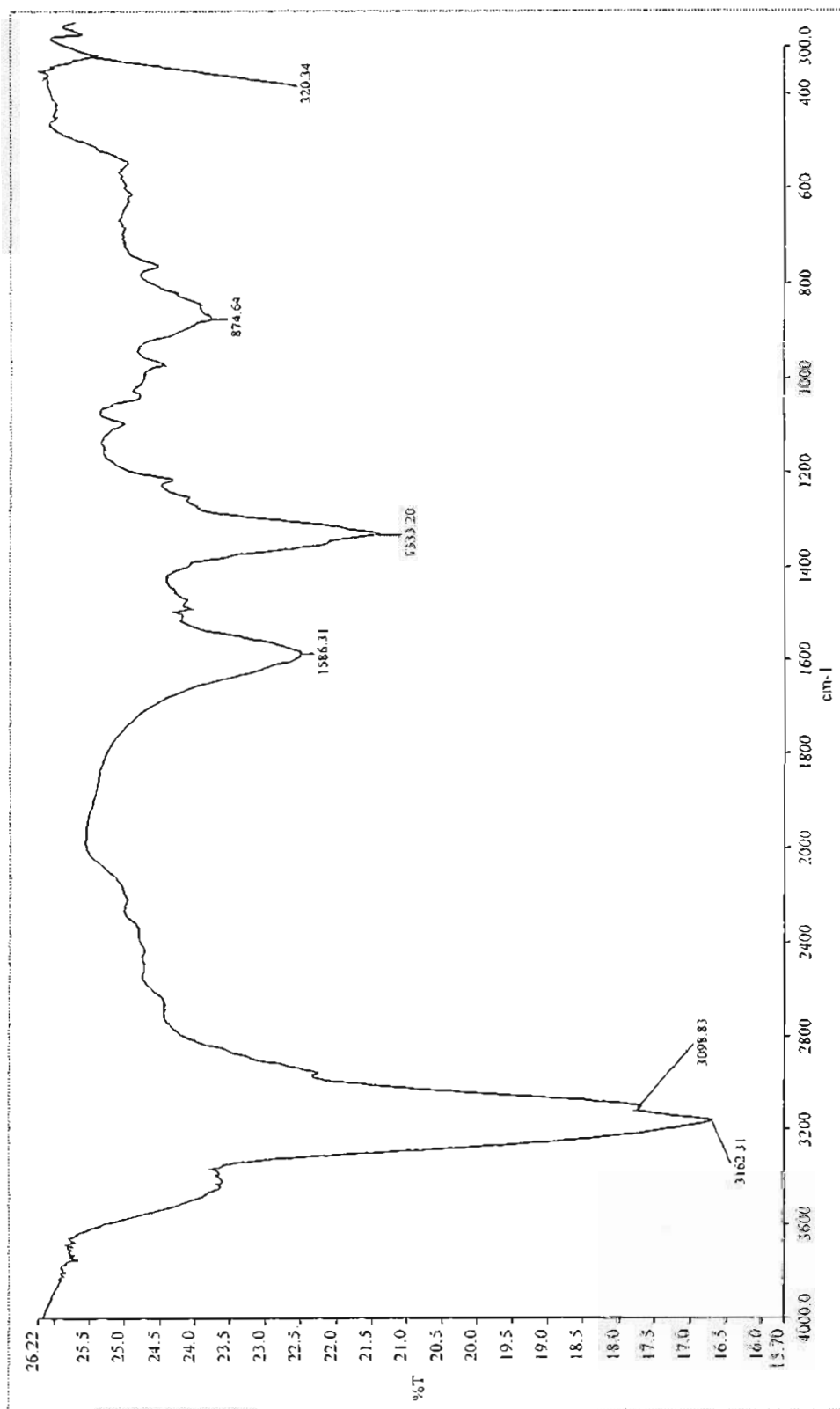
Figure A26: Infrared Spectrum of [{trans-PtCl(NH₃)₂}₂-H₂N(CH₂)₄NH₂]Cl₂ [DiPtBut-Chloro] in KBr.
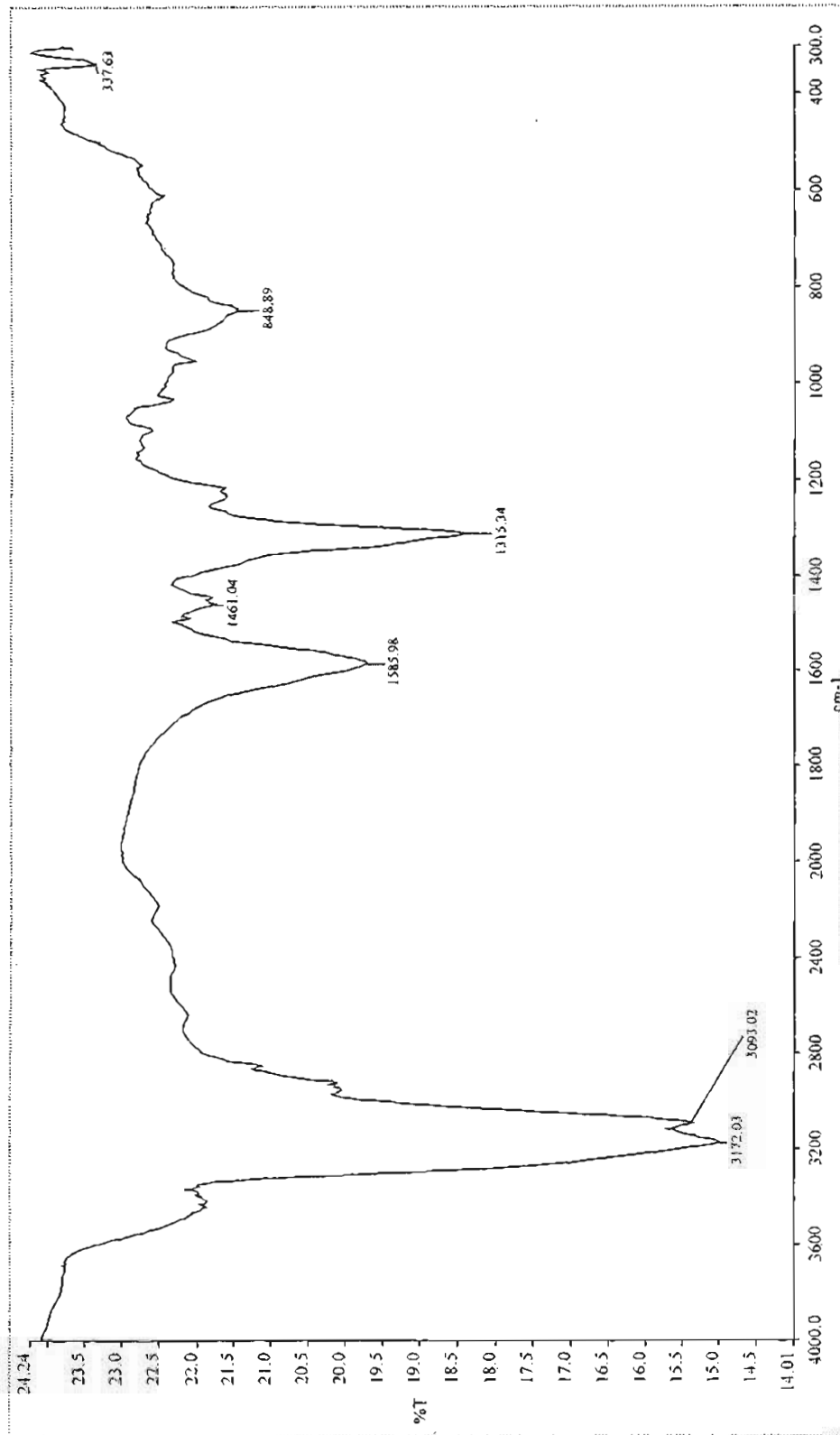
Figure A27:   Infrared Spectrum of [{trans-PtCl(NH_3)_2}_2-H_2N(CH_2)_6NH_2](NO_3)_2 [DiPtHex-Chloro] in KBr.
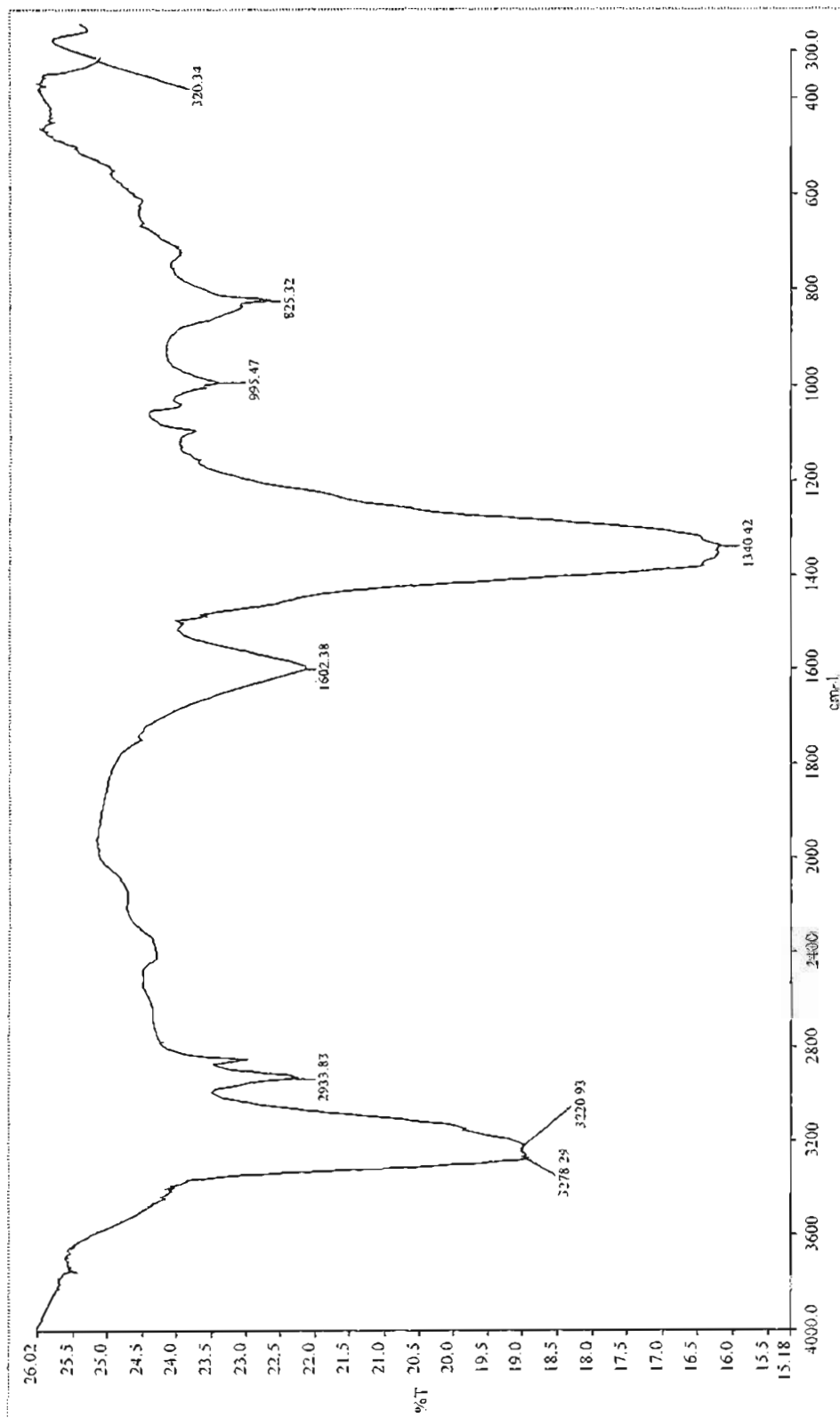
Figure A28: ^{1}H-NMR Spectrum of [{trans-PtCl(NH$_3$)$_2$}$_2$-H$_2$N(CH$_2$)$_2$NH$_2$]Cl$_2$ [DiPtEn-Chloro] in D$_2$O.

ppm (t1)
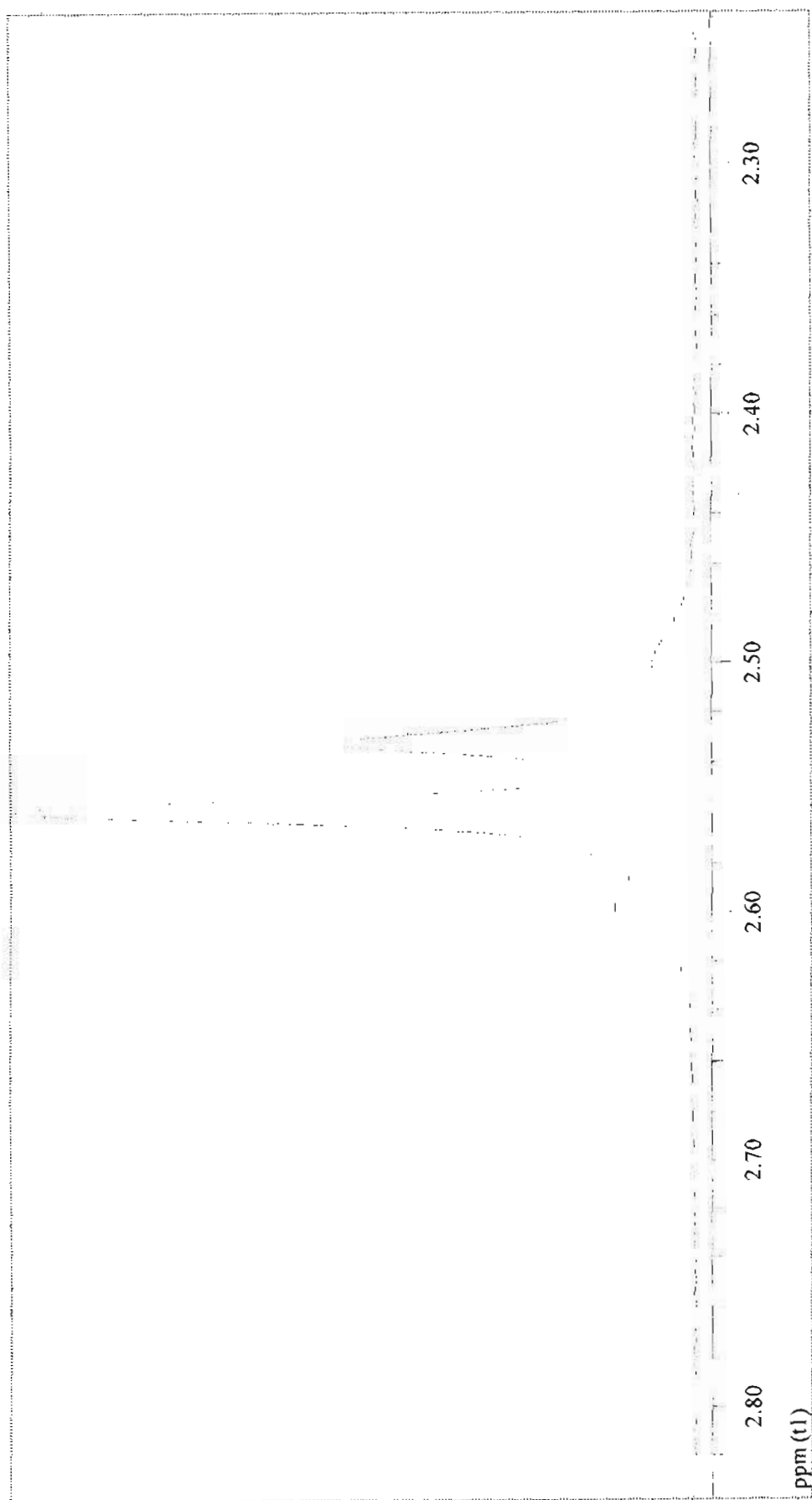
Figure A29: ^{1}H-NMR Spectrum of [[trans-PtCl(NH$_3$)$_2$]$_2$-H$_2$N(CH$_2$)$_2$NH$_2$]Cl$_2$ [DiPtProp-Chloro] in D$_2$O.
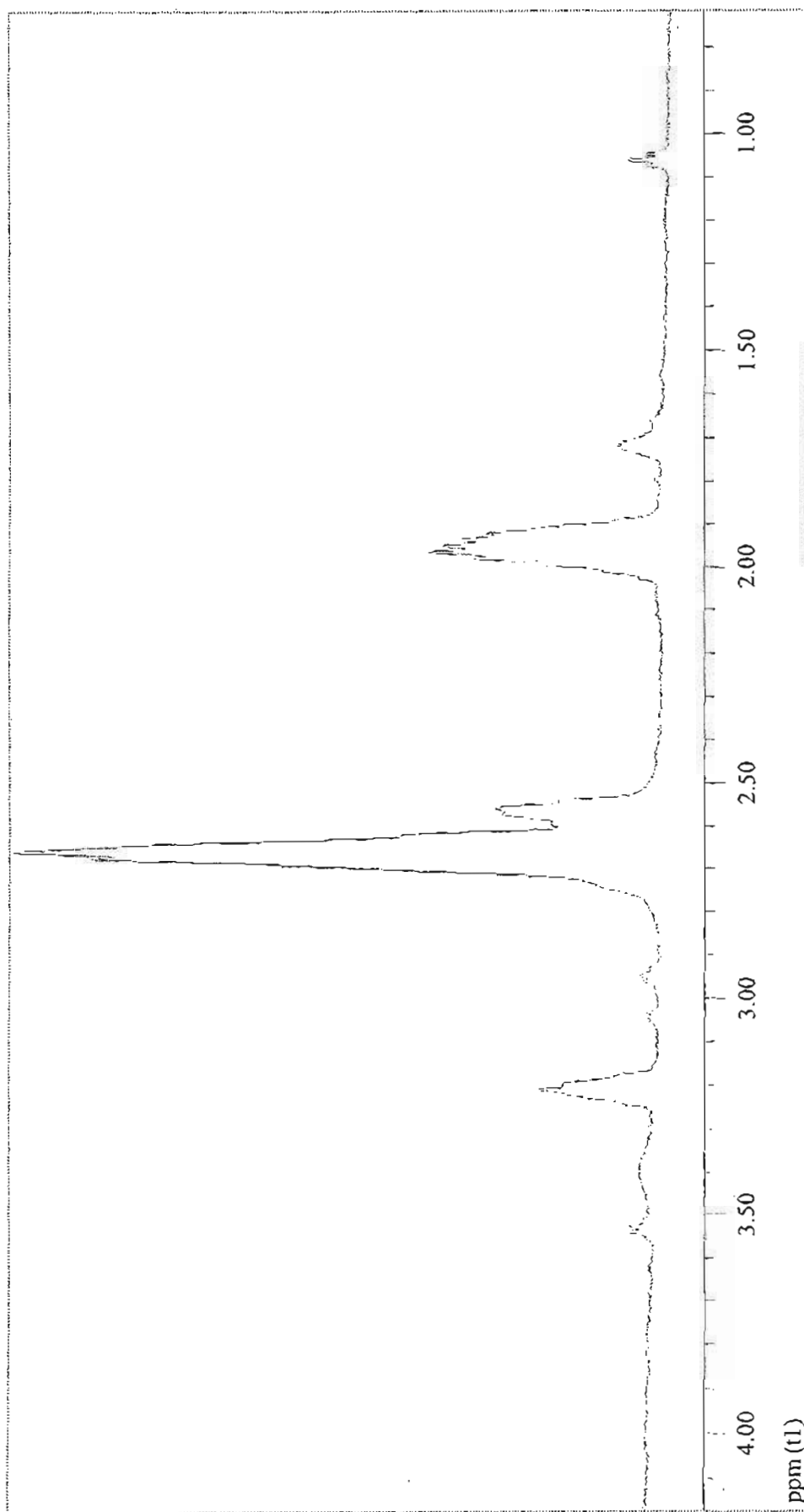
Figure A30: ^{1}H-NMR Spectrum of [{trans-PtCl(NH$_3$)$_2$}$_2$-H$_2$N(CH$_2$)$_4$NH$_2$]Cl$_2$ [DiPtBut-Chloro] in D$_2$O.

ppm (t1)
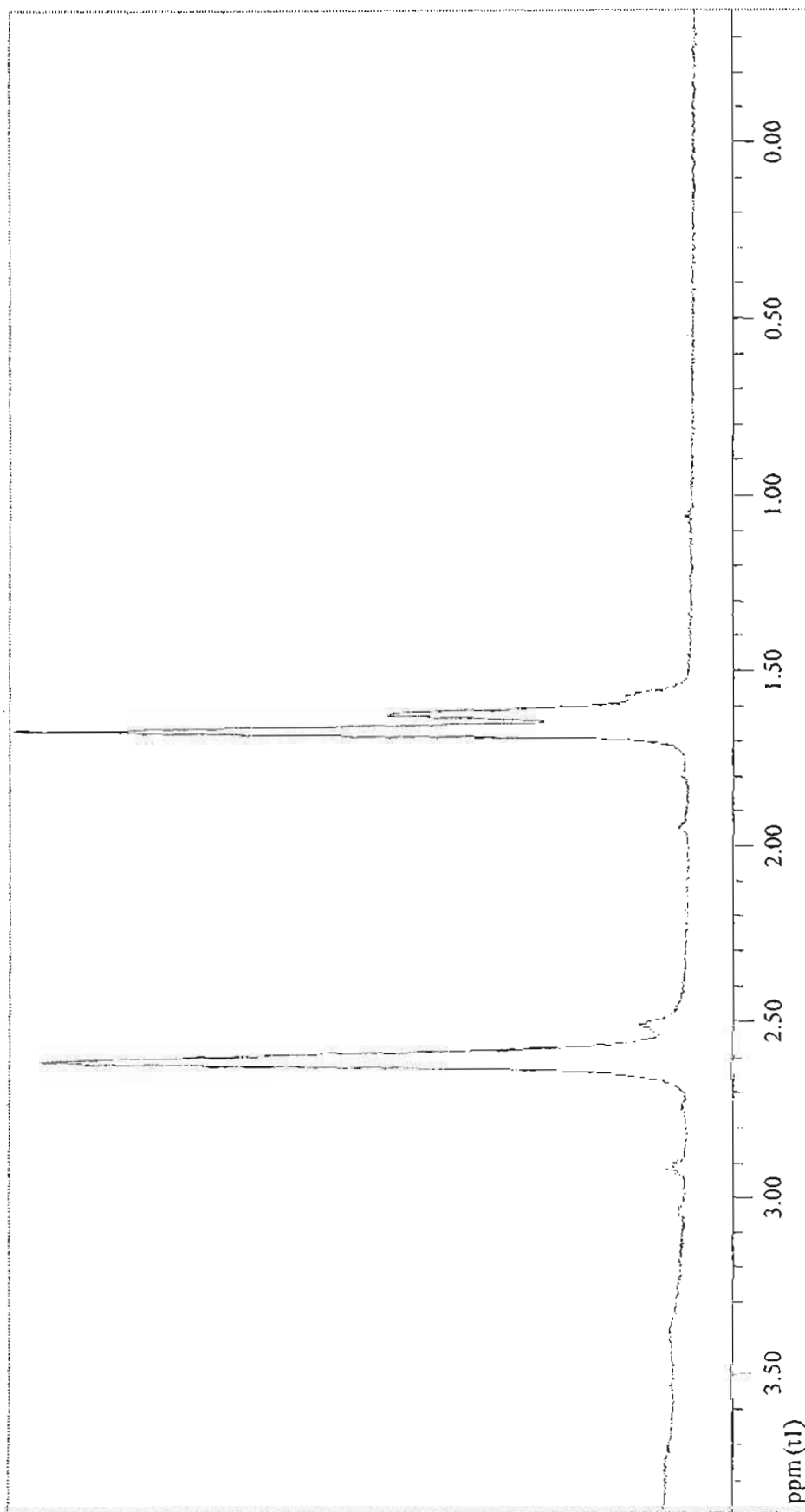
Figure A31: ^{195}Pt-NMR Spectrum of [{trans-PtCl(NH$_3$)$_2$}$_2$-H$_2$N(CH$_2$)$_2$NH$_2$]Cl$_2$ [DiPtEn-Chloro] in D$_2$O.

-2400.835

A-24
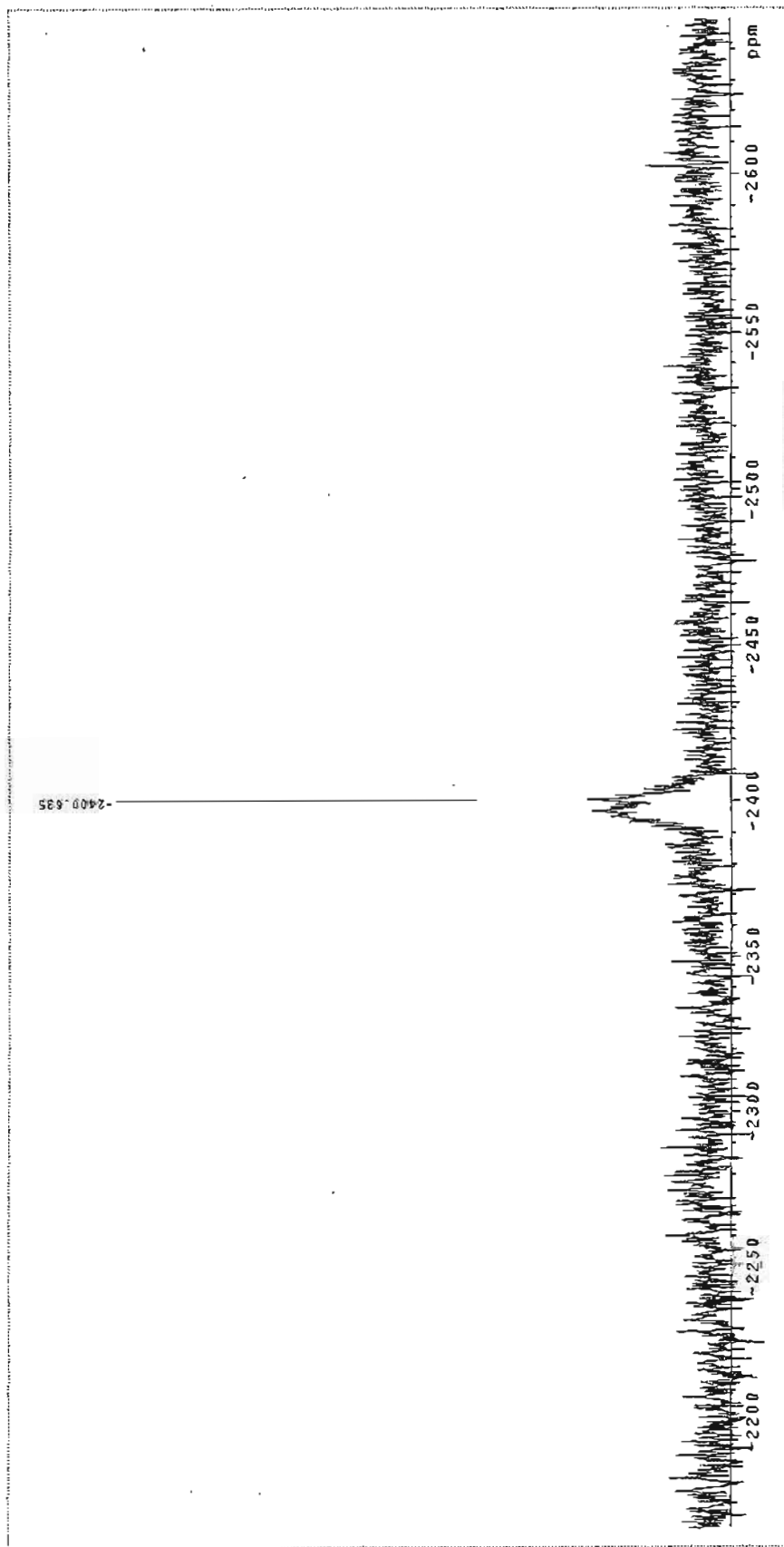
Figure A32: ^{195}Pt-NMR Spectrum of [{trans-PtCl(NH$_3$)$_2$}$_2$-H$_2$N(CH$_2$)$_3$NH$_2$]Cl$_2$ [DiPttProp-Chloro] in D$_2$O.
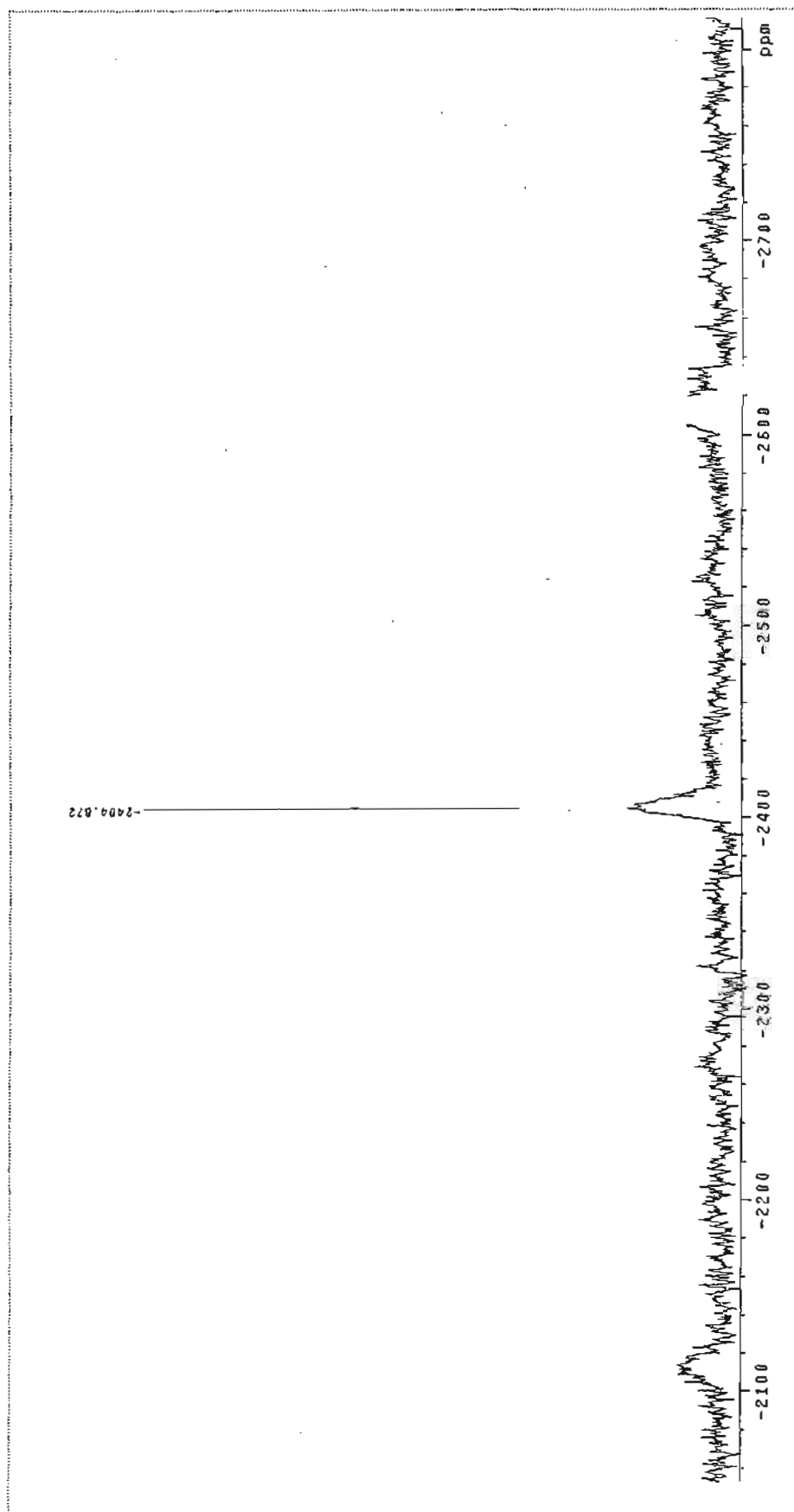
Figure A33: ^{195}Pt-NMR Spectrum of [{trans-PtCl(NH$_3$)$_2$}$_2$-H$_2$N(CH$_2$)$_4$NH$_2$]Cl$_2$ [**DiPtBut-Chloro**] in D$_2$O.
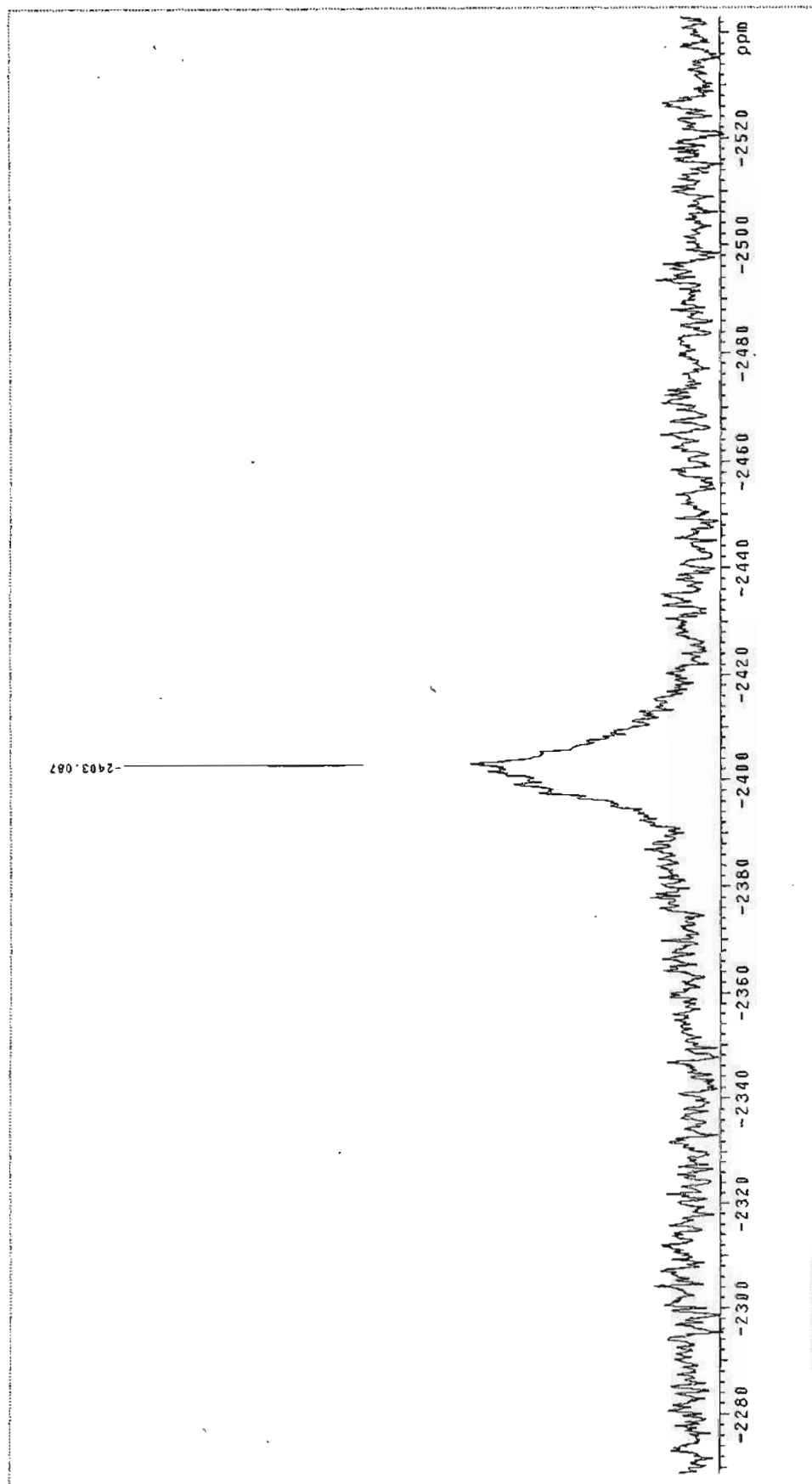
Figure A34: ^{195}Pt-NMR Spectrum of [{trans-PtCl(NH$_3$)$_2$}$_2$H$_2$N(CH$_2$)$_6$NH$_2$](NO$_3$)$_2$ [DiPtHex-Chloro] in D$_2$O.
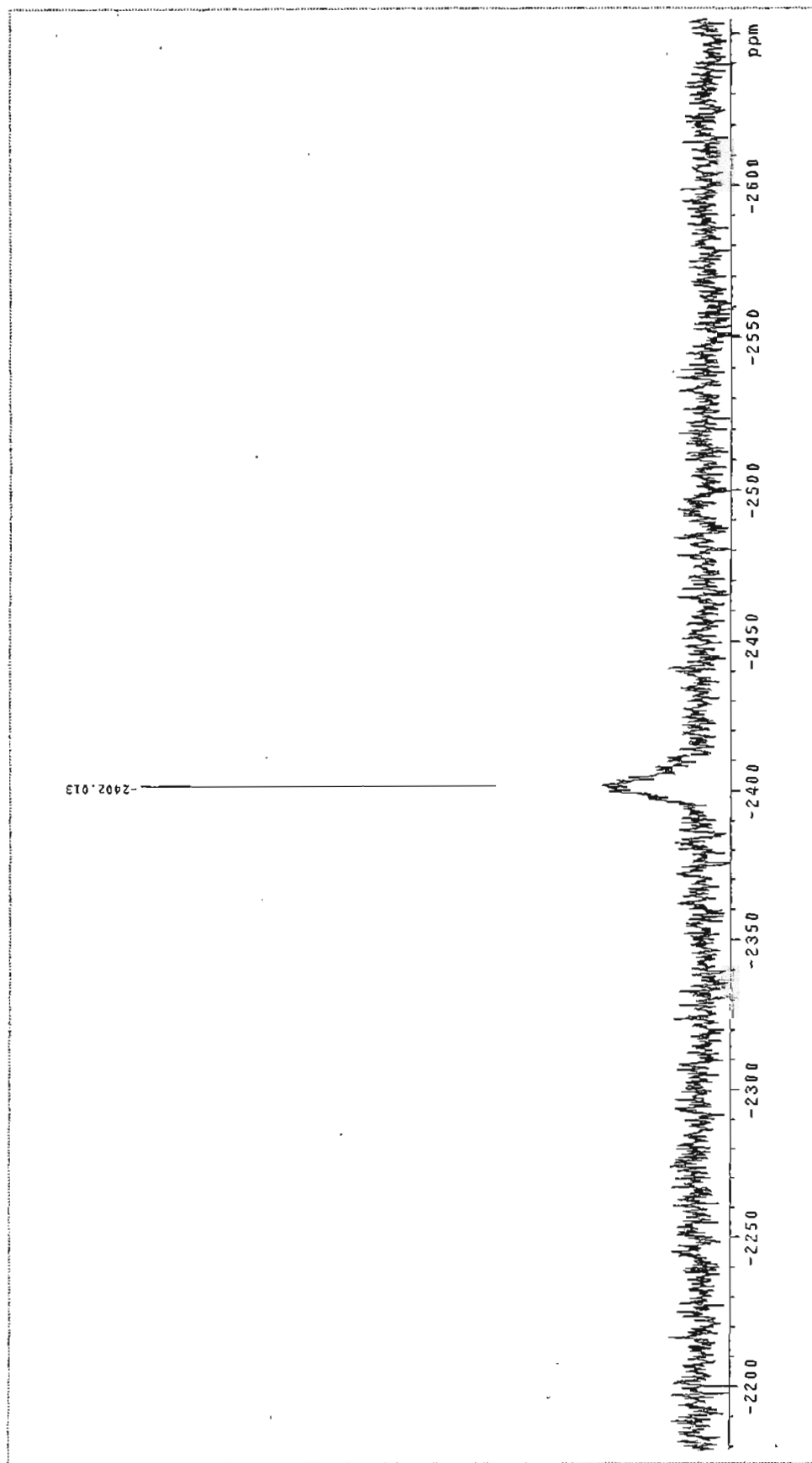
Appendix B

<u>*Draft Publication*</u>

Role of Bridging Diamine Linkers on the Rate of Ligand Substitution in a Series of Dinuclear Pt[II] Complexes

D. Jaganyi, V. M. Munisamy & D. Reddy

School of Chemistry, University of KwaZulu-Natal, Pietermaritzburg, 3209, South Africa

Abstract

A series of dinuclear platinum[II] complexes of the type [{*trans*-Pt(H_2O)(NH_3)$_2$}$_2$-NH_2(CH_2)$_n$$H_2$N]$^{4+}$ (where n = 2, 3, 4 and 6) were synthesized to investigate the influence of the bridging diamine linker on the reactivity of the platinum centres. The pK_a values were determined and the rates of substitution of the aqua moieties by a series of neutral nucleophiles *viz.* thiourea (TU), 1,3-dimethyl-2-thiourea (DMTU) and 1,1,3,3-tetramethyl-2-thiourea (TMTU) was studied as a function of concentration and temperature. All reactions studied gave excellent fits to a single exponential and obeyed the simple rate law, k_{obs} = k_2[Nu], with the exception of the reaction involving [{*trans*-Pt(H_2O)(NH_3)$_2$}$_2$-NH_2(CH_2)$_2$$H_2$N]($ClO_4$)$_4$ and TU, which was found to exhibit second-order kinetics with the observed rate constants, $k_{obs(1,2)}$ being expressed by the equation, $k_{obs(1,2)}$ = $k_{(1,2)}$[Nu]. Negative activation entropies support an associative mode of substitution. The results obtained suggest that the rate of substitution is definitely influenced by the length of the diamine chain, with the rate of substitution decreasing as the length of the diamine chain increases.

Introduction

Platinum coordination compounds are effective chemotherapeutic agents used for the treatment of testicular cancer, and are used in combination regimens for a variety of other tumours including ovarian, cervical, bladder, lung, and those of the head and neck. *cis*-diamminedichloroplatinum[II] and its analogue *cis*-diammine(1,1 cyclobutyldicarboxylato) are effective anticancer drugs approved for the treatment of several human malignancies.[1-7] Although these drugs are among the most successful antitumour compounds developed in recent years, they display limited activity against some of the most common forms of the disease, such as colon and breast cancer. In addition, a variety of adverse effects and acquired resistance are observed in patients

undergoing chemotherapy.[7] These limitations have provided the impetus for the development of new and improved platinum antitumour drugs and these have mainly focused on the development of new derivatives that display improved therapeutic properties.

Multinuclear platinum complexes comprising of either di- or trinuclear platinum centres linked by variable length diamine chains constitute a new and discrete class of platinum-based anticancer agents. Development of these complexes were driven by the hypothesis that complexes with distinctly different DNA binding mechanisms may exhibit unique biological activity in comparison to the current mononuclear clinically used agents.[8-12]

Di- or trinuclear compounds are bifunctional platinating agents because only two Pt-Cl bonds are present. Their intrinsic differences are dictated by the separation between the two platinating centres and the overall charge on the molecule, which is caused by the presence of the extra "noncoordinating" tetraammineplatinum moiety. These structures display biological activity that differs substantially from that of cisplatin.[10,12]

There are several aspects of the DNA binding profiles of these complexes that are remarkably different to that found for cisplatin and other mononuclear platinum[11] complexes. Firstly, these compounds are capable of forming bifunctional DNA adducts that are structurally different to that of cisplatin, especially long-range (Pt, Pt) interstrand cross-links.[12,13] These cross-links represent a new class of DNA adducts of anticancer agents, situated in the major groove by virtue of guanine N7 binding. In principle, the bifunctional DNA binding modes of dinuclear complexes may be manipulated by the geometry of the complex, especially with regard to the relationship of the leaving groups to the diamine bridge, and the nature of the diamine bridge itself as well as the other ligands present within the platinum coordination sphere.[10]

An interesting aspect in the chemistry of bis(platinum) complexes containing two platinum centres linked by a diamine bridge is their mode of substitution. Bis(platinum) complexes with two identical coordination spheres are equally likely to react at either metal centre. In a substitution reaction this equivalence is broken upon reaction of the

first Pt centre. There now exists a competition between the two non-equivalent platinum centres and the final product will therefore be dependant on the incoming ligand.

Comprehensive studies on the role of DNA binding properties and product formation have been conducted on bis(platinum) complexes, with the results being interpreted in terms of charge, hydrogen bonding, length and flexibility of the bridging ligand. However, there is limited information available with regard to the reactivity and thermodynamic properties of the two platinum centres. Such data is only available for $[\{trans\text{-}PtCl(NH_3)_2\}_2\text{-}H_2N(CH_2)_6NH_2]^{2+}$ (BBR3005) and $[(trans\text{-}PtCl(NH_3)_2)_2\{\mu\text{-}trans\text{-}Pt(NH_3)_2(H_2N(CH_2)_6NH_2)_2\}]^{4+}$ (BBR3464) and suggests that the reactivity and properties of the first platinum centre is independent of the state of the second and *vice versa*.[8,11] Data available in literature is insufficient to formulate a relationship between the reactivity of the two platinum centres and the nature of the bridging ligand.

In an effort to gain more insight into the role of the bridging diamine linker, the following study was undertaken whereby the influence of four different bridges on the reactivity of each of the platinum centres was investigated. The variation of the bridging diamine spacer enabled a systematic study of the influence of chain length and flexibility of the bridge on the thermodynamic and kinetic properties of the two platinum centres.

Experimental

Materials and procedures

All the reactions involving the synthesis of the dinuclear platinum (II) complexes were carried out in air unless otherwise stated. Dimethylformamide and ethanol were purified using standard literature procedures.[14] *trans*-diamminedichloroplatinum(II) was purchased from Strem chemicals and used as supplied. The diamines: 1,2-ethanediamine, 1,4-butanediamine and 1,6-hexanediamine were all purchased from Aldrich and used without further purification. 1,6-hexanediamine was stored in a dessicator when not in use. 1,3-propanediamine was purchased from Fluka and used without purification. The nucleophiles, thiourea (TU), 1,3-dimethyl-2-thiourea (DMTU)

and 1,1,3,3-tetramethyl-2-thiourea (TMTU) were purchased from Aldrich and used without further purification. All other reagents were of analytical reagent quality.

Synthesis and Preparation of Complex Solutions

[{trans-PtCl(NH$_3$)$_2$}$_2$-H$_2$N(CH$_2$)$_n$NH$_2$]Cl$_2$ (where n = 2-4, 6) were synthesized as described previously.[15,16] The corresponding aqua analogues for the n = 2-4 complexes were prepared by dissolving a known amount of the chloro complex in 0.001 M perchloric acid and then adding a stoichiometric excess (with respect to chloride) of AgClO$_4$ (150-200%).[17] The mixture was then stirred overnight at 40-50 °C. The precipitated silver chloride was removed by filtration through a 0.45 μm nylon membrane filter using a Millipore filtration apparatus. The pH of the solution was thereafter adjusted to *ca.* 10-11 via the careful addition of 0.1 M NaOH. This process resulted in the precipitation of a gelatinous brown solid, Ag$_2$O, which was then separated from the mixture by filtering it through a 0.45 μm nylon membrane. This procedure was repeated to ensure that complete removal of the brown Ag$_2$O precipitate had been achieved. The pH of the resulting solution was adjusted to 2 by the careful addition of perchloric acid (10.6 M). A method formulated by Burgacic[18] was used to prepare the aqua analogue of the n = 6 complex.

Physical measurements and instrumentation

^{1}H NMR spectra were recorded on a Varian Gemini 500 spectrophotometer at 25 °C, referenced to the proton signal of the solvent using transmitter presaturation of H$_2$O resonance. Infrared spectra were recorded as KBr discs on a Perkin Elmer Spectrum One FTIR spectrometer. Elemental analysis was performed using a Carlo Erba Elemental Analyser 1106. UV-Vis spectra for the determination of the pK_a values were recorded on a Varian Cary 100 Bio Spectrophotometer. The pH of the solutions were recorded using a Jenway 4330 Conductivity / pH meter fitted with a Micro 4.5 mm diameter glass electrode. Calibration of the electrode was achieved through the use of buffers of pH 4, 7 and 10 at 25 °C. Spectrophotometric pH titrations of the aqua complex solutions, from pH 2-10 were performed using NaOH as the base. A large volume (100 ml) of the complex solution was used so as to avoid absorbance changes

due to dilution effects. Initially, crushed pellets of NaOH were used to obtain a pH change from 2-3. All subsequent pH measurements were obtained by dipping a needle into a saturated solution of NaOH and thereafter into the complex solution. To avoid precipitation of $KClO_4$ within the electrode the KCl solution was replaced with a 3 M NaCl solution. It was found that if the pH electrode was dipped into the test solution for a long period of time, it resulted in the formation of the chloro complex. It was therefore necessary to take 0.6 ml aliquots from the complex solution, which was then transferred into narrow vials for the pH measurements. These were then discarded after each measurement.

Kinetic Analyses

All kinetic measurements were performed under pseudo first-order conditions using either an Applied Photophysics SX. 18MV (v 4.33) or a Varian Cary 100 Bio Scanning Kinetic Utility, both coupled to a temperature-control unit and an online data acquisition system. The pseudo-first-order conditions were achieved by having the nucleophile in at least 10-fold excess. The ionic strength of the solution was maintained at 0.1 M through the use of $NaClO_4$.

DFT Calculations

Density functional theory (DFT) calculations (pseudopotential method[19-21], B3LYP functional[22], LACVP** basis set[23]) were performed using Spartan® '04 for Windows®.

Results

In an attempt to understand the influence of chain length and flexibility of the bridging ligand in the dinuclear platinum complexes on the kinetic and thermodynamic properties of each of the platinum centres, a series of four dinuclear bridged complexes was synthesized and characterized. Their structures together with their corresponding abbreviations are shown in **Figure 1**. The similarities and differences between these complexes was first studied by determining the pK_a values of the coordinated water moieties. The rate of substitution of the coordinated aqua moieties from the dinuclear platinum[II] complexes, **DiPtEn, DiPtProp, DiPBut and DiPtHex** by a series of neutral

B-5

nucleophiles *viz.* thiourea (TU), 1,3-dimethyl-2-thiourea (DMTU) and 1,1,3,3-tetramethyl-2-thiourea (TMTU) was investigated as a function of concentration and temperature under pseudo first-order conditions by monitoring the substitution reactions using either conventional stopped-flow techniques or UV/Visible spectrophotometry.
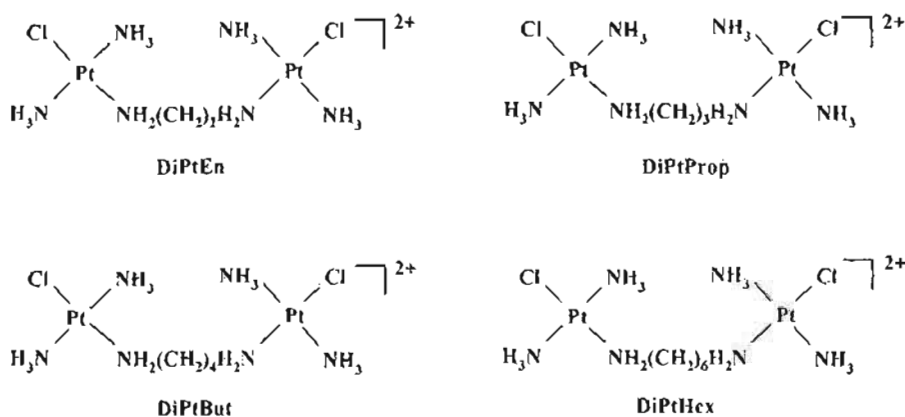
Figure 1: Schematic structures and abbreviations used for the investigated complexes.

Acidity and Complex Formation

A typical example of the spectral changes observed during the pH titration is shown in **Figure 2** and the overall process involving the dissociation of the aqua complex may be represented by **Scheme 1.**
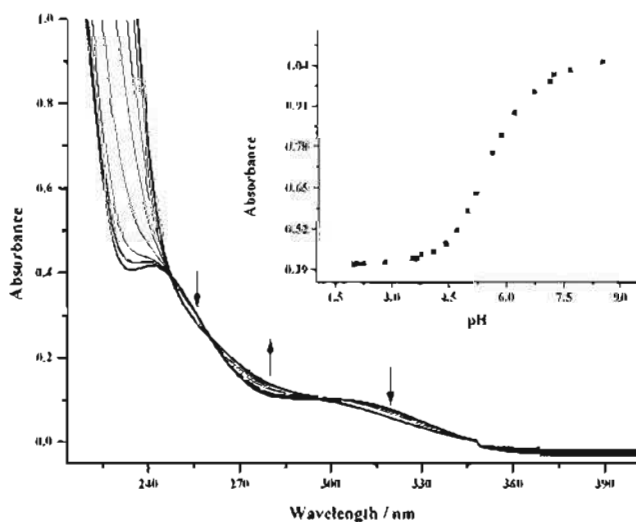
Figure 2: UV/Vis Spectra obtained for **DiPtBut** as a function of pH in the range 2-10 at 25 °C. Inset: Corresponding pK_a graph at 280 nm.

$$[H_2O-Pt_1-L-Pt_2-OH_2]^{4+} + 2 H_2O$$

$$\Big\Updownarrow K_{a1}$$

$$[HO-Pt_1-L-Pt_2-OH_2]^{3+} + H_2O + H_3O^+$$

$$\Big\Updownarrow K_{a2}$$

$$[HO-Pt_1-L-Pt_2-OH]^{2+} + 2 H_3O^+$$
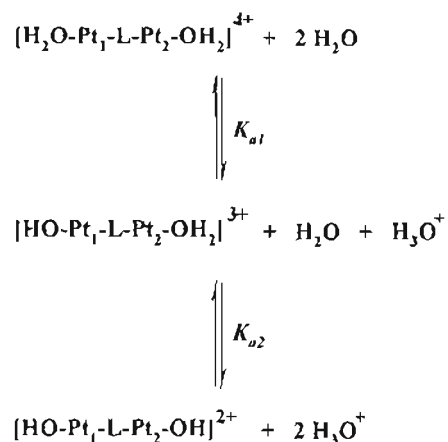
Scheme 1:   A general representation of an acid-base equilibria.

The pK_a values were thereafter determined by plotting absorbance against pH at a specific wavelength. This is shown in **Figure 2**. Using a non-linear least squares procedure the data points were fitted and the results obtained are summarized in **Table 1**.

Kinetics of Reactions with Nucleophiles

Reactions involving **DiPtEn** were fast enough to be monitored using stopped-flow techniques whilst the other reactions involving the other complexes were followed using the UV-Visible spectrophotometer. The typical kinetic traces obtained using these two methods are shown in **Figures 3** and **4** respectively.
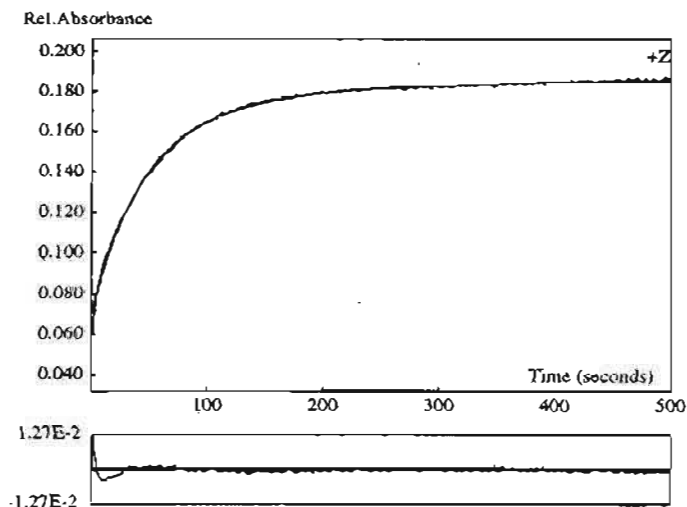
Figure 3: Fit of a double exponential and residuals for the reaction of **DiPtEn** (0.499 mM) with thiourea (50 X, 49.90 mM) followed at 340 nm, I = 0.2 M NaClO$_4$, T = 298.15 K.
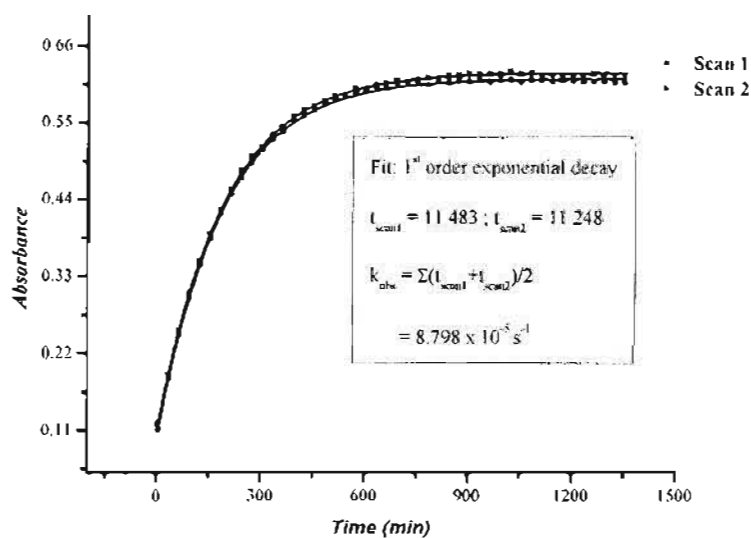
Figure 4: Fit of a first-order exponential decay for the reaction of **DiPtBut** (0.689 mM) with 1,1,3,3-tetramethyl-2-thiourea (40 X, 55.12 mM) followed at 365 nm, I = 0. 2 M (ClO$_4$⁻), T = 298.15 K.

All kinetic traces obtained were initially fitted using a non-linear curve fit on Origin 7.5® using a second-order exponential decay function. It was found however that only the reaction between **DiPtEn** + TU exhibited second-order exponential decay. As such a

double exponential fit was used to fit the observed time dependant spectra. The substitution process for this reaction is shown in **Scheme 2**.

$$[H_2O\text{-}Pt_1\text{-}L\text{-}Pt_2\text{-}OH_2]^{4+} + 2 H_2O$$

$$+ Tu \downarrow k_1$$

$$[Tu\text{---}Pt_1\text{---}L\text{---}Pt_2\text{---}OH_2]^{4+}$$

$$+ Tu \downarrow k_2$$

$$[Tu\text{-}Pt_1\text{-}L\text{-}Pt_2\text{-}Tu]^{4+}$$
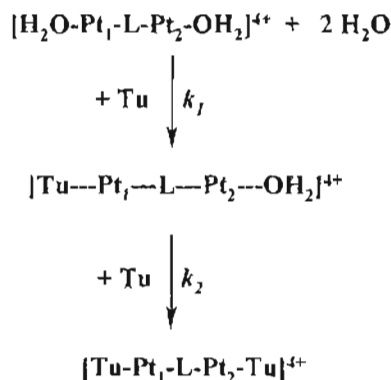
Scheme 2:   Reaction scheme illustrating the mode of substitution of the aqua species from the dinuclear platinum^{II} species exhibiting second-order kinetics.

The pseudo-first order rate constants, (k_{obs1} and $k_{obs2} = k_{obs(1,2)}$) obtained hereafter were plotted against the concentration of the entering nucleophile (TU). A linear dependence on the nucleophile concentration was observed for this reaction. The corresponding plot obtained for the reaction of **DiPtEn** + Tu is shown in **Figure 5** for k_{obs1} and k_{obs2}. The results obtained imply that $k_{obs(1,2)}$ may be expressed as follows:

$$k_{obs(1,2)} = k_{(1,2)}[Nu] \qquad\qquad 1$$

where $k_{(1,2)}$ represents the second-order rate constants.
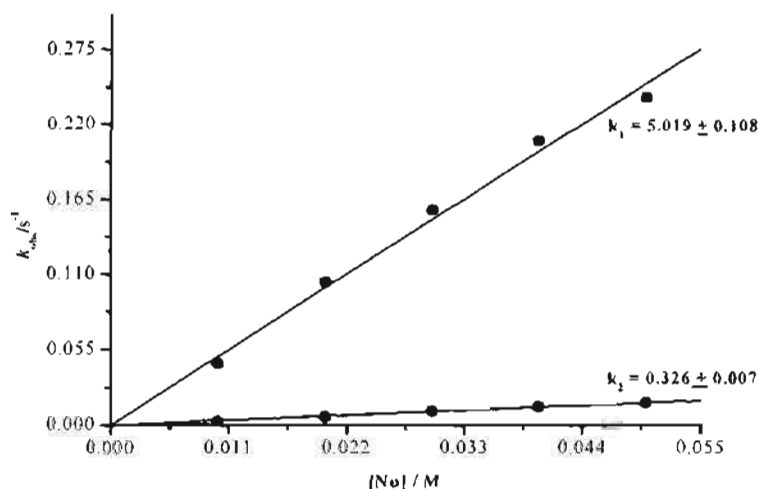
Figure 5:   Plots of $k_{obs(1,2)}$ versus [Nu] for the reaction of **DiPtEn** with TU at 298.15 K.

Since no meaningful intercept was obtained, it was concluded that the reverse reaction was too slow to make a significant contribution on the $k_{obs(1,2)}$ values or was completely absent. A difference of approximately 15 times was observed between the values of the second-order rate constants, k_1 and k_2. This distinction between k_1 and k_2 was however, only observed for the reaction of **DiPtEn** with TU as the nucleophile.

Reactions of the remaining complexes, **DiPtProp**, **DiPtBut** and **DiPtHex** with all nucleophiles and **DiPtEn** with the DMTU and TMTU were found to be first-order with respect to the incoming nucleophiles and gave excellent fits to a single exponential, a process that can be represented by **Scheme 3**.

$$[H_2O\text{-}Pt_1\text{-}L\text{-}Pt_2\text{-}OH_2]^{4+} + 2\,Tu$$

$$\Big\downarrow k_1$$

$$[TU\text{---}Pt_1\text{---}L\text{---}Pt_2\text{---}TU]^{4+} + 2\,H_2O$$
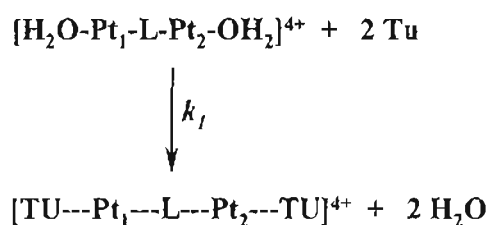
Scheme 3:   Reaction scheme illustrating the mode of substitution of the aqua species from the dinuclear platinum^{II} species exhibiting first-order kinetics.

The pseudo first-order rate constants k_{obs}, was plotted against the concentration of the incoming nucleophiles. Once again, a linear dependence with no meaningful intercept was obtained. Therefore, k_{obs} can be represented by *Equation 2*.

$$k_{obs} = k_2[Nu] \qquad\qquad 2$$

Representative plots of the second-order rate constants, k_2 obtained from those reactions exhibiting first-order kinetics are shown in **Figure 6**. The values of the second order rate constants, k_1 and all the k_2's, which resulted from the direct attack of the nucleophile were obtained from the slopes of these plots at 298.15 K and are summarized in **Table 1**.
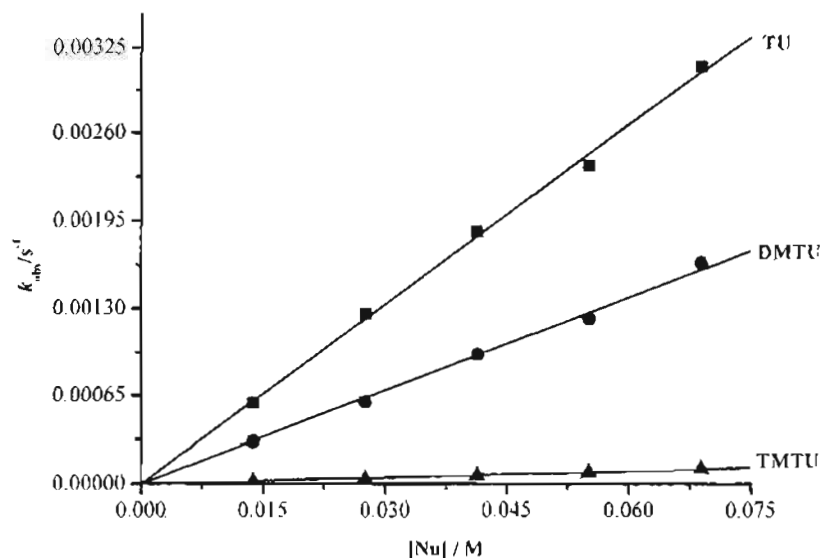
Figure 6: Plots of k_{obs} versus [Nu] for the reaction of **DiPtBut** with a series of nucleophiles *viz*. TU, DMTU and TMTU at 298.15 K.

Table 1: Summary of rate constants and their corresponding standard deviations for the displacement of the coordinated water molecules by TU, DMTU and TMTU; I = 0.2 M (NaClO$_4$), T = 298.15 K.

Nucleophile	$k_2 / 10^{-3} \, M^{-1} s^{-1}$			
	DiPtEn	DiPtProp	DiPtBut	DiPtHex
TU	5029.24 ± 0.01 $(335.6 \pm 7.5)^{\dagger}$	70.1 ± 1.0	44.4± 0.6	31.2 ± 0.2
DMTU	131.8 ± 0.01	33.7 ± 0.1	23.1 ± 0.4	17.1 ± 0.1
TMTU	7.23 ± 0.12	2.33 ± 0.02	1.61 ± 0.02	1.01 ± 0.02
pK_a	4.98 ± 0.09	5.30 ± 0.12	5.50 ± 0.02	5.62 ± 0.03‡

[†] *Second-order rate constant, k_2, calculated for the second substitution step.*

[‡] *Data obtained from literature.*[8,10]

The temperature dependence of the rate constant, k_2 was studied over the range of 15-35 °C or 20-40 °C depending on the reactivity of the complex. A typical plot obtained is illustrated in **Figure 7**. The corresponding activation parameters were calculated using the Eyring equation and are tabulated in **Table 2**.

Figure 7:   Plots of $\ln(k_2/T)$ versus $1/T$ for the reaction of **DiPtHex** with a series of nucleophiles *viz.* TU, DMTU and TMTU at various temperatures, whilst keeping the nucleophile concentration constant at *ca.* 50 X greater than that of the metal complex.
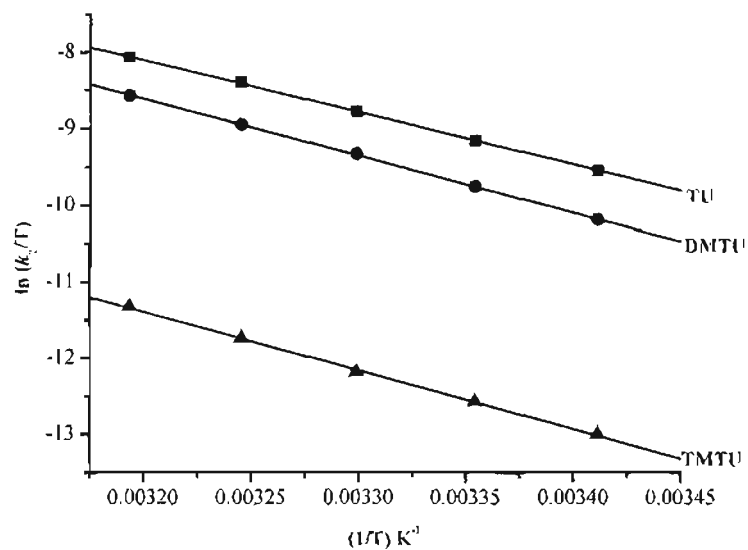
Table 2: Summary of activation parameters and the corresponding standard deviations for the displacement of the coordinated water molecules by TU, DMTU and TMTU; $I = 0.2$ M (NaClO$_4$).

Complex	Nucleophile	$\Delta H^{\neq}$ (kJ mol^{-1})	$\Delta S^{\neq}$ (J K^{-1} mol^{-1})
DiPtEn	**TU**	48.7 ± 6.1	-67.6 ± 19.9
		$(48.7 \pm 1.1)^{\dagger}$	$(-69.4 \pm 3.8)^{\dagger}$
	DMTU	45.8 ± 2.5	-108 ± 8.4
	TMTU	59.9 ± 2.8	-82.1 ± 9.5
DiPtProp	**TU**	38.2 ± 1.5	-138 ± 5
	DMTU	38.7 ± 2.2	-144 ± 7
	TMTU	54.6 ± 2.3	-113 ± 8
DiPtBut	**TU**	49.1 ± 1.6	-107 ± 5
	DMTU	55.7 ± 1.5	-90.5 ± 4.9
	TMTU	60.6 ± 1.7	-95.6 ± 5.6
DiPtHex	**TU**	56.5 ± 0.6	-84.6 ± 1.8
	DMTU	61.6 ± 0.5	-72.4 ± 1.7
	TMTU	64.1 ± 1.1	-87.5 ± 3.6

† *Calculated activation parameters ($\Delta H^{\neq}$ and $\Delta S^{\neq}$) for the second substitution step.*

DFT Calculations

The investigated complexes, **DiPtEn**, **DiPtProp**, **DiPtBut** and **DiPtHex** were modeled using computational techniques in order to assist in explaining the kinetic trends that were observed and to determine how the molecular structures of the complexes are likely to influence the reactivity of the metal centres.

The complexes were all modeled as cations with a +4 charge using the computational software package Spartan® '04 for Windows® using B3LYP density functional method (DFT) and the LACVP+** pseudopotential basis set. The geometry-optimised structures are shown in **Figure 8**.

DiPtEn

$[\{trans\text{-}Pt(OH_2)(NH_3)_2\}_2 - H_2N(CH_2)_2NH_2]^{4+}$

DiPtProp

$[\{trans\text{-}Pt(OH_2)(NH_3)_2\}_2 - H_2N(CH_2)_3NH_2]^{4+}$

DiPtBut

$[\{trans\text{-}Pt(OH_2)(NH_3)_2\}_2 - H_2N(CH_2)_4NH_2]^{4+}$

DiPtHex

$[\{trans\text{-}Pt(OH_2)(NH_3)_2\}_2 - H_2N(CH_2)_6NH_2]^{4+}$
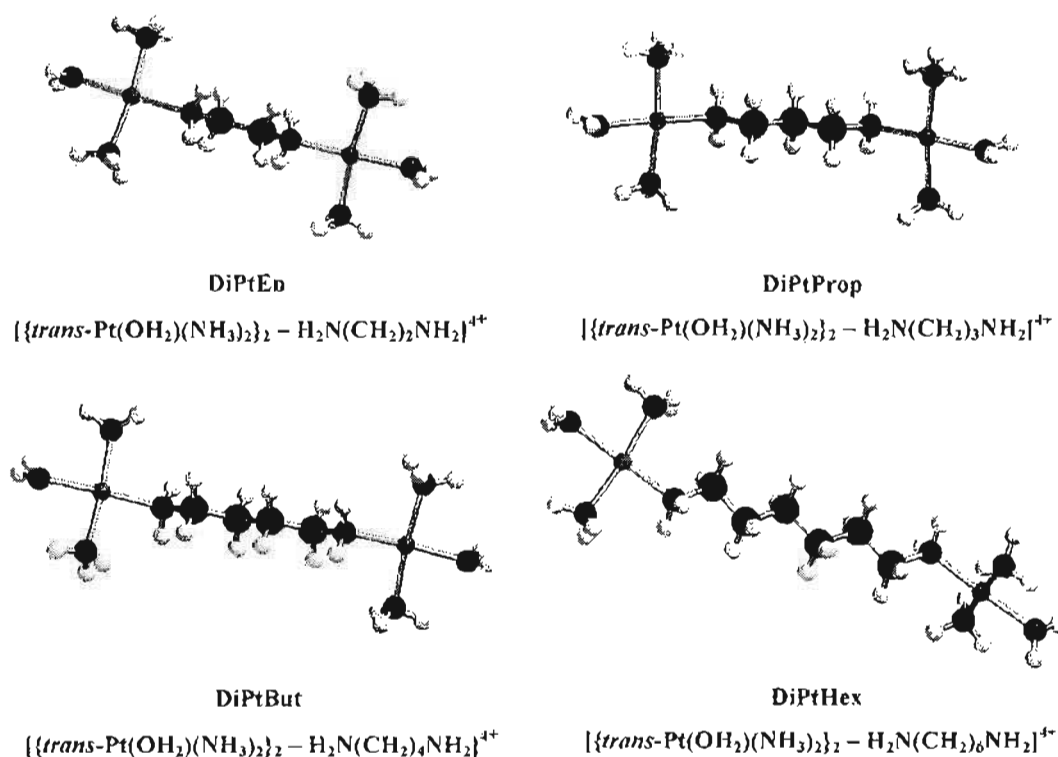
Figure 8: Geometry optimized structures of complexes **DiPtEn**, **DiPtProp**, **DiPtBut** and **DiPtHex**.

From the modeled structures, bond lengths and bond angles were obtained and are given in **Table 3**. In addition the HOMO and LUMO energies were calculated including the energy gap between them. These are shown in **Table 4**.

Table 3:   Summary of selected bond lengths and bond angles for each of the investigated complexes from geometry optimization studies using the B3LYP/LACVP+** level of theory.

	Dinuclear Platinum[II] Complexes			
	DiPtEn	**DiPtProp**	**DiPtBut**	**DiPtHex**
Pt – OH$_2$ / Å	2.107	2.117	2.124	2.134
Pt – *trans* N[†] / Å	2.125	2.105	2.093	2.084
Pt – *cis* N[††] / Å	2.109	2.107	2.101	2.105
cis N –Pt – *cis* N / ° on the side of H$_2$O	172.73	173.57	174.01	174.60

[†] *trans to the leaving group. i.e. OH$_2$;* [††] *cis to the leaving group,. i.e. OH$_2$*

Table 4:   Summary of the HOMO and LUMO values obtained for each of the investigated complexes from geometry optimization studies using the B3LYP/LACVP+** level of theory.

Complex	HOMO / eV	LUMO / eV	ΔE / eV
DiPtEn	-19.62	-14.74	4.88
DiPtProp	-19.06	-14.04	5.02
DiPtBut	-18.58	-13.49	5.09
DiPtHex	-17.90	-12.76	5.14

Figure 9 shows the linear correlation between chain length and the energy gap between HOMO and LUMO orbitals. The only complex that does not fit on this line is **DiPtEn**. This is probably due to the stronger interaction between the metal centres due to the shortness of the backbone chain joining the metals.
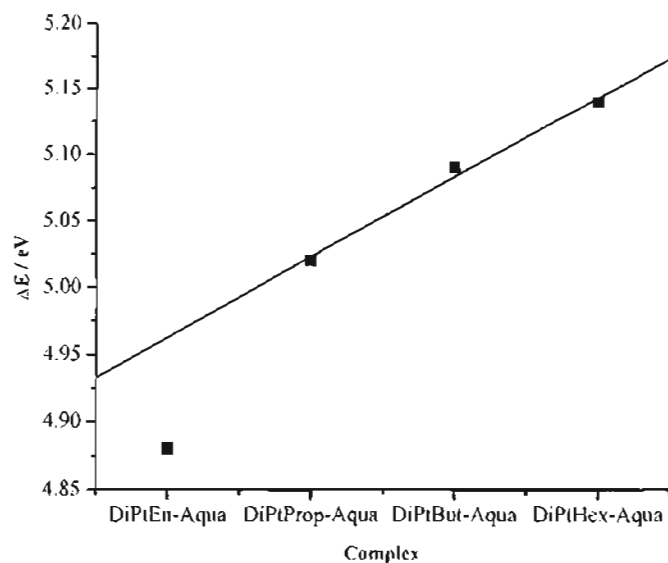
Figure 9: The linear correlation between chain length and the energy gap between HOMO and LUMO orbitals.

From the data tabulated in **Table 3**, it can be observed that upon increasing the length of the diamine chain, the Pt-OH$_2$ and Pt-*trans* N bond lengths are most affected, with the bond lengths increasing and decreasing respectively. The process of increasing the chain length increases the electron density around the *trans*-atom to the platinum through the inductive process, which is equal in both directions. This is supported by an equal decrease and increase of the bonds at the platinum centre. The increase in σ-donor capacity at the *trans*-donor atom results in the shortening of the Pt-N bond length *trans* to the H$_2$O molecule, and consequently a lengthening of the Pt-H$_2$O bond length.

The frontier orbital energies in **Table 4** show a clear increasing trend along the series. This is in line with the expectation, since electron donating groups are known to raise the energy of a molecular orbital, unlike electron withdrawing groups, which lowers the energy. This means as one increases the CH$_2$ groups, the substitution reactions should be expected to be slower due to the increasing of the energy gap.

B-16

Discussion

What has the study achieved? It has shown that the pK_a value for the coordinated water increases with increasing length of the diamine linker. This trend is supported by the computational calculations on the $Pt-OH_2$ bond length, which were also found to increase as the distance between the two platinum atoms was increased. One can infer from this that the water molecule becomes more labile with the increase of the diamine linker. This means that the O-H bond becomes increasingly more difficult to break resulting in higher pK_a's. This observation is in agreement with what is in literature.[24,25]

The lengthening of the $Pt-OH_2$ bond can be accounted for, by looking at the bond *trans* to the water molecules. The theoretical calculation shows a decrease in length of this bond. It can therefore be concluded that there is a net increase in σ-donicity toward the platinum centre *i.e.* the well-known *trans*-effect is influencing the basicity of the complex by promoting ground-state destabilization. This is manifested in the elongation of the $M-OH_2$ bonds *trans* to the σ-bound nitrogen atom of the diamine linker. This observation is probably the same with that observed for metal-halide and metal-water *trans* to the σ-bound carbon atom.[26,27]

It has been shown that the pK_a value obtained for the coordinated water moiety at the platinum[11] centre is a good indicator of the electrophilicity of the metal centre.[18,26] Electron withdrawing π-acceptor effects tends to stabilize the electron rich hydroxo species in comparison to the aqua species and result in lower pK_a values.[19,27] Alternatively, the pK_a value increases if the σ-donor capacity of the ligand *trans* to the aqua moiety is enhanced.[11] Thus, as the length of the bridging diamine chain increases from 2 to 6, so too does the effective σ-donor capacity due to the greater number of CH_2 groups resulting in an increase in the pK_a value as already explained. In this investigation it was not possible to distinguish between the two deprotonation steps, similar to Davies *et al*.[8,11] Interestingly, the dinuclear complexes studied by Hofmann and van Eldik[17] displayed the two pK_a's. This difference is likely to be due to the ligand system around the platinum metal or the inability of the UV/Visible being able to distinguish the two values.

The reactivity of these di-platinum complexes were determined and found to be dependent on the length of the diamine linker as well. Looking at the pK_a values and the HOMO-LUMO energy gap, it is reasonable to expect the reactivity of these complexes to decrease from **DiPtEn** to **DiPtHex**.[28-30] This was indeed found to be the case. From the bond length of $M-OH_2$ one would have expected the trend to be in the opposite direction due to the lability of the water molecules as indicated by the theoretical calculation. However, this is contrary to the result obtained. The interpretation of this is that, whilst the *trans*-effect is operational in these molecules and increases from the **En** to the **Hex** ligand, it does not appear to be the controlling factor. It is obvious, that the rate of substitution increases due to either the ground-state destabilization or transition state stabilization. In this case destabilization of the ground-state does occur as supported by the computational calculations showing an increase in the $M-OH_2$ bond length. These increase with the increasing of the linking chain. In addition to this effect, the shortening of the Pt-N bond in the *trans* position to the water molecules results in destabilization of the transition state. This is thought to be due to the increase in σ-donicity to the metal centre. This decreases the electrophilic character of the metal centre with a net effect of repelling the incoming nucleophile. In this case it is most likely that the two effects play a simultaneous role, with the latter being more dominant.

The retardation on the rate of substitution from **DiPtEn** to **DiPtHex** can also be attributed to steric hindrance around the Pt centre. Analysis of the geometry-optimized structures tends to suggest that as the chain length of the diamine linker increases, so too does the flexibility of the complex. It would appear that as the CH_2 groups are increased, the number of rotations about these bonds increases, leading to a greater number of possible conformers for the diplatinum complexes. This increased flexibility consequently leads to a greater degree of steric influence and in all probability do directly influence the path that the incoming nucleophile adopts in approaching the metal centre. If it is assumed that these complexes from **DiPtProp** can form curvature in solution, it becomes obvious that the axial attack from one side will be greatly reduced. It is most likely that this steric hindrance by itself may account for a bigger percentage of the factors influencing the reactivity of these complexes.

In comparing the reactivity of the aqua complexes it can be summarized that the substitution behaviour of the complexes clearly depends on the length of the diamine linker. The increasing of the CH_2 groups increases the σ-donicity around the platinum centre, as reflected by the shortening of the Pt-N bond length and higher pK_a for the ionisation of the aqua ligand. This results in a net decrease in the electrophilicity at the metal centre. In addition, increasing of the CH_2 unit increases the flexibility of the complexes, resulting in increased steric hindrance. Both these factors contribute towards the decrease in the rate of substitution of the coordinated water molecule.

Substitution reactions with sterically less hindered thiourea (Tu) is about 10^2 times faster for **DiPtEn** when compared to the other complexes. The reason for the observed trend across the complexes has been accounted for, what requires explanation is the big difference between **DiPtEn** and the other complexes. The reason for this enhanced reactivity is due to the interaction between the two Pt^{II} centres, apart from all other factors, which are also operational. This is strongly supported by the fact that this was the only complex where absolute values of k_1 and k_2 could be differentiated. The findings compare well with Farrell's[11] study involving 1,1/t,t where there was no measurable difference in the rate constants obtained for the first and second substitution reactions involving chloride when the bridge was longer by two CH_2 groups. Substitution reactions with the sterically hindered nucleophiles, DMTU and TMTU show a clear dependence on the steric bulk of the nucleophiles. The most sterically hindered nucleophile, TMTU reacting significantly slower than the less hindered TU.

On the basis of the activation parameters there is no direct correlation that is evident between the reactivity and activation enthalpy, $\Delta H^{\neq}$. But a trend exists when looking at the activation entropy. $\Delta S^{\neq}$, which is playing an important role in these reactions. Comparing the complexes where the CH_2 group is greater than 3, where Pt$\cdots$Pt interactions are insignificant, the value of $\Delta S^{\neq}$ is seen to be less negative as the length of the diamine linker increases. This is true for all the nucleophiles irrespective of the steric bulkness. This observation can be attributed to a larger number of different conformers that exists as a result of the greater flexibility of the bridging backbone.

The mechanism of the substitution reactions for all these complexes remains associative in nature as supported by the large and negative values of $\Delta S^{\ddagger}$, indicating that the structure of the transition state is more compact than that of either the reactant or product species. This is consistent with the substitution mechanism for square-planar systems[27], even though dissociative mechanisms have been observed but in very limited cases.[31,32]

Conclusions

The study has investigated the effect of increasing the CH_2 group to the $[\{trans\text{-}Pt(OH_2)(NH_3)_2\}_2\text{-}H_2N(CH_2)_n\text{-}NH_2]^{4+}$ complexes. The results have shown that the reactivity of these complexes depends on the length of the diamine linker. This increases the σ-donicity to the platinum centre, increasing the pK_a of the coordinated water and decreases the electrophilicity of the metal centre. Other factors that slow down the rate of substitution, is the increasing steric hindrance due to the flexibility of the complexes as the chain becomes longer. It is also observed that when $n \geq 3$, the Pt···Pt interactions diminishes, and it is not possible to distinguish the two rate constants. The associative substitution mechanism remains operational in all the systems investigated. This study has shed some light in trying to understand for the first time the influence the linker backbone has on the binuclear complexes with regards to their folding abilities, Pt···Pt distance and interactions.

Acknowledgements

References

1. Lippert, B., *Cisplatin: Chemistry and Biochemistry of a Leading Anticancer Drug*, Wiley-VCH, NY, **1999**, pp 2-36.

2. Kelland, L.R., Farrell, N.F., *Platinum Based Drugs in Cancer Therapy*, JAI Press, Greenwich, CT, **1996**.

3. Jamieson, E.R., Lippard, S.J., *Chem. Rev.*, *99*, **1999**, 2467.

4. Wong, E. & Giandomenico, C.M., *Chem. Rev.*, *99*, **1999**, 2451.

5. Oehlsen, M.E., Qu, Y., Farrel, N., *Inorg. Chem.*, *42*, **2003**, 5498.

6. Chaney, S.G. & Sancar, A., *J. Natl. Cancer Inst.*, *88*, **1996**, 1346.

7. Kasparkova, J., Farrell, N., Brabec, V., *Jnl. Biol. Chem.*, *275*, **2000**, 15789.

8. Davies, M.S., Thomas, D.S., Hegmans, A., Berners-Price, S.J., Farrell, N., *Inorg. Chem.*, *41*, **2002**, 1101.

9. Hegmans, A., Qu, Y., Kelland, LR., Roberts, J.D., Farrell, N., *Inorg. Chem.*, *40*, **2001**, 6108.

10. Cox, J.W., Berners-Price, S.J., Davies, M.S., Qu, Y., Farrell, N., *J. Amer. Chem. Soc.*, *123*, **2001**, 1316.

11. Davies, M.S., Cox, J.W., Berners-Price, S.J., Barklage, W., Qu, Y., Farrell, N., *Inorg. Chem.*, *39*, **2000**, 1710.

12. Farrell, N.,., Qu, Y., Bierbach, U., Valsecchi, M., Menta, E., Lippert, B (Ed.), *Cisplatin : Chemistry and Biochemistry of a Leading Anticancer Drug*, Wiley-VCH, NY, 1999, pp 469-496.

13. Zaludova, R., Zaikovska, A., Kasparkova, J., Balcarova, Z., Kleinwachter, V., Vrana, O., Farrell, N., *Eur. J. Biochem.*, *246*, **1997**, 508.

14. Perrin, D.D., Armarego, W.L.F., Perrin, D.R., *Purification of Laboratory Chemicals*, 2nd Ed., Pergamon, Oxford, **1980**, pp 229, 249.

15. Farrell, N., Qu, Y., Feng, L., van Houten, B., *Biochemistry*, *29*, **1990**, 9522.

16. Farrell, N. & Qu, Y., *Inorg. Chem.*, *31*, **1992**, 930.

17. Hofmann, A. & van Eldik, R., *J. Chem. Soc. Dalton Trans.*, **2003**, 2979.

18. Bugarčič, Z.D., Petrović, B.V.; Jelić, R., *Trans. Met. Chem.*, *26*, **2001**, 668.

19. Hehre, W.J., *A Guide to Molecular Mechanics and Quantum Chemical Calculations*, Wavefunction, Irvine, **2003**.

20. Friesner, R.A., *Chem. Phys. Lett.*, *116*, **1985**, 39.

21. Friesner, R.A., *Annu. Rev. Phys. Chem.*, *42*, **1991**, 341.

22. Becke, A.D., *J. Chem. Phys.*, *98*, **1993**, 5648.

23. Hay, P.J. & Wadt, W.R., *J. Chem. Phys.*, *82*, **1985**, 299

24. Hofmann, A., Jaganyi, D., Munro, O.Q., Liehr, G., van Eldik, R., *Inorg. Chem.*, *42*, **2003**, 1688.

25. Ryabov, A.D., Kazankov, G.M., Yatsimirky, A.K., *et.al.*, *Inorg. Chem.*, *32*, **1992**, 3083.

26. Castan., P., Laud, J., Wimmer, S., Wimmer, F.L., *J. Chem. Soc. Dalton Trans.*, **1991**, 1155.

27. Jaganyi, D. & Tiba, F., *Trans. Met. Chem.*, *28*, **2003**, 803.

28. Jaganyi, D., Hofmann, A., van Eldik, R., *Agnew. Chem. Int. Ed.*, *40*, **2001**, 1680.

29. Otto, S., Elding, L.I., *J. Chem. Soc. Dalton Trans.*, **2002**, 2354.

30. Romeo, R., Plutino, M.R., Scolaro, L.M., Stoccoro, S., Minghetti, G., *Inorg. Chem.*, *39*, **2000**, 4749.

31. Romeo, R., Monsu-Scolaro, L., Plutino, M.R., *et al.*, *Inorg. Chim. Acta.*, *350*, **2003**, 143.

32. Romeo, R., Grassi, A., Monsu-Scolaro, L., *Inorg. Chem.*, *31*, **1992**, 4383.